

See discussions, stats, and author profiles for this publication at: <https://www.researchgate.net/publication/339913143>

# DIFFRACTION GRATING HANDBOOK, eighth edition

Book · March 2020

---

CITATIONS

2

READS

2,398

1 author:



Christopher Palmer

MKS Instruments, Rochester, New York, United States

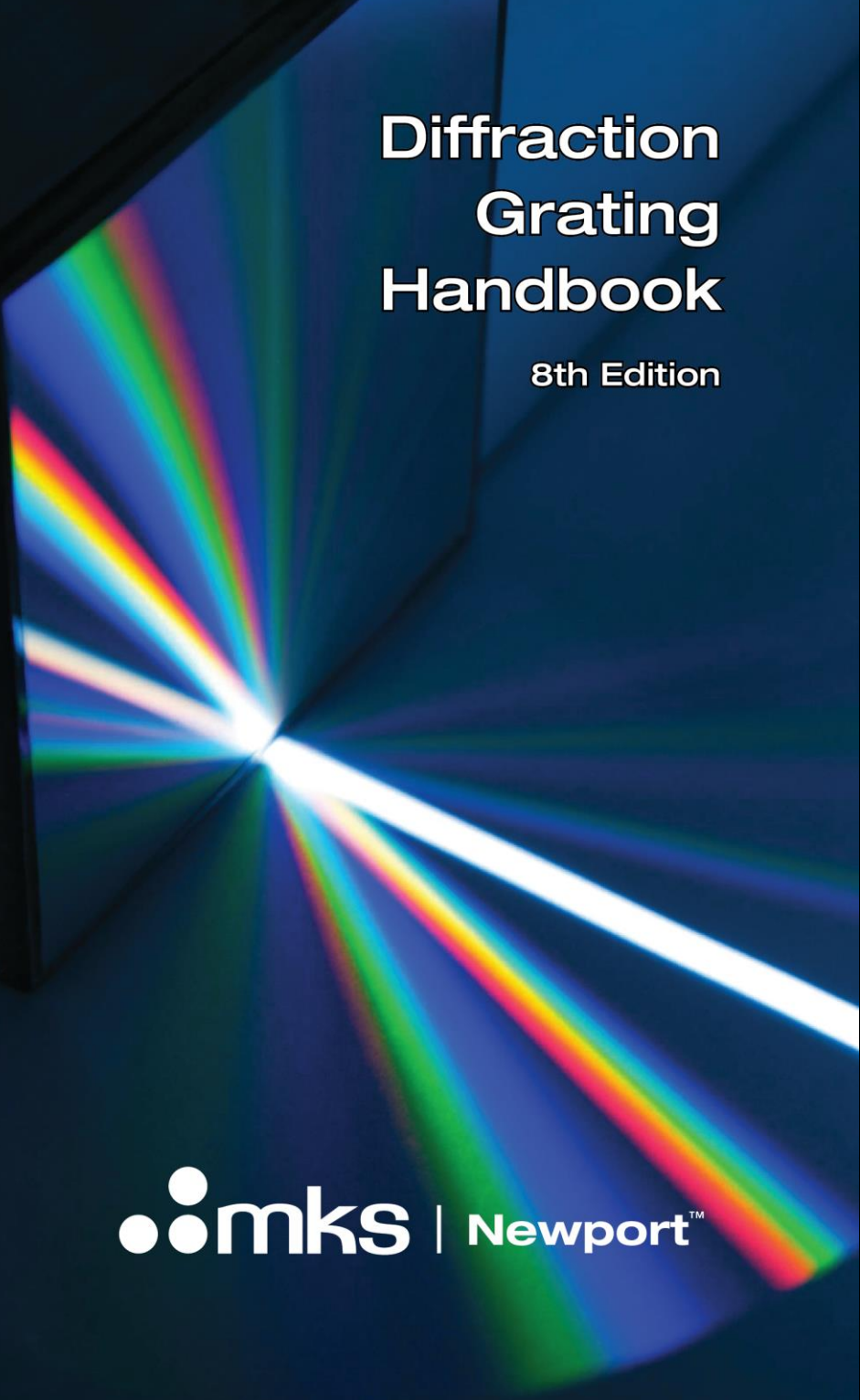
29 PUBLICATIONS 678 CITATIONS

SEE PROFILE

Some of the authors of this publication are also working on these related projects:

Project

Diffraction Grating Handbook - 8th edition [View project](#)

A photograph of a diffraction grating held at an angle. Light passes through it, creating a vibrant, multi-colored rainbow spectrum that fans out against a dark background.

# Diffraction Grating Handbook

8th Edition

 mks | Newport™

# DIFFRACTION GRATING HANDBOOK

eighth edition

**Christopher Palmer**

Richardson Gratings™  
MKS Instruments, Inc.



705 St. Paul Street, Rochester, New York 14605 USA

tel: +1 585 248 4100, fax: +1 585 248 4111

e-mail: [gratings@mksinst.com](mailto:gratings@mksinst.com)

web site: <http://www.gratinglab.com/>

Copyright 2020, MKS Instruments, Inc., All Rights Reserved



# CONTENTS

<b>PREFACE TO THE EIGHTH EDITION</b>	<b>11</b>
<b>1. SPECTROSCOPY AND GRATINGS</b>	<b>13</b>
1.0. INTRODUCTION	13
1.1. THE DIFFRACTION GRATING	14
1.2. A BRIEF HISTORY OF GRATING DEVELOPMENT	15
1.3. HISTORY OF RICHARDSON GRATINGS	16
1.4. DIFFRACTION GRATINGS FROM RICHARDSON GRATINGS	17
<b>2. THE PROPERTIES OF DIFFRACTION GRATINGS</b>	<b>19</b>
2.1. THE GRATING EQUATION	19
2.2. DIFFRACTION ORDERS	24
2.2.1. <i>Existence of diffraction orders</i>	24
2.2.2. <i>Overlapping of diffracted spectra</i>	25
2.3. DISPERSION	26
2.3.1. <i>Angular dispersion</i>	26
2.3.2. <i>Linear dispersion</i>	27
2.4. RESOLVING POWER, SPECTRAL RESOLUTION, AND SPECTRAL BANDPASS	28
2.4.1. <i>Resolving power</i>	28
2.4.2. <i>Spectral resolution</i>	30
2.4.3. <i>Spectral Bandpass</i>	31
2.4.4. <i>Resolving power vs. resolution</i>	31
2.5. FOCAL LENGTH AND $f$ /NUMBER	32
2.6. ANAMORPHIC MAGNIFICATION	34
2.7. FREE SPECTRAL RANGE	35
2.8. ENERGY DISTRIBUTION (GRATING EFFICIENCY)	35
2.9. SCATTERED LIGHT AND STRAY LIGHT	37
2.10. SIGNAL-TO-NOISE RATIO (SNR)	38
<b>3. RULED GRATINGS</b>	<b>39</b>
3.0. INTRODUCTION	39
3.1. RULING ENGINES	39

3.1.1. <i>The Michelson engine</i>	39
3.1.2. <i>The Mann engine</i>	40
3.1.3. <i>The MIT 'B' engine</i>	40
3.1.4. <i>The MIT 'C' engine</i>	41
3.2. THE RULING PROCESS	42
3.3. VARIED LINE-SPACE (VLS) GRATINGS	43
<b>4. HOLOGRAPHIC GRATINGS</b>	<b>45</b>
4.0. INTRODUCTION	45
4.1. PRINCIPLE OF MANUFACTURE	45
4.1.1. <i>Formation of an interference pattern</i>	45
4.1.2. <i>Formation of the grooves</i>	46
4.2. CLASSIFICATION OF HOLOGRAPHIC GRATINGS	47
4.2.1. <i>Single-beam interference</i>	47
4.2.2. <i>Double-beam interference</i>	48
4.3. THE HOLOGRAPHIC RECORDING PROCESS	50
4.4. DIFFERENCES BETWEEN RULED AND HOLOGRAPHIC GRATINGS	52
4.4.1. <i>Differences in grating efficiency</i>	52
4.4.2. <i>Differences in scattered light</i>	52
4.4.3. <i>Differences and limitations in the groove profile</i>	53
4.4.4. <i>Range of obtainable groove frequencies</i>	54
4.4.5. <i>Differences in the groove patterns</i>	54
4.4.6. <i>Differences in the substrate shapes</i>	55
4.4.7. <i>Differences in the size of the master substrate</i>	56
4.4.8. <i>Differences in generation time for master gratings</i>	56
<b>5. REPLICATED GRATINGS</b>	<b>57</b>
5.0. INTRODUCTION	57
5.1. THE REPLICATION PROCESS	57
5.2. REPLICA GRATINGS VS. MASTER GRATINGS	61
5.3. STABILITY OF REPLICATED GRATINGS	63
5.4. DUAL-BLAZE GRATINGS	66
<b>6. PLANE GRATINGS AND THEIR MOUNTS</b>	<b>69</b>
6.1. GRATING MOUNT TERMINOLOGY	69
6.2. PLANE GRATING MONOCHROMATOR MOUNTS	69
6.2.1. <i>The Czerny-Turner monochromator</i>	70

6.2.2. <i>The Ebert monochromator</i>	71
6.2.3. <i>The Monk-Gillieson monochromator</i>	72
6.2.4. <i>The Littrow monochromator</i>	73
6.2.5. <i>Double &amp; triple monochromators</i>	73
6.2.6. <i>The constant-scan monochromator</i>	75
<b>6.3. PLANE GRATING SPECTROGRAPH MOUNTS</b>	<b>76</b>
<b>7. CONCAVE GRATINGS AND THEIR MOUNTS</b>	<b>79</b>
7.0. INTRODUCTION	79
7.1. CLASSIFICATION OF GRATING TYPES	79
7.1.1. <i>Groove patterns</i>	80
7.1.2. <i>Substrate (blank) shapes</i>	80
7.2. CLASSICAL CONCAVE GRATING IMAGING	81
7.3. NONCLASSICAL CONCAVE GRATING IMAGING	88
7.4. REDUCTION OF ABERRATIONS	90
7.5. CONCAVE GRATING MOUNTS	94
7.5.1. <i>The Rowland circle spectrograph</i>	94
7.5.2. <i>The Wadsworth spectrograph</i>	96
7.5.3. <i>Flat-field spectrographs</i>	96
7.5.4. <i>Imaging spectrographs and monochromators</i>	98
7.5.5. <i>Constant-deviation monochromators</i>	98
<b>8. IMAGING PROPERTIES OF GRATING SYSTEMS</b>	<b>101</b>
8.1. CHARACTERIZATION OF IMAGING QUALITY	101
8.1.1. <i>Geometric raytracing and spot diagrams</i>	101
8.1.2. <i>Linespread calculations</i>	103
8.2. INSTRUMENTAL IMAGING	103
8.2.1. <i>Magnification of the entrance aperture</i>	103
8.2.2. <i>Effects of the entrance aperture dimensions</i>	106
8.2.3. <i>Effects of the exit aperture dimensions</i>	107
8.3. INSTRUMENTAL BANDPASS	111
<b>9. EFFICIENCY CHARACTERISTICS OF DIFFRACTION GRATINGS</b>	<b>113</b>
9.0. INTRODUCTION	113
9.1. GRATING EFFICIENCY AND GROOVE SHAPE	116
9.2. EFFICIENCY CHARACTERISTICS FOR TRIANGULAR-GROOVE GRATINGS	117

9.3.	EFFICIENCY CHARACTERISTICS FOR SINUSOIDAL-GROOVE GRATINGS	122
9.4.	THE EFFECTS OF FINITE CONDUCTIVITY	126
9.5.	DISTRIBUTION OF ENERGY BY DIFFRACTION ORDER	127
9.6.	USEFUL WAVELENGTH RANGE	130
9.7.	BLAZING OF RULED TRANSMISSION GRATINGS	130
9.8.	BLAZING OF HOLOGRAPHIC REFLECTION GRATINGS	131
9.9.	OVERCOATING OF REFLECTION GRATINGS	132
9.10.	THE RECIPROCITY THEOREM	134
9.11.	CONSERVATION OF ENERGY	134
9.12.	GRATING ANOMALIES	136
9.12.1.	<i>Rayleigh anomalies</i>	136
9.12.2.	<i>Resonance anomalies</i>	136
9.13.	GRATING EFFICIENCY CALCULATIONS	138
<b>10.</b>	<b>STRAY LIGHT CHARACTERISTICS OF GRATINGS AND GRATING SYSTEMS</b>	<b>141</b>
10.0.	INTRODUCTION	141
10.1.	GRATING SCATTER	141
10.1.1.	<i>Surface irregularities in the grating coating</i>	143
10.1.2.	<i>Dust, scratches &amp; pinholes on the surface of the grating</i>	143
10.1.3.	<i>Irregularities in the position of the grooves</i>	143
10.1.4.	<i>Irregularities in the depth of the grooves</i>	144
10.1.5.	<i>Spurious fringe patterns due to the recording system</i>	144
10.1.6.	<i>The perfect grating</i>	145
10.2.	INSTRUMENTAL STRAY LIGHT	146
10.2.1.	<i>Grating scatter</i>	146
10.2.2.	<i>Other diffraction orders from the grating</i>	146
10.2.3.	<i>Overfilling optical surfaces</i>	146
10.2.4.	<i>Direct reflections from other surfaces</i>	147
10.2.5.	<i>Optical effects due to the sample or sample cell</i>	148
10.2.6.	<i>Thermal emission</i>	148
10.3.	ANALYSIS OF OPTICAL RAY PATHS IN A GRATING-BASED INSTRUMENT	149
10.4.	DESIGN CONSIDERATIONS FOR REDUCING STRAY LIGHT	152

<b>11. TESTING AND CHARACTERIZING DIFFRACTION GRATINGS</b>	<b>155</b>
11.1. THE MEASUREMENT OF SPECTRAL DEFECTS	155
11.1.1. <i>Rowland ghosts</i>	155
11.1.2. <i>Lyman ghosts</i>	158
11.1.3. <i>Satellites</i>	159
11.2. THE MEASUREMENT OF GRATING EFFICIENCY	159
11.3. THE MEASUREMENT OF DIFFRACTED WAVEFRONT QUALITY	161
11.3.1. <i>The Foucault knife-edge test</i>	161
11.3.2. <i>Direct wavefront testing</i>	161
11.4. THE MEASUREMENT OF RESOLVING POWER	164
11.5. THE MEASUREMENT OF SCATTERED LIGHT	165
11.6. THE MEASUREMENT OF INSTRUMENTAL STRAY LIGHT	168
11.6.1. <i>The use of cut-off filters</i>	168
11.6.2. <i>The use of monochromatic light</i>	169
11.6.3. <i>Signal-to-noise and errors in absorbance readings</i>	170
<b>12. SELECTION OF DISPERSING SYSTEMS</b>	<b>173</b>
12.1. REFLECTION GRATING SYSTEMS	173
12.1.1. <i>Plane reflection grating systems</i>	173
12.1.2. <i>Concave reflection grating systems</i>	173
12.2. TRANSMISSION GRATING SYSTEMS	174
12.3. GRATING PRISMS (GRISMS)	177
12.4. GRAZING INCIDENCE SYSTEMS	179
12.5. ECHELLES	179
12.6. IMMERSED GRATINGS	183
<b>13. APPLICATIONS OF DIFFRACTION GRATINGS</b>	<b>185</b>
13.1. GRATINGS FOR INSTRUMENTAL ANALYSIS	185
13.1.1. <i>Atomic and molecular spectroscopy</i>	185
13.1.2. <i>Fluorescence spectroscopy</i>	187
13.1.3. <i>Colorimetry</i>	187
13.1.4. <i>Raman spectroscopy</i>	188
13.1.5. <i>Hyperspectral systems</i>	188
13.2. GRATINGS IN LASER SYSTEMS	189
13.2.1. <i>Laser tuning</i>	189
13.2.2. <i>Pulse stretching and compression</i>	191

<b>13.3. GRATINGS IN ASTRONOMICAL APPLICATIONS</b>	<b>192</b>
<i>13.3.1. Ground-based astronomy</i>	192
<i>13.3.2. Space-borne astronomy</i>	196
<i>13.3.3. Space travel</i>	197
<b>13.4. GRATINGS IN SYNCHROTRON RADIATION BEAMLINES</b>	<b>197</b>
<b>13.5. SPECIAL USES FOR GRATINGS</b>	<b>197</b>
<i>13.5.1. Gratings as filters</i>	197
<i>13.5.2. Gratings as biosensors</i>	199
<i>13.5.3. Gratings in fiber-optic telecommunications</i>	200
<i>13.5.4. Gratings as beam splitters</i>	201
<i>13.5.5. Gratings as optical couplers</i>	201
<i>13.5.6. Gratings in metrological applications</i>	201
<b>14. ADVICE FOR USING GRATINGS</b>	<b>203</b>
<b>14.1. CHOOSING A SPECIFIC GRATING</b>	<b>203</b>
<b>14.2. APPEARANCE</b>	<b>204</b>
<i>14.2.1. Ruled gratings</i>	204
<i>14.2.2. Holographic gratings</i>	204
<b>14.3. GRATING MOUNTING</b>	<b>205</b>
<b>14.4. GRATING SIZE</b>	<b>205</b>
<b>14.5. SUBSTRATE MATERIAL</b>	<b>205</b>
<b>14.6. GRATING COATINGS</b>	<b>205</b>
<b>15. HANDLING GRATINGS</b>	<b>207</b>
<b>15.1. THE GRATING SURFACE</b>	<b>207</b>
<b>15.2. PROTECTIVE COATINGS</b>	<b>207</b>
<b>15.3. GRATING COSMETICS AND PERFORMANCE</b>	<b>207</b>
<b>15.4. UNDOING DAMAGE TO THE GRATING SURFACE</b>	<b>209</b>
<b>15.5. GUIDELINES FOR HANDLING GRATINGS</b>	<b>209</b>
<b>16. GUIDELINES FOR SPECIFYING GRATINGS</b>	<b>211</b>
<b>16.1. REQUIRED SPECIFICATIONS</b>	<b>211</b>
<b>16.2. SUPPLEMENTAL SPECIFICATIONS</b>	<b>215</b>
<b>16.3. ADDITIONAL REQUIRED SPECIFICATIONS FOR CONCAVE ABERRATION-REDUCED GRATINGS</b>	<b>216</b>

<b>APPENDIX A. SOURCES OF ERROR IN MONOCHROMATOR-MODE EFFICIENCY MEASUREMENTS OF PLANE DIFFRACTION GRATINGS</b>	<b>219</b>
A.o. INTRODUCTION	219
A.1. OPTICAL SOURCES OF ERROR	221
A.1.1. <i>Wavelength error</i>	221
A.1.2. <i>Fluctuation of the light source intensity</i>	223
A.1.3. <i>Bandpass</i>	223
A.1.4. <i>Superposition of diffracted orders</i>	224
A.1.5. <i>Degradation of the reference mirror</i>	225
A.1.6. <i>Collimation</i>	225
A.1.7. <i>Stray light or “optical noise”</i>	226
A.1.8. <i>Polarization</i>	226
A.1.9. <i>Unequal path length</i>	227
A.2. MECHANICAL SOURCES OF ERROR	228
A.2.1. <i>Alignment of incident beam to grating rotation axis</i>	228
A.2.2. <i>Alignment of grating surface to grating rotation axis</i>	228
A.2.3. <i>Orientation of the grating grooves (tilt adjustment)</i>	228
A.2.4. <i>Orientation of the grating surface (tip adjustment)</i>	229
A.2.5. <i>Grating movement</i>	229
A.3. ELECTRICAL SOURCES OF ERROR	229
A.3.1. <i>Detector linearity</i>	229
A.3.2. <i>Changes in detector sensitivity</i>	230
A.3.3. <i>Sensitivity variation across detector surface</i>	231
A.3.4. <i>Electronic noise</i>	231
A.4. ENVIRONMENTAL FACTORS	231
A.4.1. <i>Temperature</i>	231
A.4.2. <i>Humidity</i>	232
A.4.3. <i>Vibration</i>	232
A.5. SUMMARY	232
<b>APPENDIX B. LIE ABERRATION THEORY FOR GRATING SYSTEMS</b>	<b>235</b>
<b>FURTHER READING</b>	<b>239</b>
<b>GRATING PUBLICATIONS BY MKS PERSONNEL</b>	<b>243</b>
<b>INDEX</b>	<b>249</b>



# PREFACE TO THE EIGHTH EDITION

“No single tool has contributed more to the progress of modern physics than the diffraction grating ...”<sup>1</sup>

MKS Instruments is proud to build upon the heritage of technical excellence that began when Bausch & Lomb established what became the Richardson Grating Laboratory and produced its first high-quality master grating in the late 1940s. A high-fidelity replication process was subsequently developed to make duplicates of the tediously generated master gratings. This replication process became the key to converting diffraction gratings from academic curiosities to commercially-available optical components, which in turn enabled gratings to supplant prisms as the optical dispersing element of choice in modern laboratory instrumentation. The advantage of replica gratings lies not only in their greater availability and lower cost, but in making possible the provision of exact duplicates whenever needed.

Since its introduction in 1970, the *Diffraction Grating Handbook* has been a primary source of information of a general nature regarding diffraction gratings. In 1982, Dr. Michael Hutley of the National Physical Laboratory published *Diffraction Gratings*, a monograph that addresses in more detail the nature and uses of gratings, as well as their manufacture. In 1997, Dr. Erwin Loewen, the emeritus director of the Bausch & Lomb grating laboratory who wrote the original *Handbook*, wrote with Dr. Evgeny Popov (now with the Laboratoire d’Optique Électromagnétique) a very thorough and complete monograph entitled *Diffraction Gratings and Applications*. Readers of this *Handbook* who seek additional insight into the many aspects of diffraction grating behavior, manufacture and use are encouraged to turn to these two excellent books.

Christopher Palmer  
Rochester, New York, USA  
March 2020  
[chris.palmer@mksinst.com](mailto:chris.palmer@mksinst.com)

---

<sup>1</sup> G. R. Harrison, “The production of diffraction gratings. I. Development of the ruling art,” *J. Opt. Soc. Am.* **39**, 413-426 (1949).



# 1. SPECTROSCOPY AND GRATINGS

“It is difficult to point to another single device that has brought more important experimental information to every field of science than the diffraction grating. The physicist, the astronomer, the chemist, the biologist, the metallurgist, all use it as a routine tool of unsurpassed accuracy and precision, as a detector of atomic species to determine the characteristics of heavenly bodies and the presence of atmospheres in the planets, to study the structures of molecules and atoms, and to obtain a thousand and one items of information without which modern science would be greatly handicapped.”

— J. Strong, “The Johns Hopkins University and diffraction gratings,” *J. Opt. Soc. Am.* **50**, 1148-1152 (1960), quoting G. R. Harrison.

## 1.0. INTRODUCTION

Optical spectroscopy is the study of electromagnetic spectra – the wavelength composition of light – due to atomic and molecular interactions. For many years, spectroscopy has been important in the study of physics, and it is now equally important in astronomical, biological, chemical, metallurgical and other analytical investigations. The first experimental tests of quantum mechanics involved verifying predictions regarding the spectrum of hydrogen with grating spectrometers. In astrophysics, diffraction gratings provide clues to the composition of and processes in stars and planetary atmospheres, as well as offer clues to the large-scale motions of objects in the universe. In chemistry, toxicology and forensic science, grating-based instruments are used to determine the presence and concentration of chemical species in samples. In telecommunications, gratings are being used to increase the capacity of fiber-optic networks using wavelength division multiplexing (WDM). Gratings have also found many uses in tuning and spectrally shaping laser light, as well as in chirped pulse amplification applications.

The diffraction grating is of considerable importance in spectroscopy, due to its ability to separate (disperse) polychromatic light into its constituent monochromatic components. In recent years, the spectroscopic quality of diffraction gratings has greatly improved, and Richardson Gratings has been a leader in this development.

The extremely high accuracy required of a modern diffraction grating dictates that the mechanical dimensions of diamond tools, ruling engines, and optical recording hardware, as well as their environmental conditions, be controlled to the very limit of that which is physically possible. A lower degree of accuracy results in gratings that are ornamental but have little technical or scientific value. The challenge to produce precision diffraction gratings has attracted the attention of some of the world's most capable scientists and technicians. Only a few have met with any appreciable degree of success, each limited by the technology available.

### **1.1. THE DIFFRACTION GRATING**

A *diffraction grating* is a collection of reflecting (or transmitting) elements separated by a distance comparable to the wavelength of light under study. It may be thought of as a collection of diffracting elements, such as a pattern of transparent slits (or apertures) in an opaque screen, or a collection of reflecting grooves on a substrate. In either case, the fundamental physical characteristic of a diffraction grating is the spatial modulation of the refractive index. Upon diffraction, an electromagnetic wave incident on a grating will have its electric field amplitude, or phase, or both, modified in a predictable manner, due to the (often but not always periodic) variation in refractive index in the region near the surface of the grating.<sup>2</sup> Diffraction from or through a grating generates one or more discrete sets of diffracted waves, created via constructive interference.

A *reflection grating* consists of a grating superimposed on a reflective surface, whereas a *transmission grating* consists of a grating superimposed on a transparent surface.

A *master grating* (also called an *original grating*) is a grating whose surface-relief pattern is created “from scratch”, either by mechanical ruling (see Chapter 3) or holographic recording (see Chapter 4). A *replica grating* is one whose surface-relief pattern is generated by casting or molding the relief pattern of another grating (see Chapter 5).

---

<sup>2</sup> M. Born and E. Wolf, *Principles of Optics*, 7<sup>th</sup> expanded ed., Cambridge University Press (Cambridge, England: 1999).

## 1.2. A BRIEF HISTORY OF GRATING DEVELOPMENT

The first diffraction grating was made by an American astronomer, David Rittenhouse, in 1785, who reported constructing a half-inch wide grating with fifty-three apertures.<sup>3</sup> He did not develop this prototype further, and there is no evidence that he tried to use it for serious scientific experiments.

In 1821, most likely unaware of Rittenhouse's work, Joseph von Fraunhofer began his work on diffraction gratings,<sup>4</sup> who saw the value that grating dispersion could have for the new science of spectroscopy. Fraunhofer's persistence resulted in gratings of sufficient quality to enable him to measure the absorption lines of the solar spectrum, now generally referred to as Fraunhofer lines. He also derived the equations that govern the dispersive behavior of gratings. Fraunhofer was interested only in making gratings for his own experiments, and upon his death his equipment disappeared.

By 1850, F.A. Nobert, a Prussian instrument maker, began to supply scientists with gratings superior to Fraunhofer's. About 1870, the scene of grating development returned to America, where L.M. Rutherford, a New York lawyer with an avid interest in astronomy, became interested in gratings. In just a few years, Rutherford learned to rule reflection gratings in speculum metal that were far superior to any that Nobert had made. Rutherford developed gratings that surpassed even the most powerful prisms. He made very few gratings, though, and their uses were limited.

Rutherford's part-time dedication, impressive as it was, could not match the tremendous strides made by H.A. Rowland, professor of physics at the Johns Hopkins University. Rowland's 1882 work established the grating as the primary optical element of spectroscopic technology.<sup>5</sup> Rowland constructed sophisticated ruling engines and

---

<sup>3</sup> D. Rittenhouse, "Explanation of an optical deception," *Trans. Amer. Phil. Soc.* **2**, 37-42 (1786); "An optical problem, proposed by Mr. Hopkinson, and solved by Mr. Rittenhouse", *Trans. Amer. Phil. Soc.* **2**, 201-206 (1786).

<sup>4</sup> J. Fraunhofer, "Kurzer Bericht von den Resultaten neuerer Versuche über die Gesetze des Lichtes, und die Theorie derselben," *Ann. D. Phys.* **74**, 337-378 (1823).

<sup>5</sup> H. A. Rowland, "Preliminary notice of results accomplished on the manufacture and theory of gratings for optical purposes," *Phil. Mag. Suppl.* **13**, 469-474 (1882); H. A. Rowland, "On Mr. Glazebrook's Paper on the aberration of concave gratings", *Philos. Mag.* **16**, 210 (1883); G. R. Harrison and E. G. Loewen, "Ruled gratings and wavelength tables," *Appl. Opt.* **15**, 1744-1747 (1976).

invented the concave grating, a device of spectacular value to modern spectroscopists. He continued to rule gratings until his death in 1901.

After Rowland's great success, many people set out to rule diffraction gratings. The few who were successful sharpened the scientific demand for gratings. As the advantages of gratings over prisms and interferometers for spectroscopic work became more apparent, the demand for diffraction gratings far exceeded the supply.

### **1.3. HISTORY OF RICHARDSON GRATINGS**

In 1947, the Bausch & Lomb Optical Company decided to make precision gratings available commercially. In 1950, through the encouragement of Prof. George R. Harrison of MIT, David Richardson and Robert Wiley of Bausch & Lomb succeeded in producing their first high-quality ruled master grating. This grating was ruled on a rebuilt engine that had its origins in the University of Chicago laboratory of Prof. Albert A. Michelson, the first American to be awarded a Nobel Prize in Physics (in 1907) for "his optical precision instruments and the spectroscopic and metrological investigations carried out with their aid."<sup>6</sup> A high-fidelity replication process was subsequently developed, which was crucial to making *replicas*, duplicates of the painstakingly-ruled master gratings.

Over four decades, Bausch & Lomb created hundreds of unique master gratings, covering of very wide range of sizes, groove spacings and groove profiles. In particular, the control of groove shape (or blazing) has increased spectral efficiency dramatically since the early days of grating manufacture. Interferometric and servo control systems made it possible to break through the accuracy barrier previously set by the mechanical constraints inherent in the ruling engines.<sup>7</sup>

In 1985, Milton Roy Company acquired Bausch & Lomb's gratings and spectrometer operations, which it sold in 1995 to Life Sciences International plc as part of Spectronic Instruments, Inc. At this time, the gratings operations took the name Richardson Grating Laboratory. In 1997, Spectronic Instruments was acquired by Thermo Electron Corporation (now Thermo Fisher Scientific), and a few years later the gratings operation was renamed Thermo RGL for a time before being

---

<sup>6</sup> "The Nobel Prize in Physics 1907," nobelprize.org.

<sup>7</sup> G. R. Harrison and G. W. Stroke, "Interferometric control of grating ruling with continuous carriage advance," *J. Opt. Soc. Am.* **45**, 112-121 (1955).

transferred to Thermo Electron's subsidiary, Spectra-Physics. In 2004, Spectra-Physics was acquired by Newport Corporation.

Newport was acquired by MKS Instruments, Inc., a global provider of instruments, subsystems and process control solutions that measure, monitor, deliver, analyze, power and control critical parameters of advanced manufacturing processes to improve process performance and productivity. MKS' products are derived from its core competencies in pressure measurement and control, flow measurement and control, gas and vapor delivery, gas composition analysis, residual gas analysis, leak detection, control technology, ozone generation and delivery, power, reactive gas generation, vacuum technology, lasers, photonics, sub-micron positioning, vibration control, optics, and laser-based manufacturing solutions. MKS also provide services relating to the maintenance and repair of our products, installation services and training. Its primary served markets include semiconductor, industrial technologies, life and health sciences, research and defense.

During these changes, Richardson Gratings has continued to uphold the traditions of precision and quality established by Bausch & Lomb over seventy years ago.

#### **1.4. DIFFRACTION GRATINGS FROM RICHARDSON GRATINGS**

MKS' Richardson Gratings occupies two manufacturing facilities in Rochester, New York, USA. These facilities contain the ruling engines and the holographic recording chambers, which are used for making master gratings, as well as the replication and associated testing and inspection facilities for manufacturing replicated gratings in commercial quantities. In order to reduce risk, we qualify the manufacture and testing of the gratings we produce for our OEM (original equipment manufacturer) customers in both facilities.

To achieve the high spectral resolution characteristic of high-quality gratings, a precision of better than 1 nm in the spacing of the grooves must be maintained. For ruled gratings, such high precision requires extraordinary control over temperature fluctuation and vibration in the ruling engine environments. This control has been established by the construction of specially-designed ruling cells that provide environments in which temperature stability is maintained at  $\pm 0.01$  °C for weeks at a time, as well as vibration isolation that suppresses ruling engine displacement to less than 0.025  $\mu\text{m}$ . The ruling cells can maintain

reliable control over the important environmental factors for periods of several weeks, the time required to rule large, finely-spaced gratings.

In addition to burnishing gratings with a diamond tool, an optical interference pattern can be used to produce holographic gratings. The creation of master holographic gratings requires a very high degree of stability of the recording optical system to obtain the best contrast and fringe structure, which in turn provides the correct groove pattern and groove profile. MKS produces holographic gratings in its dedicated recording facilities, in whose controlled environment thermal gradients and air currents are minimized and fine particulates are filtered from the air. These master holographic gratings are replicated in a process identical to that for ruled master gratings.

## 2. THE PROPERTIES OF DIFFRACTION GRATINGS

### 2.1. THE GRATING EQUATION

When monochromatic light is incident on a grating surface, it is diffracted into discrete directions. We can picture each grating groove as being a very small, slit-shaped source of diffracted light. The light diffracted by each groove combines to form a set of diffracted wavefronts. The usefulness of a grating depends on the fact that there exists a unique set of discrete angles along which, for a given spacing  $d$  between grooves, the diffracted light from each facet is in phase with the light diffracted from any other facet, leading to constructive interference.

Diffraction by a grating can be visualized from the geometry in Figure 2-1, which shows a light ray of wavelength  $\lambda$  incident at an angle  $\alpha$  and diffracted by a grating (of *groove spacing*  $d$ , also called the *pitch*) along a set of angles  $\{\beta_m\}$ . These angles are measured from the grating normal, which is shown as the dashed line perpendicular to the grating surface at its center. The sign convention for these angles depends on whether the light is diffracted on the same side or the opposite side of the grating as the incident light. In diagram (a), which shows a *reflection grating*, the angles  $\alpha > 0$  and  $\beta_1 > 0$  (since they are measured counter-clockwise from the grating normal) while the angles  $\beta_0 < 0$  and  $\beta_{-1} < 0$  (since they are measured clockwise from the grating normal). Diagram (b) shows the case for a *transmission grating*. In both cases, the sign conventions are such that, for the  $m = 0$  order,  $\beta_0 = -\alpha$ .

By convention, angles of incidence and diffraction are measured *from* the grating normal *to* the beam. This is shown by arrows in the diagrams. In both diagrams, the sign convention for angles is shown by the plus and minus symbols located on either side of the grating normal. For either reflection or transmission gratings, the algebraic signs of two angles differ if they are measured from opposite sides of the grating normal. Other sign conventions exist, so care must be taken in calculations to ensure that results are self-consistent.

Another illustration of grating diffraction, using wavefronts (surfaces of constant phase), is shown in Figure 2-2. The geometrical path difference between light from adjacent grooves is seen to be  $d \sin\alpha + d \sin\beta$ .

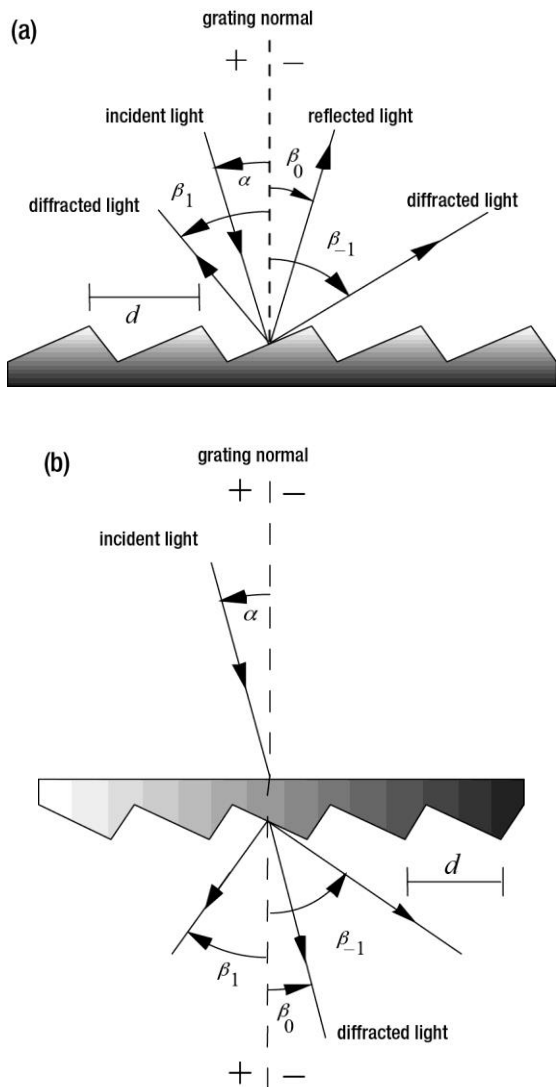


*Figure 2-1. Diffraction by a plane grating.* A beam of monochromatic light of wavelength  $\lambda$  is incident on a grating and diffracted along several discrete paths. The triangular grooves come out of the page; the rays lie in the plane of the page. The sign convention for the angles  $\alpha$  and  $\beta$  is shown by the + and - signs on either side of the grating normal. (a) A *reflection grating*: the incident and diffracted rays lie on the same side of the grating. (b) A *transmission grating*: the diffracted rays lie on the opposite side of the grating from the incident ray.

[Since  $\beta < 0$ , the term  $d \sin \beta$  is negative.] The principle of constructive interference dictates that only when this difference equals the wavelength  $\lambda$  of the light, or some integral multiple thereof, will the light from adjacent grooves be in phase (leading to constructive interference). At all other angles, the Huygens wavelets originating from the groove facets will interfere destructively.

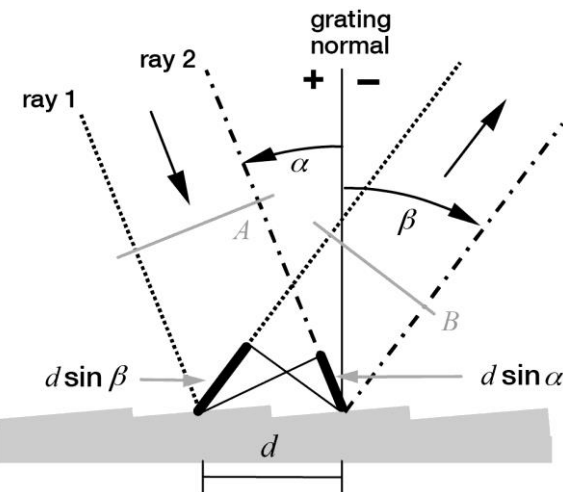


*Figure 2-2. Geometry of diffraction, showing planar wavefronts.* Two parallel rays, labeled 1 and 2, are incident on the grating one groove spacing  $d$  apart and are in phase with each other at wavefront A. Upon diffraction, the principle of constructive interference implies that these rays are in phase at diffracted wavefront B if the difference in their path lengths,  $d \sin \alpha + d \sin \beta$ , is an integral number of wavelengths; this in turn leads to the grating equation. [Huygens wavelets not shown.]

These relationships are expressed by the *grating equation*

$$m\lambda = d(\sin \alpha + \sin \beta), \quad (2-1)$$

which governs the angular locations of the principal intensity maxima when light of wavelength  $\lambda$  is diffracted from a grating of groove spacing  $d$ . Here  $m$  is the *diffraction order* (or *spectral order*), which is an integer. For a particular wavelength  $\lambda$ , all values of  $m$  for which  $|m\lambda/d| < 2$  correspond to propagating (rather than evanescent) diffraction orders. The special case  $m = 0$  leads to the law of reflection  $\beta = -\alpha$ .

It is sometimes convenient to write the *grating equation* as

$$Gm\lambda = \sin \alpha + \sin \beta, \quad (2-2)$$

where  $G = 1/d$  is the *groove frequency* or *groove density*, more commonly called "grooves per millimeter".

Eq. (2-1) and its equivalent Eq. (2-2) are the common forms of the grating equation, but their validity is restricted to cases in which the incident and diffracted rays lie in a plane which is perpendicular to the grooves (at the center of the grating). Most grating systems fall within this category, which is called *classical* (or *in-plane*) *diffraction*. If the incident light beam is not perpendicular to the grooves, though, the grating equation must be modified:

$$Gm\lambda = \cos\varepsilon (\sin\alpha + \sin\beta). \quad (2-3)$$

Here  $\varepsilon$  is the angle between the incident light path and the plane perpendicular to the grooves at the grating center (the plane of the page in Figure 2-2). If the incident light lies in this plane,  $\varepsilon = 0$  and Eq. (2-3) reduces to the more familiar Eq. (2-2). In geometries for which  $\varepsilon \neq 0$ , the diffracted spectra lie on a cone rather than in a plane, so such cases are termed *conical diffraction*.

For a grating of groove spacing  $d$ , there is a purely mathematical relationship between the wavelength and the angles of incidence and diffraction. In a given spectral order  $m$ , the different wavelengths of polychromatic wavefronts incident at angle  $\alpha$  are separated in angle:

$$\beta(\lambda) = \sin^{-1} \left( \frac{m\lambda}{d} - \sin\alpha \right). \quad (2-4)$$

When  $m = 0$ , the grating acts as a mirror, and the wavelengths are not separated ( $\beta = -\alpha$  for all  $\lambda$ ); this is called *specular reflection* or simply the *zero order*.

A special but common case is that in which the light is diffracted back toward the direction from which it came (*i.e.*,  $\alpha = \beta$ ); this is called the *Littrow configuration*, for which the grating equation becomes

$$m\lambda = 2d \sin\alpha, \quad \text{in Littrow.} \quad (2-5)$$

In many applications a constant-deviation monochromator mount is used, in which the wavelength  $\lambda$  is changed by rotating the grating about the axis coincident with its central ruling, with the directions of incident and diffracted light remaining unchanged. The *deviation angle*  $2K$  between the incidence and diffraction directions (also called the *angular deviation*) is

$$2K = \alpha - \beta = \text{constant}, \quad (2-6)$$

while the *scan angle*  $\phi$ , which varies with  $\lambda$  and is measured from the grating normal to the bisector of the beams, is

$$2\phi = \alpha + \beta. \quad (2-7)$$

Note that  $\phi$  changes with  $\lambda$  (as do  $\alpha$  and  $\beta$ ). In this case, the grating equation can be expressed in terms of  $\phi$  and the *half deviation angle*  $K$  as

$$m\lambda = 2d \cos K \sin \phi. \quad (2-8)$$

Here  $K$  is called the half deviation angle because the angle between the incident and diffracted beams is  $2K$ . This version of the grating equation is useful for monochromator mounts (see Chapter 7). Eq. (2-8) shows that the wavelength diffracted by a grating in a monochromator mount is directly proportional to the sine of the scan angle  $\phi$  through which the grating rotates, which is the basis for monochromator drives in which a *sine bar* rotates the grating to scan wavelengths (see Figure 2-3).

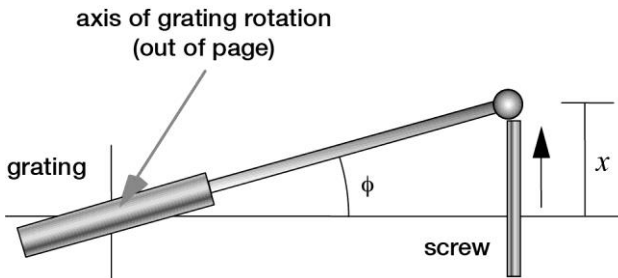


Figure 2-3. A sine bar mechanism for wavelength scanning. As the screw is extended linearly by the distance  $x$  shown, the grating rotates through an angle  $\phi$  in such a way that  $\sin \phi$  is proportional to  $x$ .

For the constant-deviation monochromator mount, the incidence and diffraction angles can be expressed simply in terms of the scan angle  $\phi$  and the half-deviation angle  $K$  via

$$\alpha(\lambda) = \phi(\lambda) + K \quad (2-9)$$

and

$$\beta(\lambda) = \phi(\lambda) - K, \quad (2-10)$$

where we show explicitly that  $\alpha$ ,  $\beta$  and  $\phi$  depend on the wavelength  $\lambda$ .

## 2.2. DIFFRACTION ORDERS

Generally, several integers  $m$  will satisfy the grating equation – we call each of these values a *diffraction order*.

### 2.2.1. Existence of diffraction orders

For a particular groove spacing  $d$ , wavelength  $\lambda$  and incidence angle  $\alpha$ , the grating equation (2-1) is generally satisfied by more than one diffraction angle  $\beta$ . In fact, subject to restrictions discussed below, there will be several discrete angles at which the condition for constructive interference is satisfied. The physical significance of this is that the constructive reinforcement of wavelets diffracted by successive grooves merely requires that each ray be retarded (or advanced) in phase with every other; this phase difference must therefore correspond to a real distance (path difference) which equals an integral multiple of the wavelength. This happens, for example, when the path difference is one wavelength, in which case we speak of the positive first diffraction order ( $m = 1$ ) or the negative first diffraction order ( $m = -1$ ), depending on whether the rays are advanced or retarded as we move from groove to groove. Similarly, the second order ( $m = 2$ ) and negative second order ( $m = -2$ ) are those for which the path difference between rays diffracted from adjacent grooves equals two wavelengths.

The grating equation reveals that only those spectral orders for which  $|m\lambda/d| < 2$  can exist; otherwise,  $|\sin\alpha + \sin\beta| > 2$ , which is physically meaningless. This restriction prevents light of wavelength  $\lambda$  from being diffracted in more than a finite number of orders. Specular reflection, for which  $m = 0$ , is always possible; that is, the *zero order* always exists (it simply requires  $\beta = -\alpha$ ). In most cases, the grating equation allows light of wavelength  $\lambda$  to be diffracted into both negative and positive orders as well. Explicitly, spectra of all orders  $m$  exist for which

$$-2d < m\lambda < 2d, \quad m \text{ an integer.} \quad (2-11)$$

For  $\lambda/d \ll 1$ , a large number of diffracted orders will exist.

As seen from Eq. (2-1), the distinction between negative and positive spectral orders is that

$$\begin{aligned} \beta &> -\alpha && \text{for positive orders } (m > 0), \\ \beta &< -\alpha && \text{for negative orders } (m < 0), \text{ and} \\ \beta &= -\alpha && \text{for specular reflection } (m = 0). \end{aligned} \quad (2-12)$$

This sign convention requires that  $m > 0$  if the diffracted ray lies to the left (the counter-clockwise side) of the zero order ( $m = 0$ ), and  $m < 0$  if the diffracted ray lies to the right (the clockwise side) of the zero order. This convention is shown graphically in Figure 2-4.

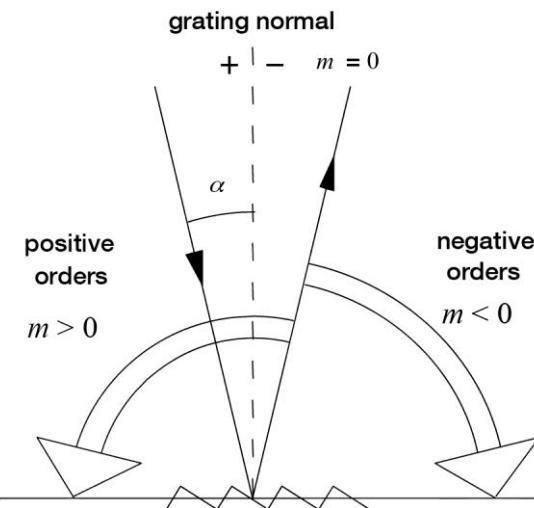
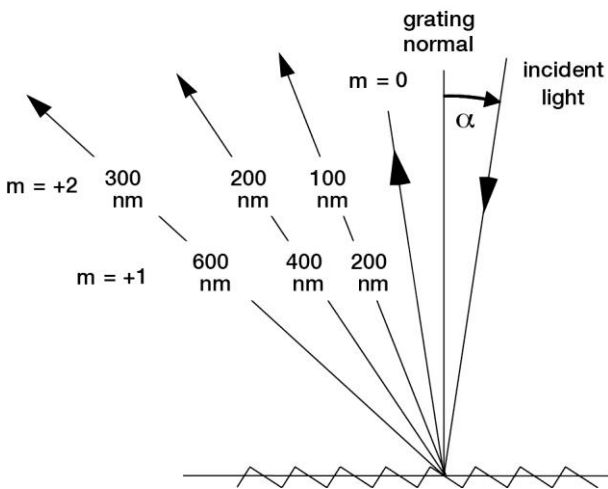


Figure 2-4. Sign convention for the spectral order  $m$ . In this example  $\alpha$  is positive.

### 2.2.2. Overlapping of diffracted spectra

The most troublesome aspect of multiple order behavior is that successive spectra overlap, as shown in Figure 2-5. It is evident from the grating equation that light of wavelength  $\lambda$  diffracted by a grating along direction  $\beta$  will be accompanied by integral fractions  $\lambda/2, \lambda/3, etc.$ ; that is, for any grating instrument configuration, the light of wavelength  $\lambda$  diffracted in the  $m = 1$  order will coincide with the light of wavelength  $\lambda/2$  diffracted in the  $m = 2$  order, *etc.* In this example, the red light (600 nm) in the first spectral order will overlap the ultraviolet light (300 nm) in the second order. A detector sensitive at both wavelengths would see both simultaneously. This superposition of wavelengths, which would lead to ambiguous spectroscopic data, is inherent in the grating equation itself and must be prevented by suitable filtering (called *order sorting*), since the detector cannot generally distinguish between light of different wavelengths incident on it (within its range of sensitivity). [See also Section 2.7 below.]



*Figure 2-5. Overlapping of spectral orders.* The light for wavelengths 100, 200 and 300 nm in the 2<sup>nd</sup> order is diffracted in the same direction as the light for wavelengths 200, 400 and 600 nm in the 1<sup>st</sup> order. In this diagram, light is incident from the right, so  $\alpha < 0$ .

## 2.3. DISPERSION

The primary purpose of a diffraction grating is to disperse light spatially by wavelength. A beam of white light incident on a grating will be separated into its component wavelengths upon diffraction from the grating, with each wavelength diffracted along a different direction. *Dispersion* is a measure of the separation (either angular or spatial) between diffracted light of different wavelengths. Angular dispersion expresses the spectral range per unit angle, and linear resolution expresses the spectral range per unit length.

### 2.3.1. Angular dispersion

The angular spread  $\Delta\beta$  of a spectrum of order  $m$  between the wavelength  $\lambda$  and  $\lambda + \Delta\lambda$  can be obtained by differentiating the grating equation, assuming the incidence angle  $\alpha$  to be constant. The change  $D$  in diffraction angle per unit wavelength is therefore

$$D = \frac{d\beta}{d\lambda} = \frac{m}{d \cos \beta} = \frac{m}{d} \sec \beta = Gm \sec \beta, \quad (2-13)$$

where  $\beta$  is given by Eq. (2-4). The quantity  $D$  is called the *angular dispersion*. As the groove frequency  $G = 1/d$  increases, the angular

dispersion increases (meaning that the angular separation between wavelengths increases for a given order  $m$ ).

In Eq. (2-13), it is important to realize that the quantity  $m/d$  is not a ratio which may be chosen independently of other parameters; substitution of the grating equation into Eq. (2-13) yields the following general equation for the angular dispersion:

$$D = \frac{d\beta}{d\lambda} = \frac{\sin \alpha + \sin \beta}{\lambda \cos \beta}. \quad (2-14)$$

For a given wavelength, this shows that the angular dispersion may be considered to be solely a function of the angles of incidence and diffraction. This becomes even more clear when we consider the Littrow configuration ( $\alpha = \beta$ ), in which case Eq. (2-14) reduces to

$$D = \frac{d\beta}{d\lambda} = \frac{2}{\lambda} \tan \beta, \quad \text{in Littrow.} \quad (2-15)$$

When  $|\beta|$  increases from  $10^\circ$  to  $63^\circ$  in Littrow use, the angular dispersion can be seen from Eq. (2-15) to increase by a factor of ten, regardless of the spectral order or wavelength under consideration. Once the diffraction angle  $\beta$  has been determined, the choice must be made whether a fine-pitch grating (small  $d$ ) should be used in a low diffraction order, or a coarse-pitch grating (large  $d$ ) such as an echelle grating (see Section 12.5) should be used in a high order. [The fine-pitched grating, though, will provide a larger free spectral range; see Section 2.7 below.]

### 2.3.2. Linear dispersion

For a given diffracted wavelength  $\lambda$  in order  $m$  (which corresponds to an angle of diffraction  $\beta$ ), the *linear dispersion* of a grating system is the product of the angular dispersion  $D$  and the effective focal length  $r'(\beta)$  of the system:

$$r'D = r' \frac{d\beta}{d\lambda} = \frac{mr'}{d \cos \beta} = \frac{mr'}{d} \sec \beta = Gmr' \sec \beta. \quad (2-16)$$

The quantity  $r'\Delta\beta = \Delta l$  is the change in position along the spectrum (a real distance, rather than a wavelength). We have written  $r'(\beta)$  for the focal length to show explicitly that it may depend on the diffraction angle  $\beta$  (which, in turn, depends on  $\lambda$ ).

The *reciprocal linear dispersion*, formerly called the *plate factor*  $P$ , is more often considered; it is simply the reciprocal of  $r'D$ ,

$$P = \frac{d \cos \beta}{mr'}, \quad (2-17)$$

usually measured in nm/mm (where  $d$  is expressed in nm and  $r'$  is expressed in mm). The quantity  $P$  is a measure of the change in wavelength (in nm) corresponding to a change in location along the spectrum (in mm). [It should be noted that the terminology *plate factor* is used by some authors to represent the quantity  $1/\sin \phi$ , where  $\phi$  is the angle the spectrum makes with the line perpendicular to the diffracted rays (see Figure 2-6); in order to avoid confusion, we call the quantity  $1/\sin \phi$  the *obliquity factor*.] When the image plane for a particular wavelength is not perpendicular to the diffracted rays (*i.e.*, when  $\phi \neq 90^\circ$ ),  $P$  must be multiplied by the obliquity factor to obtain the correct reciprocal linear dispersion in the image plane.

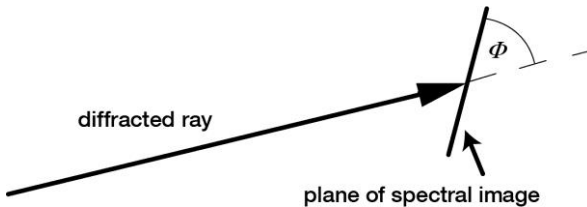


*Figure 2-6. The obliquity angle  $\phi$ . The spectral image recorded need not lie in the plane perpendicular to the diffracted ray (*i.e.*,  $\phi \neq 90^\circ$ ).*

## 2.4. RESOLVING POWER, SPECTRAL RESOLUTION, AND SPECTRAL BANDPASS

### 2.4.1. Resolving power

The *resolving power*  $R$  of a grating is a measure of its ability to separate adjacent spectral lines of average wavelength  $\lambda$ . It is usually expressed as the dimensionless quantity

$$R = \frac{\lambda}{\Delta\lambda}. \quad (2-18)$$

Here  $\Delta\lambda$  is the *limit of resolution*, the difference in wavelength between two lines of equal intensity that can be distinguished (that is, the peaks of two wavelengths  $\lambda_1$  and  $\lambda_2$  for which the separation  $|\lambda_1 - \lambda_2| < \Delta\lambda$  will be

ambiguous). Often the *Rayleigh criterion* is used to determine  $\Delta\lambda$  – that is, the intensity maxima of two neighboring wavelengths are resolvable (*i.e.*, identifiable as distinct spectral lines) if the intensity maximum of one wavelength coincides with the intensity minimum of the other wavelength.<sup>8</sup>

The theoretical resolving power of a planar diffraction grating is given in elementary optics textbooks as

$$R = mN, \quad (2-19)$$

where  $m$  is the diffraction order and  $N$  is the total number of grooves illuminated on the surface of the grating. For negative orders ( $m < 0$ ), the absolute value of  $R$  is considered.

A more meaningful expression for  $R$  is derived below. The grating equation can be used to replace  $m$  in Eq. (2-19):

$$R = \frac{Nd(\sin \alpha + \sin \beta)}{\lambda}. \quad (2-20)$$

If the groove spacing  $d$  is uniform over the surface of the grating, and if the grating substrate is planar, the quantity  $Nd$  is simply the ruled width  $W$  of the grating, so

$$R = \frac{W(\sin \alpha + \sin \beta)}{\lambda}. \quad (2-21)$$

As expressed by Eq. (2-21),  $R$  is not dependent explicitly on the spectral order or the number of grooves; these parameters are contained within the ruled width and the angles of incidence and diffraction. Since

$$|\sin \alpha + \sin \beta| < 2, \quad (2-22)$$

the maximum attainable resolving power is

$$R_{\text{MAX}} = \frac{2W}{\lambda}, \quad (2-23)$$

regardless of the order  $m$  or number of grooves  $N$  under illumination. This maximum condition corresponds to the grazing Littrow configuration, *i.e.*,  $|\alpha| \approx 90^\circ$  (grazing incidence) and  $\alpha \approx \beta$  (Littrow).

It is useful to consider the resolving power as being determined by the maximum phase retardation of the extreme rays diffracted from the

<sup>8</sup> D. W. Ball, *The Basics of Spectroscopy*, SPIE Press (2001), ch. 8.

grating.<sup>9</sup> Measuring the difference in optical path lengths between the rays diffracted from opposite sides of the grating provides the maximum phase retardation; dividing this quantity by the wavelength  $\lambda$  of the diffracted light gives the resolving power  $R$ .

The degree to which the theoretical resolving power is attained depends not only on the angles  $\alpha$  and  $\beta$ , but also on the optical quality of the grating surface, the uniformity of the groove spacing, the quality of the associated optics in the system, and the width of the slits (or detector elements). Any departure of the diffracted wavefront greater than  $\lambda/10$  from a plane (for a plane grating) or from a sphere (for a spherical grating) will result in a loss of resolving power due to aberrations at the image plane. The grating groove spacing must be kept constant to within about one percent of the wavelength at which theoretical performance is desired. Experimental details, such as slit width, air currents, and vibrations can seriously interfere with obtaining optimal results.

The practical resolving power of a diffraction grating is limited by the spectral width of the spectral lines emitted by the source. For this reason, systems with revolving powers greater than  $R = 500,000$  are not usually required except for the study of spectral line shapes, Zeeman effects, and line shifts, and are not needed for separating individual spectral lines.

A convenient test of resolving power is to examine the isotopic structure of the mercury emission line at  $\lambda = 546.1$  nm (see Section 11.4). Another test for resolving power is to examine the line profile generated in a spectrograph or scanning spectrometer when a single mode laser is used as the light source. The *full width at half maximum intensity* (FWHM) can be used as the criterion for  $\Delta\lambda$ . Unfortunately, resolving power measurements are the convoluted result of all optical elements in the system, including the locations and dimensions of the entrance and exit slits and the auxiliary lenses and mirrors, as well as the quality of these elements. Their effects on resolving power measurements are necessarily superimposed on those of the grating.

#### 2.4.2. Spectral resolution

While resolving power can be considered a characteristic of the grating and the angles at which it is used, the ability to resolve two wavelengths  $\lambda_1$  and  $\lambda_2 = \lambda_1 + \Delta\lambda$  generally depends not only on the

---

<sup>9</sup> N. Abramson, "Principle of least wave change," *J. Opt. Soc. Am.* **A6**, 627-629 (1989).

grating but on the dimensions and locations of the entrance and exit slits (or detector elements), the aberrations in the images, and the magnification of the images. The minimum wavelength difference  $\Delta\lambda$  (also called the *limit of resolution*, *spectral resolution* or simply *resolution*) between two wavelengths that can be resolved unambiguously can be determined by convoluting the image of the entrance aperture (at the image plane) with the exit aperture (or detector element). This measure of the ability of a grating system to resolve nearby wavelengths is arguably more relevant than is resolving power, since it considers the imaging effects of the system. While resolving power is a dimensionless quantity, resolution has spectral units (usually nanometers).

### 2.4.3. Spectral Bandpass

The (*spectral*) *bandpass*  $B$  of a spectroscopic system is the range of wavelengths of the light that passes through the exit slit (or falls onto a detector element). It is often defined as the difference in wavelengths between the points of half-maximum intensity on either side of an intensity maximum. Bandpass is a property of the spectroscopic system, not of the diffraction grating itself.

For a system in which the width of the image of the entrance slit is roughly equal to the width of the exit slit, an estimate for bandpass is the product of the exit slit width  $w'$  and the reciprocal linear dispersion  $P$ :

$$B \approx w' P. \quad (2-24)$$

An instrument with smaller bandpass can resolve wavelengths that are closer together than an instrument with a larger bandpass. The spectral bandpass of an instrument can be reduced by decreasing the width of the exit slit (down to a certain limit; see Chapter 8), but usually at the expense of decreasing light intensity as well.

See Section 8.3 for additional comments on instrumental bandpass.

### 2.4.4. Resolving power vs. resolution

In the literature, the terms *resolving power* and *resolution* are sometimes interchanged. While the word *power* has a very specific meaning (energy per unit time), the phrase *resolving power* does not involve *power* in this way; as suggested by Hutley, though, we may think of resolving power as “ability to resolve”.<sup>10</sup>

---

<sup>10</sup> M. C. Hutley, *Diffraction Gratings*, Academic Press (New York, New York: 1982), p. 29.

The comments above regarding resolving power and resolution pertain to planar classical gratings used in collimated light (plane waves). The situation is complicated for gratings on concave substrates or with groove patterns consisting of unequally spaced lines, which restrict the usefulness of the previously defined simple formulas, though they may still yield useful approximations. Even in these cases, though, the concept of maximum retardation is still a useful measure of the resolving power, and the convolution of the image and the exit slit is still a useful measure of resolution.

## 2.5. FOCAL LENGTH AND $f$ /NUMBER

For gratings (or grating systems) that image as well as diffract light, or disperse light that is not collimated, a *focal length* may be defined. If the beam diffracted from a grating of a given wavelength  $\lambda$  and order  $m$  converges to a focus, then the distance between this focus and the grating center is the focal length  $r'(\lambda)$ . [If the diffracted light is collimated, and then focused by a mirror or lens, the focal length is that of the refocusing mirror or lens and not the distance to the grating.] If the diffracted light is diverging, the focal length may still be defined, although by convention we take it to be negative (indicating that there is a virtual image behind the grating). Similarly, the incident light may diverge toward the grating (so we define the incidence or entrance slit distance  $r(\lambda) > 0$ ) or it may converge toward a focus behind the grating (for which  $r(\lambda) < 0$ ). Usually gratings are used in configurations for which  $r$  does not depend on wavelength (though the focal length  $r'$  usually depends on  $\lambda$ ).

In Figure 2-7, a typical concave grating configuration is shown; the monochromatic incident light (of wavelength  $\lambda$ ) diverges from a point source at A and is diffracted toward B. Points A and B are distances  $r$  and  $r'$ , respectively, from the grating center O. In this figure, both  $r$  and  $r'$  are positive.

Calling the width (or diameter) of the grating (in the dispersion plane)  $W$  allows the *input* and *output f/numbers* (also called *focal ratios*) to be defined:

$$f/\text{no}_{\text{INPUT}} = \frac{r}{W}, \quad f/\text{no}_{\text{OUTPUT}} = \frac{r'(\lambda)}{W}. \quad (2-25)$$

Usually the input  $f$ /number is matched to the  $f$ /number of the light cone leaving the entrance optics (*e.g.*, an entrance slit or fiber) to use as much of the grating surface for diffraction as possible. This increases the

amount of diffracted energy while not overfilling the grating (which would generally contribute to instrumental stray light; see Chapter 10).

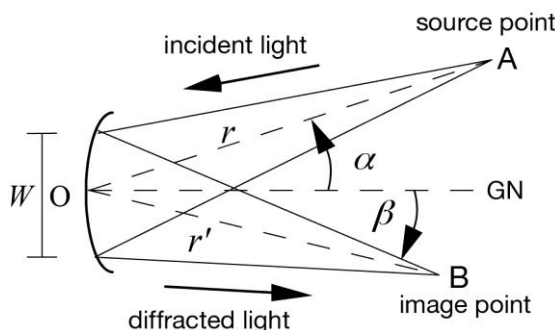


*Figure 2-7. Geometry for focal distances and focal ratios ( $f/\text{numbers}$ ). GN is the grating normal (perpendicular to the grating at its center, O),  $W$  is the width of the grating (its dimension perpendicular to the groove direction, which is out of the page), and A and B are the source and image points, respectively.*

For oblique (non-normal) incidence or diffraction, Eqs. (2-25) are often modified by replacing  $W$  with the projected width of the grating:

$$f/\text{no}_{\text{INPUT}} = \frac{r}{W \cos \alpha}, \quad f/\text{no}_{\text{OUTPUT}} = \frac{r'(\lambda)}{W \cos \beta}. \quad (2-26)$$

These equations account for the reduced width of the grating as seen by the entrance and exit slits; moving toward oblique angles (*i.e.*, increasing  $|\alpha|$  or  $|\beta|$ ) decreases the projected width and therefore increases the  $f/\text{number}$ .

The focal length is an important parameter in the design and specification of grating spectrometers, since it governs the overall size of the optical system (unless folding mirrors are used). The ratio between the input and output focal lengths determines the projected width of the entrance slit that must be matched to the exit slit width or detector element size. The  $f/\text{number}$  is also important, as it is generally true that spectral aberrations decrease as  $f/\text{number}$  increases. Unfortunately, increasing the input  $f/\text{number}$  results in the grating subtending a smaller solid angle as seen from the entrance slit; this will reduce the amount of light energy the grating collects and consequently reduce the intensity of the diffracted beams. This trade-off prohibits the formulation of a simple rule for choosing the input and output  $f/\text{numbers}$ , so sophisticated

design procedures have been developed to minimize aberrations while maximizing collected energy. See Chapters 7 and 8 for a discussion of the imaging properties and Chapter 9 for a description of the efficiency characteristics of grating systems.

## 2.6. ANAMORPHIC MAGNIFICATION

For a given wavelength  $\lambda$ , we may consider the ratio of the width of a collimated diffracted beam to that of a collimated incident beam to be a measure of the effective magnification of the grating (see Figure 2-8). From this figure we see that this ratio is

$$\frac{b}{a} = \frac{\cos \beta}{\cos \alpha}. \quad (2-27)$$

Since  $\alpha$  and  $\beta$  depend on  $\lambda$  through the grating equation (2-1), this magnification will vary with wavelength. The ratio  $b/a$  is called the *anamorphic magnification*; for a given wavelength  $\lambda$ , it depends only on the angular configuration in which the grating is used.

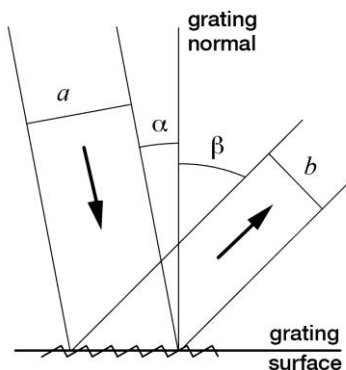


Figure 2-8. Anamorphic magnification. The ratio  $b/a$  of the beam widths equals the anamorphic magnification; from the grating equation (2-1) we see that this ratio will not equal unity unless  $m = 0$  (specular reflection) or  $\alpha = \beta$  (the Littrow configuration).

The magnification of an object not located at infinity (so that the incident rays are not collimated) is discussed in Chapter 8.

## 2.7. FREE SPECTRAL RANGE

For a given set of incidence angle  $\alpha$  and diffraction angle  $\beta$ , the grating equation is satisfied for a different wavelength  $\lambda$  for each integral diffraction order  $m$ . Thus, light of several wavelengths (each in a different order) will be diffracted along the same direction: light of wavelength  $\lambda$  in order  $m$  is diffracted along the same direction as light of wavelength  $\lambda/2$  in order  $2m$ , etc.

The range of wavelengths in a given spectral order for which superposition of light from adjacent orders does not occur is called the *free spectral range*  $F_\lambda$ . It can be calculated directly from its definition: in order  $m$ , the wavelength of light that diffracts along the direction of  $\lambda$  in order  $m+1$  is  $\lambda + \Delta\lambda$ , where

$$\lambda + \Delta\lambda = \frac{m+1}{m} \lambda, \quad (2-28)$$

from which

$$F_\lambda = \Delta\lambda = \frac{\lambda}{m}. \quad (2-29)$$

The concept of free spectral range applies to all gratings capable of operation in more than one diffraction order, but it is particularly important in the case of echelles, because they operate in high orders with correspondingly short free spectral ranges.

Free spectral range and order sorting are intimately related, since grating systems with greater free spectral ranges may have less need for filters (or cross-dispersers) that absorb or diffract light from overlapping spectral orders. This is one reason why first-order applications are widely popular.

## 2.8. ENERGY DISTRIBUTION (GRATING EFFICIENCY)

The distribution of light energy of a given wavelength diffracted by a grating into the various spectral orders depends on many parameters: the power and polarization of the incident light, the angles of incidence and diffraction, the (complex) index of refraction of the materials at the surface of the grating, the groove spacing and the groove profile. A complete treatment of grating efficiency requires the vector formulation of electromagnetic theory (*i.e.*, Maxwell's equations) applied to corrugated surfaces, which has been studied in detail over the past few

decades. While the theory does not yield conclusions easily, certain rules of thumb can be useful in making approximate predictions.

The simplest and most widely used rule of thumb regarding grating efficiency (for reflection gratings) is the *blaze condition*

$$m\lambda = 2d\sin\theta_B, \quad (2-30)$$

where  $\theta_B$  (often called the *blaze angle* of the grating) is the angle between the face of the groove and the plane of the grating (see Figure 2-9). When the blaze condition is satisfied, the incident and diffracted rays follow the law of reflection when viewed from the facet; that is, we have

$$\alpha - \theta_B = \beta - \theta_B. \quad (2-31)$$

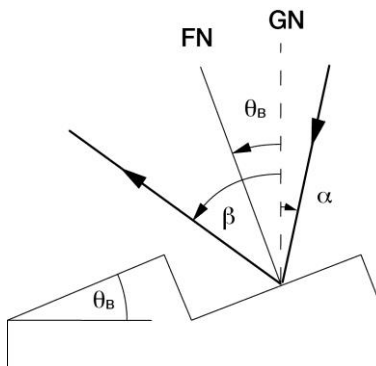


Figure 2-9. *Blaze condition.* The angles of incidence  $\alpha$  and diffraction  $\beta$  are shown in relation to the facet angle  $\theta_B$  for the blaze condition. GN is the grating normal and FN is the facet normal. When the facet normal bisects the angle between the incident and diffracted rays, the blaze condition (Eq. (2-30)) is satisfied.

Because of this relationship, it is often said that when a grating is used at the blaze condition, the facets act as tiny mirrors. This is not strictly true; since the dimensions of the facet are often on the order of the wavelength itself, ray optics does not provide an adequate physical model. Nonetheless, this is a useful way to remember the conditions under which a grating can be used to enhance efficiency.

Eq. (2-30) generally leads to the highest efficiency when the following condition is also satisfied:

$$2K = \alpha - \beta = 0, \quad (2-32)$$

where  $2K$  was defined above as the angle between the incident and diffracted beams (see Eq. (2-6)). Eqs. (2-30) and (2-32) collectively define the *Littrow blaze condition*. When Eq. (2-32) is not satisfied (*i.e.*,  $\alpha \neq \beta$  and therefore the grating is not used in the Littrow configuration), efficiency is generally seen to decrease as one moves further off Littrow (*i.e.*, as  $|2K|$  increases).

For a given blaze angle  $\theta_B$ , the Littrow blaze condition provides the *blaze wavelength*  $\lambda_B$ , the wavelength for which the efficiency is maximal when the grating is used in the Littrow configuration:

$$\lambda_B = \frac{2d}{m} \sin \theta_B, \quad \text{in Littrow.} \quad (2-33)$$

Many grating catalogs specify the *first-order Littrow blaze wavelength* for each grating:

$$\lambda_B = 2d \sin \theta_B, \quad \text{in Littrow } (m = 1). \quad (2-34)$$

Unless a diffraction order is specified, quoted values of  $\lambda_B$  are generally assumed to be for the first diffraction order, in Littrow.

The blaze wavelength  $\lambda_B$  in order  $m$  will decrease as the off-Littrow angle  $\alpha - \theta_B$  increases from zero, according to the relation

$$\lambda_B = \frac{2d}{m} \sin \theta_B \cos(\alpha - \theta_B). \quad (2-35)$$

Computer programs are commercially available that accurately predict grating efficiency for a wide variety of groove profiles over wide spectral ranges.

The topic of grating efficiency is addressed more fully in Chapter 9.

## 2.9. SCATTERED LIGHT AND STRAY LIGHT

All light that reaches the detector of a grating-based instrument from anywhere other than the grating, by any means other than diffraction as governed by Eq. (2-1), for any spectral order other than the primary diffraction order of use, is called *instrumental stray light* (or more commonly, simply *stray light*). All components in an optical system contribute to stray light, as will any baffles, apertures, and partially reflecting surfaces. Unwanted light originating from an illuminated grating itself is often called *scattered light* or *grating scatter*.

Instrumental stray light can introduce inaccuracies in the output of an absorption spectrometer used for chemical analysis. These instruments usually employ a “white light” (broad spectrum) light source and a monochromator to isolate a narrow spectral range from the white light spectrum; however, some of the light at other wavelengths will generally reach the detector, which will tend to make an absorbance reading too low (*i.e.*, the sample will seem to be slightly more transmissive than it would in the absence of stray light). In most commercial benchtop spectrometers, such errors are on the order of 0.1 to 1 percent (and can be much lower with proper instrument design) but in certain circumstances (*e.g.*, in Raman spectroscopy), instrumental stray light can lead to significant errors. Grating scatter and instrumental stray light are addressed in more detail in Chapter 10.

## 2.10. SIGNAL-TO-NOISE RATIO (SNR)

The *signal-to-noise ratio* (SNR) is the ratio of diffracted energy to unwanted light energy.\* While we might be tempted to conclude that increasing diffraction efficiency will increase SNR, stray light usually plays the limiting role in the achievable SNR for a grating system.

Instruments using replicated gratings from ruled master gratings can have quite high SNRs. Instruments using holographic gratings sometimes have even higher SNRs, since they have no ghosts<sup>†</sup> due to periodic errors in groove location and lower interorder stray light. Improvements in master ruling technology and coatings has improved the quality of replicated grating from ruled masters so that they may now be used in applications requiring extremely high SNRs, such as Raman spectroscopy.

As SNR is a property of the optical instrument, not of the grating only, there exist no clear rules of thumb regarding what type of grating will provide higher SNR. See Chapter 12 for a discussion of the sources of unwanted optical energy at the detector in a grating system.

---

\* This statement ignores electrical and other non-optical contributions to the noise in the instrument.

<sup>†</sup> Ghosts are false spectral lines due to irregularities in the groove pattern; see Chapter 11 for more detail.

## 3. RULED GRATINGS

### 3.0. INTRODUCTION

The first diffraction gratings made for commercial use were mechanically ruled, manufactured by burnishing grooves individually with a diamond tool against a thin coating of evaporated metal applied to a plane or concave surface. Replicas of such *ruled gratings* are used in many types of lasers, spectroscopic instrumentation and fiber-optic telecommunications equipment.

### 3.1. RULING ENGINES

The most vital component in the production of ruled diffraction gratings is the apparatus, called a *ruling engine*, on which master gratings are ruled. MKS has four ruling engines in operation, each producing a substantial number of high-quality master gratings every year. Each of these engines produces gratings with very low Rowland ghosts, high resolving power, and high efficiency uniformity.

Selected diamonds, whose crystal axis is oriented for optimum behavior, are used to shape the grating grooves. The ruling diamonds are carefully shaped by skilled diamond toolmakers to produce the exact groove profile required for each grating. The carriage that moves the diamond back and forth during ruling must maintain its position to better than a few nanometers for ruling times that may last from one day to several weeks.

The mechanisms for advancing the grating carriages on all MKS ruling are designed to make it possible to rule gratings with a wide choice of groove frequencies. The *Diffraction Grating Catalog* published by MKS lists the range of groove frequencies available.

#### 3.1.1. The Michelson engine

In 1947 Bausch & Lomb acquired its first ruling engine from the University of Chicago; this engine was originally designed by Michelson in the 1910s and rebuilt by Gale. It underwent further refinement, which greatly improved its performance, and has produced a continuous supply of high-quality gratings of up to 200 x 250 mm ruled area.

The Michelson engine originally used an interferometer system to plot the error curve of the lead screw, from which an appropriate me-

chanical correction cam was derived. In 1990, this system was superseded by the addition of a digital computer servo control system based on a laser interferometer. The Michelson engine is unusual in that it covers the widest range of groove frequencies of any ruling engine: it can rule gratings as coarse as 32 grooves per millimeter (g/mm) and as fine as 5,400 g/mm.

### **3.1.2. The Mann engine**

The second ruling engine installed at MKS has been producing gratings since 1953, was originally built by the David W. Mann Co. of Lincoln, Massachusetts. Bausch & Lomb equipped it with an interferometric control system following the technique of Harrison of MIT.<sup>11</sup> The Mann engine can rule areas up to 110 x 110 mm, with virtually no detectable ghosts and nearly theoretical resolving power.

While the lead screws of the ruling engines are lapped to the highest precision attainable, there are always residual errors in both threads and bearings that must be compensated to produce the highest quality gratings. The Mann engine is equipped with an automatic interferometer servo system that continually adjusts the grating carriage to the correct position as each groove is ruled. In effect, the servo system simulates a perfect screw.

### **3.1.3. The MIT 'B' engine**

The third ruling engine at MKS was built by Harrison and moved to Rochester in 1968. It has the capacity to rule plane gratings to the greatest precision ever achieved; these gratings may be up to 420 mm wide, with grooves (between 20 and 1500 per millimeter) up to 320 mm long. It uses a double interferometer control system, based on a frequency-stabilized laser, to monitor not only table position but to correct residual yaw errors as well. This engine produces gratings with nearly theoretical resolving powers, virtually eliminating Rowland ghosts and minimizing stray light. It has also ruled almost perfect echelle gratings, the most demanding application of a ruling engine.

---

<sup>11</sup> G. R. Harrison and J. E. Archer, "Interferometric calibration of precision screws and control of ruling engines," *J. Opt. Soc. Am.* **41**, 495 (1951); G. R. Harrison and G. W. Stroke, "Interferometric control of grating ruling with continuous carriage advance," *J. Soc. Opt. Am.* **45**, 112 (1955); G. R. Harrison, N. Sturgis, S. C. Baker and G. W. Stroke, "Ruling of large diffraction grating with interferometric control", *J. Opt. Soc. Am.* **47**, 15 (1957).

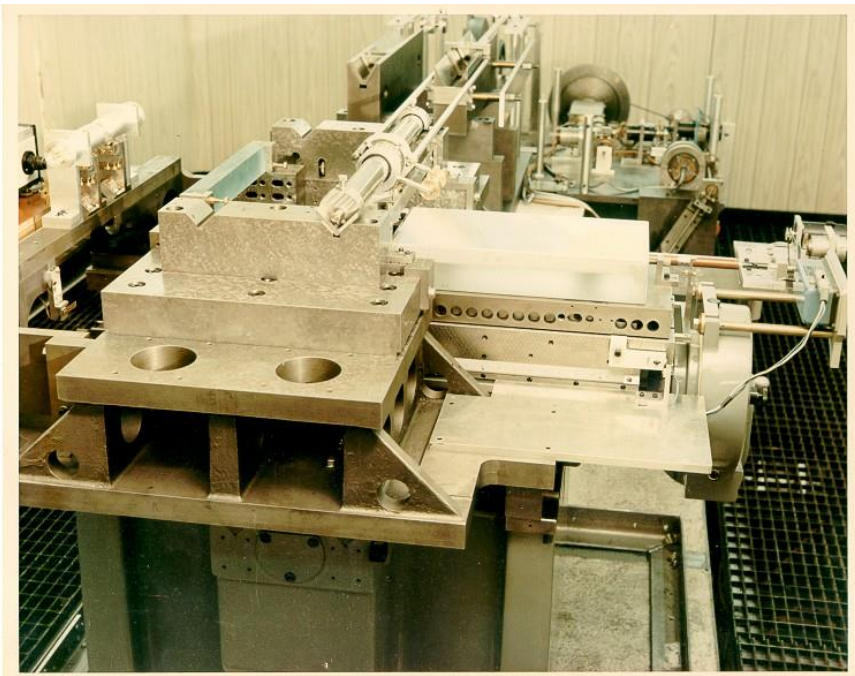


*Figure 3-1. MIT 'B' Engine.* This ruling engine, built by Professor George Harrison of the Massachusetts Institute of Technology and now in operation at MKS, is shown with its cover removed.

### **3.1.4. The MIT 'C' engine**

The fourth MKS ruling engine was also built by Harrison in the 1960s and transferred in the 1970s to the Association of Universities for Research in Astronomy (AURA) in Tucson, Arizona, where it was installed to support the Kitt Peak National Observatory. At that time the original control system was upgraded to a solid-state system using integrated circuit technology. In 1995 the engine was acquired by and moved to Richardson Gratings. A laser-based control system was developed that uses two interferometers for translation and yaw correction. The 'C' engine has a grating carriage travel of 813 mm and can rule gratings with a groove length of 460 mm; this engine has ruled gratings up to 400 mm x 600 mm with good wavefront and efficiency characteristics, comparable to those of 'B' engine rulings.

### **3.2. THE RULING PROCESS**

Master gratings are ruled on carefully selected well-annealed substrates of several different materials. The choice is generally between BK-7 optical glass, special grades of fused silica, or a special grade of Schott ZERODUR®. The optical surfaces of these substrates are polished to closer than  $\lambda/10$  for green light (about 50 nm), then coated with a reflective film (usually aluminum or gold).

Compensating for changes in temperature and atmospheric pressure is especially important in the environment around a ruling engine. Room temperature must be held constant to within 0.01 °C for small ruling engines (and to within 0.005 °C for larger engines). Since the interferometric control of the ruling process uses monochromatic light, whose wavelength is sensitive to the changes of the refractive index of air with pressure fluctuations, atmospheric pressure must be compensated for by the system. A change in pressure of 2.5 mm of mercury (300 Pa) results in a corresponding change in wavelength of one part per million.<sup>12</sup> This change is negligible if the optical path of the interferometer is near zero but becomes significant as the optical path increases during the ruling. If this effect is not compensated, the carriage control system of the ruling engine will react to this change in wavelength, causing a variation in groove spacing.

The ruling engine must also be isolated from those vibrations that are easily transmitted to the diamond. This may be done by suspending the engine mount from springs that isolate vibrations between frequencies from 2 or 3 Hz (which are of no concern) to about 60 Hz, above which vibration amplitudes are usually too small to have a noticeable effect on ruled master grating quality.<sup>13</sup>

The actual ruling of a master grating is a long, slow and painstaking process. The set-up of the engine, prior to the start of the ruling, requires great skill and patience. The critical alignment requires the use of a high-power interference microscope, or an electron microscope for more finely spaced grooves.

After each microscopic examination, the diamond is readjusted until the operator is satisfied that the groove shape is appropriate for the

---

<sup>12</sup> H. W. Babcock, "Control of a ruling engine by a modulated interferometer," *Appl. Opt.* **1**, 415-420 (1962).

<sup>13</sup> G. R. Harrison, "Production of diffraction gratings. I. Development of the ruling art," *J. Opt. Soc. Am.* **39**, 413-426 (1949).

particular grating being ruled. This painstaking adjustment, although time consuming, results in very "bright" gratings with nearly all the diffracted light energy concentrated in a specific angular range of the spectrum. This ability to concentrate the light selectively at a certain part of the spectrum is what distinguishes blazed diffraction gratings from all others.

Finished master gratings are carefully tested to be certain that they have met specifications completely. The wide variety of tests run to evaluate all the important properties include spectral resolution, efficiency, Rowland ghost intensity, and surface accuracy. Wavefront interferometry is used when appropriate. If a grating meets all specifications, it is then used as a master for the production of our replica gratings.

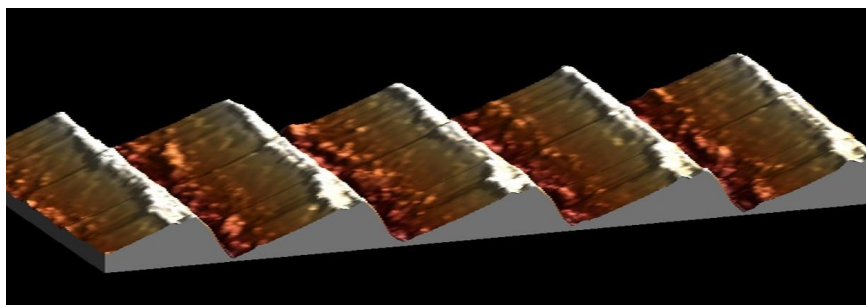


Figure 3-2. Atomic force micrograph of a ruled grating. This grating was ruled with 400 g/mm (groove spacing of 2.5  $\mu\text{m}$ ). The horizontal and vertical scales are not the same.

### 3.3. VARIED LINE-SPACE (VLS) GRATINGS

For over a century, great effort has been expended in keeping the spacing between successive grooves uniform as a master grating is ruled. In an 1893 paper, Cornu realized that variations in the groove spacing modified the curvature of the diffracted wavefronts.<sup>14</sup> While periodic and random variations were understood to produce stray light, a uniform variation in groove spacing across the grating surface was recognized by Cornu to change the location of the focus of the spectrum, which need not be considered a defect if properly taken into account. He determined that

<sup>14</sup> M. A. Cornu, "Vérifications numériques relatives aux propriétés focales des réseaux diffringents plans," *Comptes Rendus Acad. Sci.* **117**, 1032-1039 (1893).

a planar classical grating, which by itself would have no focusing properties if used in collimated incident light, would focus the diffracted light if ruled with a systematic 'error' in its groove spacing. He was able to verify this by ruling three gratings whose groove positions were specified to vary as each groove was ruled. Such gratings, in which the pattern of straight parallel grooves has a variable yet well-defined (though not periodic) spacing between successive grooves, are now called *varied line-space (VLS) gratings*. VLS gratings have not found use in commercial instruments but are occasionally used in spectroscopic systems for synchrotron light sources.

## 4. HOLOGRAPHIC GRATINGS

### 4.0. INTRODUCTION

Since the late 1960s, a method distinct from mechanical ruling has also been used to manufacture diffraction gratings.<sup>15</sup> This method involves the photographic recording of a stationary interference fringe field. Such *interference gratings*, more commonly known as *holographic gratings*, have several characteristics that distinguish them from ruled gratings.

In 1901 Aimé Cotton produced experimental holographic gratings,<sup>16</sup> fifty years before the concepts of holography were developed by Gabor. A few decades later, Michelson considered the interferometric generation of diffraction gratings obvious, but recognized that an intense monochromatic light source and a photosensitive material of sufficiently fine granularity did not then exist.<sup>17</sup> In the mid-1960s, ion lasers and photoresists became available; the former provides a strong monochromatic line and the latter is photoactive at the molecular level, rather than at the crystalline level (such as photographic film).

### 4.1. PRINCIPLE OF MANUFACTURE

#### 4.1.1. Formation of an interference pattern

When two sets of coherent equally polarized monochromatic optical plane waves of equal intensity intersect each other, a standing wave pattern will be formed in the region of intersection if both sets of waves are of the same wavelength  $\lambda$  (see Figure 4-1).<sup>\*</sup> The combined intensity dis-

---

<sup>15</sup> D. Rudolph and G. Schmahl, "Verfahren zur Herstellung von Röntgenlinsen und Beugungsgittern," *Umschau Wiss. Tech.* **78**, 225 (1967); G. Schmahl, "Holographically made diffraction gratings for the visible, UV and soft x-ray region," *J. Spectrosc. Soc. Japan* **23**, 3-11 (1974); A. Labeyrie and J. Flamand, "Spectroscopic performance of holographically made diffraction gratings," *Opt. Commun.* **1**, 5 (1969).

<sup>16</sup> A. Cotton, "Resaux obtenus par la photographie des ordes stationnaires," *Seances Soc. Fran. Phys.* 70-73 (1901).

<sup>17</sup> A. A. Michelson, *Studies in Optics* (U. Chicago, 1927; reprinted by Dover Publications, 1995).

\* Most descriptions of holographic grating recording stipulate coherent beams, but such gratings may also be made using incoherent light; see M. C. Hutley, "Improvements in or relating to the formation of photographic records," UK Patent no. 1384281 (1975).

tribution forms a set of straight equally-spaced fringes (bright and dark lines). Thus, a photographic plate would record a fringe pattern, since the regions of zero field intensity would leave the film unexposed while the regions of maximum intensity would leave the film maximally exposed. Regions between these extremes, for which the combined intensity is neither maximal nor zero, would leave the film partially exposed. The combined intensity varies sinusoidally with position as the interference pattern is scanned along a line. If the beams are not of equal intensity, the minimum intensity will no longer be zero, thereby decreasing the contrast between the fringes. As a consequence, all portions of the photographic plate will be exposed to some degree.

The centers of adjacent fringes (that is, adjacent lines of maximum intensity) are separated by a distance  $d$ , where

$$d = \frac{\lambda}{2 \sin \theta} \quad (4-1)$$

and  $\theta$  is the half the angle between the beams. A small angle between the beams will produce a widely spaced fringe pattern (large  $d$ ), whereas a larger angle will produce a fine fringe pattern. The lower limit for  $d$  is  $\lambda/2$ , so for visible recording light, thousands of fringes per millimeter may be formed.

#### 4.1.2. Formation of the grooves

Master holographic diffraction gratings are recorded in photoresist, a material whose intermolecular bonds are either strengthened or weakened by exposure to light. Commercially available photoresists are more sensitive to some wavelengths than others; the recording laser line must be matched to the type of photoresist used. The proper combination of an intense laser line and a photoresist that is highly sensitive to this wavelength will reduce exposure time.

Photoresist gratings are chemically developed after exposure to reveal the fringe pattern. A photoresist may be *positive* or *negative*, though the latter is rarely used. During chemical development, the portions of a substrate covered in positive photoresist that have been exposed to light are dissolved, while for negative photoresist the unexposed portions are dissolved. Upon immersion in the chemical developer, a surface relief pattern is formed: for positive photoresist, valleys are formed where the bright fringes were, and ridges where the dark fringes were. At this stage a master holographic grating has been produced; its grooves are

sinusoidal ridges. This grating may be coated and replicated like master ruled gratings.

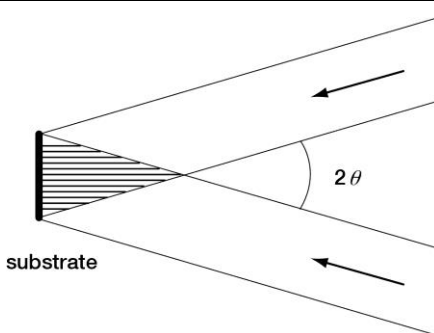


Figure 4-1. Formation of interference fringes. Two collimated beams of wavelength  $\lambda$  form an interference pattern composed of straight equally spaced planes of intensity maxima (shown as the horizontal lines). A sinusoidally varying interference pattern is found at the surface of a substrate placed perpendicular to these planes.

Lindau has developed simple theoretical models for the groove profile generated by making master gratings holographically and shown that even the application of a thin metallic coating to the holographically-produced groove profile can alter that profile.<sup>18</sup>

## 4.2. CLASSIFICATION OF HOLOGRAPHIC GRATINGS

### 4.2.1. Single-beam interference

An interference pattern can be generated from a single collimated monochromatic coherent light beam if it is made to reflect back upon itself. A standing wave pattern will be formed, with intensity maxima forming planes parallel to the wavefronts. The intersection of this interference pattern with a photoresist-covered substrate will yield on its surface a pattern of grooves, whose spacing  $d$  depends on the angle  $\theta$  between the substrate surface and the planes of maximum intensity (see Figure 4-2)<sup>19</sup>; the relation between  $d$  and  $\theta$  is identical to Eq. (4-1), though it must be emphasized that the recording geometry behind the

<sup>18</sup> S. Lindau, "The groove profile formation of holographic gratings," *Opt. Acta* **29**, 1371-1381 (1982).

<sup>19</sup> N. K. Sheridan, "Production of blazed holograms," *Appl. Phys. Lett.* **12**, 316-318 (1968).

single-beam holographic grating (or *Sheridon grating*) is different from that of the double-beam geometry for which Eq. (4-1) was derived.

The groove depth  $h$  for a Sheridon grating is dictated by the separation between successive planes of maximum intensity (nodal planes); explicitly,

$$h = \frac{\lambda_0}{2n}, \quad (4-2)$$

where  $\lambda_0$  is the wavelength of the recording light and  $n$  the refractive index of the photoresist. This severely limits the range of available blaze wavelengths, typically to those between 200 and 250 nm.

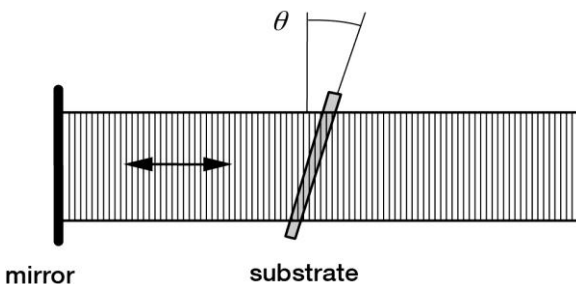


*Figure 4-2. Sheridon recording method.* A collimated beam of light, incident from the right, is retroreflected by a plane mirror, which forms a standing wave pattern whose intensity maxima are shown. A transparent substrate, inclined at an angle  $\theta$  to the fringes, will have its surfaces exposed to a sinusoidally varying intensity pattern.

#### 4.2.2. Double-beam interference

The double-beam interference pattern shown in Figure 4-1 is a series of straight parallel fringe planes, whose intensity maxima (or minima) are equally spaced throughout the region of interference. Placing a substrate covered in photoresist in this region will form a groove pattern defined by the intersection of the surface of the substrate with the fringe planes. If the substrate is planar, the grooves will be straight, parallel and equally spaced, though their spacing will depend on the angle between the substrate surface and the fringe planes. If the substrate is concave, the grooves will be curved and unequally spaced, forming a series of circles of different radii and spacings. Regardless of the shape of the substrate, the intensity maxima are equally spaced planes, so the grating recorded will be a classical equivalent holographic grating (more often called simply a

classical grating). This name recognizes that the groove pattern (on a planar surface) is identical to that of a planar classical ruled grating. Thus, all holographic gratings formed by the intersection of two sets of plane waves are called classical equivalents, even if their substrates are not planar (and therefore their groove patterns are not straight equally spaced parallel lines).

If two sets of spherical wavefronts are used instead, as in Figure 4-3, a *first generation holographic grating* is recorded. The surfaces of maximum intensity are now confocal hyperboloids (if both sets of wavefronts are converging, or if both are diverging) or ellipsoids (if one set is converging and the other diverging). This interference pattern can be obtained by focusing the recording laser light through pinholes (to simulate point sources). Even on a planar substrate, the fringe pattern will be a collection of unequally spaced curves. Such a groove pattern will alter the curvature of the diffracted wavefronts, regardless of the substrate shape, thereby providing focusing. Modification of the curvature and spacing of the grooves can be used to reduce aberrations in the spectral images; as there are three degrees of freedom in such a recording geometry, three aberrations can be reduced (see Chapter 6).

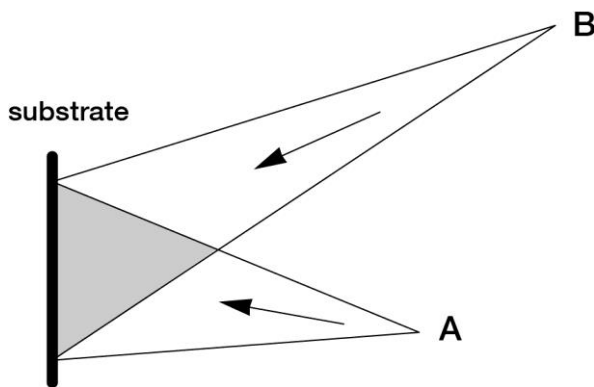


Figure 4-3. First-generation recording method. Laser light focused through pinholes at A and B forms two sets of spherical wavefronts, which diverge toward the grating substrate. The standing wave region is shaded; the intensity maxima are confocal hyperboloids.

The addition of auxiliary concave mirrors or lenses into the recording beams can render the recording wavefronts toroidal (that is, their curvature in two perpendicular directions will generally differ). The

grating thus recorded is a *second generation holographic grating*.<sup>20</sup> The additional degrees of freedom in the recording geometry (e.g., the location, orientation and radii of the auxiliary mirrors) provide for the reduction of additional aberrations above the three provided by first generation holographic gratings.<sup>21</sup>

The use of aspheric recording wavefronts can be further accomplished by using aberration-reduced gratings in the recording system; the first set of gratings is designed and recorded to produce the appropriate recording wavefronts to make the second grating.<sup>22</sup> Another technique is to illuminate the substrate with light from one real source, and reflect the light that passes through the substrate by a mirror behind it, so that it interferes with itself to create a stationary fringe pattern.<sup>23</sup> Depending on the angles involved, the curvature of the mirror and the curvature of the front and back faces of the substrate, a number of additional degrees of freedom may be used to reduce high-order aberrations. [Even more degrees of freedom are available if a lens is placed in the recording system thus described.<sup>24</sup>]

### 4.3. THE HOLOGRAPHIC RECORDING PROCESS

Holographic gratings are recorded by placing a light-sensitive surface in an interferometer. The generation of a holographic grating of spectroscopic quality requires a stable optical bench and laser as well as high-quality optical components (mirrors, collimating optics, etc.). Ambient light must be eliminated so that fringe contrast is maximal. Thermal gradients and air currents, which change the local index of refraction in the beams of the interferometer, must be avoided. MKS

---

<sup>20</sup> C. Palmer, "Theory of second-generation holographic gratings," *J. Opt. Soc. Am.* **A6**, 1175-1188 (1989); T. Namioka and M. Koike, "Aspheric wavefront recording optics for holographic gratings," *Appl. Opt.* **34**, 2180-2186 (1995).

<sup>21</sup> M. Duban, "Holographic aspheric gratings printed with aberrant waves," *Appl. Opt.* **26**, 4263-4273 (1987).

<sup>22</sup> E. A. Sokolova, "Concave diffraction gratings recorded in counterpropagating beams," *J. Opt. Technol.* **66**, 1084-1088 (1999); E. A. Sokolova, "New-generation diffraction gratings," *J. Opt. Technol.* **68**, 584-589 (2001).

<sup>23</sup> E. A. Sokolova, "Geometric theory of two steps recorded holographic diffraction gratings," *Proc. SPIE* **3540**, 113-324 (1998); E. Sokolova, B. Kruizinga, T. Valkenburg and J. Schaarsberg, "Recording of concave diffraction gratings in counterpropagating beams using meniscus blanks," *J. Mod. Opt.* **49**, 1907-1917 (2002).

<sup>24</sup> E. Sokolova, B. Kruizinga and I. Golubenko, "Recording of concave diffraction gratings in a two-step process using spatially incoherent light," *Opt. Eng.* **43**, 2613-2622 (2004).

records master holographic gratings in a clean room specially-designed to meet these requirements.

During the recording process, the components of the optical system must be of nearly diffraction-limited quality, and mirrors, pinholes and spatial filters must be adjusted as carefully as possible. Any object in the optical system receiving laser illumination may scatter this light toward the grating, which will contribute to stray light. Proper masking and baffling during recording are essential to the successful generation of a holographic grating, as is single-mode operation of the laser throughout the duration of the exposure.

The substrate on which the master holographic grating is to be produced must be coated with a highly uniform, virtually defect-free coating of photoresist. Compared with photographic film, photoresists are somewhat insensitive to light during exposure, due to the molecular nature of their interaction with light. As a result, typical exposures may take from minutes to hours, during which time an extremely stable fringe pattern (and, therefore, optical system) is required. After exposure, the substrate is immersed in a developing agent, which forms a surface relief fringe pattern; coating the substrate with metal then produces a master holographic diffraction grating.

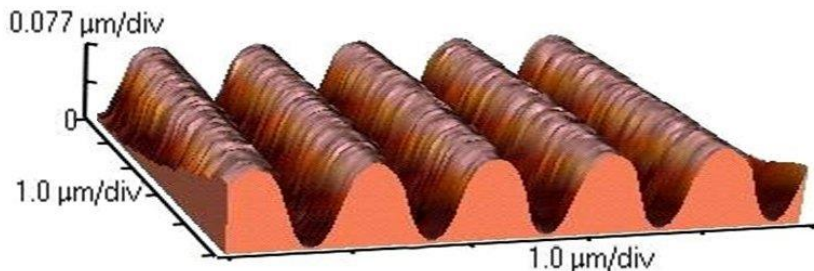


*Figure 4-4. Atomic force micrograph of a holographic grating.* A sinusoidal holographic grating with 1000 g/mm (1  $\mu\text{m}$  groove spacing) is shown. The horizontal and vertical scales are not the same.

## **4.4. DIFFERENCES BETWEEN RULED AND HOLOGRAPHIC GRATINGS**

Due to the distinctions between the fabrication processes for ruled and holographic gratings, each type of grating has advantages and disadvantages relative to the other, some of which are described below.

### **4.4.1. Differences in grating efficiency**

The efficiency curves of ruled and holographic gratings generally differ considerably, though this is a direct result of the differences in groove profiles and not strictly due to method of making the master grating. For example, holographic gratings made using the Sheridan method described in Section 4.2.1 above have nearly triangular groove profiles, and therefore have efficiency curves that look more like those of ruled gratings than those of sinusoidal-groove holographic gratings.

There exist no clear rules of thumb for describing the differences in efficiency curves between ruled and holographic gratings; the best way to gain insight into these differences is to look at representative efficiency curves of each grating type. Chapter 9 in this *Handbook* contains a number of efficiency curves; the paper<sup>25</sup> by Loewen *et al.* on which this chapter is based contains even more efficiency curves, and the book *Diffractive Gratings and Applications*<sup>26</sup> by Loewen and Popov has an extensive collection of efficiency curves and commentary regarding the efficiency behavior of plane reflection gratings, transmission gratings, echelle gratings and concave gratings.

### **4.4.2. Differences in scattered light**

Since holographic gratings do not involve burnishing grooves into a thin layer of metal, the surface irregularities on its grooves differ from those of mechanically ruled gratings. Moreover, errors of ruling, which are a manifestation of the fact that ruled gratings have one groove formed after another, are nonexistent in interferometric gratings, for which all grooves are formed simultaneously. Holographic gratings, if properly made, can be entirely free of both small periodic and random groove

---

<sup>25</sup> E. G. Loewen, M. Nevière and D. Maystre, "Grating efficiency theory as it applies to blazed and holographic gratings," *Appl. Opt.* **16**, 2711-2721 (1977).

<sup>26</sup> E. G. Loewen and E. Popov, *Diffractive Gratings and Applications*, Marcel Dekker, Inc. (1997).

placement errors found on even the best mechanically ruled gratings. Holographic gratings may offer advantages to spectroscopic systems in which light scattered from the grating surface is performance-limiting, such as in the study of the Raman spectra of solid samples, though proper instrumental design is essential to ensure that the performance of the optical system is not limited by other sources of stray light.

While holographic gratings generally exhibit lower scattered light than early ruled gratings, modern control systems and improved master coatings have led to ruled masters whose replicas exhibit scattered light as low as that of replicas of holographic masters. Some commercially-available Raman spectrometers now use ruled gratings, since their scattered light properties are suitable even for such a demanding application.

#### **4.4.3. Differences and limitations in the groove profile**

The groove profile has a significant effect on the light intensity diffracted from the grating (see Chapter 9). While ruled gratings may have triangular or trapezoidal groove profiles, holographic gratings usually have sinusoidal (or nearly sinusoidal) groove profiles (see Figure 4-5). A ruled grating and a holographic grating, identical in every way except in groove profile, will have demonstrably different efficiencies (diffraction intensities) for a given wavelength and spectral order. Moreover, ruled gratings are more easily blazed (by choosing the proper shape of the burnishing diamond) than are holographic gratings, which are usually blazed by ion bombardment (ion etching). Differences in the intensity diffracted into the order in which the grating is to be used implies differences in the intensities in all other orders as well; excessive energy in other orders usually makes the suppression of stray light more difficult.

The distribution of groove profile characteristics across the surface of a grating may also differ between ruled and holographic gratings. For a ruled concave grating, the facet angles are not aligned identically, and the effective blaze wavelength varies from one side of the grating to the other. A holographic grating, on the other hand, usually demonstrates much less variation in efficiency characteristics across its surface. Gratings have been ruled by changing the facet angle at different places on the substrate during ruling. These so-called "multipartite" gratings, in which the ruling is interrupted and the diamond reoriented at different places across the width of the grating, demonstrate enhanced efficiency but do not provide

the resolving power expected from an uninterrupted ruling (since each section of grooves may be out of phase with the others).<sup>27</sup>

---

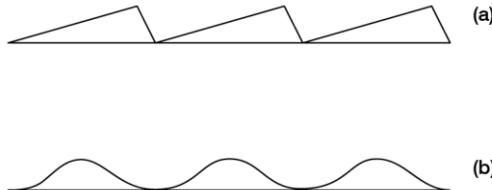


*Figure 4-5. Ideal groove profiles for ruled and holographic gratings. (a) Triangular grooves, representing the profile of a typical mechanically ruled grating. (b) Sinusoidal grooves, representing the profile of a typical holographic grating.\**

---

#### 4.4.4. Range of obtainable groove frequencies

The number of grooves per millimeter for ruled and holographic gratings can vary over a very wide range. Gratings of both types can be made with very coarse groove patterns – as low as 30 g/mm for ruled gratings and as low as 1 g/mm for holographic gratings. As an upper limit, both holographic and ruled gratings have been produced with groove densities up to 10,000 grooves per millimeter.

#### 4.4.5. Differences in the groove patterns

Classical ruled plane gratings, which constitute the vast majority of ruled gratings, have straight equally-spaced grooves. Classical ruled concave gratings have unequally spaced grooves that form circular arcs on the grating surface, but this groove pattern, when projected onto the plane tangent to the grating at its center, is still a set of straight equally spaced lines. [It is the projected groove pattern that governs imaging.<sup>28</sup>] Even ruled varied line-space (VLS) gratings (see Chapter 3) do not

---

<sup>27</sup> M. C. Hutley and W. R. Hunter, "Variation of blaze of concave diffraction gratings," *Appl. Opt.* **20**, 245-250 (1981).

\* Holographic gratings may also be made with quasi-triangular grooves (using the Sheridan method and by ion etching) as well as other groove profiles (e.g., circular bumps, trapezoids); different groove profile provide different efficiency characteristics.

<sup>28</sup> C. Palmer and W. R. McKinney, "Imaging theory of plane-symmetric varied line-space grating systems," *Opt. Eng.* **33**, 820-829 (1994).

contain curved grooves, except on curved substrates. The aberration reduction possible with ruled gratings is therefore limited to that possible with straight grooves, though this limitation is due to the mechanical motions possible with present-day ruling engines rather than with the burnishing process itself.

Holographic gratings, on the other hand, need not have straight grooves. Groove curvature can be modified to reduce aberrations in the spectrum, thereby improving the throughput and spectral resolution of imaging spectrometers. A common spectrometer mount is the *flat-field spectrograph*, in which the spectrum is imaged onto a flat detector array and several wavelengths are monitored simultaneously. Holographic gratings can significantly improve the imaging of such a grating system, whereas classical ruled gratings are not suitable for forming well-focused planar spectra without auxiliary optics.

#### 4.4.6. Differences in the substrate shapes

The interference pattern used to record holographic gratings is not dependent on the substrate shape or dimension, so gratings can be recorded interferometrically on substrates of low *f*/number more easily than they can be mechanically ruled on these substrates. Consequently, holographic concave gratings lend themselves more naturally to systems with short focal lengths. Holographic gratings of unusual curvature can be recorded easily; of course, there may still remain technical problems associated with the replication and testing of such gratings.

The substrate shape affects both the grating efficiency characteristics its imaging performance.

- Grating efficiency depends on the groove profile as well as the angle at which the light is incident and diffracted; for a concave grating, both the groove profile and the local angles vary with position on the grating surface. This leads to the efficiency curve being the sum of the various efficiency curves for small regions of the grating, each with its own groove profile and incidence and diffraction angles.
- Grating imaging depends on the directions of the diffracted rays over the surface of the grating, which in turn are governed by the local groove spacing and curvature (*i.e.*, the *groove pattern*) as well as the local incidence angle. For a conventional plane grating used in collimated light, the groove pattern is the same everywhere on the grating surface, as is the incidence angle, so all diffracted rays are parallel. For a grating on a concave substrate, though, the groove

pattern is generally position-dependent, as is the local incidence angle, so the diffracted rays are not parallel – thus the grating has focal (imaging) properties as well as dispersive properties.

#### **4.4.7. Differences in the size of the master substrate**

While ruled master gratings can generally be as large as 320 x 420 mm, holographic master gratings are rarely this large, due to the requirement that the recording apparatus contain very large, high-quality lenses or mirrors, and well as due to the decrease in optical power farther from the center of the master grating substrate.

#### **4.4.8. Differences in generation time for master gratings**

A ruled master grating is formed by burnishing each groove individually; to do so, the ruling diamond may travel a very large distance to rule one grating. For example, a square grating of dimensions 100 x 100 mm with 1000 grooves per millimeter will require the diamond to move 10 km (over six miles), which may take several weeks to rule.

In the fabrication of a master holographic grating, on the other hand, the grooves are created simultaneously. Exposure times vary from a few minutes to tens of minutes, depending on the intensity of the laser light used and the spectral response (sensitivity) of the photoresist at this wavelength. Even counting preparation and development time, holographic master gratings are produced much more quickly than ruled master gratings. Of course, an extremely stable and clean optical recording environment is necessary to record precision holographic gratings. For plane gratings, high-grade collimating optics are required, which can be a limitation for larger gratings.

## 5. REPLICATED GRATINGS

### 5.0. INTRODUCTION

Decades of research and development have contributed to the process for manufacturing replicated diffraction gratings (*replicas*) of spectroscopic quality. This process is capable of producing thousands of duplicates of master gratings which equal the quality and performance of the master gratings themselves. The replication process has reduced the price of a typical diffraction grating by a factor of one hundred or more, compared with the cost of acquiring a master grating, as well as greatly increasing their commercial availability.

### 5.1. THE REPLICATION PROCESS

The process for making replica gratings results in a grating whose grooves are formed in a very thin layer of resin that adheres strongly to the surface of the substrate material. The optical surface of a reflection replica is usually coated with aluminum (Al), but gold (Au) or silver (Ag) is recommended for greater diffracted energy in certain spectral regions. Transmission gratings have no reflective coating.

Most commercially-available surface-relief gratings are made using a casting process, which faithfully reproduces the three-dimension nature of the grating surface. It is for this reason that photographic replication techniques are not generally sufficient.<sup>29</sup>

The casting process for the production of a replicated diffraction grating is a series of sequential steps:

1. *Submaster selection.* The replication process starts with the selection of a suitable *submaster* grating that has the desired specifications (groove frequency, blaze angle, size, etc.). [A submaster grating is a grating replicated from a master, or from another submaster, but is itself used not as a final optical product but as a mold for the replication of product gratings; for this reason, it is not strictly required that a submaster grating meet all of the performance specifications of the product grating (e.g., it need not have a suitably reflective coating).]

---

<sup>29</sup> E. G. Loewen and E. Popov, *Diffraction Gratings and Applications*, Marcel Dekker, Inc. (1997), p. 577.

2. *Application of parting agent.* A parting agent is applied to the surface of the submaster grating. The parting agent serves no optical purpose and should have no deleterious optical effects but aids in the separation of the delicate submaster and product grating surfaces. Since the replicated optical surface is intended to match that of the submaster as closely as possible, the parting agent must be very thin and conformal to the surface of the submaster.<sup>30</sup>
3. *Application of transfer coating.* After the parting agent is applied, a reflective coating (usually aluminum) is applied to the surface of the submaster. This coating will form the optical surface of the product grating upon separation. To obtain an optical quality coating, this step is performed in a vacuum deposition chamber. [Since this coating is applied to the submaster, but transfers to the product grating upon separation, it is called a *transfer coating*.] Typical transfer coating thicknesses are about one micron.
4. *Cementing* A substrate is then cemented with a layer of resin to the grooved surface of the master grating; this layer can vary in thickness, but it is usually tens of microns thick. It is the resin that holds the groove profile and replicates it from the submaster to the product; the transfer coating is much too thin for this purpose. The “sandwich” formed by the substrate and submaster cemented together is shown in Figure 5-1.

Since the resin is in the liquid state when it is applied to the submaster, it must harden sufficiently to ensure that it can maintain the groove profile faithfully when the product grating is separated from the submaster. This hardening, or curing, is usually accomplished by a room-temperature cure period (lasting from hours to days) or by heating the resin to accelerate the curing, though gratings can also be replicated using a UV-curable resin.<sup>31</sup>

5. *Separation.* After the resin is fully cured, the groove profile is faithfully replicated in the resin when the submaster and product are separated. The parting agent serves as the weak interface and allows the separation to take place between the submaster coating and the

---

<sup>30</sup> E. G. Loewen, Replication of Mirrors and Diffraction Gratings, SPIE Tutorial T10 (1983).

<sup>31</sup> S. D. Fantone, “Replicating optical surfaces using UV curing cements: a method,” *Appl. Opt.* **22**, 764 (1983); R. J. M. Zwiers and G. C. M. Dortant, “Aspheric lenses produced by a fast high-precision replication process using UV-curable coatings,” *Appl. Opt.* **24**, 4483-4488 (1985).

transfer metallic coating. The groove profile on the product is the inverse of the groove profile on the submaster; if this profile is not symmetric with respect to this inversion, the efficiency characteristics of the product grating will generally differ from those of the submaster grating. In such cases, an additional replication must be done to invert the inverted profile, resulting in a profile identical to that of the original submaster. However, for certain types of gratings, inversion of the groove increases efficiency significantly.

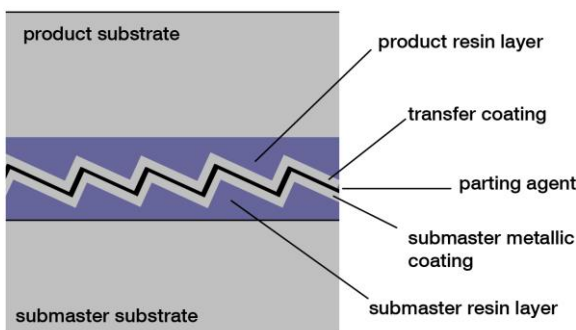


Figure 5-1. The replication "sandwich". The substrates, the resin layers, the metallic coatings, and the parting agent are shown.

At this stage, if a transmission grating is desired, the transfer coating is removed from the product, leaving the groove structure intact in the transparent resin.

6. *Inspection.* After separation, both the submaster and the product gratings are inspected for surface or substrate damage. The product grating may also be tested for key performance characteristics (e.g., efficiency, wavefront flatness (or curvature), scattered light, alignment of the grooves to a substrate edge) depending on requirements.

The product grating formed by this replication process may be used as an optical component, or it may serve as a mold (replication tool) by being considered a submaster. In this way, a single master grating can make several submasters, each of which can make several more submasters, etc., to form a *replication tree* (see Figure 5-2).

The replication tree shown in Figure 5-2 illustrates two important features of replication: extension horizontally (within a generation) and

vertically (to subsequent generations). Replication within a generation is accomplished by the successive replication of a single grating (much as a parent can have many children). Replication to additional generations is accomplished by forming a replica (child), which itself forms a replica (grandchild), etc. Thus replication can extend both within generations ( $X-1$ ,  $X-2$ ,  $X-3$ ,  $X-4$ , ...), all of which are replicated directly from the master) and to subsequent generations ( $X-1$ ,  $X-1-3$ ,  $X-1-3-1$ ,  $X-1-3-1-4$ , ...), each of which is replicated from the submaster before it) to create a large number of replicas from a single master grating.

As an example, consider a master grating  $X$  from which five *first-generation replicas* are made ( $X-1$  through  $X-5$ ). Each of these is used as a submaster to form five replicas:  $X-1$  forms  $X-1-1$  through  $X-1-5$ ,  $X-2$  forms  $X-2-1$  through  $X-2-5$ , and so on. This forms twenty-five *second-generation replicas*. If each of these replicas is itself replicated five times, we arrive at 125 *third-generation replicas* ( $X-1-1-1$ ,  $X-1-1-2$ , ... through  $X-5-5-5$ ). This example illustrates that a large number of replicas can be made from a single master grating, assuming a conservative number of replicas and a reasonable number of generations.

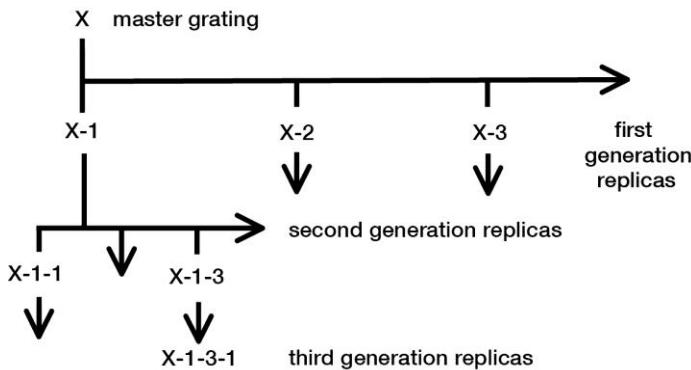


*Figure 5-2. A replication tree.* Master  $X$  is replicated to create several first-generation replicas ( $X-1$ ,  $X-2$ , ...), which themselves are replicated to form second-generation replicas ( $X-1-1$ , ...), etc.

The number  $N$  of replicas of a particular generation that can be made from a single master can be estimated using the following formula,

$$N = R^g, \quad (5-1)$$

where  $R$  is the number of replications per generation and  $g$  is the number of generations. Reasonable values of  $R$  are 5 to 10 (though values well above 20 are not unheard of), and  $g$  generally ranges from 3 to 9. Conservatively, then, for  $R = 5$  and  $g = 3$ , we have  $N = 125$  third-generation replicas; at the other end of the ranges we have  $R = 10$  and  $g = 9$  so that  $N = 1,000,000,000$  ninth-generation replicas. Of course, one billion replicas of a single grating have never been required, but even if it were, Eq. (5-1) assumes that each replica in every generation (except the last generation) is replicated  $R$  times, whereas in practice most gratings cannot be replicated too many times before being damaged or otherwise rendered unusable. That is, some branches of the replication tree are truncated prematurely as a result of manufacturing defects, i.e., because the manufacturing yield is less than 100%. Consequently, Eq. (5-1) must be taken as an unreasonable upper limit, which becomes unrealistically high as either  $R$  or  $g$  increases beyond small numbers. In practice,  $N$  is often in the thousands when required, and can be even higher if extra care is taken to ensure that the submasters in the replication tree are not damaged.

## 5.2. REPLICA GRATINGS VS. MASTER GRATINGS

There are two fundamental differences between master gratings and replica gratings: how they are made and what they are made of.

*Manufacturing process.* Replica gratings are made by the replication process outlined in Section 5.1 above – they are resin castings of master gratings. The master gratings themselves, though, are not castings: their grooves are created either by burnishing (in the case of ruled gratings) or by optical exposure and chemical development (in the case of holographic gratings).

*Composition.* Replica gratings are composed of a metallic coating on a resin layer, which itself rests on a substrate (usually glass). Master gratings also usually have glass substrates but have no resin (the grooves of a ruled master are contained entirely within a metallic layer on the substrate, and those of a holographic master are contained entirely within a layer of photoresist or similar photosensitive material).

The differences in manufacturing processes for master gratings and replica gratings naturally provide an advantage in both production time and unit cost to replica gratings, thereby explaining their popularity, but the replication process itself must be designed and carried out to ensure

that the performance characteristics of the replicated grating match those of the master grating. Exhaustive experimentation has shown how to eliminate loss of resolution between master and replica – this is done by ensuring that the surface figure of the replica matches that of the master, and that the grooves are not displaced or distorted as a result of replication. The efficiency of a replica matches that of its master when the groove profile is reproduced faithfully. Other characteristics, such as scattered light, are generally matched as well, provided care is taken during the transfer coating step to ensure a dense metallic layer. [Even if the layer were not dense enough, so that its surface roughness caused increased scattered light from the replica when compared with the master, this would be diffuse scatter; scatter in the dispersion plane, due to irregularities in the groove spacing, would be faithfully replicated by the resin and does not depend significantly on the quality of the coating.] Circumstances in which a master grating is shown to be superior to a replicated grating are quite rare and can often be attributed to flaws or errors in the particular replication process used, not to the fact that the grating was replicated.

In one respect, replicated gratings can provide an advantage over master gratings: those cases where the ideal groove profile is not obtainable in a master grating, but the inverse profile is obtainable. Echelle gratings, for example, are ruled so that their grooves exhibit a sharp trough but a relatively less sharp peak. By replicating, the groove profile is inverted, leaving a first-generation replica with a sharp peak. The efficiency of the replica will be considerably higher than the efficiency of the master grating. In such cases, only odd-generation replicas are used as products, since the even-generation replicas have the same groove profile (and therefore the same efficiency characteristics) as the master itself.\*

The most prominent hazard to a grating during the replication process, either master or replica, is scratching, since the grating surface consists of a thin metal coating on a resin layer. Scratches involve damage to the groove profile, which generally leads to increased stray light, though in some applications this may be tolerable. Scratches faithfully replicate from master to submaster to product, and cannot be

---

\* By convention, a master grating is designated as the zeroth (0) generation, so the second-, fourth- and subsequent even-generation submasters from the master will have the same groove profile, and the first-, third- and subsequent odd-generation submasters will have inverted groove profiles.

repaired, since the grating surface is not a polished surface, and an overcoating will not repair the damaged grooves.

Another hazard during replication is surface contamination from fingerprints; should this happen, a grating can sometimes (but not always) be cleaned or recoated to restore it to its original condition. [In use, accidentally evaporated contaminants, typical of vacuum spectrometry pumping systems, can be especially harmful when baked on the surface of the grating with ultraviolet radiation.]

### 5.3. STABILITY OF REPLICATED GRATINGS

*Temperature.* There is no evidence of deterioration or change in standard replica gratings with age or when exposed to thermal variations from the boiling point of nitrogen (77 K = -196 °C) to 110 °C and above. In addition to choosing the appropriate resin, the cure cycle can be modified to result in a grating whose grooves will not distort under high temperature.

Gratings replicated onto substrates made of low thermal expansion materials behave as the substrate dictates: the resin and aluminum, which have much higher thermal expansion coefficients, are present in very thin layers compared with the substrate thickness and therefore do not expand and contract appreciably with temperature changes since they are fixed rigidly to the substrate.

*Relative Humidity.* Standard replicas generally do not show signs of degradation in normal use in high relative humidity environments, but some applications (*e.g.*, fiber-optic telecommunications) require extended exposure to very high humidity environments. Coatings and epoxies that resist the effects of water vapor are necessary for these applications.

Instead of a special resin, the metallic coating on a reflection grating made with standard resin is often sufficient to protect the underlying resin from the effects of water vapor. A transmission grating that requires protection from environmental water vapor can be so protected by applying a dielectric coating (*e.g.*, SiO) to its grooved surface.<sup>32</sup>

*Temperature and Relative Humidity.* Fiber optic telecommunications applications often require diffraction gratings that

---

<sup>32</sup> E. G. Loewen and E. Popov, *Diffraction Gratings and Applications*, Marcel Dekker, Inc. (1997), p. 582.

meet harsh environmental standards, particularly those in the Telcordia document GR-1221, “Generic Reliability Assurance Requirements for Passive Optical Components”. Special resin materials, along with specially-designed proprietary replication techniques, have been developed to produce replicated gratings that can meet this demanding requirement with no degradation in performance.

*High Vacuum.* Even the highest vacuum, such as that of outer space, has no effect on replica gratings. Concerns regarding outgassing from the resin are addressed by recognizing that the resin is fully cured. However, some outgassing may occur in high vacuum, which may be a problem for gratings used in synchrotron beamlines; in certain cases, ruled master gratings are used instead.

*Energy Density of the Beam.* For applications in which the energy density at the surface of the grating is very high (as in some pulsed laser applications), enough of the energy incident on the grating surface may be absorbed to cause damage to the surface. In these cases, it may be necessary to make the transfer coat thicker than normal, or to apply a second metallic layer (an overcoat) to increase the opacity of the metal film(s) sufficiently to protect the underlying resin from exposure to the light and to permit the thermal energy absorbed from the pulse to be dissipated without damaging the groove profile. Using a metal rather than glass substrate is also helpful in that it permits the thermal energy to be dissipated; in some cases, a water-cooled metal substrate is used for additional benefit.<sup>33</sup>

Pulsed lasers often require optical components with high damage thresholds, due to the short pulse duration and high energy of the pulsed beam. For gratings used in the infrared, gold is generally used as the reflective coating (since it is more reflective than aluminum in the near IR).

A continuous-wave laser operating at  $\lambda = 10.6 \mu\text{m}$  was reported by Huguley and Loomis<sup>34</sup> to generate damage to the surface of replicated grating at about  $150 \text{ kW/cm}^2$  or above.

Gill and Newnam<sup>35</sup> undertook a detailed experimental study of laser-induced damage of a set of master gratings and a set of replicated

---

<sup>33</sup> F. M. Anthony, “High heat load optics: an historical overview,” *Opt. Eng.* **34**, 313-320 (1995).

<sup>34</sup> C. A. Huguley and J. S. Loomis, “Optical material damage from  $10.6 \mu\text{m}$  CW radiation,” in *Damage in Laser Materials*, A. J. Glass and A. H. Guenther, eds., *Nat. Bur. Stand. (U.S.) Spec. Publ.* **435** (1975).

gratings using 30-ps pulses at  $\lambda = 1.06 \mu\text{m}$ . They reported that the damage threshold for the holographic gratings they tested was a factor of 1.5 to 5 times higher than for the ruled gratings they tested. Differences in the damage threshold for S- vs. P-polarized light were also observed: the threshold for S-polarized light was 1.5 to 6 times higher than for P-polarized light, though how this correlates to grating efficiency in these polarization states is not clear. The (holographic) master gratings tested exhibited lower damage thresholds than did the replicated gratings. Some of the experimental results reported by Gill and Newnam are reproduced in Table 5-1.

Increasing the thickness of the reflective layer can, in certain circumstances, greatly increase the damage threshold of a replicated grating used in pulsed beams, presumably by reducing the maximum temperature which the metallic coating reaches during illumination.<sup>36</sup>

Damage Threshold ( $\text{J/cm}^2$ ) at $\lambda = 1.06 \mu\text{m}$				
	P polarization		S polarization	
	Au coating	Al coating	Au coating	Al coating
1800 g/mm holographic #1	2.6	0.3	1.2	0.1
1800 g/mm holographic #2	1.0	0.3	0.8	0.1
600 g/mm ruled	1.1	0.2	0.4	0.1
300 g/mm ruled	0.5	0.3	0.1	0.1

Table 5-1. Damage thresholds reported by Gill and Newnam. For these gratings, the difference in damage threshold measurements between Au and Al coatings, between P- and S-polarization, and between the 1800 g/mm holographic gratings and 300 and 600 g/mm ruled gratings are evident.

Increasing the thickness of the reflective layer can, in certain circumstances, greatly increase the damage threshold of a replicated

<sup>35</sup> D. H. Gill and B. E. Newnam, "Picosecond-pulse damage studies of diffraction gratings," in *Damage in Laser Materials*, H. E. Bennett, A. H. Guenther, D. Milam and B. E. Newnam, eds., *Nat. Bur. Stand. (U.S.) Spec. Publ.* **727** (1986), pp. 154-161.

<sup>36</sup> R. W. C. Hansen, "Replica grating radiation damage in a normal incidence monochromator," *Rev. Sci. Instrum.* **67** (9), 1-5 (1996).

grating used in pulsed beams, presumably by reducing the maximum temperature which the metallic coating reaches during illumination.<sup>37</sup>

Experimental damage thresholds for continuous wave (cw) beams, reported by Loewen and Popov<sup>38</sup>, are given in Table 5-2.

Coating defects can play a critical role in the incidence of laser damage, as reported by Steiger and Brausse,<sup>39</sup> who studied optical components illuminated by a pulsed Nd:YAG laser operating at  $\lambda = 1.06 \mu\text{m}$ .

<i>Grating type</i>	<i>Damage Threshold (power density)</i>
Standard replica grating on glass substrate	40 to 80 W/cm <sup>2</sup>
Standard replica grating on copper substrate	c. 100 W/cm <sup>2</sup>
Standard replica grating on water-cooled copper substrate	150 to 250 W/cm <sup>2</sup>

Table 5-2. Damage thresholds for continuous wave (cw) beams.

Coating defects can play a critical role in the incidence of laser damage, as reported by Steiger and Brausse, who studied optical components illuminated by a pulsed Nd:YAG laser operating at  $\lambda = 1.06 \mu\text{m}$ .

#### 5.4. DUAL-BLAZE GRATINGS

Using the replication process described above, replica gratings made from two different master gratings may be combined to make a single grating.

Two (or more) gratings with different groove spacings may be combined in this way. Since the dispersion from each groove pattern will differ, though, the spectra will generally be imaged separately. An optical

<sup>37</sup> R. W. C. Hansen, "Replica grating radiation damage in a normal incidence monochromator," *Rev. Sci. Instrum.* **67** (9), 1-5 (1996).

<sup>38</sup> E. G. Loewen and E. Popov, *Diffraction Gratings and Applications*, Marcel Dekker, Inc. (1997), p. 485.

<sup>39</sup> B. Steiger and H. Brausse, "Interaction of laser radiation with coating defects," *Proc. SPIE* **2428**, 559-567 (1995).

component of this nature would serve as two distinct gratings whose positions and orientations are fixed relative to each other.

Gratings with the same groove spacing, however, may be combined in this way to form a component that behaves like a single grating, but with an efficiency curve formed by the weighted average of the efficiencies of the sections (weighted by the illuminated areas of each section). Such *dual-blaze gratings* can provide efficiency curves that are not achievable with conventionally produced gratings, due to limitations in the available groove profiles. The relative areas of the two sections can be chosen to tailor the efficiency behavior of the entire grating.

Dual-blaze gratings are made by carefully replicating submasters from two different gratings together to produce a dual-blaze submaster, which itself is replicated using conventional means. Gratings made in this way have exhibited wavefront distortions of  $\lambda/4$  or less, and exhibit efficiency characteristics that cannot be obtained from single ruled gratings, in that their efficiency curves have lower and broader peaks (see Figure 5-3).

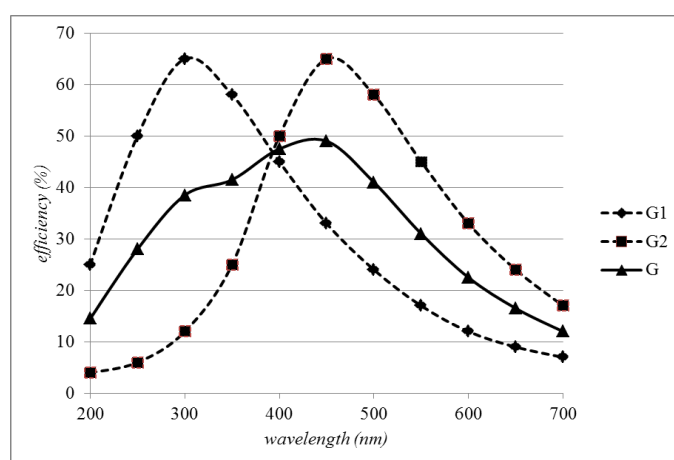


Figure 5-3. Efficiency curve of a dual-blaze grating. Two ruled gratings G1 and G2, of the same groove spacing but blazed at 250 nm and 450 nm, and combined to form a dual-blaze grating G. Equal areas of each of the two grating are illuminated to create a grating with the solid efficiency curve.



## 6. PLANE GRATINGS AND THEIR MOUNTS

### 6.1. GRATING MOUNT TERMINOLOGY

The auxiliary collimating and focusing optics that modify the wavefronts incident on and diffracted by a grating, as well as the angular configuration in which it is used, is often called its *mount*. Grating mounts are a class of *spectrometer*, a term that usually refers to any spectroscopic instrument, regardless of whether it scans wavelengths individually or entire spectra simultaneously, or whether it employs a prism or grating. For this discussion we consider grating spectrometers only.

A *monochromator* is a spectrometer that images a single wavelength or wavelength band at a time onto an exit slit; the spectrum is scanned by the relative motion of the entrance and/or exit optics (usually slits) with respect to the grating. A *spectrograph* is a spectrometer that images a range of wave-lengths simultaneously, either onto photographic film or a series of detector elements, or through several exit slits (sometimes called a *polychromator*). The defining characteristic of a spectrograph is that an entire section of the spectrum is recorded at once.

### 6.2. PLANE GRATING MONOCHROMATOR MOUNTS

A *plane grating* is one whose surface is flat. Plane gratings are normally used in collimated incident light, which is dispersed by wavelength but is not focused. Plane grating mounts generally require auxiliary optics, such as lenses or mirrors, to collect and focus the energy. Some simplified plane grating mounts illuminate the grating with converging light, though the focal properties of the system will then depend on wavelength. For simplicity, only plane reflection grating mounts are discussed below, though each mount may have a transmission grating analogue.

### 6.2.1. The Czerny-Turner monochromator<sup>40</sup>

This design involves a classical plane grating illuminated by collimated light. The incident light is usually diverging from a source or slit, and collimated by a concave mirror (the *collimator*), and the diffracted light is focused by a second concave mirror (the *camera*); see Figure 6-1. Ideally, since the grating is planar and classical, and used in collimated incident light, no aberrations should be introduced into the diffracted wavefronts. In practice, since spherical mirrors are often used, aberrations are contributed by their use off-axis.<sup>41</sup>

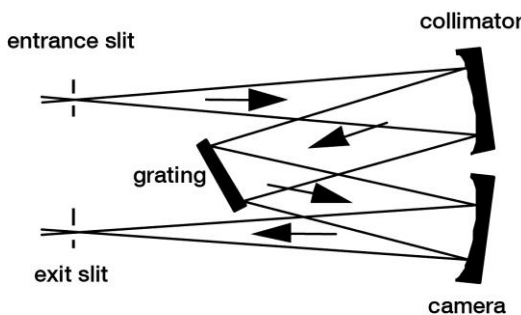


Figure 6-1. The Czerny-Turner mount. The plane grating provides dispersion and the concave mirrors provide focusing.

Like all monochromator mounts, the wavelengths are imaged individually. The spectrum is scanned by rotating the grating; this moves the grating normal relative to the incident and diffracted beams, which (by Eq. (2-1)) changes the wavelength diffracted toward the second mirror. Since the light incident on and diffracted by the grating is collimated, the spectrum remains at focus at the exit slit for each wavelength, since only the grating can introduce wavelength-dependent focusing properties.

<sup>40</sup> A. Shafer, L. Megil and L. Doppelman, "Optimization of Czerny-Turner spectrometers," *J. Opt. Soc. Am.* **54**, 879-888 (1964); J. M. Simon, M. A. Gil and A. N. Fantino, "Czerny-Turner monochromator: astigmatism in the classical and in the crossed beam dispositions," *Appl. Opt.* **25**, 3715-3720 (1986); K. M. Rosfjord, R. A. Villalaz and T. K. Gaylord, "Constant-bandwidth scanning of the Czerny-Turner monochromator," *Appl. Opt.* **39**, 568-572 (2000).

<sup>41</sup> R. F. James and R. S. Sternberg, *The Design of Optical Spectrometers*, Chapman and Hall (London: 1969).

Aberrations\* caused by the auxiliary mirrors include astigmatism and spherical aberration (each of which is contributed additively by the mirrors); as with all concave mirror geometries, astigmatism increases as the angle of reflection increases. Coma, though generally present, can be eliminated at one wavelength through proper choice of the angles of reflection at the mirrors; due to the anamorphic (wavelength-dependent) tangential magnification of the grating, the images of the other wavelengths experience higher-order coma (which becomes troublesome only in special systems).

### 6.2.2. The Ebert monochromator<sup>42</sup>

This design is a special case of a Czerny-Turner mount in which a single relatively large concave mirror serves as both the collimator and the camera (Figure 6-2). Its use is limited, since stray light and aberrations are difficult to control – the latter effect being a consequence of the relatively few degrees of freedom in design (compared with a Czerny-Turner monochromator). This can be seen by recognizing that the Ebert monochromator is a special case of the Czerny-Turner monochromator in which both concave mirror radii are the same, and for which their centers of curvature coincide. However, an advantage that the Ebert mount provides is the avoidance of relative misalignment of the two mirrors.

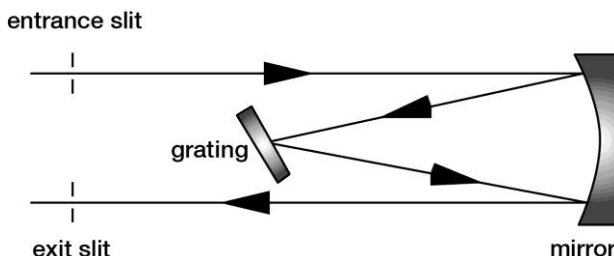


Figure 6-2. The Ebert mount. A single concave mirror replaces the two concave mirrors found in Czerny-Turner mounts.

\* See Chapter 7 for a discussion of aberrations.

<sup>42</sup> H. Ebert, *Wied. Ann.* **38**, 489 (1889); H. Kayser, *Handbuch der Spectroscopie* (1900), vol. 1.

Fastie improved upon the Ebert design by replacing the straight entrance and exit slits with curved slits, which yields higher spectral resolution.<sup>43</sup>

### 6.2.3. The Monk-Gillieson monochromator<sup>44</sup>

In this mount (see Figure 6-3), a plane grating is illuminated by converging light. Usually light diverging from an entrance slit (or fiber) is rendered converging by off-axis reflection from a concave mirror (which introduces aberrations, so the light incident on the grating is not composed of perfectly spherical converging wavefronts). The grating diffracts the light, which converges toward the exit slit; the spectrum is scanned by rotating the grating to bring different wavelengths into focus at or near the exit slit. Often the angles of reflection (from the primary mirror), incidence and diffraction are small (measured from the appropriate surface normals), which keeps aberrations (especially off-axis astigmatism) to a minimum.

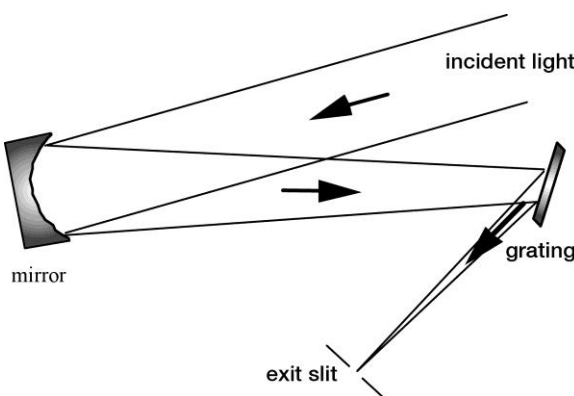


Figure 6-3. The Monk-Gillieson mount. A plane grating is used in converging light.

<sup>43</sup> W. G. Fastie, "A small plane grating monochromator," *J. Opt. Soc. Am.* **42**, 641-647 (1952); W. G. Fastie, "Image forming properties of the Ebert monochromator," *J. Opt. Soc. Am.* **42**, 647-652 (1952).

<sup>44</sup> G. S. Monk, "A mounting for the plane grating," *J. Opt. Soc. Am.* **17**, 358 (1928); A. Gillieson, "A new spectrographic diffraction grating monochromator," *J. Sci. Instr.* **26**, 334-339 (1949); T. Kaneko, T. Namioka and M. Seya, "Monk-Gillieson monochromator," *Appl. Opt.* **10**, 367-381 (1971); M. Koike and T. Namioka, "Grazing-incidence Monk-Gillieson monochromator based on surface normal rotation of a varied line-spacing grating," *Appl. Opt.* **41**, 245-257 (2002).

Since the incident light is not collimated, the grating introduces wavelength-dependent aberrations into the diffracted wavefronts (see Chapter 7). Consequently, the spectrum cannot remain in focus at a fixed exit slit when the grating is rotated (unless this rotation is about an axis displaced from the central groove of the grating<sup>45</sup>). For low-resolution applications, the Monk-Gillieson mount enjoys a certain amount of popularity, since it represents the simplest and least expensive spectrometric system imaginable.

#### 6.2.4. The Littrow monochromator<sup>46</sup>

A grating used in the Littrow or autocollimating configuration diffracts light of wavelength  $\lambda$  back along the incident light direction (Figure 6-4). In a *Littrow monochromator*, the spectrum is scanned by rotating the grating; this reorients the grating normal, so the angles of incidence  $\alpha$  and diffraction  $\beta$  change (even though  $\alpha = \beta$  for all  $\lambda$ ). The same auxiliary optics can be used as both collimator and camera, since the diffracted rays retrace the incident rays. Usually the entrance slit and exit slit (or image plane) will be offset slightly along the direction parallel to the grooves so that they do not coincide; this will generally introduce out-of-plane aberrations. True Littrow monochromators are quite popular in laser tuning applications (see Chapter 13).

#### 6.2.5. Double & triple monochromators<sup>47</sup>

Two monochromator mounts used in series form a *double monochromator*. The exit slit of the first monochromator usually serves as the entrance slit for the second monochromator (see Figure 6-5), though some systems have been designed without an intermediate slit. Stray light in a double monochromator with an intermediate slit is much lower than in a single monochromator: it is approximately the product of ratios of stray light intensity to parent line intensity for each single monochromator.

---

<sup>45</sup> D. J. Schroeder, "Optimization of converging-beam grating monochromators," *J. Opt. Soc. Am.* **60**, 1022 (1970).

<sup>46</sup> J. F. James and R. S. Sternberg, *The Design of Optical Spectrometers*, Chapman and Hall (London: 1969); R. Masters, C. Hslech and H. L. Pardue, "Advantages of an off-Littrow mounting of an echelle grating," *Appl. Opt.* **27**, 3895-3897 (1988).

<sup>47</sup> R. L. Christensen and R. J. Potter, "Double monochromator systems," *Appl. Opt.* **2**, 1049-1054 (1963); F. R. Lipsett, G. Oblinsky and S. Johnson, "Varioilluminator (subtractive double monochromator with variable bandpass)," *Appl. Opt.* **12**, 818 (1973).

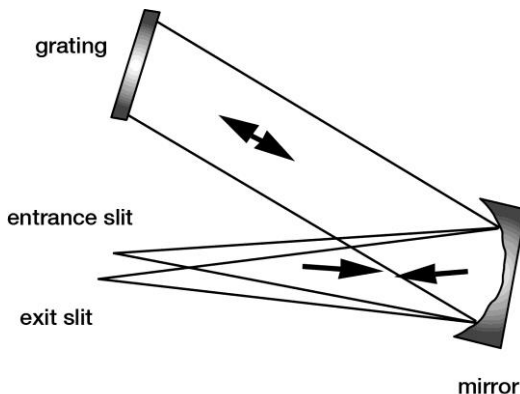


*Figure 6-4. The Littrow monochromator mount. The entrance and exit slits are slightly above and below the dispersion plane; they are shown separated for clarity.*

A double monochromator may be designed to have either *additive dispersion* or *subtractive dispersion*.

- In the case of additive dispersion, the reciprocal linear dispersion of the entire system is the sum of the reciprocal linear dispersions of each monochromator: that is, the spectrum that is dispersed by the first monochromator is further dispersed in passing through the second monochromator.
- In the case of subtractive dispersion, the entire system is designed so that the spectral dispersion at the exit slit of the second monochromator is essentially zero. A subtractive-dispersion monochromator has the property that the light leaving its exit slit is spectrally uniform: the homogeneous combination of all wavelengths is transmitted through the intermediate slit, instead of a spectrum of continuous varying wavelength as seen in single monochromators and additive-dispersion double monochromators. Such instruments have found use in Raman spectroscopy systems (in which spectral features very close to the exciting laser wavelength can be observed), and in fluorescence and luminescence excitation.<sup>48</sup>

<sup>48</sup> F. R. Lipsett, G. Bechtold, F. D. Blair, F. V. Cairns and D. H. O'Hara, "Apparatus for measurement of luminescence spectra with a digital recording system," *Appl. Opt.* **9**, 1312 (1970); R. L. McCreery, *Raman Spectroscopy for Chemical Analysis*, Wiley-Interscience (New York, New York: 2000), pp. 168 ff.

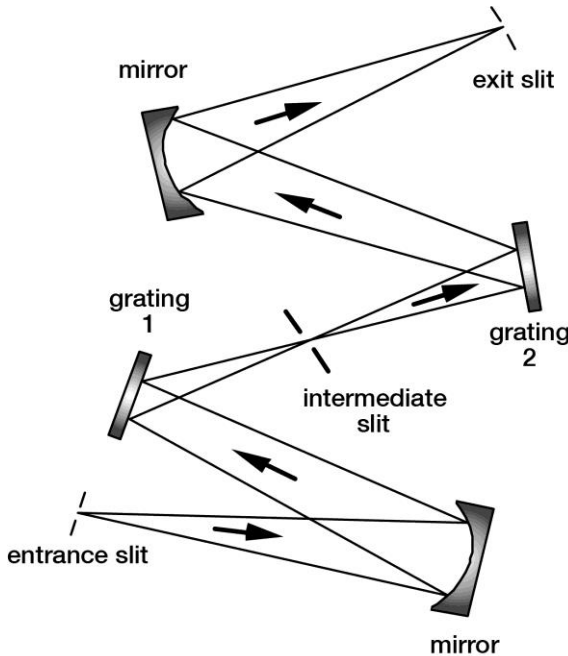


*Figure 6-5. A double monochromator mount. An intermediate slit between the two monochromators is shown.*

A *triple monochromator* mount consists of three monochromators in series. These mounts are used when the demands to reduce instrumental stray light are extraordinarily severe.<sup>49</sup>

#### 6.2.6. The constant-scan monochromator

The vast majority of monochromator mounts are of the constant deviation variety: the grating is rotated to bring different wavelengths into focus at the (stationary) exit slit. This mount has the practical advantage of requiring a single rotation stage and no other moving parts, but it has the disadvantage of being “on blaze” at only one wavelength – at other wavelengths, the incidence and diffraction angles do not satisfy the blaze condition

$$m\lambda = d (\sin \alpha + \sin \beta) = 2d \sin \theta_B, \quad (2-30)$$

<sup>49</sup> A. Walsh and J. B. Willis, “Multiple monochromators. IV. A triple monochromator and its application to near infrared, visible and ultraviolet spectroscopy,” *J. Opt. Soc. Am.* **43**, 989-993 (1953).

where  $\theta_B$  is the facet angle.

An alternative design that may be considered is the constant-scan monochromator, so called because in the grating equation

$$m\lambda = 2d \cos K \sin \phi \quad (2-8)$$

it is the scan angle  $\phi$  rather than the half-deviation angle  $K$  that remains fixed. In this mount, the bisector of the entrance and exit arms must remain at a constant angle to the grating normal as the wavelengths are scanned; the angle  $2K(\lambda) = \alpha(\lambda) - \beta(\lambda)$  between the two arms must expand and contract to change wavelength.

Constant-scan plane grating monochromators have been designed<sup>50</sup> but have not been widely adopted, due to the complexity of the required mechanisms for the precise movement of the slits. Hunter described a constant-scan monochromator for the vacuum ultraviolet in which the entrance and exit slits moved along the Rowland circle (see Section 7.2 below).<sup>51</sup> The imaging properties of the constant-scan monochromator with fixed entrance and exit arms have not been fully explored, but since each wavelength remains on blaze, there may be applications where this design proves advantageous. [As noted in Section 2.8, though, the efficiency will drop as  $|2K|$  increases, *i.e.* as the monochromator is used farther off-Littrow.]

### 6.3. PLANE GRATING SPECTROGRAPH MOUNTS<sup>52</sup>

The plane grating monochromator mounts described in Section 6.2 have an exit slit through which a narrow spectral region passes; the center wavelength of this spectra region is changed by rotating the grating. Alternatively, a wide spectral region can be imaged at once by

---

<sup>50</sup> C. Kunz, R. Haensel and B. Sonntag, "Grazing-incidence vacuum-ultraviolet monochromator with fixed exit slit for use with distant sources," *J. Opt. Soc. Am.* **58**, 1415 (1968); H. Deitrich and C. Kunz, "A grazing incidence vacuum ultraviolet monochromator with fixed exit slit," *Rev. Sci. Inst.* **43**, 434-442 (1972).

<sup>51</sup> W. R. Hunter, "On-blaze scanning monochromator for the vacuum ultraviolet," *Appl. Opt.* **21**, 1634-1642 (1982); W. R. Hunter and J. C. Rife, "Higher-order suppression in an on-blaze plane-grating monochromator," *Appl. Opt.* **23**, 293-299 (1984).

<sup>52</sup> R. F. Jarrell, "Stigmatic plane grating spectrograph with order sorter," *J. Opt. Soc. Am.* **45**, 259-269 (1955); J. Reader, "Optimizing Czerny-Turner spectrographs: a comparison between analytic theory and ray tracing," *J. Opt. Am. Soc.* **59**, 1189-1196 (1969); M. A. Gil, J. M. Simon and A. N. Fantino, "Czerny-Turner spectrograph with a wide spectral range," *Appl. Opt.* **27**, 4069-4072 (1988); N. C. Das, "Aberration properties of a Czerny-Turner

leaving the grating fixed and using a series of exits slits (or an array of detector elements) in a focal plane. Such optical systems are called *spectrographs*.

Often the imaging properties of a plane grating spectrograph (with no auxiliary optics) are acceptable over only a portion of the spectrum of interest, which requires the use of additional lenses or mirrors to provide additional focusing power to render the focal curve as close to the line (or curve) represented by the slits or detector array.

---

spectrograph using plane-holographic diffraction grating," *Appl. Opt.* **30**, 3589-3597 (1991).



## 7. CONCAVE GRATINGS AND THEIR MOUNTS

### 7.0. INTRODUCTION

A concave reflection grating can be modeled as a concave mirror that disperses; it can be thought to reflect and focus light by virtue of its concavity, and to disperse light by virtue of its groove pattern. The groove pattern can also contribute to focusing for an *aberration-reduced concave grating*.

Since their invention by Henry Rowland over one hundred years ago,<sup>53</sup> concave diffraction gratings have played an important role in spectrometry. Compared with plane gratings, they offer one important advantage: they provide the focusing (imaging) properties to the grating that otherwise must be supplied by separate optical elements. For spectroscopy below 110 nm, for which the reflectivity of available mirror coatings is low, concave gratings allow for systems free from focusing mirrors that would reduce throughput two or more orders of magnitude.

Many configurations for concave spectrometers have been designed. Some are variations of the Rowland circle, while some place the spectrum on a flat field, which is more suitable for charge-coupled device (CCD) array instruments. The Seya-Namioka concave grating monochromator is especially suited for scanning the spectrum by rotating the grating around its own axis.

### 7.1. CLASSIFICATION OF GRATING TYPES

The imaging characteristics of a concave grating system are governed by the size, location and orientation of the entrance and exit optics (the *mount*), the aberrations due to the grating, and the aberrations due to any auxiliary optics in the system. [In this chapter we address only simple systems, in which the concave grating is the single optical element; auxiliary mirrors and lenses are not considered.] The imaging properties of the grating itself are determined completely by the shape of its substrate (its *curvature* or *figure*) and the spacing and curvature of the grooves (its *groove pattern*).

---

<sup>53</sup> H. A. Rowland, “Preliminary notice of the results accomplished in the manufacture and theory of gratings for optical purposes,” *Philos. Mag.* **13**, 469 (1882).

Gratings are classified both by their groove patterns and by their substrate curvatures. In Chapter 6, we restricted our attention to plane classical gratings and their mounts. In this chapter, more general gratings and grating systems are considered.

### 7.1.1. Groove patterns

A *classical grating* is one whose grooves, when projected onto the tangent plane, form a set of straight equally-spaced lines. Until the 1980s, the vast majority of gratings were classical, in that any departure from uniform spacing, groove parallelism or groove straightness was considered a flaw. Classical gratings are made routinely both by mechanical ruling and interferometric (holographic) recording.

A *first generation holographic grating* has its grooves formed by the intersection of a family of confocal hyperboloids (or ellipsoids) with the grating substrate. When projected onto the tangent plane, these grooves have both unequal spacing and curvature. First generation holographic gratings are formed by recording the master grating in a field generated by two sets of spherical wavefronts, each of which may emanate from a point source or be focused toward a virtual point.

A *second generation holographic grating* has the light from its point sources reflected by concave mirrors (or transmitted through lenses) so that the recording wavefronts are toroidal.<sup>54</sup>

A *varied line-space (VLS) grating* is one whose grooves, when projected onto the tangent plane, form a set of straight parallel lines whose spacing varies from groove to groove. Varying the groove spacing across the surface of the grating moves the tangential focal curve, while keeping the groove straight and parallel keeps the sagittal focal curve fixed.\*

### 7.1.2. Substrate (blank) shapes

A *concave grating* is one whose surface is concave, regardless of its groove pattern or profile, or the mount in which it is used. Examples are spherical substrates (whose surfaces are portions of a sphere, which are definable with one radius) and toroidal substrates (definable by two

---

<sup>54</sup> C. Palmer, "Theory of second-generation holographic diffraction gratings," *J. Opt. Soc. Am.* **6**, 1175-1188 (1989); T. Namioka and M. Koike, "Aspheric wavefront recording optics for holographic gratings," *Appl. Opt.* **34**, 2180-2186 (1995).

\* The tangential and sagittal focal curves are defined in Section 7.1.2 below.

radii). Spherical substrates are by far the most common type of concave substrates, since they are easily manufactured and tolerated, and can be replicated in a straightforward manner. Toroidal substrates are much more difficult to align, tolerance and replicate, but astigmatism (see below) can generally be corrected better than by using a spherical substrate.<sup>55</sup> More general substrate shapes are also possible, such as ellipsoidal or paraboloidal substrates<sup>56</sup>, but tolerancing and replication complications relegate these grating surfaces out of the mainstream. Moreover, the use of aspheric substrates whose surfaces are more general than those of the toroid do not provide any additional design freedom for the two lowest-order aberrations (defocus and astigmatism; see below)<sup>57</sup>; consequently, there have been very few cases in commercial instrumentation for which the improved imaging due to aspheric substrates has been worth the cost.

The shape of a concave grating (considering only spheres & toroids) can be characterized either by its radii or its curvatures. The radii of the slice of the substrate in the principal (dispersion) plane is called the *tangential radius R*, while that in the plane parallel to the grooves at the grating center is called the *sagittal radius ρ*. Equivalently, we can define the *tangential curvature 1/R* and the *sagittal curvature 1/ρ*. For a spherical substrate,  $R = \rho$ .

A *plane grating* is one whose surface is planar. While plane gratings can be thought of as a special case of concave gratings (for which the radii of curvature of the substrate become infinite), we treat them separately here (see the previous chapter). In the equations that follow, the case of a plane grating is found simply by letting  $R$  (and  $\rho$ )  $\rightarrow \infty$ .

## 7.2. CLASSICAL CONCAVE GRATING IMAGING

In Figure 7-1, a classical grating is shown; the Cartesian axes are defined as follows: the  $x$ -axis is the outward *grating normal* to the grating surface at its center (point O), the  $y$ -axis is tangent to the grating surface at O and perpendicular to the grooves there, and the  $z$ -axis

---

<sup>55</sup> H. Haber, "The torus grating," *J. Opt. Soc. Am.* **40**, 153-165 (1950).

<sup>56</sup> T. Namioka, "Theory of the ellipsoidal concave grating. I," *J. Opt. Soc. Am.* **51**, 4-12 (1961).

<sup>57</sup> C. Palmer, "Limitations of aberration correction in spectrometer imaging," *Proc. SPIE* **1055**, 359-369 (1989).

completes the right-handed triad of axes (and is therefore parallel to the grooves at O). Light from point source A( $\xi, \eta, 0$ ) is incident on a grating at point O; light of wavelength  $\lambda$  in order  $m$  is diffracted toward point B( $\xi', \eta', 0$ ). Since point A was assumed, for simplicity, to lie in the  $xy$  plane, to which the grooves are perpendicular at point O, the image point B will lie in this plane as well; this plane is called the *principal plane* (also called the *tangential plane* or the *dispersion plane* (see Figure 7-2). Ideally, any point P( $x, y, z$ ) located on the grating surface will also diffract light from A to B.

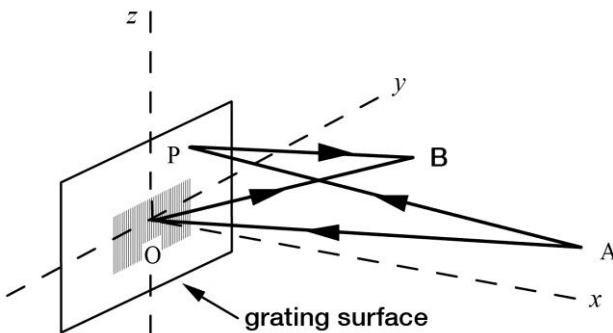


*Figure 7-1. Grating geometry of use.* The grating surface centered at O diffracts light from point A to point B. P is a general point on the grating surface. The x-axis points out of the grating from its center, the z-axis points along the central groove, and the y-axis completes the right-handed triad.

The plane through points O and B perpendicular to the principal plane is called the *sagittal plane*, which is unique for this wavelength. The *grating tangent plane* is the plane tangent to the grating surface at its center point O (*i.e.*, the  $yz$  plane). The imaging effects of the groove spacing and curvature can be completely separated from those due to the curvature of the substrate if the groove pattern is projected onto this plane.

The imaging of this optical system can be investigated by considering the optical path difference  $OPD$  between the *pole ray* AOB (where O is the center of the grating) and the *general ray* APB (where P is an arbitrary point on the grating surface). Application of Fermat's principle to this path difference, and the subsequent expansion of the results in power series of the coordinates of the tangent plane ( $y$  and  $z$ ), yields expressions for the aberrations of the system.

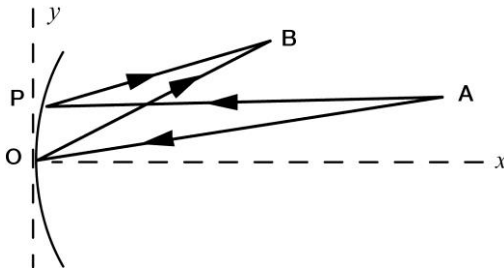


Figure 7-2. Geometry of use – the principal plane. Points A, B and O lie in the  $xy$  (principal) plane; the general point P on the grating surface may lie outside this plane. The z-axis comes out of the page at O.

The optical path difference is

$$OPD = \langle APB \rangle - \langle AOB \rangle + Nm\lambda, \quad (7-1)$$

where  $\langle APB \rangle$  and  $\langle AOB \rangle$  are the geometric lengths of the general and pole rays, respectively (both multiplied by the index of refraction),  $m$  is the diffraction order, and  $N$  is the number of grooves on the grating surface between points O and P. The last term in Eq. (7-1) accounts for the fact that the distances  $\langle APB \rangle$  and  $\langle AOB \rangle$  need not be exactly equal for the light along both rays to be in phase at B: due to the wave nature of light, the light is in phase at B even if there are an integral number of wavelengths between these two distances. If points O and P are one groove apart ( $N = 1$ ), the number of wavelengths in the difference  $\langle APB \rangle - \langle AOB \rangle$  determines the order of diffraction  $m$ .

From geometric considerations, we find

$$\begin{aligned} \langle APB \rangle &= \langle AP \rangle + \langle PB \rangle \\ &= \sqrt{(\xi - x)^2 + (\eta - y)^2 + z^2} + \sqrt{(\xi' - x)^2 + (\eta' - y)^2 + z^2}, \end{aligned} \quad (7-2)$$

and similarly for  $\langle AOB \rangle$ , if the medium of propagation is air ( $n \approx 1$ ). The optical path difference can be expressed more simply if the coordinates of points A and B are plane polar rather than Cartesian: letting

$$\langle AO \rangle = r, \quad \langle OB \rangle = r', \quad (7-3)$$

we may write

$$\begin{aligned} \xi &= r \cos \alpha, \quad \eta = r \sin \alpha; \\ \xi' &= r' \cos \beta, \quad \eta' = r' \sin \beta, \end{aligned} \quad (7-4)$$

where the angles of incidence and diffraction  $\alpha$  and  $\beta$  follow the sign convention described in Chapter 2.

The power series for  $OPD$  can be written in terms of the grating surface point coordinates  $y$  and  $z$ :

$$OPD = \sum_{i=0}^{\infty} \sum_{j=0}^{\infty} F_{ij} y^i z^j , \quad (7-5)$$

where  $F_{ij}$ , the expansion coefficient of the  $(ij)$  term, describes how the rays (or wavefronts) diffracted from point P toward the ideal image point B differ (in direction, or curvature, etc.) in proportion to  $y^i z^j$  from those from point O. The  $x$ -dependence of  $OPD$  has been suppressed by writing

$$x = x(y, z) = \sum_{i=0}^{\infty} \sum_{j=0}^{\infty} a_{ij} y^i z^j . \quad (7-6)$$

This equation makes use of the fact that the grating surface is usually a regular function of position, so  $x$  is not independent of  $y$  and  $z$  (e.g., if it is a spherical surface of radius  $R$ , then  $(x - R)^2 + y^2 + z^2 = R^2$ ).

By analogy with the terminology of lens and mirror optics, we call each term in series (7-5) an *aberration*, and  $F_{ij}$  its *aberration coefficient*. An aberration is absent from the image of a given wavelength (in a given diffraction order) if its associated coefficient  $F_{ij}$  is zero.

Since we have imposed a plane of symmetry on the system (the principal ( $xy$ ) plane), all terms  $F_{ij}$  for which  $j$  is odd vanish. Moreover,  $F_{00} = 0$ , since the expansion (7-5) is about the origin O. The lowest-(first-) order terms  $F_{10}$  and  $F_{01}$  in the expansion must equal zero in accordance with Fermat's principle. Setting  $F_{10} = 0$  yields the grating equation:

$$m\lambda = d (\sin \alpha + \sin \beta) . \quad (2-1)$$

By Fermat's principle, we may take this equation to be satisfied for all images. Setting  $F_{01} = 0$  yields the law of reflection in the plane perpendicular to the dispersion plane. Thus, the second-order aberration terms  $F_{20}$  and  $F_{02}$  are those of lowest order that need not necessarily vanish.

The generally accepted terminology is that a *stigmatic image* has vanishing second-order coefficients even if higher-order aberrations are still present. The second order terms describe the tangential and sagittal focusing:

$$F_{20} = \cos \alpha \left( \frac{\cos \alpha}{2r} - a_{20} \right) + \cos \beta \left( \frac{\cos \beta}{2r'} - a_{20} \right) \equiv T(r, \alpha) + T(r', \beta), \quad (7-7)$$

$$F_{02} = \left( \frac{1}{2r} - a_{02} \cos \alpha \right) + \left( \frac{1}{2r'} - a_{02} \cos \beta \right) \equiv S(r, \alpha) + S(r', \beta). \quad (7-8)$$

The coefficient  $F_{20}$  governs the tangential (or spectral) focusing of the grating system, while  $F_{02}$  governs the sagittal focusing. The associated aberrations are called *defocus* and *astigmatism*, respectively. These equations may be seen to be generalizations of the Coddington equations that describe the second-order focal properties of an aspheric mirror.<sup>58</sup> A procedure for constructing stigmatic points in a grating system is given by Güther and Polze.<sup>59</sup>

The two second-order aberrations describe the extent of a monochromatic image: defocus pertains to the blurring of the image – its extent of the image along the dispersion direction (*i.e.*, in the tangential plane). Astigmatism pertains to the extent of the image in the direction perpendicular to the dispersion direction. In more common (but sometimes misleading) terminology, defocus applies to the "width" of the image in the spectral (dispersion) direction, and astigmatism applies to the "height" of the spectral image; these terms imply that the  $xy$  (tangential) plane be considered as horizontal and the  $yz$  (sagittal) plane as vertical.

Actually, *astigmatism* more correctly defines the condition in which the tangential and sagittal foci are not coincident, which implies a line image at the tangential focus. It is a general result of the off-axis use of a concave mirror (and, by extension, a concave reflection grating as well). A complete three-dimensional treatment of the optical path difference [see Eq. (7.1)] shows that the image is actually a conical arc; image points away from the center of the ideal image are diffracted toward the longer wavelengths. This effect, which technically is not an aberration, is called (*spectral*) *line curvature*, and is most noticeable in the spectra of Paschen-Runge mounts (see later in this chapter).<sup>60</sup> Figure 7-3 shows

<sup>58</sup> W. J. Smith, *Modern Optical Engineering* (McGraw-Hill, New York, 2000), p. 317.

<sup>59</sup> R. Güther & S. Polze, "The Construction of Stigmatic Points for Concave Gratings", *Optica Acta* **29**, 659-665 (1982).

<sup>60</sup> M. C. Hutley, *Diffraction Gratings*, Academic Press (New York, 1970), pp. 224 ff.

astigmatism in the image of a wavelength diffracted off-axis from a concave grating, ignoring line curvature.

Since grating images are generally astigmatic, the focal distances  $r'$  in Eqs. (7-7) and (7-8) should be distinguished. Calling  $r'_T$  and  $r'_S$  the *tangential* and *sagittal focal distances*, respectively, we may set these equations equal to zero and solve for the focal curves  $r'_T(\lambda)$  and  $r'_S(\lambda)$ :

$$r'_T(\lambda) = \frac{\cos^2 \beta}{A + B \cos \beta}, \quad (7-9)$$

$$r'_S(\lambda) = \frac{1}{D + E \cos \beta}. \quad (7-10)$$

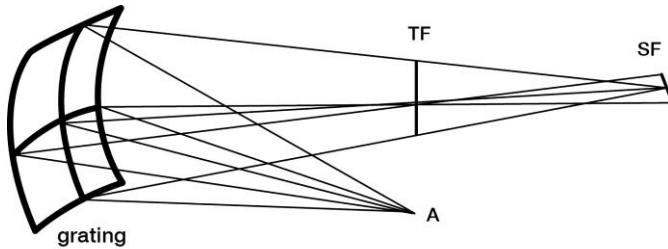


*Figure 7-3. Astigmatic focusing of a concave grating.* Light from point A is focused into a line parallel to the grooves at TF (the tangential focus) and perpendicular to the grooves at SF (the sagittal focus). Spectral resolution is maximized at TF.

Here we have defined

$$\begin{aligned} A &= B \cos \alpha - \frac{\cos^2 \alpha}{r}, & B &= 2 a_{20}, \\ D &= E \cos \alpha - \frac{1}{r}, & E &= 2 a_{02}, \end{aligned} \quad (7-11)$$

where  $a_{20}$  and  $a_{02}$  are the coefficients in Eq. (7-6) (e.g.,  $a_{20} = a_{02} = 1/(2R)$  for a spherical grating of radius  $R$ ). Eqs. (7-9) and (7-10) are completely general for classical grating systems: they apply to any type of grating mount or configuration.

Of the two primary (second-order) focal curves, that corresponding to defocus ( $F_{20}$ ) is of greater importance in spectroscopy, since it is spectral resolution that is most crucial to grating systems. For this

reason, we do not concern ourselves with locating the image plane at the "circle of least confusion"; rather, we try to place the image plane at or near the tangential focus (where  $F_{20} = 0$ ). For concave gratings ( $a_{20} \neq 0$ ), there are two well-known solutions to the defocus equation  $F_{20} = 0$ : those of Rowland and Wadsworth.

The *Rowland circle* is a circle whose diameter is equal to the tangential radius of the grating substrate, and which passes through the grating center (point O in Figure 7-5). If the point source A is placed on this circle, the tangential focal curve also lies on this circle. This solution is the basis for the Rowland circle and Paschen-Runge mounts. For the Rowland circle mount,

$$r = \frac{\cos \alpha}{2a_{20}} = R \cos \alpha, \quad (7-12)$$

$$r'_T = \frac{\cos \beta}{2a_{20}} = R \cos \beta.$$

The sagittal focal curve is

$$r'_S = \left( \frac{\cos \alpha + \cos \beta}{\rho} - \frac{1}{R \cos \alpha} \right)^{-1} \quad (7-13)$$

(where  $\rho$  is the sagittal radius of the grating), which is always greater than  $r'_T$  (even for a spherical substrate, for which  $\rho = R$ ) unless  $\alpha = \beta = 0$ . Consequently, this mount suffers from astigmatism, which in some cases is considerable.

The *Wadsworth mount* is one in which the incident light is collimated ( $r \rightarrow \infty$ ), so that the tangential focal curve is given by

$$r'_T = \frac{\cos^2 \beta}{2a_{20}(\cos \alpha + \cos \beta)} = \frac{R \cos^2 \beta}{\cos \alpha + \cos \beta}, \quad (7-14)$$

and the sagittal focal curve is

$$r'_S = \frac{1}{2a_{02}(\cos \alpha + \cos \beta)} = \frac{\rho}{\cos \alpha + \cos \beta}. \quad (7-15)$$

In this mount, the imaging from a classical spherical grating ( $\rho = R$ ) is such that the astigmatism of the image is zero only for  $\beta = 0$ , though this is true for any incidence angle  $\alpha$ .

While higher-order aberrations are usually of less importance than defocus and astigmatism, they can be significant. The third-order aberrations, *primary* or *tangential coma*  $F_{30}$  and *secondary* or *sagittal coma*  $F_{12}$ , are given by

$$F_{30} = \frac{\sin \alpha}{r} T(r, \alpha) + \frac{\sin \beta}{r'} T(r', \beta) - a_{30} (\cos \alpha + \cos \beta), \quad (7-16)$$

$$F_{12} = \frac{\sin \alpha}{r} S(r, \alpha) + \frac{\sin \beta}{r'} S(r', \beta) - a_{12} (\cos \alpha + \cos \beta), \quad (7-17)$$

where  $T$  and  $S$  are defined in Eqs. (7-7) and (7-8). Often one or both of these third-order aberrations is significant in a spectral image and must be minimized with the second-order aberrations.

### 7.3. NONCLASSICAL CONCAVE GRATING IMAGING

For nonclassical groove patterns, the aberration coefficients  $F_{ij}$  must be generalized to account for the image-modifying effects of the variations in curvature and spacing of the grooves, as well as for the focusing effects of the concave substrate:

$$F_{ij} = M_{ij} + \frac{m\lambda}{\lambda_0} H_{ij} \equiv M_{ij} + H'_{ij}. \quad (7-18)$$

The terms  $M_{ij}$  are simply those  $F_{ij}$  coefficients for classical concave grating mounts, discussed in Section 7.2 above. The  $H'_{ij}$  coefficients describe how the groove pattern differs from that of a classical grating (for classical gratings,  $H'_{ij} = 0$  for all terms of order two or higher ( $i + j \geq 2$ )). The tangential and sagittal focal distances (Eqs. (7-9) and (7-10)) must now be generalized:

$$r'_T(\lambda) = \frac{\cos^2 \beta}{A + B \cos \beta + C \sin \beta}, \quad (7-19)$$

$$r'_S(\lambda) = \frac{1}{D + E \cos \beta + F \sin \beta}, \quad (7-20)$$

where in addition to Eqs. (7-11) we have

$$C = -2 H'_{20}, \quad F = -2 H'_{02}. \quad (7-21)$$

Here  $H'_{20}$  and  $H'_{02}$  are the terms that govern the effect of the groove pattern on the tangential and sagittal focusing. For a first generation

holographic grating, for example, the  $H_{ij}$  coefficients may be written in terms of the parameters of the recording geometry (see Figure 7-4):

$$H'_{20} = -T(r_C, \gamma) + T(r_D, \delta), \quad (7-22)$$

$$H'_{02} = -S(r_C, \gamma) + S(r_D, \delta), \quad (7-23)$$

where  $C(r_C, \gamma)$  and  $D(r_D, \delta)$  are the plane polar coordinates of the recording points. These equations are quite similar to Eqs. (7-7) and (7-8), due to the similarity between Figures 7-4 and 7-2.

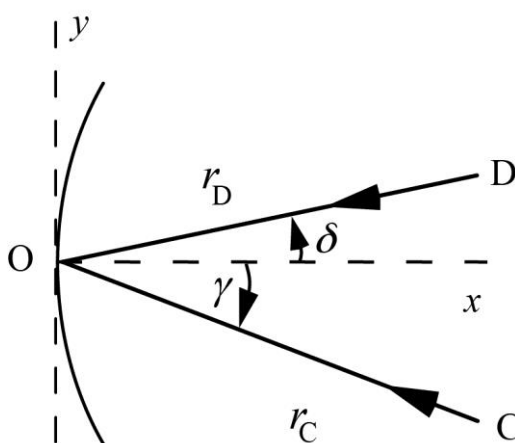


Figure 7-4. Recording parameters for a concave holographic grating. Spherical waves emanate from point sources C and D; the interference pattern forms fringes on the concave substrate centered at O.

Nonclassical concave gratings are generally produced holographically, but for certain applications, they can be made by mechanical ruling as well, by changing the groove spacing from one groove to the next during ruling<sup>61</sup>, by curving the grooves<sup>62</sup>, or both.<sup>63</sup> For such varied line-space (VLS) gratings (see Chapter 4), the terms  $H_{ij}$

<sup>61</sup> Y. Sakayanagi, "A stigmatic concave gating with varying spacing," *Sci. Light* **16**, 129-137 (1967).

<sup>62</sup> Y. Sakayanagi, *Sci. Light* **3**, 1 (1954).

<sup>63</sup> T. Harada, S. Moriyama and T. Kita, "Mechanically ruled stigmatic concave gratings," *Japan. J. Appl. Phys.* **14**, 175-179 (1974).

are written in terms of the groove spacing coefficients rather than in terms of recording coordinates.<sup>64</sup>

Several important conclusions may be drawn from the formalism developed above for grating system imaging.<sup>65</sup>

- The imaging effects of the shape of the grating substrate (manifest in the coefficients  $a_{ij}$ ) and the groove pattern (manifest in the coefficients  $H_{ij}$ ) are completely separable.
- The imaging effects of the shape of the grating substrate are contained completely in terms that are formally identical to those for the identical mirrors substrate, except that the diffraction angle is given by the grating equation (Eq. (2-1)) rather than the law of reflection.
- The imaging effects of the groove pattern are dictated completely by the spacing and curvature of the grooves when projected onto the plane tangent to the grating surface at its center.
- The  $y$ -dependence of the groove pattern governs the local groove spacing, which in turn governs the tangential aberrations of the system.
- The  $z$ -dependence of the groove pattern governs the local groove curvature, which in turn governs the sagittal aberrations of the system.

More details on the imaging properties of gratings systems can be found in Namioka<sup>66</sup> and Noda *et al.*<sup>67</sup>

#### 7.4. REDUCTION OF ABERATIONS

In the design of grating systems, there exist several degrees of freedom whose values may be chosen to optimize image quality. For monochromators, the locations of the entrance slit A and exit slit B relative to the grating center O provide three degrees of freedom (or four, if no plane of symmetry is imposed); the missing degree of freedom is

---

<sup>64</sup> C. Palmer and W. R. McKinney, "Equivalence of focusing conditions for holographic and varied line-space gratings," *Appl. Opt.* **29**, 47-51 (1990).

<sup>65</sup> C. Palmer and W. R. McKinney, "Imaging theory of plane-symmetric varied line-space grating systems," *Opt. Eng.* **33**, 820-829 (1994).

<sup>66</sup> T. Namioka, "Theory of the concave grating," *J. Opt. Soc. Am.* **49**, 446 (1959).

<sup>67</sup> H. Noda, T. Namioka and M. Seya, "Geometric theory of the grating," *J. Opt. Soc. Am.* **64**, 1031-1036 (1974).

restricted by the grating equation, which sets the angular relationship between the lines AO and BO. For spectrographs, the location of the entrance slit A as well as the location, orientation and curvature of the image field provide degrees of freedom (though the grating equation must be satisfied). In addition, the curvature of the grating substrate provides freedom, and the aberration coefficients  $H'_{ij}$  for a holographic grating (or the equivalent terms for a VLS grating) can be chosen to improve imaging. Even in systems for which the grating use geometry (the mount) has been specified, there exist several degrees of freedom due to the aberration reduction possibilities of the grating itself.

Algebraic techniques can find sets of design parameter values that minimize image size at one or two wavelengths, but to optimize the imaging of an entire spectral range is usually so complicated that computer implementation of a design procedure is essential. MKS has developed a set of proprietary computer programs to design and analyze grating systems. These programs allow selected sets of parameter values governing the use and recording geometries to vary within prescribed limits. Optimal imaging is found by comparing the imaging properties for systems with different sets of parameters values.

Design techniques for grating systems that minimize aberrations may be classified into two groups: those that consider wavefront aberrations and those that consider ray deviations. The wavefront aberration theory of grating systems was developed by Beutler<sup>68</sup> and Namioka<sup>69</sup>, and was presented in Section 7.2. The latter group contains both the familiar raytrace techniques used in commercial optical design software and the Lie aberration theory developed by Dragt.<sup>70</sup> The principles of optical raytrace techniques are widely known and taught in college courses, and are the basis of a number of commercially-available optical design software packages, so they will not be addressed here, but the concepts of

---

<sup>68</sup> H. G. Beutler, "The theory of the concave grating," *J. Opt. Soc. Am.* **35**, 311-350 (1945).

<sup>69</sup> T. Namioka, "Theory of the concave grating," *J. Opt. Soc. Am.* **49**, 446-460 (1959).

<sup>70</sup> A. J. Dragt, "Lie algebraic theory of geometrical optics and optical aberrations," *J. Opt. Soc. Am.* **72**, 372-379 (1982); K. Goto and T. Kurosaki, "Canonical formulation for the geometrical optics of concave gratings," *J. Opt. Soc. Am.* **A10**, 452-465 (1993); C. Palmer, W. R. McKinney and B. Wheeler, "Imaging equations for spectroscopic systems using Lie Transformations. Part I – Theoretical foundations," *Proc. SPIE* **3450**, 55-66 (1998); C. Palmer, B. Wheeler and W. R. McKinney, "Imaging equations for spectroscopic systems using Lie transformations. Part II - Multi-element systems," *Proc. SPIE* **3450**, 67-77 (1998).

Lie aberration theory are not widely known – for the interested reader they are summarized in Appendix B.

Design algorithms generally identify a *merit function*, an expression that returns a single value for any set of design parameter arguments; this allows two different sets of design parameter values to be compared quantitatively. Generally, merit functions are designed so that lower values correspond to better designs – that is, the ideal figure of merit is zero.

For grating system design, several merit functions may be defined. The MKS proprietary design software uses the function

$$M = w' + ch', \quad (7-24)$$

where  $w'$  and  $h'$  are the width (in the dispersion plane) and height (perpendicular to the dispersion plane) of the image, and  $c$  is a constant weighting factor.<sup>71</sup> Minimizing  $M$  therefore reduces both the width and the height of the diffracted image. Since image width (which affects spectral resolution) is almost always more important to reduce than image height,  $c$  is generally chosen to be much less than unity. If  $w'$  is expressed not as a geometric width (say, in millimeters) but a spectral width (in nanometers), then  $M$  will have these units as well; since  $h'$  is in millimeters (there being no dispersion in the direction in which  $h'$  is measured),  $c$  will have the units of reciprocal linear dispersion (e.g., nm/mm) but it is *not* a measure of reciprocal linear dispersion –  $c$  is merely a weighting factor introduced in Eq. (7-24) to ensure that image width and image height are properly weighted in the optimization routine.

For optimization over a spectral range  $\lambda_1 \leq \lambda \leq \lambda_2$ , Eq. (7-24) can be generalized to define the merit function as the maximum value of  $w' + ch'$  over all wavelengths:

$$M = \sup_{\lambda} \{w(\lambda) + ch'(\lambda)\}, \quad (7-25)$$

where the supremum function  $\sup\{\}$  returns the maximum value of all of its arguments. Defining a merit function in the form of Eq. (7-25) minimizes the maximum value of  $w' + ch'$  over all wavelengths considered. [A more general form would allow the weighting factor to be

<sup>71</sup> W. R. McKinney and C. Palmer, "Numerical design method for aberration-reduced concave grating spectrometers," *Appl. Opt.* **26**, 3018-3118 (1987).

wavelength-specific, *i.e.*,  $c \rightarrow c(\lambda)$ , and an even more general form would allow for wavelength-dependent weighting factors for  $w(\lambda)$  as well.]

Eqs. (7-24) and (7-25) consider the ray deviations in the image plane, determined either by direct ray tracing or by converting wavefront aberrations into ray deviations. An alternative merit function may be defined using Eqs. (7-19) and (7-20), the expressions for the tangential and sagittal focal distances. Following Schroeder<sup>72</sup>, we define the quantity  $\Delta(\lambda)$  as

$$\Delta(\lambda) = \left| \frac{1}{r'_T(\lambda)} - \frac{1}{r'_S(\lambda)} \right|, \quad (7-26)$$

leading to the following merit function:

$$M = \sup_{\lambda} \{\Delta(\lambda)\}. \quad (7-27)$$

This version of  $M$  will consider second-order aberrations only (*i.e.*,  $F_{20}$  (defocus) and  $F_{02}$  (astigmatism)) to minimize the distances between the tangential and sagittal focal curves for each wavelength in the spectrum.<sup>73</sup>

Noda *et al.*<sup>74</sup> have suggested using as the merit function the integral of the square of an aberration coefficient,

$$M = \int_{\lambda_1}^{\lambda_2} d\lambda (F_{ij}(\lambda))^2, \quad (7-28)$$

where the integration is over the spectrum of interest ( $\lambda_1 \leq \lambda \leq \lambda_2$ ). Choosing defocus ( $F_{20}$ ) as the aberration term would, however, not require the design routine to minimize astigmatism as well. A number  $N$  of aberrations may be considered, but this requires the simultaneous minimization of  $N$  merit functions of the form given by Eq. (7-28).<sup>75</sup>

<sup>72</sup> D. J. Schroeder, *Astronomical Optics* (Academic Press, New York, 1987), pp. 64 & 263.

<sup>73</sup> C. Palmer, "Deviation of second-order focal curves in common plane-symmetric spectrometer mounts," *J. Opt. Soc Am. A* **7**, 1770-1778 (1990).

<sup>74</sup> H. Noda, T. Namioka and M. Seya, "Geometric theory of the grating," *J. Opt. Soc Am. A* **64**, 1031-1036 (1974).

<sup>75</sup> E. Sokolova, B. Kruizinga and I. Gulobenko, "Recording of concave diffraction gratings in a two-step process using spatially incoherent light," *Opt. Eng.* **43**, 2613-2622 (2004).

Two other merit functions have been used in the design of spectrometer systems are the Strehl ratio<sup>76</sup> and the quality factor.<sup>77</sup>

## 7.5. CONCAVE GRATING MOUNTS

As with plane grating mounts, concave grating mounts can be either monochromators or spectrographs.

### 7.5.1. The Rowland circle spectrograph

The first concave gratings of spectroscopic quality were ruled by Rowland, who also designed their first mounting. Placing the ideal source point on the Rowland circle (see Eqs. (7-12) and Figure 7-5) forms spectra on that circle free from defocus and primary coma at all wavelengths (*i.e.*,  $F_{20} = F_{30} = 0$  for all  $\lambda$ ); while spherical aberration is residual and small, astigmatism is usually severe. Originally a Rowland circle spectrograph employed a photographic plate bent along a circular arc on the Rowland circle to record the spectrum in its entirety.

Today it is more common for a series of exit slits to be cut into a circular mask to allow the recording of several discrete wavelengths photoelectrically; this system is called the *Paschen-Runge mount*. Other configurations based on the imaging properties of the Rowland circle are the *Eagle mount* and the *Abney mount*, both of which are described by Hutley<sup>78</sup> and by Meltzer.<sup>79</sup>

Unless the exit slits (or photographic plates) are considerably taller than the entrance slit, the astigmatism of Rowland circle mounts usually prevents more than a small fraction of the diffracted light from being recorded, which greatly decreases the efficiency of the instrument. Increasing the exit slit heights helps collect more light, but since the images are curved, the exit slits would have to be curved as well to maintain optimal resolution. To complicate matters further, this curvature depends on the diffracted wavelength, so each exit slit would

---

<sup>76</sup> W. T. Welford, "Aberration tolerances for spectrum line images," *Opt. Acta* **10**, 121-127 (1963).

<sup>77</sup> M. Pouey, "Comparison between far ultraviolet spectrometers," *Opt. Commun.* **2**, 339-342 (1970).

<sup>78</sup> M. C. Hutley, *Diffraction Gratings*, Academic Press (New York, 1970).

<sup>79</sup> R. J. Meltzer, "Spectrographs and Monochromators," in *Applied Optics and Optical Engineering*, vol. V (chapter 3), R. Shannon, ed., Academic Press (New York: 1969).

require a unique curvature. Few instruments have gone to such trouble, so most Rowland circle grating mounts collect only a small portion of the light incident on the grating. For this reason, these mounts are adequate for strong sources (such as the observation of the solar spectrum) but not for less intense sources (such as stellar spectra).

The imaging properties of instruments based on the Rowland circle spectrograph, such as direct readers and atomic absorption instruments, can be improved by the use of nonclassical gratings. By replacing the usual concave classical gratings with concave aberration-reduced gratings, astigmatism can be improved substantially. Rowland circle mounts modified in this manner direct more diffracted light through the exit slits, though often at the expense of degrading resolution to some degree.<sup>80</sup>

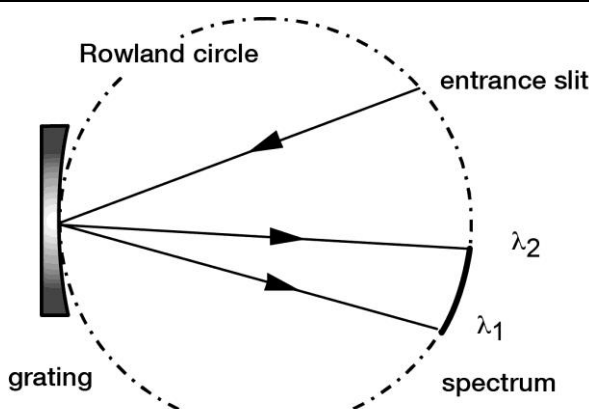


*Figure 7-5. The Rowland Circle spectrograph.* Both the entrance slit and the diffracted spectrum lie on the Rowland circle, whose diameter equals the tangential radius of curvature  $R$  of the grating and that passes through the grating center. Light of two wavelengths is shown focused at different points on the Rowland circle.

<sup>80</sup> B. J. Brown and I. J. Wilson, “Holographic grating aberration correction for a Rowland circle mount I,” *Opt. Acta (Lond.)* **28**(12), 1587–1599 (1981); B. J. Brown and I. J. Wilson, “Holographic grating aberration correction for a Rowland circle mount II,” *Opt. Acta (Lond.)* **28**(12), 1601–1610 (1981); X. Chen and L. Zeng, “Astigmatism-reduced spherical concave grating holographically recorded by a cylindrical wave and a plane wave for Rowland circle mounting,” *Appl. Opt.* **57**(25), 7281–7286 (2018).

### 7.5.2. The Wadsworth spectrograph

When a classical concave grating is illuminated with collimated light (rather than from a point source on the Rowland circle), spectral astigmatism on and near the grating normal is greatly reduced. Such a grating system is called the *Wadsworth mount* (see Figure 7-6).<sup>81</sup> The wavelength-dependent aberrations of the grating are compounded by the aberration of the collimating optics, though use of a paraboloidal mirror illuminated on-axis will reduce off-axis aberrations and spherical aberrations. The Wadsworth mount suggests itself in situations in which the light incident on the grating is naturally collimated (from, for example, astronomical sources). In other cases, an off-axis parabolic mirror would serve well as the collimating element.

### 7.5.3. Flat-field spectrographs

One of the advantages of changing the groove pattern (as on a first- or second- generation holographic grating or a VLS grating) is that the focal curves can be modified, yielding grating mounts that differ from the classical ones. A logical improvement of this kind on the Rowland circle spectrograph is the *flat-field spectrograph*, in which the tangential focal curve is removed from the Rowland circle and rendered nearly linear over the spectrum of interest (see Figure 7-7). While a grating cannot be made that images a spectrum perfectly on a line, one that forms a spectrum on a sufficiently flat surface is ideal for use in linear detector array instruments of moderate resolution. This development has had a significant effect on spectrograph design.

The relative displacement between the tangential and sagittal focal curves can also be reduced via VLS or interferometric modification of the groove pattern. In this way, the resolution of a flat-field spectrometer can be maintained (or improved) while its astigmatism is decreased; the latter effect allows more light to be transmitted through the exit slit (or onto the detector elements). An example of the process of aberration reduction is shown in Figure 7-8.

---

<sup>81</sup> F. Wadsworth, "The modern spectroscope," *Astrophys. J.* **3**, 47-62 (1896).

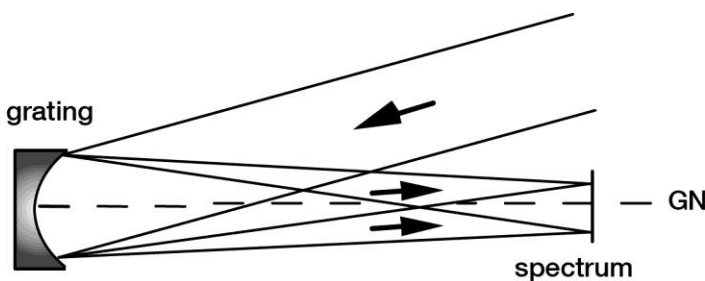


Figure 7-6. The Wadsworth spectrograph. Collimated light is incident on a concave grating; light of two wavelengths is shown focused at different points. GN is the grating normal.

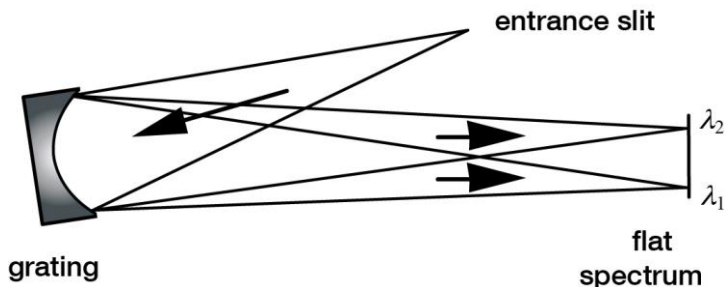


Figure 7-7. A flat-field spectrograph. The spectrum from  $\lambda_1$  to  $\lambda_2$  ( $>\lambda_1$ ) is shown imaged onto a line.

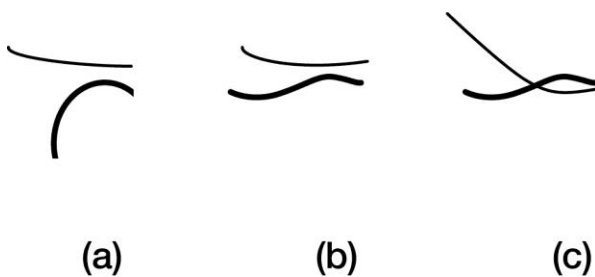


Figure 7-8. Modification of focal curves. The primary tangential focal curve ( $F_{20} = 0$ ) is thick; the primary sagittal focal curve ( $F_{02} = 0$ ) is thin. (a) Focal curves for a classical ( $H_{20} = H_{02} = 0$ ) concave grating, illuminated off the normal ( $\alpha \neq 0$ ) – the dark curve is an arc of the Rowland circle. (b) Choosing a suitable nonzero  $H_{20}$  value moves the tangential focal arc so that part of it is nearly linear, suitable for a flat-field spectrograph detector. (c) Choosing a suitable nonzero value of  $H_{02}$  moves the sagittal focal curve so that it crosses the tangential focal curve, providing a stigmatic image.

#### 7.5.4. Imaging spectrographs and monochromators<sup>82</sup>

Concave gratings may also be used in *imaging spectrographs*, which are instruments for which a spectrum is obtained for different spatial regions in the object plane. For example, an imaging spectrometer may generate a two-dimensional spatial image on a detector array, and for each such image, a spectrum is scanned (over time); alternatively, a spectrum can be recorded for a linear slice of the image, and the slice itself can be moved across the image to provide the second spatial dimension (sometimes called the “push broom” technique).

#### 7.5.5. Constant-deviation monochromators

In a constant-deviation monochromator, the angle  $2K$  between the entrance and exit arms is held constant as the grating is rotated (thus scanning the spectrum; see Figure 7-9). This angle is called the *deviation angle* or *angular deviation (AD)*. While plane or concave gratings can be used in constant-deviation mounts, only in the latter case can imaging be made acceptable over an entire spectrum without auxiliary focusing optics.

The *Seya-Namioka monochromator*<sup>83</sup> is a very special case of constant-deviation mount using a classical spherical grating, in which the deviation angle  $2K$  between the beams and the entrance and exit slit distances ( $r$  and  $r'$ ) are given by

$$2K = 70^\circ 30', \quad r = r' = R \cos(70^\circ 30'/2), \quad (7-29)$$

where  $R$  is the radius of the spherical grating substrate. The only moving part in this system is the grating, through whose rotation the spectrum is scanned. Resolution may be quite good in part of the spectrum, though it degrades farther from the optimal wavelength; astigmatism is high, but at an optimum. Replacing the grating with a classical toroidal grating can reduce the astigmatism, if the minor radius of the toroid is chosen judi-

---

<sup>82</sup> M. Descour and E. Dereliak, “Computed-tomography imaging spectrometer: experimental calibration and reconstruction results,” *Appl. Opt.* **34**, 4817-4826 (1995); P. Mouroulis, D. W. Wilson, P. D. Maker and R. E. Muller, “Convex grating types for concentric imaging spectrometers,” *Appl. Opt.* **37**, 7200-7028 (1998); M. Beasley, C. Boone, N. Cunningham, J. Green and E. Wilkinson, “Imaging spectrograph for interstellar shocks: a narrowband imaging payload for the far ultraviolet,” *Appl. Opt.* **43**, 4633-4642 (2004).

<sup>83</sup> M. Seya, “A new mounting of concave grating suitable for a spectrometer,” *Science of Light* **2**, 8-17 (1952); T. Namioka, “Theory of the concave grating. III. Seya-Namioka monochromator,” *J. Opt. Soc. Am.* **49**, 951-961 (1959).

ciously. The reduction of astigmatism by suitably designed holographic gratings is also helpful, though the best way to optimize the imaging of a constant-deviation monochromator is to relax the restrictions given by Eqs. (7-29) on the use geometry.

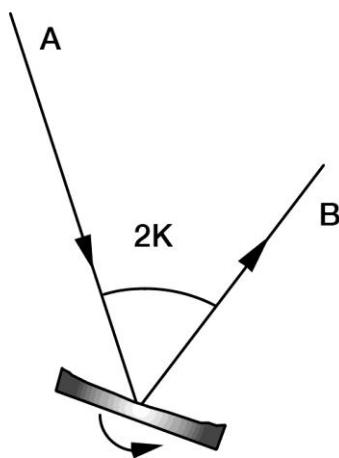


*Figure 7-9. Constant-deviation monochromator geometry.* To scan wavelengths, the entrance slit A and exit slit B remain fixed as the grating rotates. The deviation angle  $2K$  is measured from the exit arm to the entrance arm. The Seya-Namioka monochromator is a special case for which Eqs. (7-29) are satisfied.



## 8. IMAGING PROPERTIES OF GRATING SYSTEMS

### 8.1. CHARACTERIZATION OF IMAGING QUALITY

In Chapter 7, we formulated the optical imaging properties of a grating system in terms of wavefront aberrations. After arriving at a design, though, this approach is not ideal for observing the imaging properties of the system. Two tools of image analysis – spot diagrams and linespread functions – are discussed below.

#### 8.1.1. Geometric raytracing and spot diagrams

Raytracing (using the laws of geometrical optics) is superior to wavefront aberration analysis in the determination of image quality. Aberration analysis is an approximation to image analysis, since it involves expanding quantities in infinite power series and considering only a few terms. Raytracing, on the other hand, does not involve approximations, but shows (in the absence of the diffractive effects of physical optics) where each ray of light incident on the grating will diffract. It would be more exact to design grating systems with a raytracing procedure as well, though to do so would be computationally cumbersome.

The set of intersections of the diffracted rays and the image plane forms a set of points, called a *spot diagram*. In Figure 8-1, several simple spot diagrams are shown; their horizontal axes are in the plane of dispersion (the tangential plane), and their vertical axes are in the sagittal plane. In (a) an uncorrected (out-of-focus) image is shown; (b) shows good tangential focusing, and (c) shows virtually point-like imaging. All three of these images are simplistic in that they ignore the effects of line curvature as well as higher-order aberrations (such as coma and spherical aberration), which render typical spot diagrams asymmetric, as in (d).

A straightforward method of evaluating the imaging properties of a spectrometer at a given wavelength is to measure the tangential and sagittal extent of an image (often called the width  $w'$  and height  $h'$  of the image, respectively), as in Figure 8-2.

Geometric raytracing provides spot diagrams in good agreement with observed spectrometer images, except for well-focused images, in which

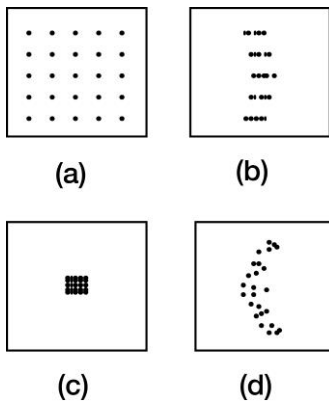


*Figure 8-1. Spot diagrams.* In (a) the image is out of focus. In (b), the image is well focused in the tangential plane only; the line curvature inherent to grating-diffracted images is shown. In (c) the image is well focused in both directions – the individual spots are not discernible. In (d) a more realistic image is shown.

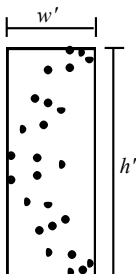


*Figure 8-2. Image dimensions.* The width  $w'$  and height  $h'$  of the image in the image plane are the dimensions of the smallest rectangle that contains the spots. The sides of the rectangle are taken to be parallel ( $w'$ ) and perpendicular ( $h'$ ) to the principal plane.

the wave nature of light dictates a minimum size for the image. Even if the image of a point object is completely without aberrations, it is not a point image, due to the diffraction effects of the pupil (which is usually the perimeter of the grating). The minimal image size, called the *diffraction limit*, can be estimated for a given wavelength by the diameter  $a$  of the Airy disk for a mirror in the same geometry:

$$a = 2.44\lambda f/\text{no}_{\text{OUTPUT}} = 2.44\lambda \frac{r'(\lambda)}{W \cos \beta}. \quad (8-1)$$

Here  $f/\text{no}_{\text{OUTPUT}}$  is the output focal ratio,  $r'(\lambda)$  is the focal distance for this wavelength, and  $W$  is the width of the grating (see Eq. (2-26), Chapter 2).

Results from raytrace analyses that use the laws of geometrical optics only should not be considered valid if the dimensions of the image are found to be near or below the diffraction limit calculated from Eq. (8-1).

### 8.1.2. Linespread calculations

A fundamental problem with geometric raytracing procedures (other than that they ignore the variations in energy density throughout a cross-section of the diffracted beam and the diffraction efficiency of the grating) is its ignorance of the effect that the size and shape of the exit aperture has on the measured resolution of the instrument.

An alternative to merely measuring the extent of a spectral image is to compute its *linespread function*, which is the convolution of the (monochromatic) image of the entrance slit with the exit aperture (the exit slit in a monochromator, or a detector element in a spectrograph). A close physical equivalent is obtained by scanning the monochromatic image by moving the exit aperture past it in the image plane and recording the light intensity passing through the slit as a function of position in this plane.

The linespread calculation thus described accounts for the effect that the entrance and exit slit dimensions have on the resolution of the grating system.

## 8.2. INSTRUMENTAL IMAGING

With regard to the imaging of actual optical instruments, it is not sufficient to state that ideal performance (in which geometrical aberrations are eliminated and the diffraction limit is ignored) is to focus a point object to a point image. All real sources are extended sources – that is, they have finite widths and heights.

### 8.2.1. Magnification of the entrance aperture

The image of the entrance slit, ignoring aberrations and the diffraction limit, will not have the same dimensions as the entrance slit itself. Calling  $w$  and  $h$  the width and height of the entrance slit, and  $w'$  and  $h'$  the width and height of its image, the *tangential* and *sagittal magnifications*  $\chi_T$  and  $\chi_S$  are

$$\chi_T \equiv \frac{w'}{w} = \frac{r' \cos \alpha}{r \cos \beta}, \quad \chi_S \equiv \frac{h'}{h} = \frac{r'}{r}. \quad (8-2)$$

These relations, which indicate that the size of the image of the entrance slit will usually differ from that of the entrance slit itself, are derived below.

Figure 8-3 shows the plane of dispersion. The grating center is at O; the  $x$ -axis is the grating normal and the  $y$ -axis is the line through the grating center perpendicular to the grooves at O. Monochromatic light of wavelength  $\lambda$  leaves the entrance slit (of width  $w$ ) located at the polar coordinates  $(r, \alpha)$  from the grating center O and is diffracted along angle  $\beta$ . When seen from O, the entrance slit subtends an angle  $\Delta\alpha = w/r$  in the

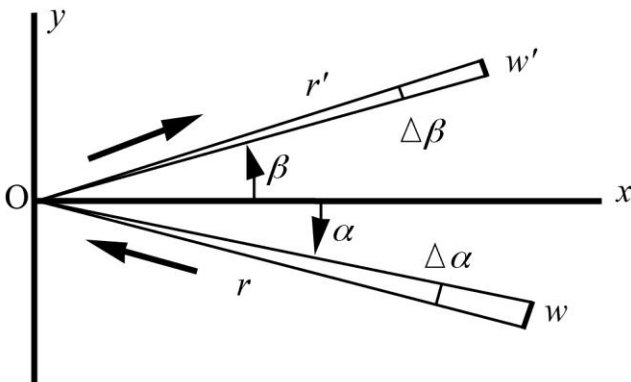


*Figure 8-3. Geometry showing tangential magnification. Monochromatic light from the entrance slit, of width  $w$ , is projected by the grating to form an image of width  $w'$ .*

dispersion ( $xy$ ) plane. Rays from one edge of the entrance slit have incidence angle  $\alpha$ , and are diffracted along  $\beta$ ; rays from the other edge have incidence angle  $\alpha + \Delta\alpha$ , and are diffracted along  $\beta - \Delta\beta$ .<sup>\*</sup> The image (located a distance  $r'$  from O), therefore subtends an angle  $\Delta\beta$  when seen from O, has width  $w' = r'\Delta\beta$ . The ratio  $\chi_T = w'/w$  is the tangential magnification.

We may apply the grating equation to the rays on either side of the entrance slit:

$$Gm\lambda = \sin\alpha + \sin\beta, \quad (8-3)$$

$$Gm\lambda = \sin(\alpha + \Delta\alpha) + \sin(\beta - \Delta\beta). \quad (8-4)$$

\* In this section, both  $\Delta\alpha$  and  $\Delta\beta$  are taken to be positive incremental angles, so by Eq. (2-1), a positive change in  $\alpha$  will lead to a negative change in  $\beta$ .

Here  $G$  ( $= 1/d$ ) is the groove frequency along the  $y$ -axis at O, and  $m$  is the diffraction order. Expanding  $\sin(\alpha + \Delta\alpha)$  in Eq. (8-4) in a Taylor series about  $\Delta\alpha = 0$ , we obtain

$$\sin(\alpha + \Delta\alpha) = \sin\alpha + (\cos\alpha)\Delta\alpha + \dots, \quad (8-5)$$

where terms of order two or higher in  $\Delta\alpha$  have been truncated. Using Eq. (8-5) (and its analogue for  $\sin(\beta - \Delta\beta)$ ) in Eq. (8-4), and subtracting it from Eq. (8-3), we obtain

$$\cos\alpha\Delta\alpha = \cos\beta\Delta\beta, \quad (8-6)$$

and therefore

$$\frac{\Delta\beta}{\Delta\alpha} = \frac{\cos\alpha}{\cos\beta}, \quad (8-7)$$

from which the first of Eqs. (8-2) follows.

Figure 8-4 shows the same situation in the sagittal plane, which is perpendicular to the principal plane and contains the pole diffracted ray. The entrance slit is located below the principal plane; consequently, its image is above this plane. A ray from the top of the center of the entrance slit is shown. Since the grooves are parallel to the sagittal plane at O, the grating acts as a mirror in this plane, so the angles  $\phi$  and  $\phi'$  are equal in magnitude.

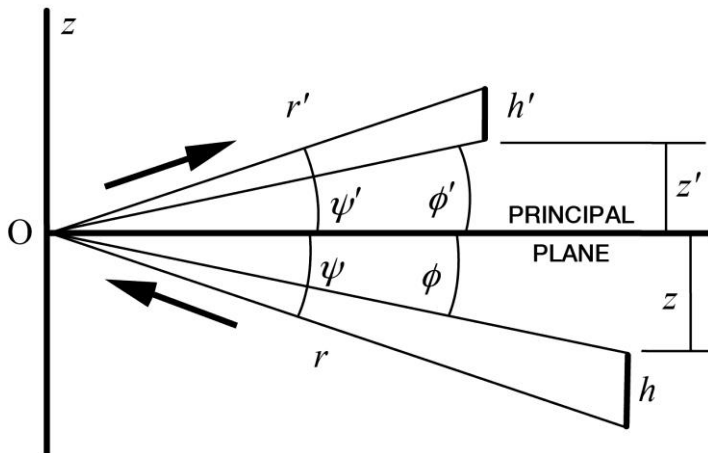


Figure 8-4. Geometry showing sagittal magnification. Monochromatic light from the entrance slit, of height  $h$ , is projected by the grating to form an image of height  $h'$ .

Ignoring signs, the tangents of these angles are equal as well:

$$\tan\phi = \tan\phi' \rightarrow \frac{z}{r} = \frac{z'}{r'}, \quad (8-8)$$

where  $z$  and  $z'$  are the distances from the entrance and exit slit points to the principal plane. A ray from an entrance slit point a distance  $|z + h|$  from this plane will image toward a point  $|z' + h'|$  from this plane, where  $h'$  now defines the height of the image. As this ray is governed by reflection as well,

$$\tan\psi = \tan\psi' \rightarrow \frac{z+h}{r} = \frac{z'+h'}{r'}. \quad (8-9)$$

Simplifying this using Eq. (8-8) yields the latter of Eqs. (8-2).

### 8.2.2. Effects of the entrance aperture dimensions

Consider a spectrometer with a point source located in the principal plane: the aberrated image of this point source has width  $\delta w'$  (in the dispersion direction) and height  $\delta h'$  (see Figure 8-5). If the point source is located out of the principal plane, it will generally be distorted, tilted and enlarged: its dimensions are now  $\delta W'$  and  $\delta H'$ . Because a point source is considered, these image dimensions are not due to any magnification effects of the system.

Now consider a rectangular entrance slit of width  $W_0$  (in the dispersion plane) and height  $H_0$ . If we ignore aberrations and line curvature (see Section 7.2) for the moment, we see that the image of the entrance slit is also a rectangle, whose width  $W_0'$  and height  $H_0'$  are magnified:

$$W_0' = \chi_T W_0, \quad H_0' = \chi_S H_0 \quad (8-10)$$

(see Figure 8-6).

Combining these two cases provides the following illustration (Figure 8-7). From this figure, we can estimate the width  $W'$  and height  $H'$  of the image of the entrance slit, considering both magnification effects and aberrations, as follows:

$$W' = \chi_T W_0 + \delta W' = \frac{r' \cos \alpha}{r \cos \beta} W_0 + \delta W', \quad (8-11a)$$

$$H' = \chi_S H_0 + \delta H' = \frac{r'}{r} H_0 + \delta H'. \quad (8-11b)$$

Eqs. (8-11) allow the imaging properties of a grating system with an entrance slit of finite area to be estimated quite well from the imaging properties of the system in which an infinitesimally small object point is considered. In effect, rays need only be traced from one point in the entrance slit (which determines  $\delta W'$  and  $\delta H'$ ), from which the image dimensions for an extended entrance slit can be calculated using Eqs. (8-10).\*

### 8.2.3. Effects of the exit aperture dimensions

The linespread function for a spectral image, as defined above, depends on the width of the exit aperture as well as on the width of the diffracted image itself. In determining the optimal width of the exit slit (or single detector element), a rule of thumb is that the width  $w''$  of the exit aperture should roughly match the width  $w'$  of the image of the entrance aperture, as explained below.

Typical linespread curves for the same diffracted image scanned by three different exit slit widths are shown in Figure 8-8. For simplicity, we have assumed  $\chi_T = 1$  for these examples. The horizontal axis is position along the image plane, in the plane of dispersion. This axis can also be thought of as a wavelength axis (that is, in spectral units); the two axes are related via the dispersion. The vertical axis is relative light intensity (or throughput) at the image plane; its bottom and top represent no intensity and total intensity (or no rays entering the slit and all rays entering the slit), respectively. Changing the horizontal coordinate represents scanning the monochromatic image by moving the exit slit across it, in the plane of dispersion. This is approximately equivalent to changing the wavelength while keeping the exit slit fixed in space.

An exit slit that is narrower than the image ( $w'' < w'$ ) will result in a linespread graph such as that seen in Figure 8-8(a). In no position of the exit slit (or, for no diffracted wavelength) do all diffracted rays fall within the slit, as it is not wide enough; the relative intensity does not reach its maximum value of unity. In (b), the exit slit width matches the width of the image:  $w'' = w'$ . At exactly one point during the scan, all of the diffracted light is contained within the exit slit; this point is the peak (at a

---

\* These equations fail to consider the effects of line curvature, so they must be regarded as approximate, though their accuracy should be acceptable for plane-symmetric grating systems (*i.e.*, those whose entrance slit is centered in the dispersion plane) provided the entrance slit is not too tall ( $H_0 \ll r$ ).

### Point Source

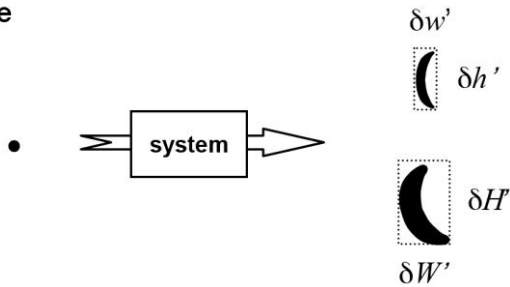


Figure 8-5. *Point source imaging.* A point source is imaged by the system; the upper image is for a point source located at the center of the entrance slit (in the dispersion plane), and the lower image shows how this image is tilted and distorted (and generally gets larger) for a point source off the dispersion plane.

### Entrance Slit – without aberrations

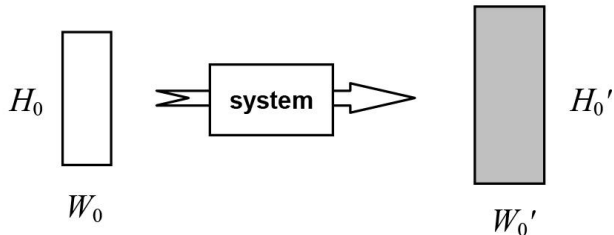


Figure 8-6. *Entrance slit imaging (without aberrations).* Ignoring aberrations and line curvature, the image of a rectangular entrance slit is also a rectangle, one that has been magnified in both directions.

### Entrance Slit – with aberrations

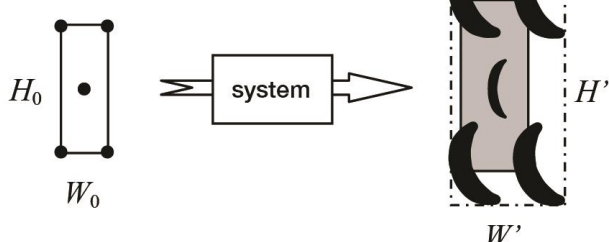
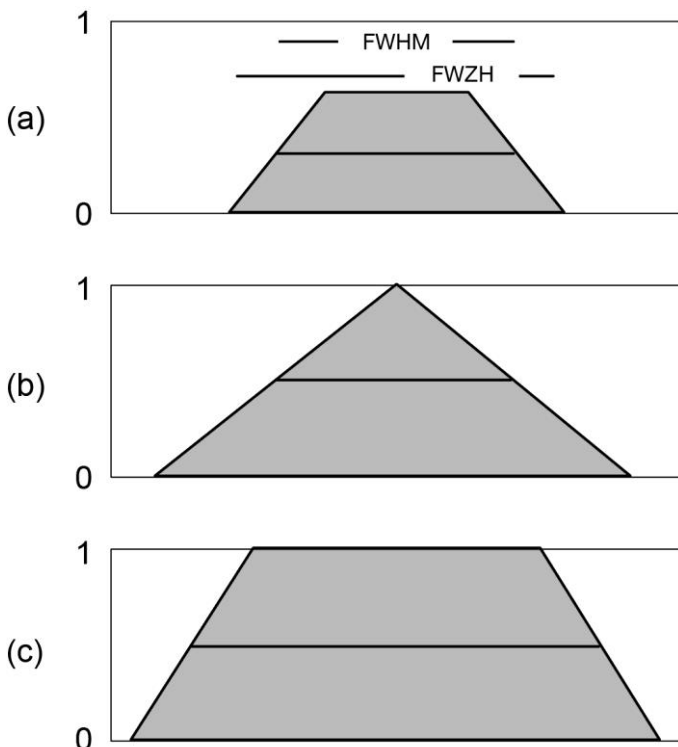


Figure 8-7. *Entrance slit imaging (including aberrations).* Superimposing the point-source images for the four corners of the entrance slit onto the (unaberrated) image of the entrance slit leads to the diagram above, showing that the rectangle in which the entire image lies has width  $W'$  and height  $H'$ .

relative intensity of unity) of the curve. In (c) the exit slit is wider than the image ( $w'' > w'$ ). The exit slit contains the entire image for many positions of the exit slit.



*Figure 8-8. Linespread curves for different exit slit widths.* The vertical axis is relative intensity at the exit aperture, and the horizontal axis is position along the image plane (in the plane of dispersion). For a given curve, the dark horizontal line shows the FWHM (the width of that portion of the curve in which its amplitude exceeds its half maximum); the FWZH is the width of the entire curve. (a)  $w'' < w'$ ; (b)  $w'' = w'$ ; (c)  $w'' > w'$ . In (a) the peak is below unity. In (a) and (b), the FWHM are approximately equal. Severely aberrated images will yield linespread curves that differ from those above (in that they will be asymmetric), although their overall shape will be similar.

In these figures the quantities FWZH and FWHM are shown. These are abbreviations for full width at zero height and full width at half maximum. The FWZH is simply the total extent of the linespread function, usually expressed in spectral units. The FWHM is the spectral extent between the two extreme points on the linespread graph that are at

half the maximum value. The FWHM is often used as a quantitative measure of image quality in grating systems; it is often called the effective spectral bandwidth. The FWZH is sometimes called the full spectral bandwidth. It should be noted that the terminology is not universal among authors and sometimes quite confusing.

As the exit slit width  $w'$  is decreased, the effective bandwidth will generally decrease. If  $w'$  is roughly equal to the image width  $w$ , though, further reduction of the exit slit width will not reduce the bandwidth appreciably. This can be seen in Figure 8-8, in which reducing  $w'$  from case (c) to case (b) results in a decrease in the FWHM, but further reduction of  $w'$  to case (a) does not reduce the FWHM.

The situation in  $w'' < w'$  is undesirable in that diffracted energy is lost (the peak relative intensity is low) since the exit slit is too narrow to collect all the diffracted light at once. The situation  $w'' > w'$  is also undesirable, since the FWHM is excessively large (or, similarly, an excessively wide band of wavelengths is accepted by the wide slit). The situation  $w'' = w'$  seems optimal: when the exit slit width matches the width of the spectral image, the relative intensity is maximized while the FWHM is minimized. An interesting curve is shown in Figure 8-9, in which the ratio FWHM/FWZH is shown vs. the ratio  $w''/w'$  for a typical grating system. This ratio reaches its single minimum near  $w'' = w'$ .

The height of the exit aperture has a more subtle effect on the imaging properties of the spectrometer, since by 'height' we mean extent in the direction perpendicular to the plane of dispersion. If the exit slit height is less than the height (sagittal extent) of the image, some diffracted light will be lost, as it will not pass through the aperture. Since diffracted images generally display curvature, truncating the sagittal extent of the image by choosing a short exit slit also reduces the width of the image (see Figure 8-10). This latter effect is especially noticeable in Paschen-Runge mounts.

In this discussion we have ignored the diffraction effects of the grating aperture: the comments above consider only the effects of geometrical optics on instrumental imaging. For cases in which the entrance and exit slits are equal in width, and this width is two or three times the diffraction limit, the linespread function is approximately Gaussian in shape rather than the triangle shown in Figure 8-8(b).

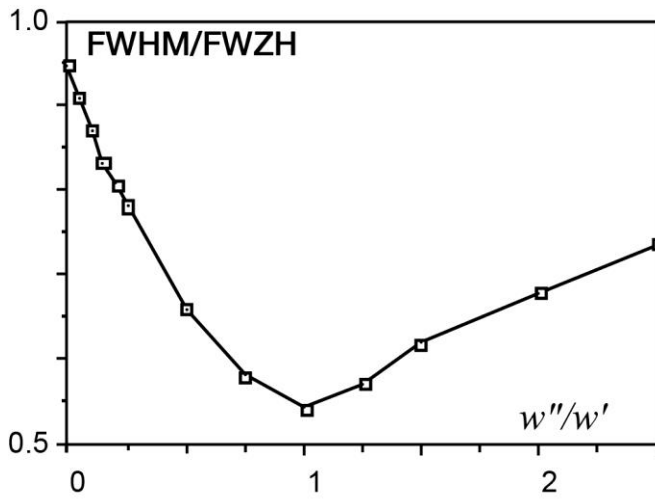


Figure 8-9.  $FWHM/FWZH$  vs.  $w''/w'$  for a typical system.

### 8.3. INSTRUMENTAL BANDPASS

The *instrumental bandpass* of an optical spectrometer depends on both the dimensions of the image of the entrance slit and the exit slit dimensions. Ignoring the effects of the image height, the instrumental bandpass  $B$  is given by

$$B = P \sup(w', w'') \quad (8-12)$$

where  $P$  is the reciprocal linear dispersion (see Eq. (2-17)),  $w'$  is the image width,  $w''$  is the width of the exit slit, and  $\sup(w', w'')$  is the greater of its arguments (*i.e.*, the two-argument version of Eq. (7-25)):

$$\sup(w', w'') = \begin{cases} w' & \text{if } w' > w'' \\ w'' & \text{otherwise} \end{cases}. \quad (8-13)$$

As  $P$  is usually expressed in nm/mm, the widths  $w'$  and  $w''$  must be expressed in millimeters to obtain the bandpass  $B$  in nanometers.

In cases where the image of the entrance slit is wider than the exit slit (that is,  $w' > w''$ ), the instrumental bandpass is said to be *imaging limited*, whereas in those cases where the exit slit is wider than the image of the entrance slit ( $w' < w''$ ), the instrumental bandpass is said to be *slit limited*. [When an imaging-limited optical system is imaging limited due

primarily to the grating, either because of the resolving power of the grating or due to its wavefront errors, the system is said to be *grating limited*.]

---

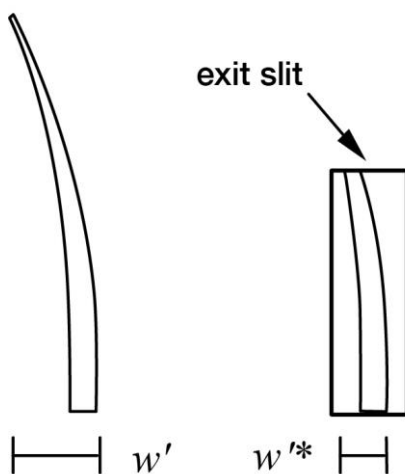


Figure 8-10. Effect of exit slit height on image width. Both the width and the height of the image are reduced by the exit slit chosen. Even if the width of the exit slit is greater than the width of the image, truncating the height of the image yields  $w'^* < w'$ . [Only the top half of each image is shown.]

---

In the design of optical spectrometers, the widths of the entrance and exit slits are chosen by balancing spectral resolution (which improves as the slits become narrower, to a limit) and optical throughput (which improves as the slits widen, up to a limit). Ideally, the exit slit width is matched to the width of the image of the entrance slit (case (b) in Figure 8-8:  $w' = w''$ ) – this optimizes both resolution and throughput. This optimum may only be achievable for one wavelength, the resolution of the other wavelengths generally being either slit-limited or imaging-limited (with suboptimal throughput likely as well).

## 9. EFFICIENCY CHARACTERISTICS OF DIFFRACTION GRATINGS

### 9.0. INTRODUCTION

Efficiency and its variation with wavelength and spectral order are important characteristics of a diffraction grating. For a reflection grating, efficiency is defined as the energy flow (power) of monochromatic light diffracted into the order being measured, relative either to the energy flow of the incident light (*absolute efficiency*) or to the energy flow of specular reflection from a polished mirror substrate coated with the same material (*relative efficiency*). [Intensity may substitute for energy flow in these definitions.] Efficiency is defined similarly for transmission gratings, except that an uncoated substrate is used in the measurement of relative efficiency.

High-efficiency gratings are desirable for several reasons. A grating with high efficiency is more useful than one with lower efficiency in measuring weak transition lines in optical spectra. A grating with high efficiency may allow the reflectivity and transmissivity specifications for the other components in the spectrometer to be relaxed. Moreover, higher diffracted energy may imply lower instrumental stray light due to other diffracted orders, as the total energy flow for a given wavelength leaving the grating is conserved (being equal to the energy flow incident on it minus any scattering and absorption).

Control over the magnitude and variation of diffracted energy with wavelength is called *blazing*, and it involves the manipulation of the micro-geometry of the grating grooves. As early as 1874, Lord Rayleigh recognized that the energy flow distribution (by wavelength) of a diffraction grating could be altered by modifying the shape of the grating grooves.<sup>84</sup> It was not until four decades later that R.W. Wood showed this to be true when he ruled a grating on which he had controlled the groove shape, thereby producing the first deliberately blazed diffraction grating.<sup>85</sup>

---

<sup>84</sup> J. W. Strutt, Lord Rayleigh, "On the manufacture and theory of diffraction gratings," *Philos. Mag.* **47**, 193-205 (1874).

<sup>85</sup> R. Wood, "The echelle grating for the infra-red," *Philos. Mag.* **20** (series 6), 770-778 (1910).

The choice of an optimal efficiency curve for a grating depends on the specific application. For some cases the desired instrumental response is linear with wavelength; that is, the ratio of intensity of light and the electronic signal into which it is transformed is to be nearly constant across the spectrum. To approach this as closely as possible, the spectral emissivity of the light source and the spectral response of the detector should be considered, from which the desired grating efficiency curve can be derived. Usually this requires peak grating efficiency in the region of the spectrum where the detectors are least sensitive; for example, a visible-light spectrometer using a silicon detector would be much less sensitive in the blue than in the red, suggesting that the grating itself be blazed to yield a peak efficiency in the blue.

A typical *efficiency curve* (a plot of absolute or relative diffracted efficiency *vs.* diffracted wavelength  $\lambda$ ) is shown in Figure 9-1. Usually such a curve shows a single maximum, at the *peak wavelength* (or *blaze wavelength*)  $\lambda_B$ . This curve corresponds to a given diffraction order  $m$ ; the peak of the curve decreases in magnitude and shifts toward shorter wavelengths as  $|m|$  increases. The efficiency curve also depends on the angles of use (*i.e.*, the angles of incidence and diffraction). Moreover, the curve depends on the groove spacing  $d$  (more appropriately, on the dimensionless parameter  $\lambda/d$ ) and the material with which the grating is coated (for reflection gratings) or made (for transmission gratings).

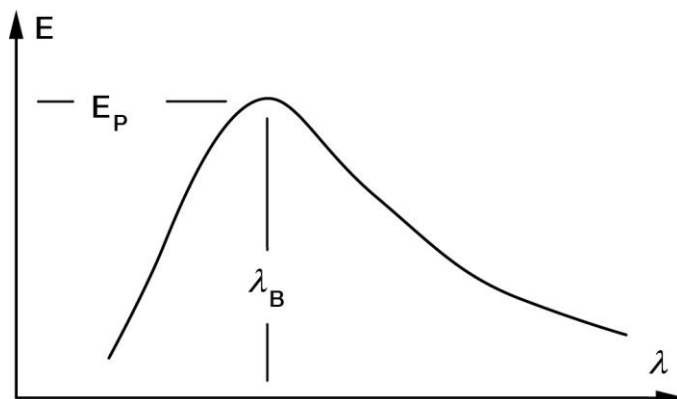


*Figure 9-1. A typical (simplified) efficiency curve.* This curve shows the efficiency  $E$  of a grating in a given spectral order  $m$ , measured *vs.* the diffracted wavelength  $\lambda$ . The peak efficiency  $E_P$  occurs at the blaze wavelength  $\lambda_B$ .

In many instances the diffracted power depends on the polarization of the incident light. *P-plane* or *TE polarized light* is polarized parallel to the grating grooves, while *S-plane* or *TM polarized light* is polarized perpendicular to the grating grooves (see Figure 9-2). For completely unpolarized incident light, the efficiency curve will be exactly halfway between the P and S efficiency curves.

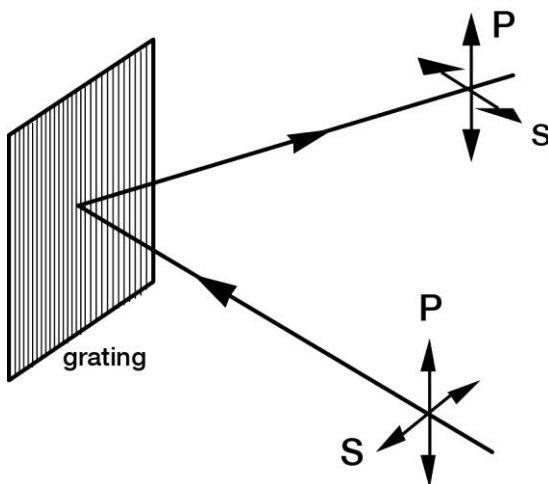
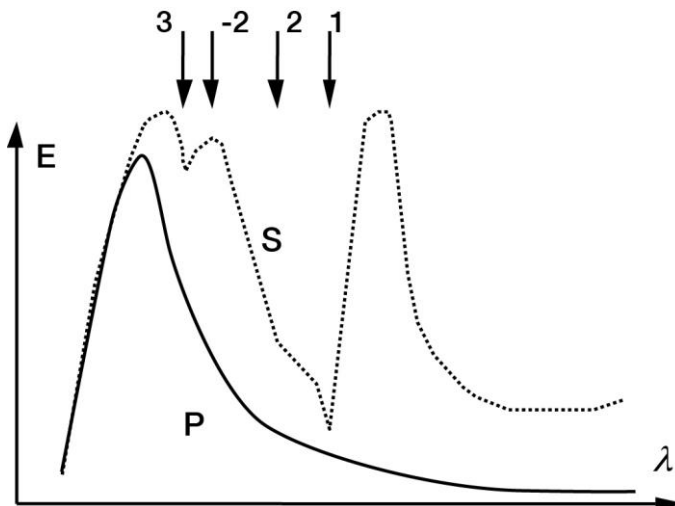


Figure 9-2. *S* and *P* polarizations. The *P* polarization components of the incident and diffracted beams are polarized parallel to the grating grooves; the *S* components are polarized perpendicular to the *P* components. Both the *S* and *P* components are perpendicular to the propagation directions.

Usually light from a single spectral order  $m$  is used in a spectroscopic instrument, so a grating with ideal efficiency characteristics would diffract all the power incident on it into this order (for the wavelength range considered). In practice, this is never true: the distribution of the power by the grating depends in a complicated way on the groove spacing and profile, the spectral order, the wavelength, and the grating material.

*Anomalies* are locations on an efficiency curve (efficiency plotted *vs.* wavelength) at which the efficiency changes abruptly. First observed by R. W. Wood, these sharp peaks and troughs in an efficiency curve are sometimes referred to as Wood's anomalies. Anomalies are rarely observed in P polarization efficiency curves, but they are often seen in S polarization curves (see Figure 9-3). Anomalies are discussed in more detail in Section 9.13.



*Figure 9-3. Anomalies in the first order for a typical grating with triangular grooves. The P efficiency curve (solid line) is smooth, but anomalies are evident in the S curve (dashed line). The passing-off locations are identified by their spectral order at the top of the figure.*

## 9.1. GRATING EFFICIENCY AND GROOVE SHAPE

The maximum efficiency of a grating is typically obtained with a simple smooth triangular groove profile, as shown in Figure 9-4, when the groove (or blaze) angle  $\theta_B$  is such that the specular reflection angle for the angle of incidence is equal (in magnitude and opposite in sign) to the angle of diffraction (see Section 2.8). Ideally, the groove facet should be flat with smooth straight edges and be generally free from irregularities on a scale comparable to a small fraction ( $< 1/10$ ) of the wavelength of light being diffracted.

Fraunhofer was well aware that the distribution of power among the various diffraction orders depended on the shape of the individual grating grooves. Wood, many decades later, was the first to achieve a degree of control over the groove shape, thereby concentrating spectral energy into one angular region. Wood's gratings were seen to light up, or *blaze*, when viewed at the correct angle.

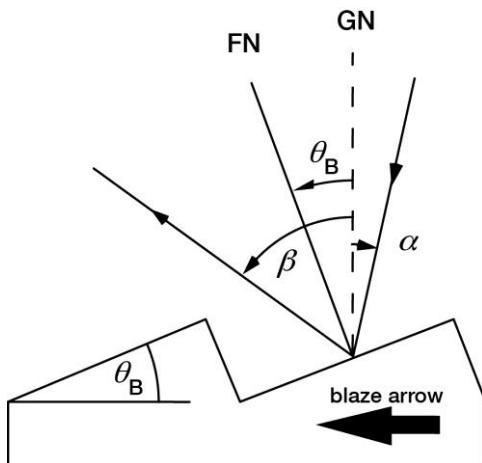


*Figure 9-4. Triangular groove geometry.* The angles of incidence  $\alpha$  and diffraction  $\beta$  are shown in relation to the facet angle  $\theta_B$ . GN is the grating normal and FN is the facet normal. When the facet normal bisects the angle between the incident and diffracted rays, the grating is used in the blaze condition. The blaze arrow (shown) points from GN to FN.

## 9.2. EFFICIENCY CHARACTERISTICS FOR TRIANGULAR-GROOVE GRATINGS

Gratings with triangular grooves can be generated by mechanical ruling, holographically using the Sheridan technique or by blazing the sinusoidal groove profile of a holographic grating by ion etching. The efficiency behavior of gratings with triangular groove profiles may be divided into six families, depending on the blaze angle:<sup>86</sup>

family	blaze angle
very low blaze angle	$\theta_B < 5^\circ$
low blaze angle	$5^\circ < \theta_B < 10^\circ$
medium blaze angle	$10^\circ < \theta_B < 18^\circ$
special low anomaly	$18^\circ < \theta_B < 22^\circ$
high blaze angle	$22^\circ < \theta_B < 38^\circ$
very high blaze angle	$\theta_B > 38^\circ$

<sup>86</sup> E. G. Loewen, M. Nevière and D. Maystre, "Grating efficiency theory as it applies to blazed and holographic gratings," *Appl. Opt.* **16**, 2711-2721 (1977).

Very low blaze angle gratings ( $\theta_B < 5^\circ$ ) exhibit efficiency behavior that is almost perfectly scalar; that is, polarization effects are virtually nonexistent. In this region, a simple picture of blazing is applicable, in which each groove facet can be considered a simple flat mirror. The diffracted efficiency is greatest for that wavelength that is diffracted by the grating in the same direction as it would be reflected by the facets. This efficiency peak occurs in the  $m = 1$  order at  $\lambda/d = 2 \sin \theta$  (provided the angle between the incident and diffracted beams is not excessive). At  $\lambda_B/2$ , where  $\lambda_B$  is the blaze wavelength, the diffracted efficiency will be virtually zero (Figure 9-5) since for this wavelength the second-order efficiency will be at its peak. Fifty-percent absolute efficiency is obtained from roughly  $0.7\lambda_B$  to  $1.8\lambda_B$ .

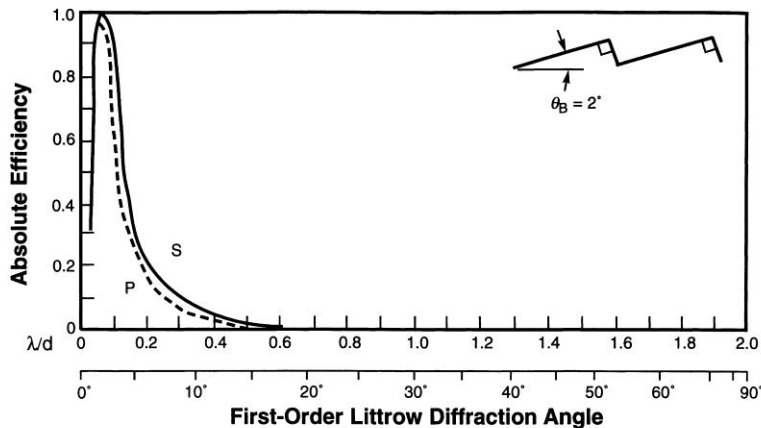


Figure 9-5. First-order theoretical efficiency curve:  $2^\circ$  blaze angle and Littrow mounting ( $2K = 0$ ). Solid curve, S-plane; dashed curve, P-plane.

For low blaze angle gratings ( $5^\circ < \theta_B < 10^\circ$ ), polarization effects will occur within their usable range (see Figure 9-6). In particular, a strong anomaly is seen near  $\lambda/d = 2/3$ . Also observed is the theoretical S-plane theoretical efficiency peak of 100% exactly at the nominal blaze, combined with a P-plane peak that is lower and at a shorter wavelength. It is characteristic of all P-plane curves to decrease monotonically from their peak toward zero as  $\lambda/d \rightarrow 2$ , beyond which diffraction is not

possible (see Eq. (2-1)). Even though the wavelength band over which 50% efficiency is attained in unpolarized light is from  $0.67\lambda_B$  to  $1.8\lambda_B$ , gratings of this type (with 1200 groove per millimeter, for example) are widely used, because they most effectively cover the wavelength range between 200 and 800 nm (in which most ultraviolet-visible (UV-Vis) spectrophotometers operate).

---

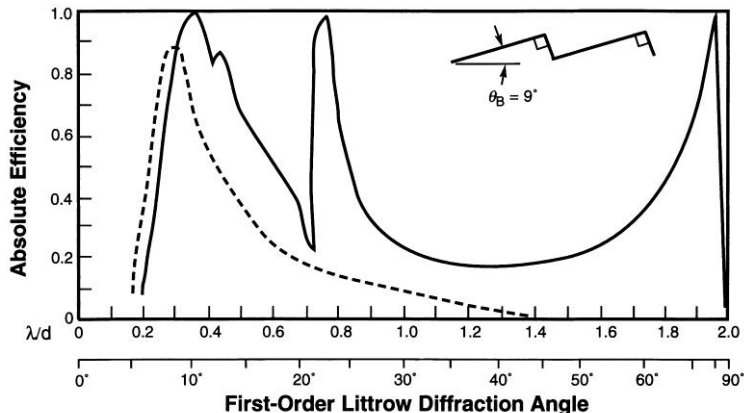


Figure 9-6. Same as Figure 9-5, except  $9^\circ$  blaze angle.

---

A typical efficiency curve for a *medium blaze angle* grating ( $10^\circ < \theta_B < 18^\circ$ ) is shown in Figure 9-7. As a reminder that for unpolarized light the efficiency is simply the arithmetic average of the S- and P-plane efficiencies, such a curve is shown in this figure only, to keep the other presentations simple.

The *low-anomaly blaze angle* region ( $18^\circ < \theta_B < 22^\circ$ ) is a special one. Due to the fact that the strong anomaly that corresponds to the  $-1$  and  $+2$  orders passing off ( $\lambda/d = 2/3$ ) occurs just where these gratings have their peak efficiency, this anomaly ends up being severely suppressed (Figure 9-8). This property is quite well maintained over a large range of angular deviations (the angle between the incident and diffracted beams), namely up to  $2K = 25^\circ$ , but it depends on the grooves having an apex angle near  $90^\circ$ . The relatively low P-plane efficiency of this family of blazed gratings holds the 50% efficiency band from  $0.7\lambda_B$  to  $1.9\lambda_B$ .

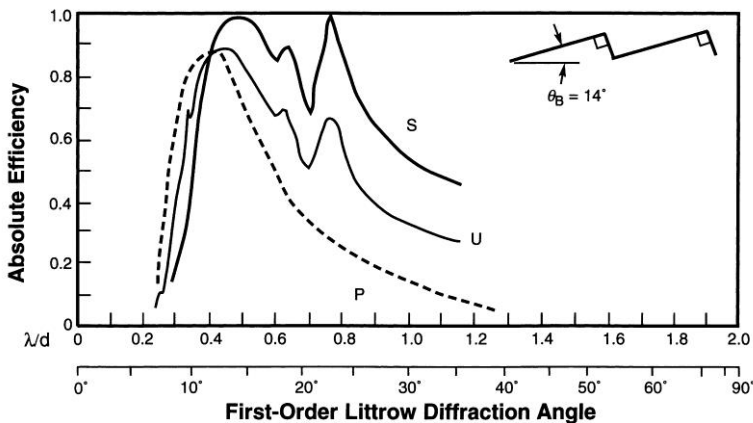


Figure 9-7. Same as Figure 9-5, except  $14^\circ$  blaze angle. The curve for unpolarized light (marked U) is also shown; it lies exactly halfway between the S and P curves.

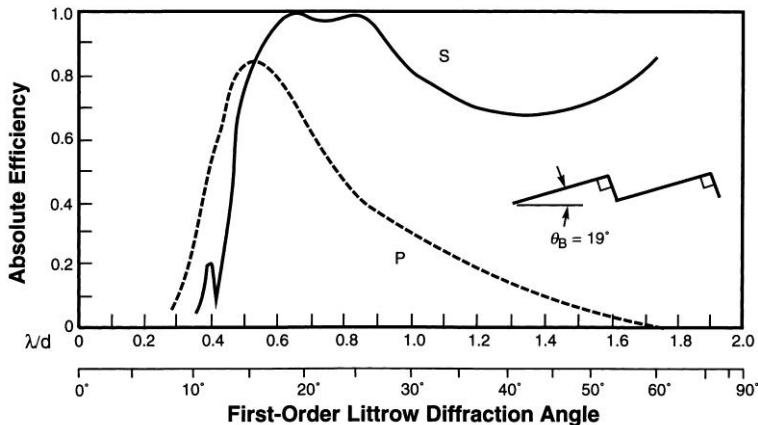


Figure 9-8. Same as Figure 9-5, except  $19^\circ$  blaze angle.

High blaze angle gratings ( $22^\circ < \theta_B < 38^\circ$ ) are widely used, despite the presence of a very strong anomaly in their efficiency curves (Figure 9-9). For unpolarized light, the effect of this anomaly is greatly attenuated by its coincidence with the P-plane peak. Another method for reducing

anomalies for such gratings is to use them at angular deviations  $2K$  above  $45^\circ$ , although this involves some sacrifice in efficiency and wavelength range. The 50% efficiency is theoretically attainable in the Littrow configuration from  $0.6\lambda_B$  to  $2\lambda_B$ , but in practice the long-wavelength end corresponds to such an extreme angle of diffraction that instrumental difficulties arise.

---

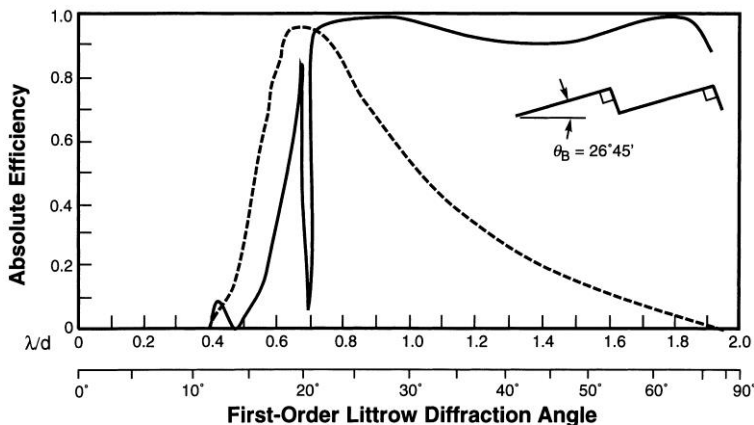


Figure 9-9. Same as Figure 9-5, except  $26^\circ 45'$  blaze angle.

---

Theoretically, all gratings have a second high-efficiency peak in the S-plane at angles corresponding to the complement of the blaze angle ( $90^\circ - \theta_B$ ); in practice, this peak is fully developed only on steeper groove-angle gratings, and then only when the steep face of the groove is not too badly deformed by the lateral plastic flow inherent in the diamond tool burnishing process. The strong polarization observed at all high angles of diffraction limits the useable efficiency in unpolarized light, but it makes such gratings very useful for tuning lasers, especially molecular lasers. The groove spacing may be chosen so that the lasing band corresponds to either the first or second of the S-plane high-efficiency plateaus. The latter will give at least twice the dispersion (in fact the maximum possible), as it is proportional to the tangent of the angle of diffraction under the Littrow conditions typical of laser tuning.

*Very-high blaze angle* gratings ( $\theta_B > 38^\circ$ ) are rarely used in the first order; their efficiency curves are interesting only because of the high P-plane values (Figure 9-10). In high orders they are often used in tuning dye lasers, where high

---

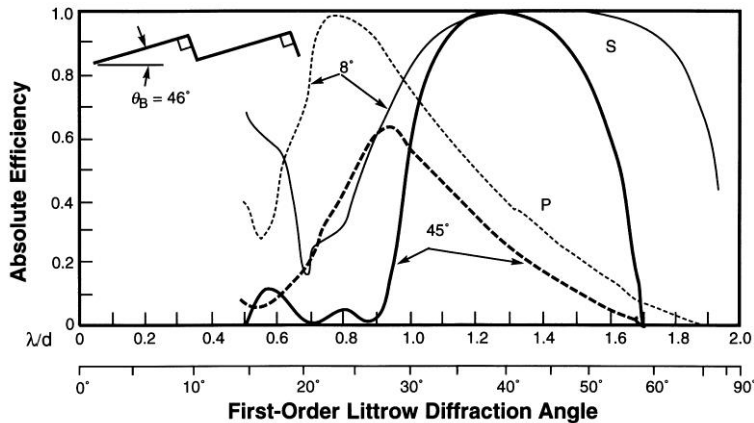


Figure 9-10. Same as Figure 9-5, except  $46^\circ$  blaze angle and  $8^\circ$  and  $45^\circ$  between the incident and diffracted beams (shown as light and heavy lines, respectively).

---

dispersion is important and where tuning through several orders can cover a wide spectral region with good efficiency. Efficiency curves for this family of gratings are shown for two configurations. With an angular deviation of  $2K = 8^\circ$ , the efficiency does not differ too much from Littrow; when  $2K = 45^\circ$ , the deep groove results in sharp reductions in efficiency. Some of the missing energy shows up in the zeroth order, but some of it can be absorbed by the grating.

### 9.3. EFFICIENCY CHARACTERISTICS FOR SINUSOIDAL-GROOVE GRATINGS

A sinusoidal-groove grating can be obtained by the interferometric (holographic) recording techniques described in Chapter 4. Sinusoidal gratings have a somewhat different diffracted efficiency behavior than do triangular-groove gratings and are treated separately.

It is convenient to consider five domains of sinusoidal-groove gratings,<sup>87</sup> with progressively increasing modulation  $\mu$ , where

$$\mu = \frac{h}{d}, \quad (9-1)$$

$h$  is the groove height and  $d$  is the groove spacing:

domain	modulation
very low	$\mu < 0.05$
low	$0.05 < \mu < 0.15$
medium	$0.15 < \mu < 0.25$
high	$0.25 < \mu < 0.4$
very high	$\mu > 0.4$

*Very low modulation* gratings ( $\mu < 0.05$ ) operate in the scalar domain,<sup>88</sup> where the theoretical efficiency peak for sinusoidal grooves is only 34% (Figure 9-11). This figure may be readily scaled, and specification is a simple matter as soon as it becomes clear that the peak wavelength always occurs at  $\lambda_B = 3.4h = 3.4\mu d$ . A blazed grating with an equivalent peak wavelength will require a groove depth 1.7 times greater.

*Low modulation* gratings ( $0.05 < \mu < 0.15$ ) are quite useful in that they have a low but rather flat efficiency over the range  $0.35 < \lambda/d < 1.4$  (Figure 9-12). This figure includes not only the infinite conductivity values shown on all previous ones but includes the effects of finite conductivity by adding the curves for an 1800 g/mm aluminum surface. The most significant effect is in the behavior of the anomaly, which is the typical result of the finite conductivity of real metals.

Figure 9-13 is a good example of a *medium modulation* grating ( $0.15 < \mu < 0.25$ ). It demonstrates an important aspect of such sinusoidal gratings, namely that reasonable efficiency requirements confine first-order applications to values of  $\lambda/d > 0.45$ , which makes them generally unsuitable for systems covering wide spectral ranges

<sup>87</sup> E. G. Loewen, M. Nevière and D. Maystre, "Grating efficiency theory as it applies to blazed and holographic gratings," *Appl. Opt.* **16**, 2711-2721 (1977).

<sup>88</sup> E. G. Loewen, M. Nevière and D. Maystre, "On an asymptotic theory of diffraction gratings used in the scalar domain," *J. Opt. Soc. Am.* **68**, 496-502 (1978).

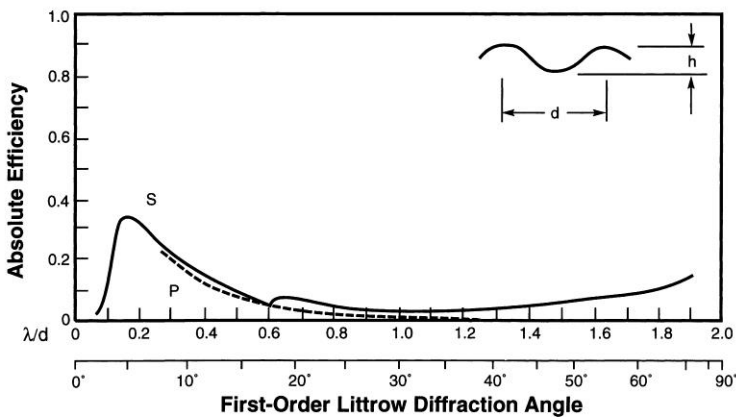


Figure 9-11. First-order theoretical efficiency curve: sinusoidal grating,  $\mu = 0.05$  and Littrow mounting ( $2K = 0$ ). Solid curve, S-plane; dashed curve, P-plane.

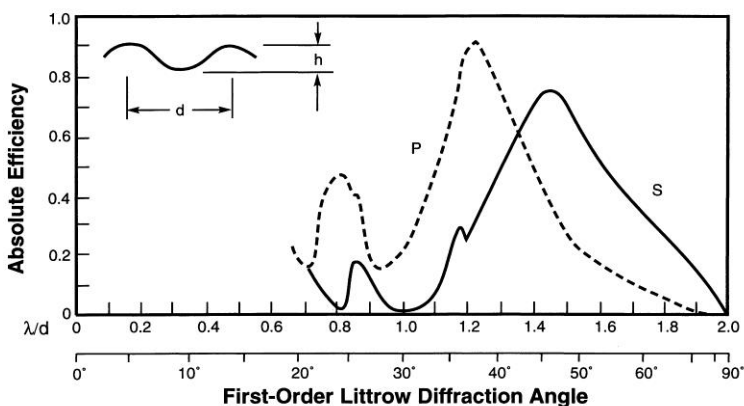


Figure 9-12. First-order theoretical efficiency curve: sinusoidal grating, aluminum coating, 1800 grooves per millimeter,  $\mu = 0.14$  and Littrow mounting. Solid curve, S-plane; dashed curve, P-plane. [For reference, the curves for a perfectly conducting surface are shown as well (light curves).]

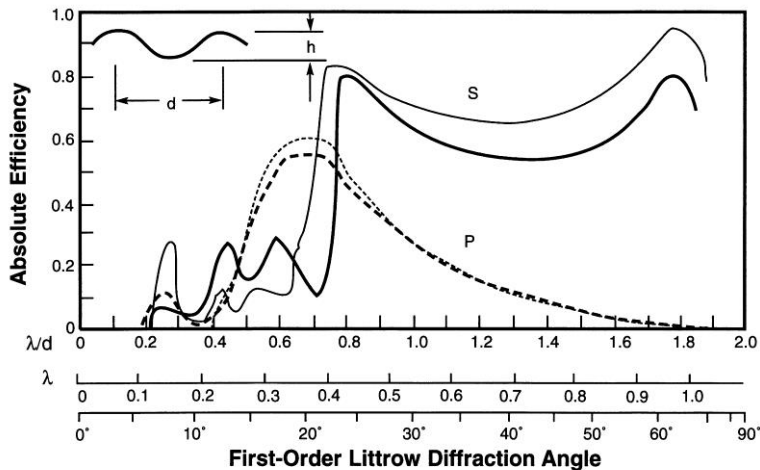


Figure 9-13. Same as Figure 9-12, except  $\mu = 0.22$  and  $8^\circ$  between incident and diffracted beams ( $2K = 8^\circ$ ).

Over this restricted region, however, efficiencies are comparable to those of triangular-groove gratings, including the high degree of polarization. This figure also demonstrates how a departure from Littrow to an angular deviation of  $2K = 8^\circ$  splits the anomaly into two branches, corresponding to the new locations of the  $-1$  and  $+2$  order passing-off conditions.

*High modulation* gratings ( $0.25 < \mu < 0.40$ ), such as shown in Figure 9-14, have the maximum useful first-order efficiencies of sinusoidal-groove gratings. Provided they are restricted to the domain in which higher orders diffract (*i.e.*,  $\lambda/d > 0.65$ ), their efficiencies are very similar to those of triangular-groove gratings having similar groove depths (*i.e.*,  $26^\circ < \theta_B < 35^\circ$ ).

*Very-high modulation* gratings ( $\mu > 0.40$ ), in common with equivalent triangular-groove gratings, have little application in the first order due to their relatively low efficiencies except perhaps over narrow wavelengths ranges and for grazing incidence applications.

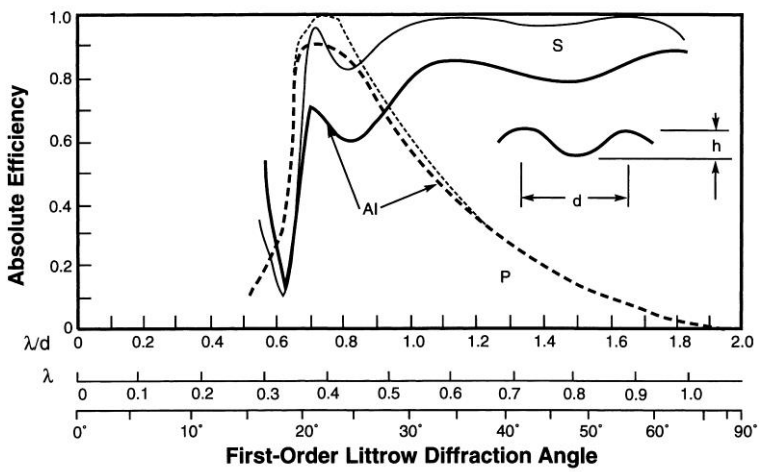


Figure 9-14. Same as Figure 9-12, except  $\mu = 0.36$ .

Very-high modulation gratings ( $\mu > 0.40$ ), in common with equivalent triangular-groove gratings, have little application in the first order due to their relatively low efficiencies except perhaps over narrow wavelengths ranges and for grazing incidence applications.

#### 9.4. THE EFFECTS OF FINITE CONDUCTIVITY

For metal-coated reflection gratings, the finite conductivity of the metal is of little importance for wavelengths of diffraction above  $4 \mu\text{m}$ , but the complex nature of the dielectric constant and the index of refraction begin to effect efficiency behavior noticeably for wavelengths below  $1 \mu\text{m}$ , and progressively more so as the wavelength decreases. In the P-plane, the effect is a simple reduction in efficiency, in direct proportion to the reflectance. In the S-plane, the effect is more complicated, especially for deeper grooves and shorter wavelengths.

Figure 9-15 shows the first-order efficiency curve for a widely-used grating: 1200 g/mm, triangular grooves, medium blaze angle ( $\theta_B = 10^\circ$ ), coated with aluminum and used with an angular deviation of  $8^\circ$ . The finite conductivity of the metal causes a reduction in efficiency; also, severe modification of the anomaly is apparent. It is typical that the anomaly is broadened and shifted toward a longer wavelength compared with the infinite conductivity curve. Even for an angular deviation as

small as  $8^\circ$ , the single anomaly in the figure is separated into a double anomaly.

---

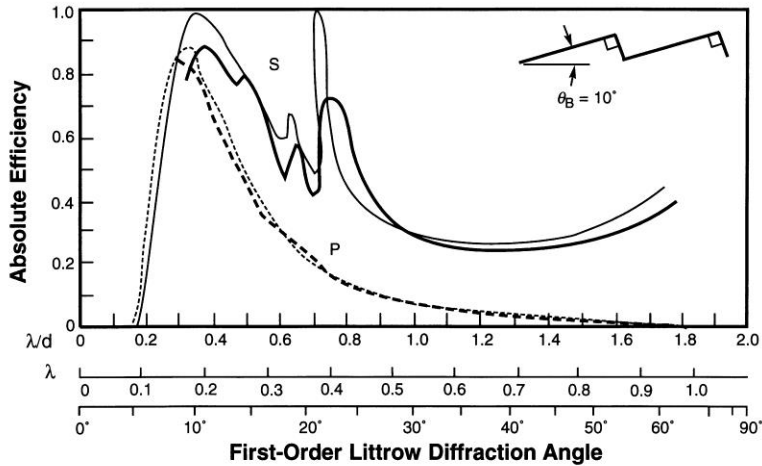


*Figure 9-15. First-order theoretical efficiency curve: triangular-groove grating, aluminum coating, 1200 grooves per millimeter,  $10^\circ$  blaze angle and  $2K = 8^\circ$ . Solid curves, S-plane; dashed curves, P-plane. For reference, the curves for a perfectly conducting surface are shown as well (light curves).*

For sinusoidal gratings, the situation is shown in Figures 9-12 and 9-14. Figure 9-13 is interesting in that it clearly shows a series of new anomalies that are traceable to the role of aluminum.

With scalar domain gratings (either  $\theta_B < 5^\circ$  or  $\mu < 0.10$ ), the role of finite conductivity is generally (but not always) to reduce the efficiency by the ratio of surface reflectance.<sup>89</sup>

## 9.5. DISTRIBUTION OF ENERGY BY DIFFRACTION ORDER

Gratings are most often used in higher diffraction orders to extend the spectral range of a single grating to shorter wavelengths than can be

---

<sup>89</sup> E. G. Loewen, M. Nevière and D. Maystre, "On an asymptotic theory of diffraction gratings used in the scalar domain," *J. Opt. Soc. Am.* **68**, 496-502 (1978).

covered in lower orders. For blazed gratings, the second-order peak will be at one-half the wavelength of the nominal first-order peak, the third-order peak at one-third, etc. Since the ratio  $\lambda/d$  will be progressively smaller as  $|m|$  increases, polarization effects will become less significant; anomalies are usually negligible in diffraction orders for which  $|m| > 2$ . Figures 9-16 and 9-17 show the second- and third-order theoretical Littrow efficiencies, respectively, for a blazed grating with  $\theta_B = 26^\circ 45'$ ; they are plotted as a function of  $m\lambda/d$  in order to demonstrate the proper angular ranges of use. These curves should be compared with Figure 9-9 for corresponding first-order behavior.

---

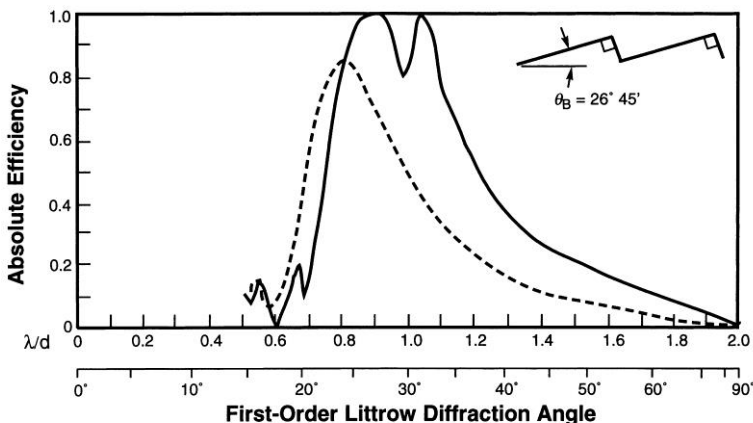


Figure 9-16. Second-order theoretical efficiency curve:  $26^\circ 45'$  blaze angle and Littrow mounting. Solid curve, S-plane; dashed curve, P-plane.

---

For gratings with sinusoidally shaped grooves, higher orders can also be used, but if efficiency is important, the choice is likely to be a finer pitch first-order grating instead. When groove modulations are very low (so that the grating is used in the scalar domain), the second-order efficiency curve looks similar to Figure 9-18, except that the theoretical peak value is about 23% (instead of 34%) and occurs at a wavelength 0.6 times that of the first-order peak, which corresponds to  $2.05h$  (instead of  $3.41h$ ), where  $h$  is the groove depth. Successive higher-order curves for gratings with sinusoidal grooves are not only closer together but drop off

more sharply with order than for gratings with triangular grooves. For sufficiently deeply modulated sinusoidal grooves, the second order can often be used effectively, though (as Figure 9-18 shows) polarization effects are relatively strong. The corresponding third-order theoretical curve is shown in Figure 9-19.

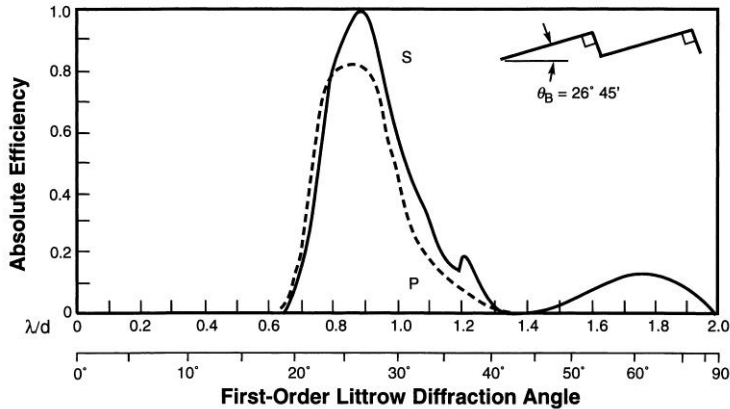


Figure 9-17. Same as Figure 9-16, except third order.

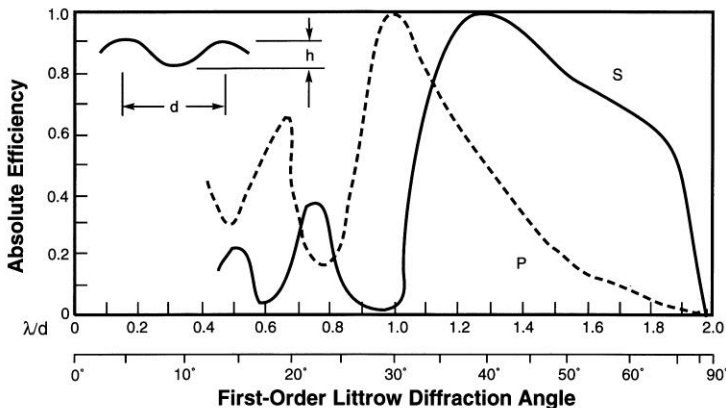


Figure 9-18. Second-order theoretical efficiency curve: sinusoidal grating,  $\mu = 0.36$  and Littrow mounting. Solid curve, S-plane; dashed curve, P-plane.

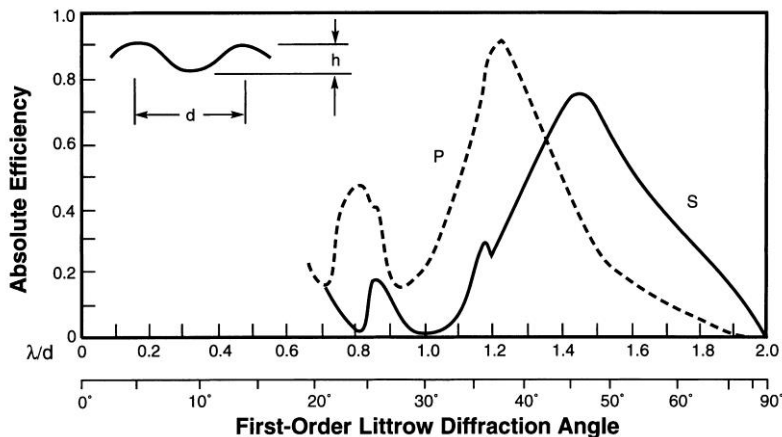


Figure 9-19. Same as Figure 9-18, except third order.

## 9.6. USEFUL WAVELENGTH RANGE

The laws governing diffracted efficiency are quite complicated, but a very rough rule of thumb can be used to estimate the useful range of wavelengths available on either side of the blaze (peak) wavelength  $\lambda_B$  for triangular-groove gratings.

For coarse gratings (for which  $d \geq 2\lambda$ ), the efficiency in the first diffraction order is roughly half its maximum (which is at  $\lambda_B$ ) at  $2\lambda_B/3$  and  $3\lambda_B/2$ . Curves of similar shape are obtained in the second and third orders, but the efficiencies are typically 20% less everywhere, as compared with the first order.

Gratings of fine pitch ( $d \approx \lambda$ ) have a somewhat lower peak efficiency than do coarse gratings, though the useful wavelength range is greater.

## 9.7. BLAZING OF RULED TRANSMISSION GRATINGS

Because they have no metallic overcoating, triangular-groove transmission gratings display far simpler efficiency characteristics than do their ruled counterparts. In particular, transmission gratings have efficiency curves almost completely free of polarization effects.

The peak wavelength generally occurs when the direction of refraction of the incident beam through a groove (thought of as a small

prism) equals the direction dictated by the grating equation. [This is in direct analogy with the model of reflection grating blazing in that the grooves are thought of as tiny mirrors; see Section 2.8.] Due to the index of refraction of the grating, though, the groove angle exceeds the blaze angle for a transmission grating.

See Section 12.2 for more information on transmission gratings.

## 9.8. BLAZING OF HOLOGRAPHIC REFLECTION GRATINGS

Although sinusoidal holographic gratings do not have the triangular groove profile found in ruled gratings, holographic gratings may still exhibit blazing characteristics (see, for example, Figure 9-18). For this reason, it is not correct to say that all blazed gratings have triangular profiles, or that all blazed gratings are ruled gratings – blazing refers to high diffraction efficiency, regardless of the profile of the grooves or the method used to generate them.

There are some cases in which it would be preferable for a holographic grating to have a triangular groove profile rather than a sinusoidal profile. The method of using standing waves to record the grooves (see Section 4.2.1) was developed by Sheridan<sup>90</sup> and improved by Hutley.<sup>91</sup>

Another useful technique for rendering sinusoidal groove profiles more nearly triangular is *ion etching*. By bombarding a surface with energetic ions, the material can be removed (etched) by an amount per unit time dependent on the angle between the beam and the local surface normal. The etching of a sinusoidal profile by an ion beam provides a continuously varying angle between the ion beam and the surface normal, which preferentially removes material at some parts of the profile while leaving other parts hardly etched. The surface evolves toward a triangular groove profile as the ions bombard it.<sup>92</sup>

---

<sup>90</sup> N. K. Sheridan, “Production of blazed holograms,” *Appl. Phys. Lett.* **12**, 316-318 (1968).

<sup>91</sup> M. C. Hutley, “Blazed interference diffraction gratings for the ultraviolet,” *Opt. Acta* **22**, 1-13 (1975); M. C. Hutley and W. R. Hunter, “Variation of blaze of concave diffraction gratings,” *Appl. Opt.* **20**, 245-250 (1981).

<sup>92</sup> Y. Aoyagi and S. Namba, *Japan. J. Appl. Phys.* **15**, 721 (1976); L. F. Johnson, “Evolution of grating profiles under ion-beam erosion,” *Appl. Opt.* **18**, 2559-2574 (1979); C. Palmer, J. Olson and M. M. Dunn, “Blazed diffraction gratings obtained by ion-milling sinusoidal photoresist gratings,” *Proc. SPIE* **2622**, 112-121 (1995).

Other method for generating blazed groove profiles have been developed,<sup>93</sup> but the Sheridan method and the method of ion etching are those most commonly used for commercially-available gratings.

## 9.9. OVERCOATING OF REFLECTION GRATINGS

The metallic coating on a reflection grating is evaporated onto the substrate. This produces a surface whose reflectivity is higher than that of the same metal electroplated onto the grating surface. The thickness of the metallic layer is chosen to enhance the diffraction efficiency throughout the spectral region of interest.

Most standard reflection gratings are furnished with an aluminum (Al) reflecting surface. While no other metal has more general application, there are several special situations where alternative surfaces or coatings are recommended. Gratings coated with gold (Au) and silver (Ag) have been used for some time for higher reflectivity in certain spectral regions, as have more exotic materials such as iridium (Ir), osmium (Os) and platinum (Pt).<sup>94</sup>

The reflectivity of aluminum drops rather sharply for wavelengths below 170 nm. While freshly deposited, fast-fired pure aluminum in high vacuum maintains its reflectivity to wavelengths shorter than 100 nm, the thin layer of oxide that grows on the aluminum (upon introduction of the coating to atmosphere) will cause a reduction in efficiency below about 250 nm.<sup>95</sup> Fortunately, a method borrowed from mirror technology makes it possible to preserve the reflectivity of aluminum to shorter wavelengths.<sup>96</sup> The process involves overcoating the grating with a thin layer of fast-fired aluminum, which is followed immediately by a coating of magnesium fluoride ( $MgF_2$ ) approximately 25 nm thick. The main

---

<sup>93</sup> M. B. Fleming and M. C. Hutley, "Blazed diffractive optics," *Appl. Opt.* **36**, 4635-4643 (1997).

<sup>94</sup> E.g., J. M. Bennett and E. J. Ashley, "Infrared reflectance and emittance of silver and gold evaporated in ultrahigh vacuum," *Appl. Opt.* **4**, 221-224 (1965); R. F. Malina and W. Cash, "Extreme ultraviolet reflection efficiencies of diamond-turned aluminum, polished nickel, and evaporated gold surfaces," *Appl. Opt.* **17**, 3309-3313 (1978); M. R. Torr, "Osmium coated diffraction grating in the Space Shuttle environment: performance," *Appl. Opt.* **24**, 2959-2961 (1985).

<sup>95</sup> R. P. Madden, L. R. Canfield and G. Hass, "On the vacuum-ultraviolet reflectance of evaporated aluminum before and during oxidation," *J. Opt. Soc. Am.* **53**, 620-625 (1963).

<sup>96</sup> G. Hass and R. Tousey, "Reflecting coatings for the extreme ultraviolet," *J. Opt. Soc. Am.* **49**, 593-602 (1959).

purpose of the MgF<sub>2</sub> coating is to protect the aluminum from oxidation. The advantage of this coating is especially marked in the region between 120 and 200 nm. While reflectivity drops off sharply below this region, it remains higher than that of gold and comparable to that of platinum, the most commonly used alternative materials, down to 70 nm.

Overcoating gratings so that their surfaces are coated with two layers of different metals sometimes leads to a change in diffraction efficiency over time. Hunter *et al.*<sup>97</sup> have found the cause of this change to be intermetallic diffusion. For example, they measured a drastic decrease (over time) in efficiency at 122 nm for gratings coated in Au and then overcoated in Al + MgF<sub>2</sub>; this decrease was attributed to the formation of intermetallic compounds, primarily AuAl<sub>2</sub> and Au<sub>2</sub>Al. Placing a suitable dielectric layer such as SiO between the two metallic layers prevents this diffusion.

As mentioned elsewhere, fingerprints are a danger to aluminized optics. It is possible to overcoat such optics, both gratings and mirrors, with dielectrics like MgF<sub>2</sub>, to prevent finger acids from attacking the aluminum. These MgF<sub>2</sub> coatings cannot be baked, as is customary for glass optics, and therefore must not be cleaned with water. Spectrographic-grade organic solvents are the only recommended cleaning agents, and they should be used sparingly and with care.

Single-layer and multilayer dielectric coatings, which are so useful in enhancing plane mirror surfaces, are less generally applicable to diffraction gratings, since in certain circumstances these coatings lead to complex guided wave effects.<sup>98</sup> For wavelengths below 30 nm, in which grazing angles of incidence and diffraction are common, multilayer coatings can enhance efficiency considerably.<sup>99</sup>

---

<sup>97</sup> W. R. Hunter, T. L. Mikes and G. Hass, "Deterioration of Reflecting Coatings by Intermetallic Diffusion," *Appl. Opt.* **11**, 1594-1597 (1972).

<sup>98</sup> M. C. Hutley, J. F. Verrill and R. C. McPhedran, "The effect of a dielectric layer on the diffraction anomalies of an optical grating," *Opt. Commun.* **11**, 207-209 (1974).

<sup>99</sup> J. C. Rife, W. R. Hunter, T. W. Barbee, Jr., and R. G. Cruddace, "Multilayer-coated blazed grating performance in the soft x-ray region," *Appl. Opt.* **28**, 1984 (1989).

## 9.10. THE RECIPROCITY THEOREM

A useful property of grating efficiency is that embodied in the *reciprocity theorem*,<sup>100</sup> which states that (under certain conditions) reversing the direction of the beam diffracted by a grating will leave its diffraction efficiency unchanged. Stated another way, the reciprocity theorem says that the grating efficiency for wavelength  $\lambda$  in order  $m$  is unchanged under the transformation  $\alpha \leftrightarrow \beta$ . This equivalence follows from the periodic nature of the grating and is strictly true for perfectly-conducting gratings and lossless dielectric gratings illuminated by an incident plane wave.<sup>101</sup>

Three consequences of the reciprocity theorem should be noted:<sup>102</sup>

- The zeroth-order efficiency  $E(\lambda,0)$  is a symmetric function (of angle  $\alpha$ ) about  $\alpha = 0$ .
- Rotation of the grating groove profile through  $180^\circ$  (while keeping  $\alpha$  constant) does not affect  $E(\lambda,0)$ ; moreover, if only two diffraction orders are propagating (say,  $m = 0$  and  $m = 1$ ), the efficiency  $E(\lambda,1)$  will be unchanged as well.
- The efficiency  $E(\lambda,m)$  for a given diffraction order  $m$  is a symmetric function of  $\sin\alpha$  about the Littrow condition ( $\alpha = \beta$ ).<sup>103</sup>

## 9.11. CONSERVATION OF ENERGY

The principle of conservation of energy requires that all the energy incident on a diffraction grating be accounted for; this can be represented mathematically (in terms of intensities), considering a single wavelength  $\lambda$ , as

$$I_{\text{in}} = I_{\text{out}} = \sum_m I_{\text{diff}}(m) + I_{\text{absorbed}} + I_{\text{scattered}}, \quad (\text{for a single } \lambda) \quad (9-2)$$

---

<sup>100</sup> R. Petit, "A tutorial introduction," in *Electromagnetic Theory of Gratings*, R. Petit, ed. (Springer-Verlag, New York, 1980), p. 12.

<sup>101</sup> E. G. Loewen and E. Popov, *Diffraction Gratings and Applications* (Marcel Dekker, New York, 1997), p. 38.

<sup>102</sup> R. C. McPhedran and M. D. Waterworth, "A theoretical demonstration of properties of grating anomalies (S-polarization)," *Opt. Acta* **19**, 877-892 (1972).

<sup>103</sup> E. G. Loewen and E. Popov, *Diffraction Gratings and Applications* (Marcel Dekker, New York, 1997), p. 38.

where the summation is over all diffraction orders  $m$  that propagate (*i.e.*, for a reflection grating, all orders for which the diffraction angle  $\beta(m)$  satisfies the inequalities  $-90^\circ \leq \beta(m) \leq +90^\circ$ ). Here the terms  $I_{\text{absorbed}}$  and  $I_{\text{scattered}}$  are the “losses” due to absorption of energy by the grating and by scattering, respectively.

It is important to recognize that Eq. (9-2) holds only for the case in which the grating and the incident beam are fixed in space, and each diffraction order is diffracted through a unique diffraction angle given by Eq. (2-4) with constant  $\alpha$ . Eq. (9-2) does *not* hold true when the intensity of each diffraction order  $m$  is measured in the Littrow configuration, since in this case the incidence angle  $\alpha$  is changed for each order such that  $\alpha = \beta_m$ . Care must be taken when adding intensities (or efficiencies) in several orders for a single wavelength: the sum of these intensities is not conserved according to Eq. (9-2) unless the grating and incident beam remain fixed while a detector is moved (in angle) from one order to the next to take the intensity measurements.

Eq. (9-2) can be used to advantage by designing an optical system for which only two diffraction orders propagate: order  $m = 1$  (or  $m = -1$ ) and order  $m = 0$  (which always exists:  $|\alpha| < 90^\circ$  implies  $|\beta(0)| < 90^\circ$ , since  $\beta(0) = -\alpha$ ). This case requires a small groove spacing  $d$  and an incidence angle  $\alpha$  such that the diffraction angle for  $m = \pm 2$  and for the other first order pass beyond  $90^\circ$ : from Eq. (2-1) this requires

$$|\sin\beta| = \left| \frac{m\lambda}{d} - \sin\alpha \right| > 1 \quad (9-3)$$

for  $m = 2$ ,  $m = -2$  and  $m = -1$  (assuming that  $m = 1$  is the order chosen to propagate). For such a system, Eq. (9-2) simplifies to become

$$I_{\text{in}} = I_{\text{out}} = I_{\text{diff}(0)} + I_{\text{diff}(1)} + I_{\text{absorbed}} + I_{\text{scattered}}, \quad (\text{for a single } \lambda) \quad (9-4)$$

where the term  $I_{\text{diff}(0)}$  corresponds to the reflected intensity and  $I_{\text{diff}(1)}$  corresponds to the intensity diffracted into the  $m = 1$  order. Choosing a groove profile that reduces the reflected intensity  $I_{\text{diff}(0)}$  will thereby increase the diffracted intensity  $I_{\text{diff}(1)}$ .

Eq. (9-2) is generally useful in measuring grating efficiency, but in the presence of anomalies (see below) they can lead to considerable inaccuracies.

## 9.12. GRATING ANOMALIES

In 1902, R. W. Wood observed that the intensity of light diffracted by a grating generally changed slowly as the wavelength was varied, but occasionally a sharp change in intensity was observed at certain wavelengths.<sup>104</sup> Called *anomalies*, these abrupt changes in the grating efficiency curve were later categorized into two groups: *Rayleigh anomalies* and *resonance anomalies*.<sup>105</sup>

### 9.12.1. Rayleigh anomalies

Lord Rayleigh predicted the spectral locations where a certain set of anomalies would be found: he suggested that these anomalies occur when light of a given wavelength  $\lambda'$  and spectral order  $m'$  is diffracted at  $|\beta| = 90^\circ$  from the grating normal (*i.e.*, it becomes an evanescent wave, passing over the grating horizon). For wavelengths  $\lambda < \lambda'$ ,  $|\beta| < 90^\circ$ , so propagation is possible in order  $m'$  (and all lower orders), but for  $\lambda > \lambda'$  no propagation is possible in order  $m'$  (but it is still possible in lower orders). Thus, there is a discontinuity in the diffracted power *vs.* wavelength in order  $m'$  at wavelength  $\lambda$ , and the power that would diffract into this order for  $\lambda > \lambda'$  is redistributed among the other propagating orders. This causes abrupt changes in the power diffracted into these other orders.

These Rayleigh anomalies, which arise from the abrupt redistribution of energy when a diffracted order changes from propagating ( $|\beta| < 90^\circ$ ) to evanescent ( $|\beta| > 90^\circ$ ), or vice versa, are also called *threshold anomalies*.<sup>106</sup>

### 9.12.2. Resonance anomalies

The second class of anomalies, which are usually much more noticeable than Rayleigh anomalies, are caused by resonance

---

<sup>104</sup> R. W. Wood, "On the remarkable case of uneven distribution of light in a diffraction grating spectrum," *Philos. Mag.* **4**, 396-402 (1902); R.W. Wood, "Ll. An experimental study of grating errors and 'ghosts'", *The London, Edinburgh, and Dublin Philosophical Magazine and Journal of Science*, 48:285, 497-508 (1924); R. W. Wood, "Anomalous diffraction gratings," *Phys. Rev.* **48**, 928-936 (1935); J. E. Stewart and W. S. Gallaway, "Diffraction anomalies in grating spectrophotometers," *Appl. Opt.* **1**, 421-430 (1962).

<sup>105</sup> A. Hessel and A. A. Oliner, "A new theory of Wood's anomalies on optical gratings," *Appl. Opt.* **4**, 1275-1297 (1965).

phenomena,<sup>107</sup> the most well-known of which are surface excitation effects.<sup>108</sup> At the interface between a dielectric and a metal, there are specific conditions under which a charge density oscillation (called a *surface plasma wave*) can be supported, which carries light intensity away from the incident beam and therefore decreases the diffraction efficiency of the grating. The efficiency curve would show a sharp drop in intensity at the corresponding conditions (see Figure 9-20).

---

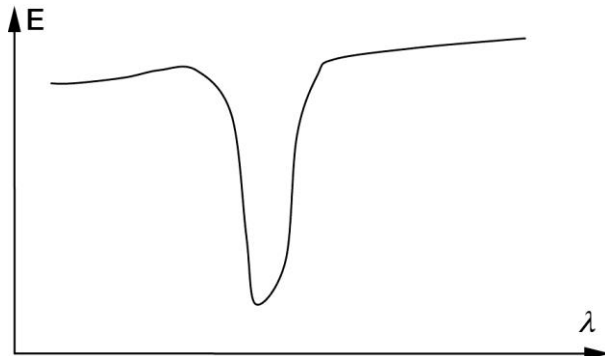


Figure 9-20. A typical (simplified) efficiency curve showing a sharp drop where the conditions are met for surface plasmon resonance. The curve over this narrow spectral region would appear to increase monotonically if the resonance condition were not met.

---

For a resonance anomaly to exist, a resonance condition must be met – this places restrictions on the wavelengths (and incidence angles) that will exhibit resonance effects for a given groove profile and refractive indices. This results from the fact that in this phenomenon – the *surface plasmon resonance* (SPR) effect<sup>109</sup> – the electromagnetic field that propagates along the metal-dielectric interface extends into each medium, so the characteristics of this propagating wave depend on the

---

<sup>106</sup> E. G. Loewen and E. Popov, *Diffraction Gratings and Applications* (Marcel Dekker, New York, 1997), ch. 8.

<sup>107</sup> U. Fano, “The theory of anomalous diffraction gratings and of quasi-stationary waves on metallic surfaces (Sommerfeld’s waves),” *J. Opt. Soc. Am.* **31**, 213-222 (1941).

<sup>108</sup> R. H. Ritchie, E. T. Arakawa, J. J. Cowan, and R. N. Hamm, “Surface-plasmon resonance effect in grating diffraction,” *Phys. Rev. Lett.* **21**, 1530-1533 (1968).

<sup>109</sup> R. H. Ritchie, E. T. Arakawa, J. J. Cowan and R. N. Hamm, “Surface-plasmon resonance effect in grating diffraction,” *Phys. Rev. Lett.* **21**, 1530-1533 (1968).

material conditions near the interface. This useful feature of SPR has led to its use in several sensing applications,<sup>110</sup> such as biosensing<sup>111</sup> and gas sensing.<sup>112</sup> SPR can also be used to characterize the surface profile of the grating itself, especially by probing the diffraction effects due to higher harmonics in the periodic structure on the grating surface.<sup>113</sup>

While diffraction gratings generally do not convert incident P-polarized light to S-polarized light (or *vice versa*) upon diffraction, it has been observed that such *polarization conversion* can occur if the grating is not illuminated in the principal plane (*i.e.*,  $\varepsilon \neq 0$  in Eq. (2-3)).<sup>114</sup> In this case, called conical diffraction (see Section 2.1), resonance effects can lead to a strong polarization conversion peak (*e.g.*, a sharp trough in the S-polarized efficiency curve coincident with a sharp peak in the P-polarized efficiency curve).

## 9.13. GRATING EFFICIENCY CALCULATIONS

Several techniques have been developed to calculate grating efficiencies, most of which have two characteristics in common: they employ Maxwell's equations whose boundary conditions are applied at the corrugated grating surface, and their difficulty in implementation varies in rough proportion to their accuracy. In this section only a brief

---

<sup>110</sup> J. Homola, S. S. Yee and G. Gauglitz, "Surface plasmon resonance sensors: review," *Sensors and Actuators B* **54**, 3-15 (1999);

<sup>111</sup> F. Caruso, M. J. Jory, G. W. Bradberry, J. R. Sambles and D. N. Furlong, "Acousto-optic surface-plasmon-resonance measurements of thin films on gold," *J. Appl. Phys.* **83**, 5 (1983); D. C. Cullen, R. G. W. Brown and R. C. Lowe, "Detection of immunocomplex formation via surface plasmon resonance on gold-coated diffraction gratings," *Biosensors* **3**, 211 (1987); J. M. Brockman and S. M. Fernández, "Grating-coupled surface plasmon resonance for rapid, label-free, array-based sensing," *American Laboratory*, 37-40 (June 2001).

<sup>112</sup> M. J. Jory, P. S. Cann and J. R. Sambles, "Surface-plasmon-polariton studies of 18-crown-6 metal-free phthalocyanide," *J. Phys. D: Appl. Phys.* **27**, 169-174 (1994)

<sup>113</sup> E. L. Wood, J. R. Sambles, N. P. Cotter and S. C. Kitson, "Diffraction grating characterization using multiple-wavelength excitation of surface plasmon polaritons," *J. Mod. Opt.* **42**, 1343-1349 (1995).

<sup>114</sup> G. P. Bryan-Brown, J. R. Sambles and M. C. Hutley, "Polarisation conversion through the excitation of surface plasmons on a metallic grating", *J. Mod. Opt.* **37**, 1227-1232 (1990); S. J. Elston, G. P. Bryan-Brown and J. R. Sambles, "Polarization conversion from diffraction gratings," *Phys. Rev. B* **44**, 6393-6400 (1991).

mention of these techniques is provided – more details may be found in Petit<sup>115</sup>, Maystre<sup>116</sup>, and Loewen and Popov<sup>117</sup>.

Grating efficiency calculations start with a description of the physical situation: an electromagnetic wave is incident upon a corrugated surface, the periodicity of which allows for a multiplicity of diffracted waves (each in a different direction, corresponding to a unique diffraction order as described in Chapter 2). Efficiency calculations seek to determine the distribution of the incident energy into each of the diffraction orders.

*Scalar theories* of grating efficiency lead to accurate results in certain cases, such as when the wavelength is much smaller than the groove spacing ( $d \ll \lambda$ ); the vectorial nature of optical radiation (manifest in the property of polarization) is not taken into account in this formalism.

*Vector* or *electromagnetic theories* can be grouped into two categories. *Differential methods* start from the differential form of Maxwell's equations for TE (P) and TM (S) polarization states, whereas *integral methods* start from the integral form of these equations. Each of these categories contains a number of methods, none of which is claimed to cover all circumstances.

Both differential and integral methods have been developed and studied extensively, and both have been implemented numerically and thoroughly tested against a wide variety of experimental data. Some of these numerical implementations are commercially available.

---

<sup>115</sup> Petit, R., ed., *Electromagnetic Theory of Gratings*, vol. 22 in “Topics in Current Physics” series (Springer-Verlag, 1980).

<sup>116</sup> D. Maystre, “Rigorous vector theories of diffraction gratings,” in *Progress in Optics*, vol. XXI, E. Wolf, ed. (Elsevier, 1984), pp. 2-67.

<sup>117</sup> E. G. Loewen and E. Popov, *Diffraction Gratings and Applications*, Marcel Dekker, Inc. (New York, 1987), ch. 10.



# 10. STRAY LIGHT CHARACTERISTICS OF GRATINGS AND GRATING SYSTEMS

## 10.0. INTRODUCTION

An annoying characteristic of all optical surfaces is their ability to scatter light. This undesirable light is often referred to as *stray radiant energy* (SRE). When this light reaches the detector of an instrument designed to measure an optical signal, the SRE contributes to the noise of the system and thereby reduces the signal-to-noise ratio (SNR).

The terminology of SRE in grating systems is not standard, so for clarity we refer to unwanted light arising from imperfections in the grating itself as *scattered light* or *grating scatter*, and unwanted light reaching the detector of a grating-based instrument as *instrumental stray light* or simply *stray light*. [We choose this definition of scattered light so that it will vanish for a perfect grating; we will see below that this does not generally cause the instrumental stray light to vanish as well.] With these definitions, some scattered light will also be stray light (if it reaches the detector); moreover, some stray light will not be scattered light (since it will not have arisen from imperfections in the grating).<sup>118</sup>

## 10.1. GRATING SCATTER

Of the radiation incident on the surface of a reflection grating, some will be diffracted according to Eq. (2-1) and some will be absorbed by the grating itself. The remainder is scattered light, which may arise from several factors, including imperfections in the shape and spacing of the grooves and roughness on the surface of the grating. An excellent

---

<sup>118</sup> This definition of stray light is not universal; while it is in agreement with K. D. Mielenz, V. R. Weidner and R. W. Burke, “Heterochromic stray light in UV absorption spectrometry: a new test method,” *Appl. Opt.* **21**, 3354-3356 (1982), it is not in agreement with the ASTM, which defines the quantity *stray radiant power* as being composed of wavelengths outside the spectral bandwidth of the monochromator (ASTM standard E387, “Standard Test Method for Estimating Stray Radiant Power Ratio of Dispersive Spectrophotometers by the Opaque Filter Method,” 2004). [See also W. Kaye, “Stray light ratio measurements,” *Anal. Chem.* **53**, 2201-2206 (1981).] The ASTM definition does not account for light of the correct wavelength that reaches the detector, but which does not follow the desired optical path.

analysis of grating scatter can be found in Sharpe & Irish,<sup>119</sup> and measured grating scatter was compared to predictions of Beckmann's scalar theory and Rayleigh's vector theory by Marx *et al.*<sup>120</sup>

Two types of scattered light are often distinguished. *Diffuse scattered light* is scattered into the hemisphere in front of the grating surface. It is due mainly to grating surface microroughness. It is the primary cause of scattered light in holographic gratings. For monochromatic light of wavelength  $\lambda$  incident on a grating, the intensity of diffuse scattered light is higher near the diffraction orders of  $\lambda$  than between these orders.\* *In-plane scatter* is unwanted energy in the dispersion plane. Due primarily to random variations in groove spacing or groove depth, its intensity is generally higher than the background diffuse scattered light.

Consider a diffraction grating consisting of a pattern of grooves whose nominal spacing is  $d$ . We have defined scattered light as all light leaving the grating due to its imperfections; this is equivalent to the operational definition that scattered light is all light energy leaving the surface of a diffraction grating that does not follow the grating equation for the nominal groove spacing  $d$ ,

$$m\lambda = d(\sin \alpha + \sin \beta). \quad (2-1)$$

This is analogous to the concept of scattered light for a mirror, which may be defined the light leaving its surface that does not follow the law of reflection for the nominal mirror surface.

This definition of grating scatter – as being caused by imperfections in the grating – does not consider light diffracted into different orders  $\{m\}$  as scattered light. That is, diffraction into multiple orders is not an artifact of grating imperfections, but a direct consequence of the phenomenon of constructive interference on which the grating operates (see Section 2.1). However, light diffracted into other orders can contribute to instrumental stray light (see Section 10.2 below).

---

<sup>119</sup> M. R. Sharpe and D. Irish, "Stray light in diffraction grating monochromators," *Opt. Acta* **25**, 861-893 (1978).

<sup>120</sup> E. Marx, T. A. Germer, T. V. Vorburger and B. C. Park, "Angular distribution of light scattered from a sinusoidal grating," *Appl. Opt.* **39**, 4473-4485 (2000).

\* This observation has led some to observe that grating scatter is "blazed".

### **10.1.1. Surface irregularities in the grating coating**

A grating surface that is rough on the scale of the incident wavelength (or somewhat smaller) will cause a small portion of the incident light to be scattered diffusely (*i.e.*, into all directions) with intensity that varies approximately with the inverse fourth power of the wavelength.<sup>121</sup> Surface roughness is due in part to the surface quality of the master grating, either ruled or holographic, since the metal coating of a ruled master, and the photoresist coating of a holographic master, are not perfectly smooth. Moreover, the addition of a reflective coating may contribute to the surface roughness due to the coating's granular structure.

### **10.1.2. Dust, scratches & pinholes on the surface of the grating**

Each speck of dust, tiny scratch, and pinhole void in the surface of a reflection grating will serve as a "scatter center" and cause diffuse scatter. This is evident upon inspecting a grating under a bright light: dust, scratches, pinholes *etc.* are easily visible and bright when looked at from many different angles (hence the diffuse nature of their scattered light).

### **10.1.3. Irregularities in the position of the grooves**

The presence of spatial frequencies in the groove pattern other than that of the groove spacing  $d$  will give rise to constructive interference of the diffracted light at angles that do not follow the grating equation for the nominal groove spacing  $d$ , but for different groove spacings  $d' \neq d$ .

Until the recent advent of interferometric control of ruling engines, mechanically ruled gratings exhibited secondary spectra, called *ghosts*, due to slight deviations in the placement of its grooves compared with their ideal locations. Ghosts that are close to and symmetric about the parent diffracted line are called *Rowland ghosts*, and are due to longer-term periodicities (on the order of millimeters), whereas *Lyman ghosts* are farther from the parent line and are caused by short-term periodicities (on the order of the groove spacing). Both Rowland and Lyman ghosts appear at angular positions given by the grating equation, but for spatial frequencies other than  $1/d$  (see Section 11.1).

---

<sup>121</sup> M. R. Sharpe and D. Irish, "Stray light in diffraction grating monochromators," *Opt. Acta* **25**, 861-893 (1978).

The presence of random (rather than periodic) irregularities in groove placement leads to a faint background between orders, rather than sharp ghosts, whose intensity varies roughly with the inverse square of the wavelength.<sup>122</sup> This background is called *grass* because it resembles blades of grass when observed using green Hg light.

Ghosts and grass are in-plane effects (that is, they are seen in and near the dispersion plane) and lead to *interorder scatter*. Holographic gratings, whose grooves are formed simultaneously, do not exhibit measurable groove placement irregularities if made properly and therefore generally exhibit lower levels of interorder scatter. With the use of sophisticated interferometric control systems on modern ruling engines, though, this advantage has been reduced when holographic gratings are compared with recently-ruled gratings.

#### **10.1.4. Irregularities in the depth of the grooves**

A distribution of groove depths about the nominal groove depth is a natural consequence of the burnishing process and the elasticity of metal coatings (in the case of ruled master gratings) or to local variations in exposure intensities and developing conditions (in the case of holographic master gratings). These variations have been shown to generate a continuous distribution of scattered light that varies with the inverse cube of the wavelength.<sup>123</sup>

#### **10.1.5. Spurious fringe patterns due to the recording system**

For holographic gratings, care must be taken to suppress all unwanted reflections and scattered light when producing the master grating. Light from optical mounts, for example, may reach the master grating substrate during exposure and leave a weak fringe pattern that causes scattered light when the grating is coated with a metal and illuminated.<sup>124</sup> A scratch on a lens in a recording beam can create a “bulls-eye” pattern on the master grating that serves as a scatter center for every replica made from that master. Recording the holographic

---

<sup>122</sup> Ibid.

<sup>123</sup> Ibid.

<sup>124</sup> M. C. Hutley, *Diffraction Gratings*, Academic Press (New York, 1970), p. 107.

master in incoherent light can reduce the stray light attributable to recording artifacts.<sup>125</sup>

### 10.1.6. The perfect grating

From the perspective of scattered light, a perfect grating would have a pattern of perfectly placed grooves (no variation in spacing from any groove to the next, and no additional pattern to the grooves leading to spacings  $d' \neq d$ ), each of the proper depth (no variation), and the surface irregularities on the grooves would be so much smaller than the wavelength of incident light that these irregularities would have no effect on the diffracted light. Moreover, this perfect grating would have no scratches, digs, blemishes or other visible surface features, and (if holographic) would contain no holographic artifacts of the recording optical system. In this ideal case, we might be forgiven in thinking that all light incident on the grating would leave according to the grating equation (2-1) for the nominal groove spacing  $d$ .

A general expression for the light intensity from a perfect grating is given by Sharpe and Irish<sup>126</sup> as

$$S(\lambda, \bar{\lambda}) = \frac{B}{N\lambda} \frac{\text{sinc}^2\left(\frac{\bar{\lambda} - \lambda_B}{\lambda}\right)}{\text{sinc}^2\left(1 - \frac{\lambda_B}{\lambda}\right)} \left(1 - \cos\left(\frac{2\pi\bar{\lambda}}{\lambda}\right)\right)^{-1} \quad (10-1)$$

where  $\lambda$  is the illumination wavelength,  $\bar{\lambda}$  is the monochromator setting (which determines the orientation of the grating: it is not a wavelength),  $\lambda_B$  is the blaze wavelength,  $B$  is the spectral bandpass of the instrument, and  $N$  is the number of grooves under illumination. We see that this equation is generally non-zero, so even a perfect grating cannot be expected to diffract no light anywhere except in its diffraction orders as given by Eq. (2-1).

---

<sup>125</sup> M. C. Hutley, "Improvements in or relating to the formation of photographic records," UK Patent no. 1384281 (1975); E. Sokolova, B. Kruizinga and I. Golubenko, "Recording of concave diffraction gratings in a two-step process using spatially incoherent light," *Opt. Eng.* **43**, 2613-2622 (2004).

<sup>126</sup> M. R. Sharpe and D. Irish, "Stray light in diffraction grating monochromators," *Opt. Acta* **25**, 861-893 (1978).

## **10.2. INSTRUMENTAL STRAY LIGHT**

Consider a spectrometer aligned so that the detector records the analytical wavelength  $\lambda$  in spectral order  $m$ . Our definition of instrumental stray light leads to its operational definition as light of either the wrong wavelength  $\lambda' \neq \lambda$  or the wrong spectral order  $m' \neq m$  that reaches the detector; this is generally a problem because most detectors are not wavelength-selective and cannot distinguish between light of wavelength  $\lambda$  and light of wavelength  $\lambda' \neq \lambda$ . Also included in our definition of stray light is any light that reaches the detector that does not follow the optical path for which the system was designed, even if this light is of wavelength  $\lambda$  and diffraction order  $m$ .

Instrumental stray light can be attributed to several factors, which are described below.

### **10.2.1. Grating scatter**

Light scattered by the grating, as discussed in Section 10.1 above, may reach the detector and contribute to instrumental stray light. This type of stray light is absent for a “perfect” grating.

### **10.2.2. Other diffraction orders from the grating**

Light of the analytical wavelength  $\lambda$  is not only diffracted into order  $m$ , but into any other orders that propagate. The zero order, which always propagates but is almost always of no value in the instrument, is particularly troublesome. The other diffracted beams are not oriented toward the detector by the grating, but if these beams are reflected by a wall, a mount or another optical component, or if these beams scatter off any interior surfaces in the instrument, some fraction of their intensity may reach the detector and contribute to instrumental stray light. This type of stray light is *not* absent even for a perfect grating, and requires proper instrumental design (*e.g.*, baffles, light traps, order-sorting filters *etc.*) to reduce.

### **10.2.3. Overfilling optical surfaces**

Fraunhofer diffraction from the illuminated edges of optical surfaces can be a significant cause of instrumental stray light. All optics in the path should be underfilled (that is, the illuminated area on the surface of each optic should fall within the edges of the optic), with masks or other apertures if necessary. Verrill has suggested that the intensity in the

incident beam fall off (from the center) according to a Gaussian function, to avoid an abrupt cut-off of intensity at the edge of the beam.<sup>127</sup>

Another important contributor to the instrumental stray light in some optical systems is the illumination of optical components downstream from the grating by light of wavelengths in the same diffraction order near the analytical wavelength  $\lambda$  (*i.e.*, the wavelength for which the monochromator is tuned). For example, in a Czerny-Turner monochromator (see Figure 6-1), the instrument may be designed so that light of wavelength  $\lambda$  underfills the concave mirror after the grating, but light of wavelengths  $\lambda \pm \Delta\lambda$  will diffract at slightly different angles and may impinge upon the edges of the mirror. These rays will scatter from the edges of the mirror and may reach the detector.<sup>128</sup>

#### 10.2.4. Direct reflections from other surfaces

A diffraction grating causes all wavelengths incident on it to diffract in different directions according to the grating equation, which in turn will illuminate the interior of the optical system.<sup>129</sup> Light in another order  $m' \neq m$  or at another wavelength  $\lambda' \neq \lambda$  for which  $m'\lambda' \neq m\lambda$  will not be diffracted toward the exit slit, but as in Section 10.2.2, this light may be reflected or scattered by other optical components, mounts or interior walls and directed toward the exit slit.

For certain wavelengths, light may reflect from another surface toward the grating and be rediffracted to the detector (called *multiply diffracted light*).<sup>130</sup> For example, in a Czerny-Turner monochromator (see Section 6.2.1), light can be diffracted by the grating back toward the first concave mirror and reflected toward the grating; this light will be diffracted again, and may reach the second mirror and then the exit slit. [Of course, the analogous situation may arise involving the second mirror

---

<sup>127</sup> J. F. Verrill, "The specification and measurement of scattered light from diffraction gratings," *Opt. Acta* **25**, 531-547 (1978).

<sup>128</sup> S. Brown and A. W. S. Tarrant, "Scattered light in monochromators," *Opt. Acta* **25**, 1175-1186 (1978).

<sup>129</sup> ASTM standard E387, "Standard Test Method for Estimating Stray Radiant Power Ratio of Dispersive Spectrophotometers by the Opaque Filter Method" (2004).

<sup>130</sup> J. J. Mitteldorf and D. O. Landon, "Multiply diffracted light in the Czerny-Turner spectrometer," *Appl. Opt.* **7**, 1431-1435 (1968); R. C. Hawes, "Multiply diffracted light in the Czerny-Turner spectrometer," *Appl. Opt.* **8**, 1063 (1969); A. B. Shafer and D. O. Landon, "Comments on Multiple Diffracted Light in a Czerny-Turner Spectrometer," *Appl. Opt.* **8**, 1063-1064 (1969).

instead of the first.] These possibilities can be eliminated by proper system design,<sup>131</sup> filtering,<sup>132</sup> or the use of masks.<sup>133</sup>

Proper instrument design and the use of baffles and light traps can reduce the effects of these unwanted reflections on instrumental stray light. Care in the analysis of the causes of stray light is especially important for monochromators, since all wavelengths in all diffraction orders (including the zero order) move as the analytical wavelength is scanned, so a wall or mount that does not cause stray light when the grating is in one orientation may be a major cause of stray light when the grating is rotated to another orientation.

Reflection (and diffuse scatter) from interior instrument walls can be reduced by using highly-absorbing paint or coatings on these surfaces and moving these surfaces as far from the optical train as possible (for this reason, it is generally more difficult to reduce stray light in smaller instruments).

Light can also scatter (or be reflected) by the exit slit.<sup>134</sup>

Tilting the detector element or array slightly, so that any reflections from its surface propagate out of the dispersion plane, can reduce the effects of this cause of stray light.

#### **10.2.5. Optical effects due to the sample or sample cell**

In analytical instruments, care must be taken to choose sample cells that are properly designed (given the characteristics of the optical path) and made of materials that do not fluoresce; otherwise the cell will be a source of stray light. Moreover, some samples will themselves fluoresce.

#### **10.2.6. Thermal emission**

For work in the far infrared, the blackbody radiation of all components in the instrument (as well as the instrument walls) will generate a background in the same spectral range as that of the analytical

---

<sup>131</sup> J. F. Verrill, "The specification and measurement of scattered light from diffraction gratings," *Opt. Acta* **25**, 531-547 (1978).

<sup>132</sup> A. Watanabe and G. C. Tabisz, "Multiply diffracted light in Ebert Monochromators," *Appl. Opt.* **6**, 1132-1134 (1967).

<sup>133</sup> C. M. Penchina, "Reduction of stray light in in-plane grating spectrometers," *Appl. Opt.* **6** 1029-1031 (1967).

<sup>134</sup> Ibid.

wavelength (e.g., at room temperature ( $293\text{ K} = 20\text{ }^{\circ}\text{C} = 68\text{ }^{\circ}\text{F}$ ), objects radiate with a spectrum that peaks around  $\lambda = 10\text{ }\mu\text{m}$ ).<sup>135</sup>

It is clear that a spectrometer containing a perfect grating (one that exhibits no detectable scattered light) will *still* have nonzero instrumental stray light. The often-made statement “the grating is the greatest cause of stray light in the system” may sometimes be true, but even a perfect grating must obey the grating equation.

### 10.3. ANALYSIS OF OPTICAL RAY PATHS IN A GRATING-BASED INSTRUMENT

Although a thorough raytrace analysis of an optical system is generally required to model the effects of scattered light, we may approach the case of a simple grating-based instrument conceptually. We consider the case in which the grating is illuminated with monochromatic light; the more general case in which many wavelengths are present can be considered by extension.

A simple case is shown in Figure 10-1. Light of wavelength  $\lambda$  enters the instrument through the entrance slit and diverges toward the grating, which diffracts the incident light into a number of orders  $\{m\}$  given by the grating equation (for all orders  $m$  for which  $\beta$  given by Eq. (2-1) is real). One of these orders (say  $m = 1$ ) is the analytical order, that which is designed to pass through the exit slit. All other propagating orders, including the ever-present  $m = 0$  order, are diffracted away from the exit slit and generally strike an interior wall of the instrument, which absorbs some of the energy, reflects some, and scatters some.

Some of the light reaching the interior walls may reflect or scatter directly toward the exit slit, but most of it does not; that which is reflected or scattered in any other direction will eventually reach another interior wall or it will return to the grating (and thereby be diffracted again).

This simple illustration allows us to draw a number of conclusions regarding the relative intensities of the various rays reaching the exit slit. We call  $E(\lambda,m)$  the diffraction efficiency of the grating (in this use geometry) at wavelength  $\lambda$  in order  $m$ ; therefore, we choose a grating for which  $E(\lambda,1)$  is maximal in this use geometry (which will minimize the efficiencies of the other propagating orders:  $E(\lambda,0)$ ,  $E(\lambda,-1)$ , etc.; see

---

<sup>135</sup> J. E. Stewart, “The effect of extraneous radiation on photometric accuracy of infrared spectrophotometers,” *Appl. Opt.* **2**, 1141-1146 (1963).

Section 9.12). We further call  $\varepsilon$  the fraction of light incident on an interior wall that is reflected and  $\phi$  the fraction that is scattered in any given direction, and stipulate that both  $\varepsilon$  and  $\phi$  are much less of unity (*i.e.*, we have chosen the interior walls to be highly absorbing). [Generally,  $\varepsilon$  and  $\phi$  depend on wavelength and incidence angle, and  $\phi$  on the direction of scatter as well, but for this analysis we ignore these dependencies.]

---

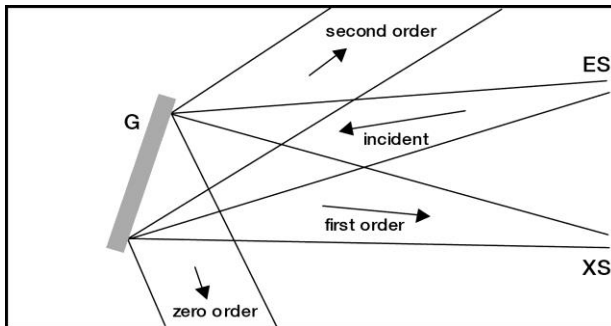


*Figure 10-1.* A simple grating system. Monochromatic light enters the system through the entrance slit *ES* and is diffracted by grating *G* into several orders by the grating; one of these orders (the analytical order) passes through the exit slit *XS*. Also shown are various rays other than that of the analytical order that may reflect or scatter off interior walls or other optics and reach the exit slit. [For simplicity, focusing elements are not shown.]

---

With these definitions, we can approximate total intensity  $I(\lambda,1)$  of the light incident on the grating that reaches the exit slit when the system is tuned to transmits wavelength  $\lambda$  in order  $m = 1$  as

$$\begin{aligned}
 I(\lambda,1) &= I_0(\lambda) E(\lambda,1) \\
 &+ I_0(\lambda) \sum_{\substack{m \\ m \neq 1}} \varepsilon E(\lambda,m) + I_0(\lambda) \sum_{\substack{m \\ m \neq 1}} \phi E(\lambda,m) \\
 &+ I_0(\lambda) \sum_{\substack{m \\ m \neq 1}} \varepsilon^2 E(\lambda,m) + I_0(\lambda) \sum_{\substack{m \\ m \neq 1}} \varepsilon \phi E(\lambda,m) \quad (10-2) \\
 &+ I_0(\lambda) \sum_{\substack{m \\ m \neq 1}} \phi^2 E(\lambda,m) + O(3)
 \end{aligned}$$

where  $I_0(\lambda)$  is the intensity incident on the grating and  $O(3)$  represents terms of order three or higher in  $\varepsilon$  and  $\phi$ .

The first term in Eq. (10-2) is the intensity in the analytical wavelength and diffraction order; in an ideal situation, this would be the only light passing through the exit slit, so we may call this quantity the “desired signal”. Subtracting this quantity from both sides of Eq. (10-2), dividing by it and collecting terms yields the fractional stray light  $S(\lambda,1)$ :

$$\begin{aligned} S(\lambda,1) &= \frac{I(\lambda,1) - I_0(\lambda)E(\lambda,1)}{I_0(\lambda)E(\lambda,1)} \\ &= \left( \varepsilon + \phi + \varepsilon^2 + \varepsilon\phi + \phi^2 + O(3) \right) \sum_{m \neq 1} \frac{E(\lambda,m)}{E(\lambda,1)}. \end{aligned} \quad (10-3)$$

The first term in Eq. (10-3) is the sum, over all other propagating orders, of the fraction of light in those diffracted orders that is reflected by an interior wall to the exit slit, divided by the desired signal; each element in this sum is generally zero unless that order strikes the wall at the correct angle. The second term is the sum, over all other orders, of the fraction of light in those orders that is scattered directly into the exit slit; the elements in this sum are generally nonzero, again divided by the desired signal. Both of these sums are linear in  $\varepsilon$  or  $\phi$  (both  $\ll 1$ ) and in  $E(\lambda,m \neq 1)$  (each of which is considerably smaller than  $E(\lambda,1)$  since we have chosen the grating to be blazed in the analytical order). The third through fifth sums represent light that is reflected off two walls into the exit slit, or scattered off two walls into the exit slit, or reflected off one wall and scattered off another wall to reach the exit slit – in all three cases, the terms are quadratic in either  $\varepsilon$  or  $\phi$  and can therefore be neglected (under our assumptions).

If we generalize this analysis for a broad-spectrum source, so that wavelengths other than  $\lambda$  are diffracted by the grating, then we obtain

$$S(\lambda,1) = \left( \varepsilon + \phi + \varepsilon^2 + \varepsilon\phi + \phi^2 + O(3) \right) \sum_{m \neq 1} \int_{\lambda_1}^{\lambda_2(m)} d\lambda' \frac{E(\lambda',m)}{E(\lambda',1)}. \quad (10-4)$$

Note that, in each term, the integral over wavelength is inside the sum, since the upper limit of integration is limited by the grating equation (2-1) for each diffraction order  $m$ . Of course, the integration limits may be

further restricted if the detector employed is insensitive in certain parts of the spectrum.

## 10.4. DESIGN CONSIDERATIONS FOR REDUCING STRAY LIGHT

From Section 10.3, we can identify some suggestions for designing a grating-based system for which instrumental stray light is reduced. We consider a grating used in first order ( $m = 1$ ).

First, start with a grating as close to the definition of “perfect” in Section 10.1.6 as possible (easier said than done), and blaze it so that the first order efficiency  $E(\lambda, m=1)$  is as high as possible and the efficiencies in the other orders,  $E(\lambda, m \neq 1)$ , are as low as possible. Provided other design considerations (e.g., dispersion) are met, it may be advantageous to choose a groove spacing  $d$  such that only the first and zero orders propagate; by the analysis in Section 10.3, this will reduce each sum in Eq. (10-2) and Eq. (10-4) to one element each (for  $m = 0$ ).

Use an entrance slit that is as small as possible, and an exit slit that is as narrow as possible (without being narrower than the image of the entrance slit) and as short as possible (without reducing the signal to an unacceptably low level).

Underfill the grating and all other optical components, preferably by using a beam with a Gaussian intensity distribution. This will ensure that essentially all the light incident on the grating will be diffracted according to the grating equation (2-1).

Next, design the system to contain as few optical components between the entrance slit and the exit slit (or detector element(s)), for two reasons: each optic is a source of scatter, and each optic will pass less than 100% of the light incident on it – both effects will reduce the signal-to-noise (SNR) ratio. Specify optical components with very smooth surfaces (a specification which is more important when a short wavelength is used, since scatter generally varies inversely with wavelength to some power greater than unity<sup>136</sup>).

Design the optical system so that the resolution is slit-limited, rather than imaging-limited (see Section 8.3); this will reduce the spectral bandwidth passing through the exit slit (whose width, multiplied by the

---

<sup>136</sup> Stover, J. C., *Optical Scattering: Measurement and Analysis* (McGraw-Hill, New York: 1990).

reciprocal linear dispersion, will equal the entire spectral range passing through the slit; otherwise, the imaging imperfections will allow some neighboring wavelengths outside this range to pass through as well).

The choice of mounting (see chapters 6 and 7) can also affect instrumental stray light. For example, a Czerny-Turner monochromator (with two concave mirrors; see Section 6.2.1) will generally have lower stray light than a comparable Littrow monochromator (with a single concave mirror; see Section 6.2.4) since the former will allow the entrance and exit slits to be located farther apart.<sup>137</sup>

Make the distances between the surfaces as large as possible to take advantage of the inverse square law that governs intensity per unit area as light propagates; an underused idea is to design the optical system in three dimension rather than in a plane – this reduces the volume taken by the optical system and also removes some optics from the dispersion plane (which will reduce stray light due to reflections and multiply diffracted light).

Use order-sorting filters where necessary (or, for echelle systems, cross-dispersers<sup>138</sup>). Also, the use of high-pass or low-pass filters to eliminate wavelengths emitted by the source but outside the wavelength range of the instrument, and to which the detector is sensitive, will help reduce stray light by preventing the detector from seeing these wavelengths.

It may be advantageous to make the interior walls not only highly absorbing but reflecting rather than scattering (*i.e.*, use a glossy black paint rather than a flat black paint). The rationale for this counterintuitive suggestion is that if all unwanted light cannot be absorbed, it is better to control the direction of the remainder by reflection rather than to allow it to scatter diffusely; controlled reflections from highly-absorbing surfaces (with only a few percent of the light reflected at each surface) will quickly extinguish the unwanted light without adding to diffuse scatter. Of course, care must be taken during design to ensure that there are no direct paths (for one or two reflections) directly to the exit slit; baffles can be helpful when such direct paths are not otherwise avoidable.

---

<sup>137</sup> J. F. Verrill, “The specification and measurement of scattered light from diffraction gratings,” *Opt. Acta* **25**, 531–547 (1978).

<sup>138</sup> R. W. Wood, *J. Opt. Soc. Am.* **37**, 733 (1947); G. R. Harrison, “The production of diffraction gratings: II. The design of echelle gratings and spectrographs,” *J. Opt. Soc. Am.* **39**, 522–528 (1949).

Avoid grazing reflections from interior walls, since at grazing angle even materials that absorb at near-normal incidence are generally highly reflecting.

Ensure that the system between the entrance slit and the detector is completely light-tight, meaning that room light cannot reach the detector, and that only light passing through the entrance slit can reach the exit slit.

Finally, hide all mounting brackets, screws, motors, *etc.* – anything that might scatter or reflect light. Any edges (including the slits) should be painted with a highly absorbing material; this includes the edges of baffles.

While it is always best to reduce instrumental stray light as much as possible, a lock-in detection scheme can be employed to significantly reduce the effects of instrumental stray light. The technique involves chopping (alternately blocking and unblocking) the principal diffraction order and using phase-sensitive detection to retrieve the desired signal.<sup>139</sup>

A useful technique at the breadboard stage (or, if necessary, the product stage) is to operate the instrument in a dark room, replace the exit slit or detector with the eye or a camera, and look back into the instrument (taking adequate precautions if intense light is used). What other than the last optical component can be seen? Are there any obvious sources of scatter, or obvious undesirable reflections? What changes as the wavelength is scanned? Before the availability of commercial stray light analysis software, this technique was often used to determine what surfaces needed to be moved, or painted black, or hidden from “the view of the exit slit” by baffles and apertures; even today, optical systems designed with such software should be checked in this manner.

---

<sup>139</sup> H. Field, “UV-VIS-IR spectral responsivity measurement system for solar cells,” National Renewable Energy Laboratory pub. CP-520-25654 (November 1998).

# 11. TESTING AND CHARACTERIZING DIFFRACTION GRATINGS

## 11.1. THE MEASUREMENT OF SPECTRAL DEFECTS<sup>140</sup>

It is fundamental to the nature of diffraction gratings that errors are relatively easy to measure, although not all attributes are equally detectable or sometimes even definable.

For example, a grating with low background (in the form of scatter or satellites) can be simply tested for Rowland ghosts on an optical bench. With a mercury lamp or a laser source, and a scanning slit connected to a detector and recorder, a ghost having intensity 0.002% of the intensity of the main line can be easily observed. The periodic error in the groove spacing giving rise to such a ghost may be less than one nanometer.

Grating ghosts are measured at MKS by making the grating part of a scanning spectrometer and illuminating it with monochromatic light, such as that from a mercury isotope lamp (isotope 198 or 202) or a helium-neon laser. On scanning both sides of the parent line, using a chart recorder and calibrated attenuators, it is easy to identify all ghost lines and to measure their intensities relative to the parent line.

The importance of ghosts in grating applications varies considerably. In most spectrophotometers, and in work with low-intensity sources, ghosts play a negligible role. In Raman spectroscopy, however, even the weakest ghost may appear to be a Raman line, especially when investigating solid samples, and hence these ghosts must be suppressed to truly negligible values.

Ghosts are usually classified as Rowland ghosts, Lyman ghosts and satellites.

### 11.1.1. Rowland ghosts

Rowland ghosts are spurious lines seen in some grating spectra that result from large-scale (millimeter) periodic errors in the spacing of the grooves (see Figure 11-1). These lines are usually located symmetrically with respect to each strong spectral line at a (spectral) distance from it

---

<sup>140</sup> For additional reading, see E. G. Loewen and E. Popov, *Diffraction Gratings and Applications*, Marcel Dekker, Inc. (1997), pp. 402-413.

that depends on the period of the error, and with an intensity that depends on the amplitude of this error.

---

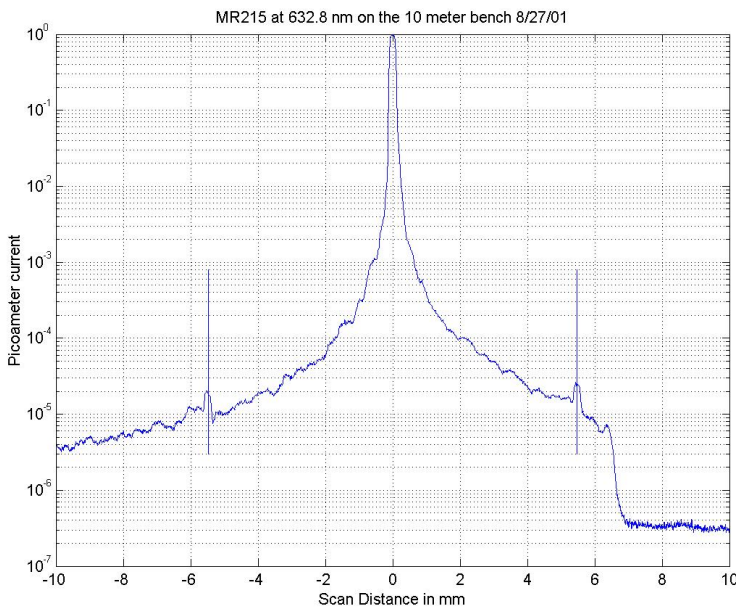


Figure 11-1. 'Ghost' trace showing Rowland ghosts caused by the periodic error of 2.54 mm in the lead screw of the MIT 'B' engine. MR215 is an echelle grating, with 52.67 g/mm, in this case tested in the 54<sup>th</sup> order.

---

If the curve of groove spacing error *vs.* position is not simply sinusoidal, there will be several ghosts on each side of the parent line representing the various orders from each of the harmonics of the error curve. On engines with mechanical drives, Rowland ghosts are associated primarily with errors in the lead or pitch of the precision screw, or with the bearings of the ruling engine. As a consequence, their location depends upon the number of grooves ruled for each complete turn of the screw. For example, if the ruling engine has a pitch of 2 mm, and a ruling is made at 1200 grooves/mm, 2400 grooves will be ruled per turn of the screw, and the ghosts in the first order can be expected to lie at  $\Delta\lambda = \pm \lambda/2400$  from the parent line  $\lambda$ , with additional ghosts located at integral multiples of  $\Delta\lambda$ . In gratings ruled on engines with interferometric feedback correction mechanisms, Rowland ghosts are usually much less

intense, but they can arise from the mechanisms used in the correction system if care is not taken to prevent their occurrence.

If the character of the periodic errors in a ruling engine were simply harmonic, which is rarely true in practice, the ratio of the diffracted intensities of the first order Rowland ghost ( $I_{RG(m=1)}$ ) to that of the parent line ( $I_{PL}$ ) is

$$\frac{I_{RG(m=1)}}{I_{PL}} = 4 \left( \frac{\pi A \sin \alpha}{\lambda} \right)^2, \quad (11-1)$$

where  $A$  is the peak simple harmonic error amplitude,  $\alpha$  is the angle of incidence, and  $\lambda$  is the diffracted wavelength.

The second-order Rowland ghost  $I_{RG(m=2)}$  will be much less intense (note the exponent):

$$\frac{I_{RG(m=2)}}{I_{PL}} = 4 \left( \frac{\pi A \sin \alpha}{\lambda} \right)^4. \quad (11-2)$$

Higher-order Rowland ghosts would be virtually invisible. The ghost intensity is independent of the diffraction order  $m$  of the parent line, and of the groove spacing  $d$ . In the Littrow configuration, Eq. (11-1) becomes

$$\frac{I_{RG(m=1)}}{I_{PL}} = \left( \frac{\pi m A}{d} \right)^2, \quad \text{in Littrow,} \quad (11-3)$$

an expression derived in 1893 by Rowland.

These simple mathematical formulas do not always apply in practice when describing higher-order ghost intensities, since the harmonic content of actual error curves gives rise to complex amplitudes that must be added vectorially and then squared to obtain intensity functions. Fortunately, the result of this complication is that ghost intensities are generally smaller than those predicted from the peak error amplitude.

The order of magnitude of the fundamental harmonic error amplitude can be derived from Eq. (11-1) or Eq. (11-3). For example, a 1200 g/mm grating used in the  $m = 1$  order in Littrow will show a 0.14% first-order ghost intensity, compared with the parent line, for a fundamental harmonic error amplitude of  $A = 10$  nm. For some applications, this ghost intensity is unacceptably high, which illustrates the importance of minimizing periodic errors of ruling. For Raman gratings and echelles, the amplitude  $A$  of the periodic error must not exceed

one nanometer; the fact that this has been accomplished is a remarkable achievement.

### 11.1.2. Lyman ghosts

Ghost lines observed at large spectral distances from their parent lines are called Lyman ghosts. They result from compounded periodic errors in the spacing of the grating grooves; the period of Lyman ghosts is on the order of a few times the groove spacing.

Lyman ghosts can be said to be in fractional-order positions (see Figure 11-2). Thus, if every other groove is misplaced so that the period contains just two grooves, ghosts are seen in the half-order positions. The number of grooves per period determines the fractional-order position of Lyman ghosts.

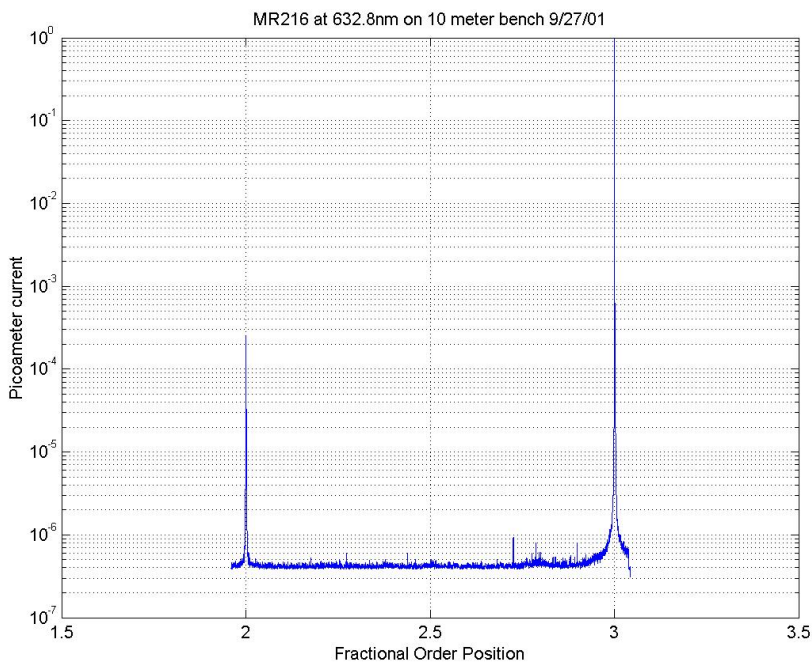


Figure 11-2. ‘Ghost’ trace showing Lyman ghosts, the small spikes between orders 2 and 3, which can be associated with fractional order positions, e.g., an error every five grooves corresponds to a fraction order of 1/5.

---

Usually it is possible to find the origin of the error in the ruling engine once its periodicity is determined. It is important that Lyman ghosts be kept to a minimum, because they are not nearly as easy to identify as Rowland ghosts.

### 11.1.3. Satellites

Satellites are false spectral lines usually occurring very close to the parent line. Individual gratings vary greatly in the number and intensity of satellites which they produce. In a poor grating, they give rise to much scattered light, referred to as *grass* (so called since this low intensity scattered light appears like a strip of lawn when viewed with green mercury light). In contrast to Rowland ghosts, which usually arise from errors extending over large areas of the grating, each satellite usually originates from a small number of randomly misplaced grooves in a localized part of the grating. With laser illumination, a relative background intensity of  $10^{-7}$  is easily observable with the eye.

## 11.2. THE MEASUREMENT OF GRATING EFFICIENCY<sup>141</sup>

Grating efficiency measurements are generally performed with a double monochromator system. The first monochromator supplies monochromatic light derived from a tungsten lamp, mercury arc, or deuterium lamp, depending on the spectral region involved. The grating being tested serves as the dispersing element in the second monochromator. In the normal mode of operation, the output is compared with that from a high-grade mirror coated with the same material as the grating. The efficiency of the grating relative to that of the mirror is reported (relative efficiency), although absolute efficiency values can also be obtained (either by direct measurement or through knowledge of the variation of mirror reflectance with wavelength). For plane reflection gratings, the wavelength region covered is usually 190 nm to 2.2  $\mu\text{m}$ ; gratings blazed farther into the infrared are often measured in higher orders. Concave reflection gratings focus as well as disperse the light, so the entrance and exit slits of the second monochromator are placed at the positions for which the grating was designed (that is, concave grating

---

<sup>141</sup> For additional reading, see E. G. Loewen and E. Popov, *Diffraction Gratings and Applications*, Marcel Dekker, Inc. (1997), pp. 413-423, and also D. J. Michels, T. L. Mikes and W. R. Hunter, "Optical grating evaluator: a device for detailed measurement of diffraction grating efficiencies in the vacuum ultraviolet," *Appl. Opt.* **13**, 1223-1229 (1974).

efficiencies are measured in the geometry in which the gratings are to be used). Transmission gratings are tested on the same equipment, with values given as the ratio of diffracted intensity to the intensity falling directly on the detector from the light source (*i.e.*, absolute efficiency).

Curves of efficiency *vs.* wavelength for plane gratings are made routinely on all new master gratings produced by MKS, both plane and concave, with light polarized in the S and P planes to assess the presence and amplitudes (if any) of anomalies. Such curves are available on the Richardson Gratings website, <http://www.gratinglab.com/> (for an example, see Figure 11-3).

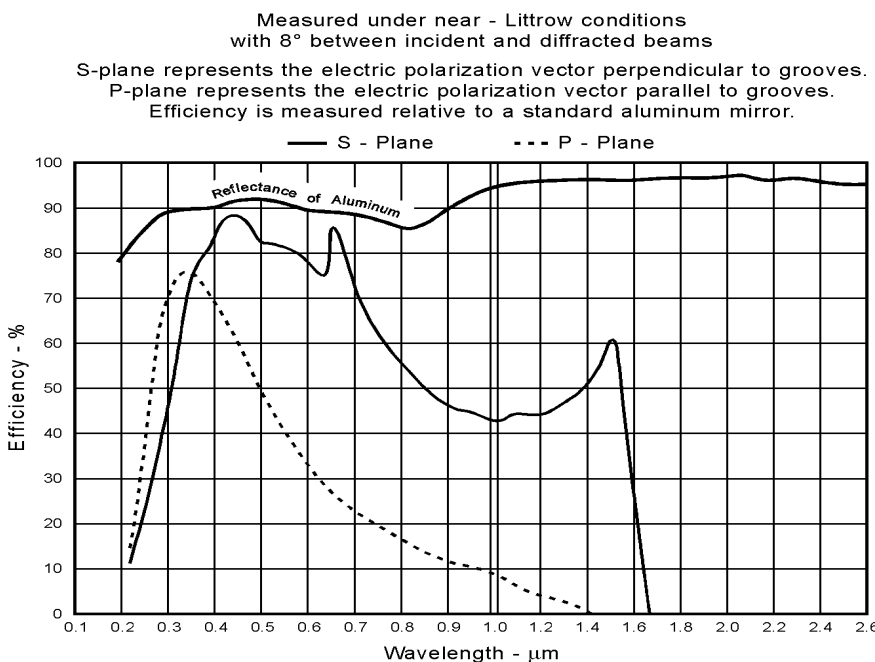


Figure 11-3. Example of an efficiency curve. This efficiency curve is specific to the particular grating under test, as well as the conditions of illumination (the incidence and diffraction angles).

## **11.3. THE MEASUREMENT OF DIFFRACTED WAVEFRONT QUALITY**

### **11.3.1. The Foucault knife-edge test**

One of the most critical tests an optical system can undergo is the Foucault knife-edge test. This test not only reveals a great deal about wavefront deficiencies but also locates specific areas (or zones) on the optical component where they originate. The test is suited equally well to plane and concave gratings (for the former, the use of very high-grade collimating optics is required). The sharper (*i.e.*, more abrupt) its knife-edge cut-off, the more likely that a grating will yield high resolution.

The sensitivity of the test depends on the radius of the concave grating (or the focal length of the collimating system), and may exceed that of interferometric testing, although the latter is more quantitative.

The Foucault test is a sensitive and powerful tool, but experience is required to interpret each effect that it makes evident. All MKS plane gratings, large plane replicas and large-radius concave gratings are checked by this method (see Figure 11-4).

### **11.3.2. Direct wavefront testing**

Any departure from perfect flatness of the surface of a plane grating, or from a perfect sphere of the surface of a concave grating, as well as variations in the groove spacing, depth or parallelism, will result in a diffracted wavefront that is less than perfect. In order to maintain resolution, this departure from perfection is generally held to  $\lambda/4$  or less, where  $\lambda$  is the wavelength of the light used in the test. To obtain an understanding of the magnitudes involved, it is necessary to consider the angle at which the grating is used. For simplicity, consider this to be the blaze angle, under Littrow conditions. Any surface figure error of height  $h$  will cause a wavefront deformation of  $2h \cos\theta$ , which decreases with increasing  $|\theta|$ . On the other hand, a groove position error  $p$  introduces a wavefront error of  $2p \sin\theta$ , which explains why ruling parameters are more critical for gratings used in high-angle configurations.

A plane grating may produce a slightly cylindrical wavefront if the groove spacing changes linearly, or if the surface figure is similarly deformed. In this special case, resolution is maintained, but focal distance will vary with wavelength.

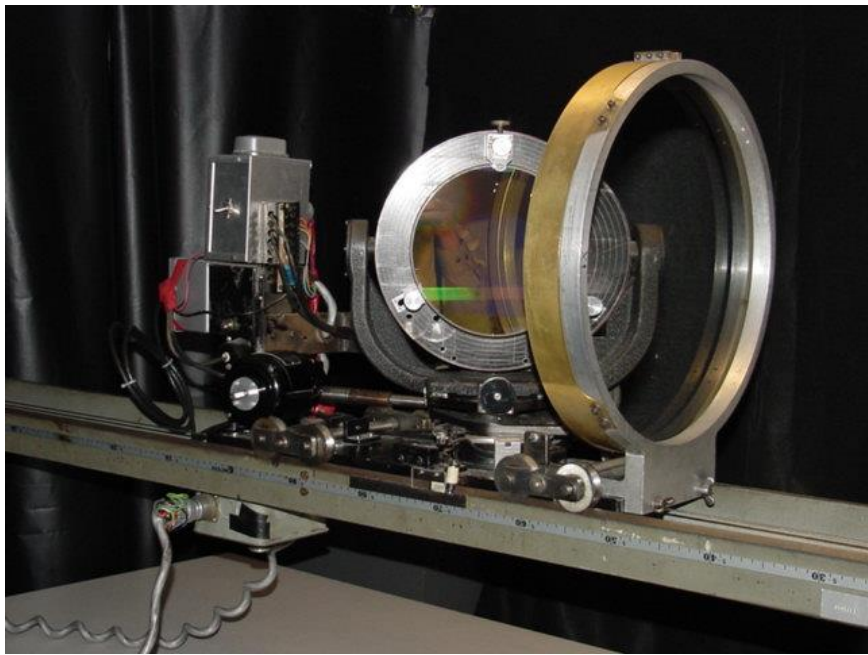


*Figure 11-4. A grating under test on the MKS 5-meter test bench. Light from a mercury source (not shown, about 5 meters to the right) is collimated by the lens (shown) which illuminates the grating (shown on a rotation stage); the same lens refocuses the diffracted light to a plane very near the light source, where the diffracted wavefront can be inspected.*

A plane grating may produce a slightly cylindrical wavefront if the groove spacing changes linearly, or if the surface figure is similarly deformed. In this special case, resolution is maintained, but focal distance will vary with wavelength.

Wavefront testing can be done conveniently by mounting a grating at its autocollimating angle (Littrow) in a Twyman-Green interferometer or a phase measuring interferometer (PMI; see Figure 11-5). MKS interferometers have apertures up to 150 mm (6 inches). With coherent laser light sources, however, it is possible to make the same measurements with a much simpler Fizeau interferometer, equipped with computer fringe analysis.

It should be noted that testing the reflected wavefront – that is, illuminating the grating in zero order – is generally inadequate since this arrangement will examine the flatness of the grating surface but tells nothing about the uniformity of the groove pattern.

Periodic errors give rise to zig-zag fringe displacements. A sudden change in groove position gives rise to a step in the fringe pattern; in the spectrum, this is likely to appear as a satellite. Curved fringes due to progressive ruling error can be distinguished from figure problems by observing fringes obtained in zero, first and higher orders. Fanning error (non-parallel grooves) will cause spreading fringes. Figure 11-6 shows a typical interferogram, for an echelle grating measured in Littrow in the diffraction order of use ( $m = 33$ ).

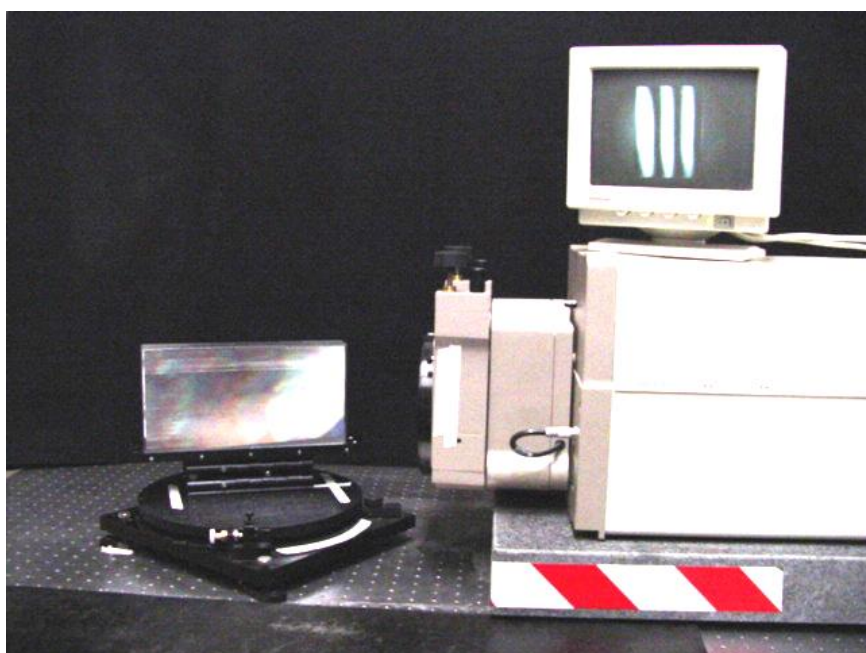
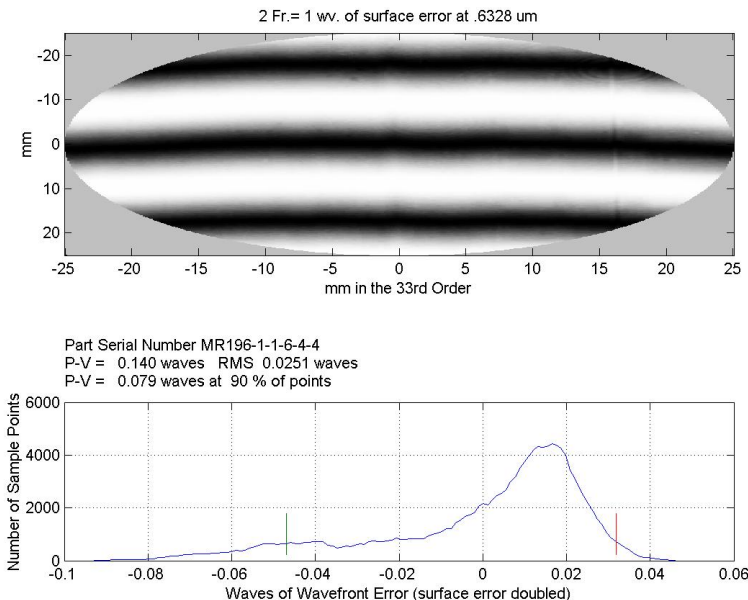


Figure 11-5. A plane grating under test on a phase measuring interferometer. The grating is tested in the Littrow configuration so that the flatness of the diffracted wavefront is evaluated.

Experience has shown that the sensitivity of standard interferograms for grating deficiencies equals or exceeds that of other plane grating testing methods only for gratings used at high angles. This is why the interferometric test is especially appropriate for the testing of echelles and other gratings used in high diffraction orders.



*Figure 11-6. Example of an interferogram and histogram generated by a Phase Measuring Interferometer (PMI). In this example, a grating is illuminated in a circular region 50 mm in diameter, and its diffracted wavefront at  $\lambda = 632.8$  nm in the  $m = 33$  order is recorded.*

## 11.4. THE MEASUREMENT OF RESOLVING POWER<sup>142</sup>

Resolving power (defined in Section 2.4) is a crucial characteristic of diffraction gratings since it is a measure of the fundamental property for which gratings are used: it quantifies the ability of the grating (when used in an optical system) to separate two nearby wavelengths. Often resolving power is specified to be great enough that the resolution of the optical system will be slit limited rather than grating limited (see Section 8.3).

Resolving power is generally measured in a spectrometer with a large focal length and very narrow slits in which the light source has fine

<sup>142</sup> For additional reading, see J. Strong, "New Johns Hopkins ruling engine," *J. Opt. Soc. Am.* **41**, 3-15 (1951), J. F. Verrill, "The limitations of currently used methods for evaluating the resolution of diffraction gratings," *Opt. Acta* **28**, 177-185 (1981), and E. G. Loewen and E. Popov, *Diffraction Gratings and Applications*, Marcel Dekker, Inc. (1997), pp. 423-432.

spectral structure; an example is the hyperfine spectrum of natural Hg near 546.1 nm (see Figure 11-7). The spectral lines are identified, and the wavelengths of those that are distinguishable ('resolvable') are subtracted, and this difference  $\Delta\lambda$  is divided into  $\lambda = 546.1$  nm according to Eq. (2-18); the smaller the wavelength difference, the greater the resolving power.

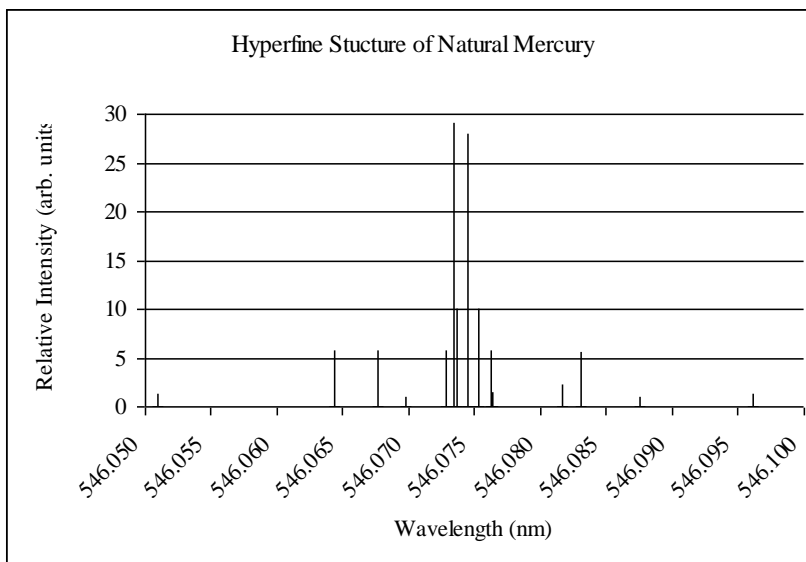


Figure 11-7. Hyperfine structure of natural Hg near 546.1 nm. Several spectral lines are identified. Visual identification of two distinct emission lines centered on  $\lambda$  and separated by  $\Delta\lambda$  implies a resolving power at least as great as  $\lambda/\Delta\lambda$ .

Resolving power is measured on MKS diffraction gratings using a specially-designed Czerny-Turner spectrograph, whose concave mirrors have very long focal lengths (10 m) so that very large astronomical gratings may be tested (see Section 13.3).

## 11.5. THE MEASUREMENT OF SCATTERED LIGHT<sup>143</sup>

As discussed in Chapters 2 and 10, light that leaves a grating surface that does not follow the grating equation (2-1) is called scattered light.

<sup>143</sup> For additional reading, see J. F. Verrill, "The specification and measurement of scattered light from diffraction gratings," *Opt. Acta* **25**, 531-547 (1978).

Scattered light is generally measured in one of two ways: either with cut-off filters (which absorb one part of the spectrum while transmitting the other part) or by using monochromatic light (from an atomic emission source or a laser, or using interference filters that transmit a narrow spectral range).

MKS has three specially-designed instruments to measure light scattered from small regions on the surface of a mirror or grating: two instruments use red HeNe light ( $\lambda = 632.8$  nm) to illuminate the grating, and the third uses a Hg source to illuminate the grating (the light reaching the detector is filtered to transmit a narrow spectral band around 254 nm). These “scatter checkers” provide several degrees of freedom so that light scattered between diffraction orders (called *inter-order scatter*) can be attributed to areas on the grating surface.

Figure 11-8 shows a simplified schematic diagram of the scatter checker. The beam from a polarized HeNe laser is spatially filtered to remove speckle and is then directed onto a concave focusing mirror that brings the beam to focus at the detector plane. The detector is a photomultiplier that, in combination with a programmable-gain current amplifier, provides eight decades of dynamic range. A PC equipped with a data acquisition card is used to process and store the detector signal.

If an absolute scatter measurement is required, measurements are made by first obtaining a reference beam profile (see Figure 11-9), or “instrument signature,” by translating the test optic out of the way and rotating the detector through the beam in incremental steps over a predetermined angular range. The test optic is then translated into the beam path and the detector passed through the reflected (or diffracted) beam from the test optic over the same angular range used to make the reference measurement. The sample and reference beam profiles are “mirror images” of one another, so it is necessary to invert one before a comparison is made. Any difference between the sample and reference beam profiles can be attributed to light scattered from the optic under test. Relative scatter measurements do not require the characterization of the instrument signature.

It is important to apply the lessons of Chapter 10 to the interpretation of grating scatter measurements. That is, even a “perfect” grating (as defined in Section 10.1.6) illuminated with monochromatic light will cause other diffraction orders to propagate, and some of this light energy may reach the detector of the scatter measuring apparatus. This is

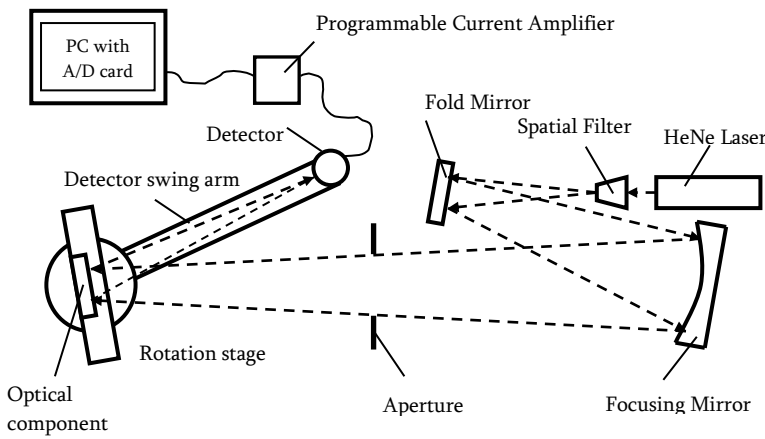


*Figure 11-8. Schematic of the MKS red HeNe scatter measuring apparatus.* To minimize the effects that other diffraction orders may have on the scattered light readings, this instrument is not enclosed so that any light that leaves the grating in a direction other than toward the detector will travel a long distance before encountering a reflecting or scattering surface.

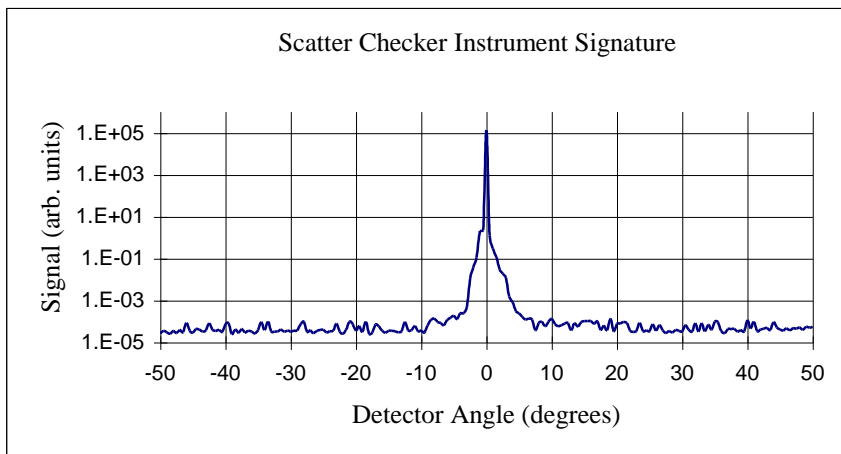


*Figure 11-9. Typical plot of data obtained from the MKS red HeNe scatter measuring instrument.* This plot of the measured signal vs. angle of rotation of the detector (from a diffracted order) shows the reference beam profile (the “instrument signature”).

important when comparing the scatter characteristics of a grating with those of a high-quality mirror (using the latter as a reference<sup>144</sup>); the mirror produces only the  $m = 0$  order (specular reflection) and will therefore exhibit lower scatter than even a “perfect” grating. This subtle point must be considered in defining the instrument signature of a grating-based optical system by using a mirror.

In analyzing grating scatter measurements, care must be taken to account for any stray light that is due to the measurement apparatus rather than the grating, as discussed in Sections 10.2 and 10.3.

## **11.6. THE MEASUREMENT OF INSTRUMENTAL STRAY LIGHT**

The consequence of undesired energy reaching the detector in a spectrometer is a reduction in photometric accuracy, since some light reaches the detector that cannot be attributed to the transmission (or absorption) of the sample at the analytical wavelength.

Instrumental stray light, like scattered light, is generally measured either with cut-off filters or monochromatic light.

### **11.6.1. The use of cut-off filters<sup>144</sup>**

Instrumental stray light is commonly measured by using a set of high-pass cut-off optical filters (whose transmission curves look like that in Figure 11-10). The spectrometer is then scanned toward shorter wavelengths and the transmittance measured; once the transmittance level has reached a steady minimum (a plateau), this reading is taken to be the stray light.<sup>145</sup>

The instrument is tuned to the analytical wavelength  $\lambda$  and a series of filters, each with a successively higher cut-off wavelength  $\lambda_c (>\lambda)$ , is placed in the beam and intensity readings taken at the detector. [Generally,  $\lambda_c$  should exceed  $\lambda$  by at least 20 nm, in the visible spectrum, to ensure than virtually no light of the analytical wavelength  $\lambda$  passes

---

<sup>144</sup> R. E. Poulsom, “Test methods in spectrophotometry: stray-light determination,” *Appl. Opt.* **3**, 99-104 (1964); A. W. S. Tarrant, “Optical techniques for studying stray light in spectrometers,” *Opt. Acta* **25**, 1167-1174 (1978); ASTM standard E387, “Standard Test Method for Estimating Stray Radiant Power Ratio of Dispersive Spectrophotometers by the Opaque Filter Method” (2004).

<sup>145</sup> K. D. Mielenz, V. R. Weidner and R. W. Burke, “Heterochromic stray light in UV absorption spectrometry: a new test method,” *Appl. Opt.* **21**, 3354-3356 (1982).

through the filter and complicates the readings.] Nonzero readings indicate the presence of stray light. A proper study requires measurements at more than one analytical wavelength since stray light properties cannot be easily extrapolated (due to the different wavelength dependencies of the causes of grating scatter and instrumental stray light noted above, and – for monochromators – the fact that all rays diffracted from or scattered by the grating change direction as the grating is rotated).

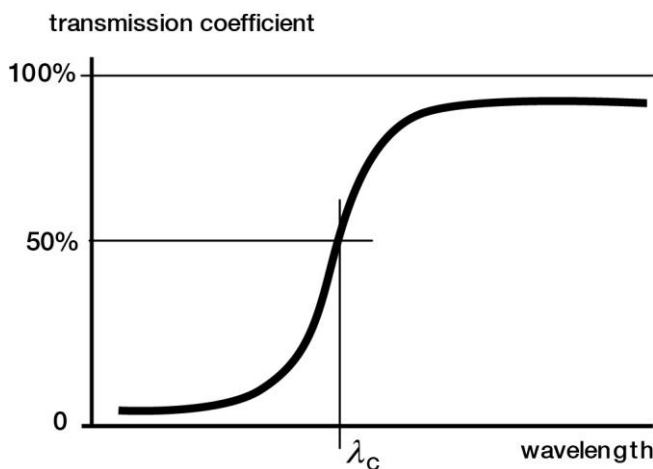


Figure 11-10. Transmission curve of a typical high-pass cut-off filter. A filter of this type is generally specified by the cut-off wavelength  $\lambda_c$ , the wavelength at which its transmission coefficient is 50%. The slope of the transmission curve near  $\lambda_c$  should be as steep as possible.

### 11.6.2. The use of monochromatic light

Another method for measuring instrumental stray light is to replace the polychromatic light source (used with cut-off filters) with a narrow-band monochromatic light source. Atomic emission sources provide narrow spectral emission lines that can be used for this purpose; lasers can be used; and broad-spectrum sources can be used in conjunction with bandpass filters.

Kaye<sup>146</sup> describes a technique in which monochromatic light is used to determine the amount of power detected at all wavelength settings for a given input wavelength; this quantity is called the *slit function*. The spectrometer (with slit widths  $w$ ) is illuminated by light whose central wavelength is  $\lambda$ , and whose spectral width  $\Delta\lambda$  is very narrow ( $\Delta\lambda \ll \lambda$ ). Scanning through the full wavelength range of the instrument (the wavelength setting being denoted by  $\bar{\lambda}$ ; see Section 10.1.6) and recording the power at each setting yields the slit function  $S_\lambda(\bar{\lambda}, w)$ , which we may write as

$$S_\lambda(\bar{\lambda}, w) = cE_\lambda M_\lambda(\bar{\lambda}, w)R_\lambda, \quad (11-4)$$

where  $E_\lambda$  is the power emitted by the source,  $M_\lambda(\bar{\lambda}, w)$  is the transmittance of the optical system (between the source and the detector),  $R_\lambda$  is the sensitivity of the detector, and  $c$  is a constant of proportionality. If we had knowledge of the slit function for all input wavelengths  $\lambda$  and for all wavelength settings  $\bar{\lambda}$ , we would be able to write for any wavelength setting the following integral:

$$S(\bar{\lambda}, w) = \int_0^\infty S_\lambda(\bar{\lambda}, w), \quad (11-5)$$

which represents the total power (for all wavelengths) recorded at wavelength setting  $\bar{\lambda}$ . In practice, the bounds of integration are not 0 and  $\infty$ , but are instead determined by the spectral sensitivity limits of the detector.

Stray light can then be expressed as the ratio of the intensities (powers) of the scattered light and principal beam.<sup>147</sup>

### 11.6.3. Signal-to-noise and errors in absorbance readings

Often the unwanted light in a spectrometer is quantified not by instrumental stray light but by the *signal-to-noise ratio* (SNR), a dimensionless quantity of more relevance to instrumental specification.

<sup>146</sup> W. Kaye, "Resolution and stray light in near infrared spectroscopy," *Appl. Opt.* **14**, 1977-1986 (1975).

<sup>147</sup> A. W. S. Tarrant, "Optical techniques for studying stray light in spectrophotometers," *Opt. Acta* **25**, 1167-1174 (1978); S. Brown and A. W. S. Tarrant, "Scattered light in monochromators," *Opt. Acta* **25**, 1175-1186 (1978).

The SNR is defined as the ratio of the signal (the desired power incident on the detector) to the noise (the undesired power, equivalent in our definition to the instrumental stray light).

Another specification of instrumental stray light is given in absorbance, a dimensionless quantity defined by

$$A = \log_{10}\left(\frac{100}{T}\right), \quad (11-6)$$

where  $T$  is the percent transmittance ( $0 \leq T \leq 100$ ). Higher values of  $A$  correspond to lower transmittances, and instrumental stray light plays an important role in the highest value of  $A$  for which the readings are accurate; an instrument for which the stray light is about 1% as intense as the signal at a given wavelength cannot provide absorbance readings of any accuracy greater than  $A \approx 2$ .

When the stray light power  $s$  is known (as a percentage of the signal), Eq. (11-6) may be modified to be made more accurate:<sup>148</sup>

$$A = \log_{10}\left(\frac{100 - s}{T - s}\right). \quad (11-7)$$

---

<sup>148</sup> A. Opler, "Spectrophotometry in the presence of stray radiation: a table of  $\log[(100 - k)/(T - k)]$ ," *J. Opt. Soc. Am.* **40**, 401-403 (1950).



## 12. SELECTION OF DISPERSING SYSTEMS

### 12.1. REFLECTION GRATING SYSTEMS

Reflection grating systems are much more common than transmission grating systems. Optical systems can be 'folded' with reflection gratings, which reflect as well as disperse, whereas transmission grating systems are 'in-line' and therefore usually of greater length. Moreover, reflection gratings are not limited by the transmission properties of the grating substrate (or resin) and can operate at much higher angles of diffraction.

#### 12.1.1. Plane reflection grating systems

The choice of existing plane reflection gratings is extensive and continually increasing. Master gratings as large as 320 mm x 420 mm have been ruled. Plane gratings have been used for ultraviolet, visible and infrared spectra for some time; they are also used increasingly for wavelengths as short as 110 nm, an extension made possible by special coatings that give satisfactory reflectivity even at such short wavelengths (see Chapter 9).

The most popular arrangement for plane reflection gratings is the Czerny-Turner mount, which uses two spherical concave mirrors between the grating and the entrance and exit slits. A single mirror arrangement (the Ebert-Fastie mount) can also be used. Both achieve spectral scanning through rotation of the grating. Collimating lenses are rarely used, since mirrors are inherently achromatic. [See Chapter 6 for a discussion of plane grating mounts.]

For special purposes, plane reflection gratings can be made on unusual materials, such as ceramics or metals, given special shapes, or supplied with holes for Cassegrain and Coudé-type telescopic systems.

#### 12.1.2. Concave reflection grating systems

The great advantage in using concave gratings lies in the fact that separate collimating and focusing optics are unnecessary. This is particularly important in the far vacuum ultraviolet region of the spectrum, for which there are no good normal-incidence reflectors. Two mirrors, each reflecting 20% of the light incident on them, will reduce throughput by a factor of twenty-five. Hence, concave grating systems are preferred

in the entire ultraviolet region. Their chief deficiency lies in their wavelength-specific imaging properties, which leads to astigmatism, which in turn limits the exit slit size (and, consequently, the energy throughput). The situation can be improved somewhat by using toroidal grating substrates; however, their use is restricted because of high costs.

Though most ruled gratings are flat, curved substrates can be ruled as well if their curvatures are not extreme. Concave gratings are not only more difficult to rule than plane gratings, since the tool must swing through an arc as it crosses the substrate, but they require the spherical master substrate to have extremely high surface accuracy and tight tolerances on surface irregularity.

Another limitation of ruled concave gratings appears when they are ruled at shallow groove angles. The ruled width is unfortunately limited by the radius of the substrate, since the diamond cannot rule useful grooves when the slope angle of the substrate exceeds the blaze angle. The automatic energy limitation that is thereby imposed can be overcome by ruling multipartite gratings, during which the ruling process is interrupted once or twice so that the diamond can be reset at a different angle. The resulting bipartite or tripartite gratings are very useful, as available energy is otherwise low in the short wavelength regions. One must not expect such gratings to have a resolving power more than that of any single section, for such an achievement would require phase matching between the grating segments to a degree that is beyond the present state of the art.

The advent of the holographic method of generating gratings has made the manufacture of concave gratings commonplace. Since the fringe pattern formed during the recording process is three-dimensional, a curved substrate placed in this volume will record fringes. Unlike ruled gratings, concave holographic gratings can be generated on substrates whose radii are fairly small (< 100 mm) and whose curvatures are fairly high ( $\sim f/1$  or beyond).

## **12.2. TRANSMISSION GRATING SYSTEMS**

In certain types of instrumentation, transmission gratings (see Figure 12-1) are much more convenient to use than reflection gratings. The most common configuration involves converting cameras into simple spectrographs by inserting a grating in front of the lens. This configuration is often used for studying the composition of falling meteors or the re-entry of space vehicles, where the distant luminous

streak becomes the entrance slit. Another application where high-speed lenses and transmission gratings can be combined advantageously is in the determination of spectral sensitivity of photographic emulsions.

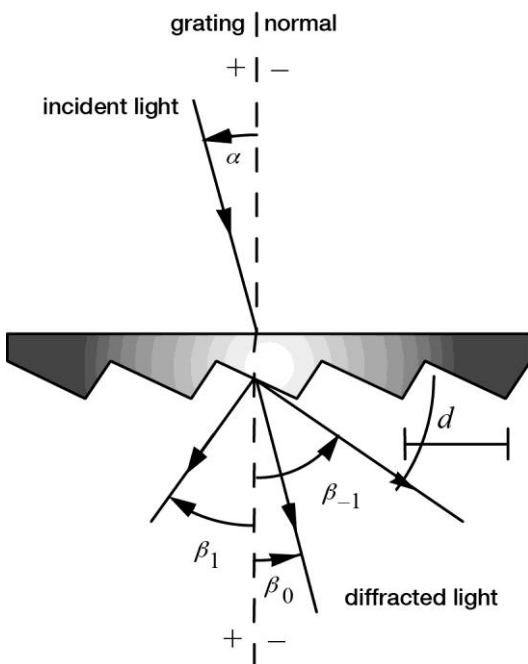


*Figure 12-1. Diffraction by a plane transmission grating.* A beam of monochromatic light of wavelength  $\lambda$  is incident on a grating at angle  $\alpha$  to the grating normal and diffracted along several discrete paths  $\{\beta_m\}$ , for diffraction orders  $\{m\}$ . The incident and diffracted rays lie on opposite sides of the grating. The configuration shown, in which the transmission grating is illuminated from the back, is most common.

Transmission gratings can be made by stripping the aluminum film from the surface of a reflection grating. However, since the substrate is now part of the imaging optics, special substrates are used, made to tighter specifications for parallelism, and those used in the visible region are given a magnesium fluoride ( $MgF_2$ ) antireflection coating on the back to reduce light loss and internal reflections. The material used to form the substrate must also be chosen for its transmission properties and for the absence of bubbles, inclusions, striae and other imperfections, none of which is a concern for reflection gratings.

In most cases, relatively coarse groove frequencies are preferred for transmission gratings, although gratings up to 600 g/mm are furnished routinely. Experimentally, transmission gratings of 1200 g/mm have been used. Energy distribution on either side of the blaze peak is very similar to that of reflection gratings in the scalar domain. For wavelengths between 220 and 300 nm, transmission gratings are made on fused silica substrates with a special resin capable of high transmission for these wavelengths.

Since transmission gratings do not have a delicate metal film they are much more readily cleaned. However, they are limited to spectral regions where substrates and resins transmit. Their main drawback is that they do not fold the optical path conveniently as a reflection grating does. Moreover, to avoid total internal reflection, their diffraction angles cannot be extreme. Even though the surface of the substrate is antireflection coated, internal reflections from the grating-air interface leads to some backward-propagating orders (that is, the transmission grating will also behave as a weak reflection grating); this limits the maximum efficiency to about 80%.<sup>149</sup> The efficiency behavior of transmission gratings can be modeled adequately over a wide spectral range and for a wide range of groove spacing by using scalar efficiency theory.<sup>150</sup>

For a reflection grating of a given groove angle  $\theta_B$  with first-order blaze wavelength  $\lambda_B$ , the transmission grating with the same groove angle will be blazed between  $\lambda_B/4$  and  $\lambda_B/3$ , depending on the index of refraction of the resin. This estimate is often very good, though it becomes less accurate for  $\theta_B > 25^\circ$ .

Although there are cases in which transmission gratings are applicable or even desirable, they are not often used: reflection gratings are much more prevalent in spectroscopic and laser systems, due primarily to the following advantages:

- Reflection gratings may be used in spectral regions where glass substrates and resins absorb light (*e.g.*, the ultraviolet).
- Reflection gratings provide much higher resolving power than equivalent transmission gratings, since the path difference

---

<sup>149</sup> M. Nevière, "Electromagnetic study of transmission gratings," *Appl. Opt.* **30**, 4540-4547 (1991).

<sup>150</sup> E. K. Popov, L. Tsonev and E. G. Loewen, "Scalar theory of transmission relief gratings," *Opt. Commun.* **80**, 307-311 (1991).

- between neighboring beams (*i.e.*, separated by a single groove) is higher in the case of the reflection grating – therefore transmission gratings much generally be wider (so that more grooves are illuminated) to obtain comparable resolving power.
- Reflection grating systems are generally smaller than transmission grating systems since the reflection grating acts as a folding mirror.

### 12.3. GRATING PRISMS (GRISMS)

For certain applications, such as a direct vision spectroscope, it is useful to have a dispersing element that will provide in-line viewing for one wavelength. This can be done by replicating a transmission grating onto the hypotenuse face of a right-angle prism. The light diffracted by the grating is bent back in-line by the refracting effect of the prism. The device is known as a *Carpenter prism*, but is more commonly called a *grism*.

The derivation of the formula for computing the required prism angle follows (refer to Figure 12-2). On introducing Snell's law, the grating equation becomes

$$m\lambda = d(n \sin \alpha + n' \sin \beta), \quad (12-1)$$

where  $n$  and  $n'$  are the refractive indices of glass and air, respectively, and  $\beta < 0$  since the diffracted ray lies on the opposite side of the normal from the incident rays ( $\alpha > 0$ ).

Taking  $n' = 1$  for air, and setting  $\alpha = -\beta = \phi$ , the prism angle, Eq. (12-1) becomes

$$m\lambda = d(n-1) \sin \phi. \quad (12-2)$$

In this derivation it is assumed that the refractive index  $n$  of the glass is the same (or very nearly the same) as the index  $n_E$  of the resin at the straight-through wavelength  $\lambda$ . While this is not likely to be true, the resulting error is often quite small.

The dispersion of a grating prism cannot be linear, owing to the fact that the dispersive effects of the prism are superimposed on those of the grating. The following steps are useful in designing a grism:

1. Select the prism material desired (*e.g.*, BK-7 glass for visible light or fused silica for ultraviolet light).

- 
2. Obtain the index of refraction of the prism material for the straight-through wavelength.

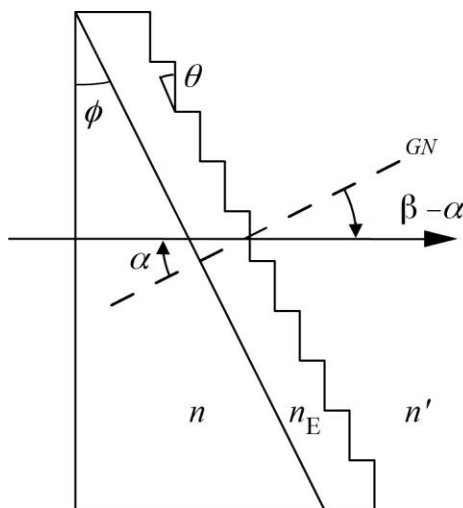


Figure 12-2. Grating prism (grism). The ray path for straight-through operation at one wavelength is shown. The refractive indices of the prism, resin and air are indicated as  $n$ ,  $n_E$  and  $n'$ , respectively; also,  $\phi$  is the prism angle and  $\theta$  is the groove angle. The incidence angle  $\alpha$  and diffraction angle  $\beta$  are measured from GN, the grating normal.

---

3. Select the grating constant  $d$  for the appropriate dispersion desired.
4. Determine the prism angle  $\phi$  from Eq. (12-2).
5. For maximum efficiency in the straight-through direction, select the grating from the *Diffraction Grating Catalog* with groove angle  $\theta$  closest to  $\phi$ .

Design equations for grism spectrometers may be found in Traub.<sup>151</sup>

---

<sup>151</sup> W. A. Traub, "Constant-dispersion grism spectrometer for channelled spectra," *J. Opt. Soc. Am.* **A7**, 1779-1791 (1990).

## 12.4. GRAZING INCIDENCE SYSTEMS<sup>152</sup>

For work in the x-ray region (roughly the wavelength range  $1 \text{ nm} < \lambda < 25 \text{ nm}$ ), the need for high dispersion and the normally low reflectivity of materials both demand that concave gratings be used at grazing incidence (*i.e.*,  $|\alpha| > 80^\circ$ , measured from the grating normal). Groove spacings of 600 to 1200 per millimeter are very effective, but exceptional groove smoothness is required on these gratings to achieve good results.

## 12.5. ECHELLES

A need has long existed for spectroscopic devices that give higher resolution and dispersion than ordinary gratings, but with a greater free spectral range than a Fabry-Perot etalon. This need is admirably filled by the echelle grating, first suggested by Harrison.<sup>153</sup> Echelles have been used in a number of applications that require compact instruments with high angular dispersion and high throughput.

Echelles are a special class of gratings with coarse groove spacings, used in high angles in high diffraction orders (rarely below  $|m| = 5$ , and sometimes used in orders beyond  $m = 100$ ). Because of spectral order overlap, some type of filtering is normally required with higher-order grating systems. This can take several forms, such as cut-off filters, detectors insensitive to longer wavelengths, or cross-dispersion in the form of prisms or low-dispersion gratings. The latter approach leads to a square display format suitable for corresponding types of array detectors; with such a system a large quantity of spectroscopic data may be recorded simultaneously.<sup>154</sup> First-order design principles for echelle spectrometers using a cross-disperser have been developed by Dantzler.<sup>155</sup>

As seen in Figure 12-3, an echelle looks like a coarse grating used at such a high angle (typically  $63^\circ$  from the normal) that the steep side of

---

<sup>152</sup> W. Cash, "Echelle spectrographs at grazing incidence," *Appl. Opt.* **21**, 710-717 (1982); L. B. Mashev, E. K. Popov and E. G. Loewen, "Optimization of the grating efficiency in grazing incidence," *Appl. Opt.* **26**, 4738-4741 (1987); L. Poletto, G. Tondello and P. Villoresi, "Optical design of a spectrometer-monochromator for the extreme-ultraviolet and soft x-ray emission of high-order harmonics," *Appl. Opt.* **42**, 6367-6373 (2003).

<sup>153</sup> G. R. Harrison, "The production of diffraction gratings II: The design of echelle gratings and spectrographs," *J. Opt. Soc. Am.* **39**, 522-528 (1949).

<sup>154</sup> D. Dravins, "High-dispersion astronomical spectrographs with holographic and ruled diffraction gratings," *Appl. Opt.* **17**, 404-414 (1978).

the groove becomes the optically active facet. Typical echelle groove spacings are 31.6, 79 and 316 g/mm, all blazed at  $63^{\circ}26'$  (although  $76^{\circ}$  is available for greater dispersion). With these grating, resolving powers greater than 1,000,000 for near-UV wavelengths can be obtained, using an echelle 10 inches wide. Correspondingly high values can be obtained throughout the visible spectrum and to 20  $\mu\text{m}$  in the infrared.

Since echelles generally operate close to the Littrow mode at the blaze condition, the incidence, diffraction and groove angles are equal (that is,

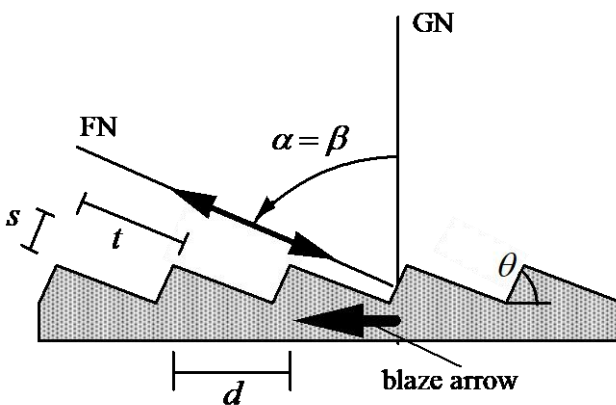


*Figure 12-3. Echelle geometry for use in the Littrow blaze condition.* The groove spacing  $d$ , step width  $t$  and step height  $s$  are shown. The double-headed arrow indicates that the grating is used in the Littrow configuration ( $\alpha = \beta$ ), and  $\beta$  was chosen to equal the groove angle  $\theta$  to satisfy the blaze condition. GN is the grating normal and FN is the facet normal. The blaze arrow (shown) points from GN toward FN.

$\alpha = \beta = \theta$ ) and the grating equation becomes

$$m\lambda = 2d \sin\beta = 2d \sin\theta = 2t, \quad (12-3)$$

where  $t = d \sin\theta$  is the width of one echelle step (see Figure 12-3).

The free spectral range is

$$F_\lambda = \frac{\lambda}{m}, \quad (2-29)$$

<sup>155</sup> A. A. Dantzler, "Echelle spectrograph software design aid," *Appl. Opt.* **24**, 4504-4508 (1985).

which can be very narrow for high diffraction orders. From Equation (12-3),  $m = 2t/\lambda$ , so

$$F_\lambda = \frac{\lambda^2}{2t} \quad (12-4)$$

for an echelle used in Littrow. In terms of wavenumbers\*, the free spectral range is

$$F_\sigma = \frac{\Delta\lambda}{\lambda^2} = \frac{1}{2t}. \quad (12-5)$$

The linear dispersion of the spectrum is, from Eq. (2-16),

$$r' \frac{\partial\beta}{\partial\lambda} = \frac{mr'}{d \cos\beta} = \frac{mr'}{s} = \frac{r'}{s} \left( \frac{2t}{\lambda} \right), \quad (12-6)$$

where  $s = d \cos\beta = d \cos\theta$  is the step height of the echelle groove (see Figure 12-3). The dispersion of an echelle used in high orders can be as high as that of fine-pitch gratings used in the first order.

The useful length  $l$  of spectrum between two consecutive diffraction orders is equal to the product of the linear dispersion and the free spectral range:

$$l = \frac{r'\lambda}{s}. \quad (12-7)$$

For example, consider a 300 g/mm echelle with a step height  $s = 6.5 \mu\text{m}$ , combined with an  $r' = 1.0$  meter focal length mirror, working at a wavelength of  $\lambda = 500 \text{ nm}$ . The useful length of one free spectral range of the spectrum is  $l = 77 \text{ mm}$ .

Typically, the spectral efficiency reaches a peak in the center of each free spectral range and drops to about half of this value at the ends of the range. Because the ratio  $\lambda/d$  is generally very small ( $\ll 1$ ) for an echelle used in high orders ( $m \gg 1$ ), polarization effects are not usually pronounced, and scalar methods may be employed in many cases to

\* A *wavenumber* is a unit proportional to inverse wavelength and is often used in the infrared. The definition of a wavenumber  $\sigma$  in inverse centimeters ( $\text{cm}^{-1}$ ) is  $\sigma = 10000/\lambda$ , where  $\lambda$  is expressed in  $\mu\text{m}$ .

compute echelle efficiency.<sup>156</sup> Echelle efficiency has been addressed in detail by Loewen *et al.*<sup>157</sup>

The steep angles and the correspondingly high orders at which echelles are used make their ruling much more difficult than ordinary gratings. Periodic errors of ruling must especially be limited to a few nanometers or even less, which is attainable only by using interferometric control of the ruling engine. The task is made even more difficult by the fact that the coarse, deep grooves require heavy loads on the diamond tool. Only ruling engines of exceptional rigidity can hope to rule echelles. This also explains why the problems escalate as the groove spacing increases.

An echelle is often referred to by its "R number", which is the tangent of the blaze angle  $\theta$ :

$$\text{R number} = \tan \theta = \frac{t}{s}. \quad (12-8)$$

The lengths  $s$  and  $t$  are shown in Figure 12-2. An R2 echelle, for example, has a blaze angle of  $\tan^{-1}(2) = 63.4^\circ$ ; an R5 echelle has a blaze angle of  $\tan^{-1}(5) = 78.7^\circ$ .

<i>R number</i>	<i>Groove angle</i>
R1	45.0°
R2	63.4°
R3	71.6°
R3.5	74.1°
R4	76.0°
R5	78.7°
R6	80.5°

*Table of common R numbers.*

<sup>156</sup> D. J. Schroeder and R. L. Hilliard, "Echelle efficiencies: theory and experiment," *Appl. Opt.* **19**, 2833-2841 (1980); B. H. Kleeman and J. Erxmeyer, "Independent electromagnetic optimization of the two coating thicknesses of a dielectric layer on the facets of an echelle grating in Littrow mount," *J. Mod. Opt.* **51**, 2093-2110 (2004).

<sup>157</sup> E. G. Loewen, D. Maystre, E. Popov and L. Tsonev, "Echelles: scalar, electromagnetic and real groove properties," *Appl. Opt.* **34**, 1707-1727 (1995); E. G. Loewen, D. Maystre, E. Popov and L. Tsonev, "Diffraction efficiency of echelles working in extremely high orders," *Appl. Opt.* **35**, 1700-1704 (1996);

Instruments using echelles can be reduced in size if the echelles are “immersed” in a liquid of high refractive index  $n$  (see Figure 12-4). This has the effect of reducing the effective wavelength by  $n$ , which is equivalent to increasing the diffraction order, resolving power and dispersion of the echelle (compared with the same echelle that is not immersed).<sup>158</sup> A prism is usually employed to couple the light to the grating surface, since at high angles most of the light incident from air to the high-index liquid would be reflected. Often an antireflection (AR) coating is applied to the normal face of the prism to minimize the amount of energy reflected from the prism.<sup>159</sup>

## 12.6. IMMERSED GRATINGS<sup>160</sup>

Unlike a grism (see Section 12.4 above), an *immersed grating* couples a prism to a reflection grating rather than a transmission grating. Instruments using gratings can be reduced in size if the gratings are “immersed” in a material of high refractive index  $n$ , usually an optically transmissive liquid or gel (see Figure 12-4). This has the effect of reducing the effective wavelength by  $n$ , which is equivalent to increasing the diffraction order, resolving power and dispersion of the grating (compared with the same grating that is not immersed).<sup>161</sup> A prism is usually employed to couple the light to the grating surface, since at high angles most of the light incident from air to the high-index liquid would be reflected. Often an antireflection (AR) coating is applied to the normal face of the prism to minimize the amount of energy reflected from the prism.<sup>162</sup>

---

---

<sup>158</sup> D. Enard and B. Delabre, “Two design approaches for high-efficiency low-resolution spectroscopy,” *Proc. SPIE* **445**, 522-529 (1984); G. Wiedemann and D. E. Jennings, “Immersion grating for infrared astronomy,” *Appl. Opt.* **32**, 1176-1178 (1993).

<sup>159</sup> C. G. Wynne, “Immersed gratings and associated phenomena. I,” *Opt. Commun.* **73**, 419-421 (1989); C. G. Wynne, “Immersed gratings and associated phenomena. II,” *Opt. Commun.* **75**, 1-3 (1990).

<sup>160</sup> D. Lee and J. R. Allington-Smith, “An experimental investigation of immersed gratings,” *Mon. Nor. R. Astron. Soc.* **312**, 57-69 (2000).

<sup>161</sup> D. Enard and B. Delabre, “Two design approaches for high-efficiency low-resolution spectroscopy,” *Proc. SPIE* **445**, 522-529 (1984); G. Wiedemann and D. E. Jennings, “Immersion grating for infrared astronomy,” *Appl. Opt.* **32**, 1176-1178 (1993).

<sup>162</sup> C. G. Wynne, “Immersed gratings and associated phenomena. I,” *Opt. Commun.* **73**, 419-421 (1989); C. G. Wynne, “Immersed gratings and associated phenomena. II,” *Opt. Commun.* **75**, 1-3 (1990).

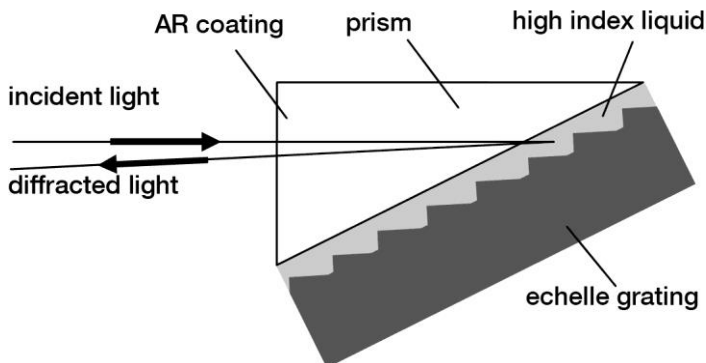


*Figure 12-4. An immersed echelle grating used near Littrow. In this example, the incident beam enters the prism normally at its face, so the prism contributes no angular dispersion to the grism (except for what little results from Snell's Law when the diffracted ray leaves the prism).*

# 13. APPLICATIONS OF DIFFRACTION GRATINGS

## 13.1. GRATINGS FOR INSTRUMENTAL ANALYSIS

The most common use for the diffraction grating is to serve as the wavelength separation device in an analytical laboratory instrument in which matter is analyzed by studying its interaction with light (this analysis is called *spectroscopy*). The spectral separation of the wavelengths is not strictly required for this interaction; instead its purpose is to provide data that can be interpreted unambiguously.

The techniques of analytical chemistry (*i.e.*, that branch of chemistry that determines the chemical composition of a substance by measuring its physical properties) may be considered qualitative or quantitative. A qualitative technique seeks to identify what is present; a quantitative technique seeks to determine how much is present. Grating-based optical systems can be used to identify or to quantify, by using the properties of light that is absorbed or emitted by a substance (called absorption spectroscopy and emission spectroscopy, respectively).

Most instruments designed for absorption spectroscopy are composed of four primary elements (see Figure 13-1): a light source, a monochromator, a sample illumination system, and a detector. Sometimes the monochromator and sample illumination system are interchanged (that is, some instruments disperse the light before it interacts with the sample, and some do this afterwards). Some instruments use a spectrograph instead of a monochromator so that the entire spectrum may be recorded at once.

### 13.1.1. Atomic and molecular spectroscopy<sup>163</sup>

The field of atomic spectroscopy started with the observation by Balmer that the discrete spectral lines emitted by a hydrogen source in the ultraviolet had wavelengths that could be predicted by a simple formula; with the development of quantum physics, the existence of a unique and predictable set of discrete emission (and absorption)

---

<sup>163</sup> *E.g.*, S. Svanberg, *Atomic and Molecular Spectroscopy*, 4<sup>th</sup> ed., Springer-Verlag (Berlin, Germany: 2004).

wavelengths for each chemical element was hypothesized and subsequently observed. We now defined atomic absorption spectroscopy as the measurement of the light absorbed by ionized atoms, and atomic emission spectroscopy as the measurement of light emitted by energized atoms or ions. Both the wavelength and the intensity of the light can be measured using monochromators and spectrographs to provide information about the atomic species.

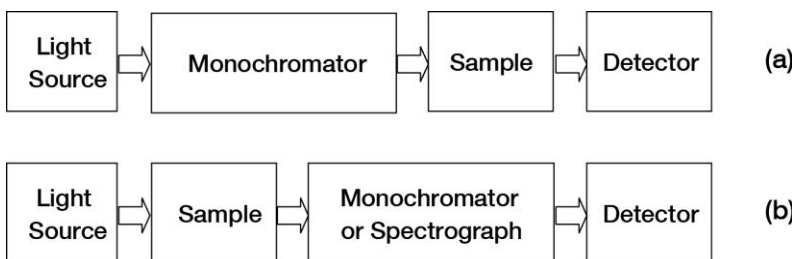


*Figure 13-1. Elements of an Absorption Spectrometer.* Light from a broad-spectrum source, such as deuterium ( $D_2$ ) or tungsten ( $W$ ), is transmitted through the absorbing sample to be analyzed and focused through the entrance slit of a monochromator (or spectrograph), and the intensity of the light at each wavelength is recorded, producing an absorption spectrum. In (a) the sample is illuminated by light after it has been spectrally tuned by the monochromator; in (b) the sample is illuminated by the broad spectrum.

Atomic absorption and emission spectrophotometers are generally used to identify elements and measure their concentrations. Primary applications include the manufacture of steel, mining, and waste & recycling. Many atomic emission instruments use an *inductively coupled plasma* (ICP) composed of the atoms to be studied as the light source.

Molecular spectroscopy instrumentation is generally designed to transmit light through a molecular species (often in a liquid suspension) and measure the absorption at each wavelength.

Atomic and molecular spectroscopy is usually undertaken in the UV, visible and IR portions of the spectrum, since atomic and molecular transition energies lie in this range. Atomic spectrophotometers are most often designed for use in the UV and visible parts of the spectrum; many go as far into the UV as the 167 nm aluminum line, which requires purging or a partial vacuum to eliminate the absorption due to the atmosphere. Instruments used for molecular spectroscopy extend to higher wavelengths than atomic spectrophotometers, through the visible and into the near-infrared. Generally, one instrument will cover only a

portion of this wide spectral range, leading to the classifications of UV spectrometers, UV-visible spectrometers, visible spectrometers and IR spectrometers.

Both the wavelength and the intensity of the light can be measured using monochromators and spectrographs to provide information about the atomic species.

### **13.1.2. Fluorescence spectroscopy<sup>164</sup>**

Many atomic and molecular species fluoresce; that is, they absorb energy in the UV-visible spectral region and rapidly emit most of that energy (the remainder being converted to heat or vibrational energy in the medium). Generally, this emission takes place on the order of nanoseconds after absorption, and (because of the energy loss) the *emission spectrum* will appear at higher wavelengths than the *excitation spectrum* (or, usually, a single excitation spectral line). Fluorescent compounds may be identified by their unique fluorescence spectra; in some applications, a non-fluorescent material may be tagged with a fluorescent dye or fluorophore so that the non-fluorescent material may be detected using fluorescence instrumentation.

Fluorescence instrumentation generally contains an excitation monochromator, serving as a tunable filter for the excitation light, and an emission spectrometer to disperse the emission spectrum (see Figure 13-2).

### **13.1.3. Colorimetry<sup>165</sup>**

*Colorimetry* is the measurement and specification of color, used in analytical chemistry, color matching, color reproduction and appearance studies. Because color as perceived cannot be associated with a single wavelength – it is a more complicated function of how the three different light receptors in the human eye respond to the entire visible spectrum when looking at an object – it is common to use a multiwavelength instrument such as a grating spectrometer.

---

<sup>164</sup> E.g., J. R. Lakowicz, *Principles of Fluorescence Spectroscopy*, 3<sup>rd</sup> ed., Springer-Verlag (New York, New York: 2006).

<sup>165</sup> E.g., C. J. Kok and M. C. Boshoff, “New spectrophotometer and tristimulus mask colorimeter,” *Appl. Opt.* **10**, 2617-2620 (1971); T. H. Chao, S. L. Zhuang, S. Z. Mao and F. T. S. Yu, “Broad spectral band color image deblurring,” *Appl. Opt.* **22**, 1439-1444 (1983).

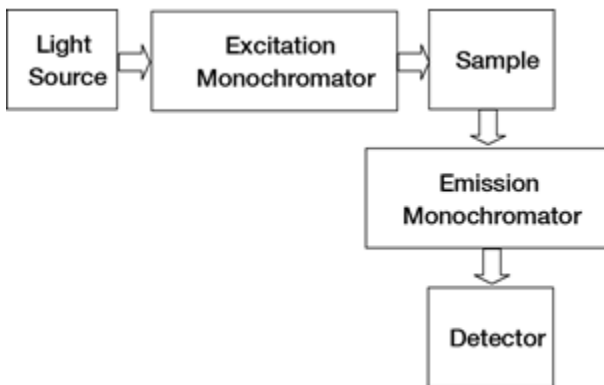


*Figure 13-2. Elements of a Fluorescence Spectrometer.* Light from a broad-spectrum source is spectrally tuned by an excitation monochromator; a spectrally narrow beam emerging from this monochromator is absorbed by the sample. The fluorescence spectrum of the sample is viewed (generally at an angle perpendicular to the excitation beam) and resolved by an emission monochromator.

---

### 13.1.4. Raman spectroscopy<sup>166</sup>

interaction of light with matter falls into two broad categories: absorption (on which absorption spectroscopy and fluorescence spectroscopy are based), and scattering. Light can scatter elastically (*i.e.*, energy is conserved) or inelastically – the latter is called Raman scattering, and the study of the spectrum of inelastically scattered light from matter is called *Raman spectroscopy*. Since the ratio of intensities of inelastically scattered light to elastically scattered light is generally under  $10^{-6}$ , the reduction of instrumental stray light in Raman spectrometers is of paramount importance.

### 13.1.5. Hyperspectral systems<sup>167</sup>

Hyperspectral imaging is a technique that creates a spectrum at each pixel in an image: it provides both spatial resolution and spectral resolution. Use of hyperspectral imaging is growing; for example,

---

<sup>166</sup> *E.g.*, E. Smith & G. Dent, *Modern Raman Spectroscopy: A Practical Approach*, John Wiley & Sons, Ltd (Chichester, England: 2005)

<sup>167</sup> *E.g.*, C.-I. Chang, *Hyperspectral Imaging: Techniques for Spectral Detection and Classification*, Kluwer (New York, New York: 2003).

hyperspectral remote sensing has been used to inspect food, detect the early outbreak of drought and disease in crops, and diagnose disease in humans.

## 13.2. GRATINGS IN LASER SYSTEMS

Diffraction gratings are also used in laser systems to perform several functions: to tune the lasing wavelength, to narrow the distribution of wavelengths in the laser, and to control the pulse shape (*vs.* time).

### 13.2.1. Laser tuning<sup>168</sup>

Lasing media have characteristic gain curves that describe the lasing intensity *vs.* wavelength. In order to “tune” the laser to a wavelength with higher gain with the gain curve, a grating can be used at one end of the resonant cavity (in place of a mirror); using a grating instead of a mirror will disperse the wavelengths in the laser, and the grating can be oriented so that the desired wavelength propagates back into the lasing medium.<sup>169</sup>

External-cavity semiconductor diode lasers are often used for their single-mode operation and spectral tunability. Plane reflection gratings can be used in the Littrow configuration to tune the lasing wavelength, as shown in Figure 13-3, or in the grazing-incidence mount.

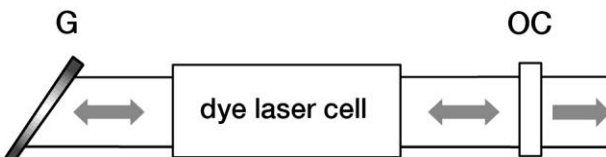


Figure 13-3. Tuning a dye laser – the grating as a total reflector in the Littrow configuration. Light from the dye laser cell is diffracted by the grating G, which is oriented so that light of the desired wavelength is redirected back toward the cell; the output beam is transmitted by an output coupler OC (which reflects most of the light back into the laser). The wavelength is tuned by rotating the grating.

<sup>168</sup> F. J. Duarte, *Tunable Laser Optics*, Academic Press (San Diego, California: 2003).

<sup>169</sup> T. M. Hard, “Laser wavelength selection and output coupling by a grating,” *Appl. Opt.* **9**, 1825-1830 (1970); A. Hardy and D. Treves, “Modes of a diffraction grating optical resonator,” *Appl. Opt.* **14**, 589-592 (1975); T. W. Hänsch, “Repetitively pulsed tunable dye laser for high resolution spectroscopy,” *Appl. Opt.* **11**, 895-898 (1971); S. O. Kanstad & G. Wang, “Laser resonators folded by diffraction gratings,” *Appl. Opt.* **17**, 87-90 (1978).

In some systems a beam expander is used to illuminate a larger area on the grating surface, to achieve high resolution and/or to reduce the power density on the grating surface (since a high-power laser may damage the grating). Since the grating will allow the zero-order to propagate as well as the (Littrow) diffraction order, the output beam may be taken from the grating as in Figure 13-4.

Grazing-incidence tuning with one grating associated with a mirror (or a second grating) can also be used to tune dye lasers without the need for a beam expander, leading to a more compact laser cavity; this is called the Littman-Metcalf design<sup>170</sup> and is shown in Figure 13-5.

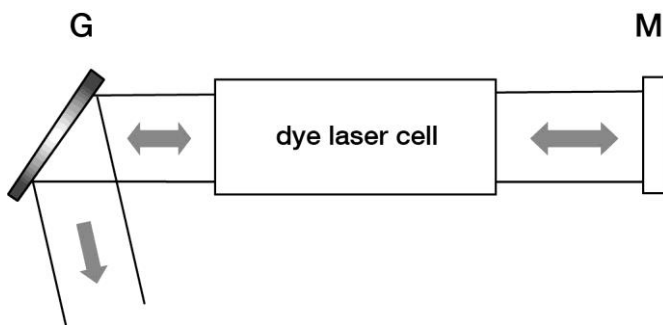


*Figure 13-4. Tuning a dye laser – the grating as output reflector.* In this case, the zero-order from the grating G is the output beam, and the output coupler in Figure 13-3 is replaced by a mirror. The wavelength is tuned by rotating the grating.

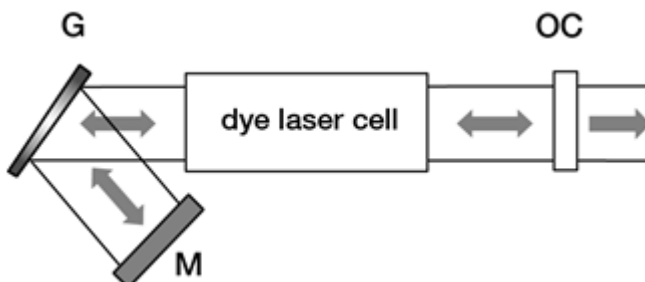


*Figure 13-5. The Littman-Metcalf arrangement.* The light diffracted by grating G is retroreflected by mirror M, which diffracts the light again back into the dye laser cell.

<sup>170</sup> M. G. Littman and H. J. Metcalf, "Spectrally narrow pulsed dye laser without beam expander," *Appl. Opt.* **17**, 2224-2227 (1978).

Molecular lasers, operating in either a pulsed or continuous-wave (cw) mode, have their output wavelength tuned by Littrow-mounted gratings. High efficiency is obtained by using the first diffraction order at diffraction angles  $|\beta| > 20^\circ$ . The output is polarized in the S-plane, since the efficiency in the P plane is quite low.

Some molecular lasers operate at powers high enough to destroy gratings. For pulsed laser tuning, extra-thick replica films may help. Due to their far greater thermal conductivity, replica gratings on metal substrates are superior to glass for cw laser applications; in some cases, the grating substrates must be water-cooled to prevent failure.

Excimer lasers – used in surgery, micromachining and photolithography – generally select a narrow spectral range from the emission profile by using an echelle grating in the Littrow configuration.<sup>171</sup> A coarse echelle ( $d > 10 \mu\text{m}$ ) is used in very high diffraction orders ( $m \gg 10$ ) at very high incidence angles ( $\alpha = 65^\circ$  to  $79^\circ$ ) in order to obtain high dispersion (see Eq. (2-15)). At such an oblique angle, a beam with circular cross section will illuminate an ellipse on the grating that is three to five times wider in the dispersion direction than it is in the cross-dispersion direction.

### 13.2.2. Pulse stretching and compression<sup>172</sup>

For optical systems employing lasers with very high peak powers, such as those that use temporally short (< 1 picosecond) yet energetic ( $\approx 1$  Joule) pulses, the required damage thresholds of the optical components in the system can exceed the performance of state-of-the-art components. Strickland and Mourou<sup>173</sup> demonstrated that such pulses can be stretched (in time) so that their pulse energy is spread out over a large time period (thereby reducing the peak power) and then compressed using a grating compressor to return the pulse to its original temporal profile. Between the two operations (stretching and compression), optical components are exposed to much lower peak powers than that of the original (or final)

---

<sup>171</sup> R Buffa, P Burlamacchi, R Salimbeni and M Matera, “Efficient spectral narrowing of a XeCl TEA laser,” *J. Phys. D: Appl. Phys.* **16** L125-L128 (1983); J. P. Partenen, “Multipass grating interferometer applied to line narrowing in excimer lasers,” *Appl. Opt.* **25**, 3810-3815 (1986).

<sup>172</sup> E. Treacy, “Optical pulse compression with diffraction gratings,” *IEEE J. Quantum Elec.* **5**, 454-458 (1969).

<sup>173</sup> D. Strickland and G. Mourou, “Compression of amplified chirped optical pulses,” *Opt. Comm.* **56**, 219-221 (1985).

pulse. By amplifying the pulse between the stretcher and compressor, higher peak power pulses may be obtained.

A dual-grating pulse stretcher is shown in Figure 13-6.

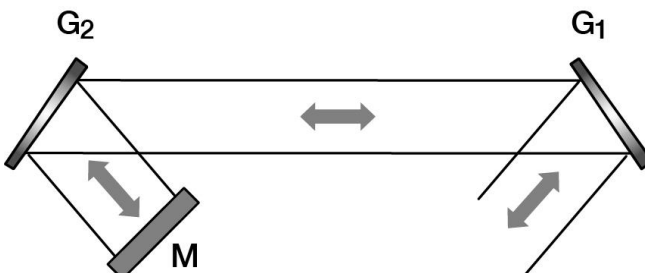


Figure 13-6. A grating-based pulse stretcher. Intermediate lenses are not shown.

### 13.3. GRATINGS IN ASTRONOMICAL APPLICATIONS

Much of what we know of the universe is due to our analysis of light reaching the earth from planets, stars and galaxies. Grating-based spectrometers play a key role in astronomical measurements. For example, the spectroscopic analysis of starlight allows us to determine the composition of stars as well as their relative velocities. The analysis of absorption lines in starlight that passes through nebulae allows us to determine the composition of the nebulae. From the analyses of these emission and absorption spectra, we can infer ages of stars, distances to galaxies, etc.

#### 13.3.1. Ground-based astronomy<sup>174</sup>

Ground-based astronomical telescopes generally have quite large apertures, to maximize the light energy collected from distant astronomical objects; this leads to the need for very large gratings to spectrally disperse the light received. Often these gratings are so large that their resolving power exceeds the value for which the spectrometer's resolution would be grating-limited; that is, in most cases the grating is 'better' than the instrument's resolution requires.

<sup>174</sup> E.g., W. Liller, "High dispersion stellar spectroscopy with an echelle grating," *Appl. Opt.* **9**, 2332-2336 (1970); D. J. Schroeder, *Astronomical Optics*, Academic Press (San Diego, California: 1987).

The MIT 'B' engine can rule large echelles and echellettes up to 320 mm x 420 mm in size (which provides a ruled area of 308 mm x 408 mm), suitable for all but the largest ground-based astronomical instruments.<sup>175</sup>

The requirement for even larger gratings for ground-based astronomical telescopes has led to three alternative solutions: a static fixture to hold smaller gratings in a larger configuration, an adjustable fixture with optical feedback to move the gratings with respect to each other (to maintain focus)<sup>176</sup>, and a *mosaic grating* produced by high-accuracy multiple replication onto a single substrate.<sup>177</sup> Such monolithic mosaic gratings have the advantage of long-term alignment stability over the other two alternatives.

In the 1990s, Richardson Gratings developed the capability to replicate two large submaster gratings onto one monolithic substrate. Except for a "dead space" between the two replicated areas, the entire face of the larger product substrate contains the groove pattern. This mosaic grating must have its two grating areas aligned to very high accuracy if the mosaic is to perform as one high-quality grating. Typical specifications for two 308 mm x 408 mm ruled areas on a 320 mm x 840 mm substrate are one arc second alignment of the groove directions, one arc second tilt between the two faces, and one micron displacement between the two grating planes.

A large mosaic echelle grating produced by Richardson Gratings for the European Southern Observatory is shown in Figure 13-7. Two submasters from MKS master grating MR160 (a 31.6 g/mm echelle blazed at 75.1°) were independently replicated onto a large monolithic substrate to form this mosaic grating; the two halves of its surface are clearly seen in the photograph.

---

<sup>175</sup> S. S. Vogt and G. D. Penrod, "HiRES: A high resolution echelle spectrometer for the Keck 10-meter telescope," in *Instrumentation for Ground-Based Astronomy*, L. B. Robinson, ed. (Springer-Verlag, New York: 1988), pp. 68-103.

<sup>176</sup> G. A. Brealey, J. M. Fletcher, W. A. Grundmann and E. H. Richardson, "Adjustable mosaic grating mounts," *Proc. SPIE* **240**, 225-228 (1980).

<sup>177</sup> H. Dekker and J. Hoose, "Very high blaze angle R4 echelle mosaic," *Proc. ESO Workshop on High Resolution Spectroscopy*, M.-H. Ulrich, ed., p. 261 (1992); J. Hoose et al., "Grand Gratings: Bigger is Better, Thanks to Mosaic Technology," *Photonics Spectra* **29**, 118-120 (December 1995); T. Blasiak and S. Zheleznyak, "History and construction of large mosaic diffraction gratings," *Proc. SPIE* **4485**, 370-377 (2002).

Figure 13-8 shows a six-inch aperture Fizeau interferogram of an echelle mosaic ( $31.6 \text{ g/mm}$ ) in the  $m = 98^{\text{th}}$  order, tested at  $\lambda = 632.8 \text{ nm}$ . The grooves are vertical in the photos and the blaze arrow is facing left. One fringe over this aperture is  $0.43 \text{ arc seconds}$ . These measurements indicate that the two sides of the mosaic are aligned to  $0.3 \text{ arc seconds}$ .

Figure 13-9 shows a focal plane scan on a ten-meter optical test bench using a mode-stabilized HeNe laser ( $\lambda = 632.8 \text{ nm}$ ) as the light source. The entrance slit width is 25 microns, and the exit slit is opened just enough to get signal through. The grating is operating in the  $m = 97^{\text{th}}$  order with full aperture illumination. The image is dominated by the wavefront characteristics of the individual segments, but still indicates a system resolving power better than  $R = 900,000$ .

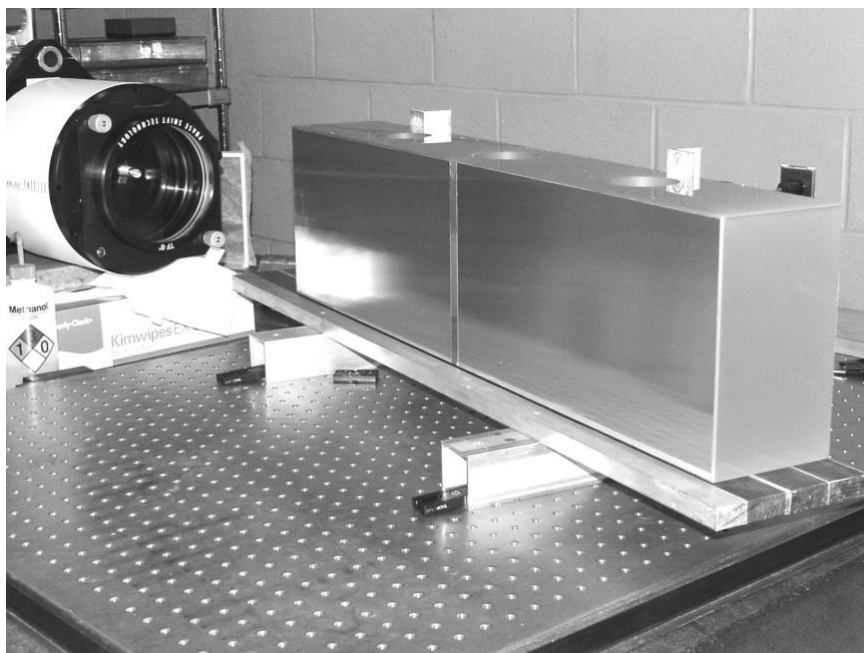
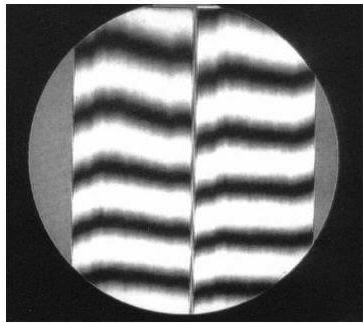
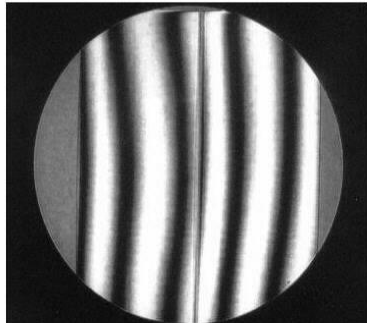


Figure 13-7. A large mosaic grating. A monolithic  $214 \times 840 \text{ mm}$  replica mosaic grating was produced from two  $214 \times 415 \text{ mm}$  submasters replicated onto a single piece of ZERODUR®.



Alignment perpendicular  
to grooves



Alignment parallel  
to grooves

Figure 13-8. Six-inch-aperture Fizeau interferograms of a 31.6 g/mm echelle mosaic produced from two 214 x 415 mm submasters. The photograph on the left shows alignment perpendicular to the grooves; that on the right shows alignment in the direction of the grooves. These interferograms were taken in the 98<sup>th</sup> diffraction order.

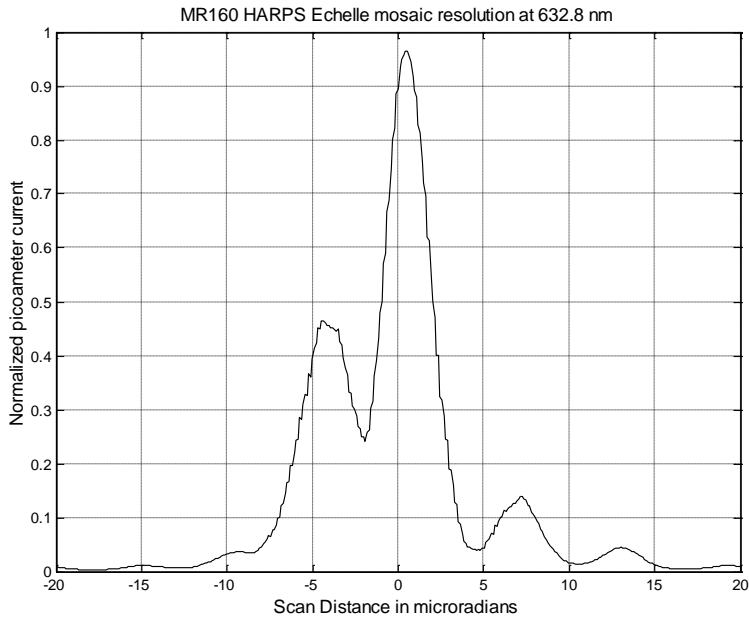


Figure 13-9. Signal trace of a 31.6 g/mm echelle mosaic at 632.8 nm in the 97<sup>th</sup> order.

The first exosolar planet seen orbiting a main sequence star was discovered in 1995 using the Elodie spectrograph at the Observatoire de Haute-Provence in France.<sup>178</sup> This discovery was the first to employ the radial velocity method (also known as Doppler spectroscopy), which detects very small periodic shifts in the wavelengths of the features of the emission spectrum of a star due to its motion about its common center of mass with nearby objects. This spectrograph uses a Richardson Gratings R4 echelle as its primary dispersive component. The 2019 Nobel Prize in Physics was awarded in part for this discovery.<sup>179</sup>

This discovery was based on the detection of a Doppler shift corresponding to a change in the star 51 Pegasi's radial velocity (over the period of the planet) of about 100 m/s. Since the construction of the Elodie spectrograph, more sensitive Doppler spectrometers have been designed and constructed and are in use in telescopes around the world; the newest instruments can detect a radial velocity change of 1 m/s.<sup>180</sup>

### 13.3.2. Space-borne astronomy<sup>181</sup>

Neither master nor replica gratings suffer in any measurable way over extended periods of time in a space environment. Since most space work involves the study of ultraviolet (UV) and extreme ultraviolet (EUV) wavelengths, special problems exist in setting and aligning the optics. For this purpose, MKS can rule gratings matching the EUV grating but with a groove spacing modified so that the mercury 546.1-nm line lies in the spectrum just where the main wavelength under study will lie. Another possibility is to rule a small section on the main grating with similar coarse spacings and then mask off this area when the alignment is complete. Sometimes special tolerances on substrate radii are required for complete interchangeability.

---

<sup>178</sup> M. Mayor & D. Queloz, "A Jupiter-mass companion to a solar-type star", *Nature* **378**, 355-359 (1995).

<sup>179</sup> Press release: The Nobel Prize in Physics 2019 ([nobelprize.org](http://nobelprize.org)).

<sup>180</sup> E.g., M. Mayor *et al.*, "Setting New Standards with HARPS," *ESO Messenger* **114**, 20 (2003).

<sup>181</sup> E.g., J. F. Seely, M. P. Kowalski, W. R. Hunter, T. W. Barbee Jr., R. G. Cruddace and J. C. Rife, "Normal-incidence efficiencies in the 115-340-Å wavelength region of replicas of the Skylab 3600-line/mm grating with multilayer and gold coatings," *Appl. Opt.* **34**, 6453-6458 (1995).

### **13.3.3. Space travel**

A method of spacecraft propulsion has been proposed by Srivastava *et al.* using ‘light sails’ propelled by powerful lasers based on Earth.<sup>182</sup> Previous designs had proposed the use of mirrors; the use of gratings instead allows for a mechanism to keep the sails from drifting out of alignment. The experimental demonstration of a light sail based on diffraction gratings was reported in 2019 by Chu *et al.*<sup>183</sup>

## **13.4. GRATINGS IN SYNCHROTRON RADIATION BEAMLINES<sup>184</sup>**

Synchrotron radiation is generated by electrons traveling in circular orbits at relativistic speeds; this radiation covers the x-ray through infrared portions of the electromagnetic spectrum and may be used to investigate the electronic properties of matter. Synchrotron beamlines are optical systems oriented tangentially to synchrotron rings, and often gratings are used to disperse the portion of the radiation in the extreme ultraviolet (UV) and vacuum ultraviolet (VUV) spectra.<sup>185</sup>

## **13.5. SPECIAL USES FOR GRATINGS<sup>186</sup>**

In addition to the “traditional” uses of gratings – in analytical instruments, lasers and astronomy – there are several additional uses for which diffraction gratings are well-suited.

### **13.5.1. Gratings as filters**

Diffraction gratings may be employed as reflectance filters when working in the far infrared, to remove the unwanted second- and higher-

---

<sup>182</sup> P. R. Srivastava *et al.*, “Stable diffractive beam rider,” *Opt. Lett.* **44**(12), 3082–3085 (2019).

<sup>183</sup> Y.-J. L. Chu *et al.*, “Experimental Verification of a Bigrating Beam Rider”, *Phys. Rev. Lett.* **123**, 244302 (2019).

<sup>184</sup> E.g., G. Margaritondo, *Introduction to Synchrotron Radiation*, Oxford University Press (New York, New York: 1988).

<sup>185</sup> D. L. Ederer, ed., *Selected Papers on VUV Synchrotron Radiation Instrumentation – Beam Line and Instrument Development*, SPIE Milestone Series vol. **MS 152**, SPIE (Bellingham, Washington: 1998).

<sup>186</sup> E.g., B. E. A. Saleh and M. C. Teich, *Fundamentals of Photonics*, 2<sup>nd</sup> ed., Wiley Interscience (Hoboken, New Jersey: 2012).

diffraction orders from the incident light.<sup>187</sup> For this purpose, small plane gratings are used that are blazed for the wavelength of the unwanted shorter-wavelength radiation. The grating acts as a mirror for the longer-wavelength light, reflecting the desired light into the instrument, while diffracting shorter wavelengths out of the optical path. The groove spacing  $d$  must be chosen so that

$$|\sin\beta| > 1 \text{ for all } \lambda > \lambda_c, \quad (13-1)$$

where  $\lambda_c$  is a wavelength between the short wavelengths to be diffracted and the long wavelengths to be reflected (see Eq. (2-1)).

A grating can also be used as a color filter if it is illuminated such that its zero-order efficiency is highly wavelength-dependent.<sup>188</sup>

It should be recognized that a diffraction grating by itself cannot serve as a spectral bandpass filter. The grating provides spectral dispersion but not spectral resolution, so the analogue of a thin-film filter designed to pass a narrow spectral band would be the combination of a grating and a slit (see Figure 13-10). A grating monochromator (as described in Chapter 3) may be thought of as a tunable filter – rotating the grating tunes the central wavelength in the transmitted spectral band, and the exit slit serves to narrow this band.

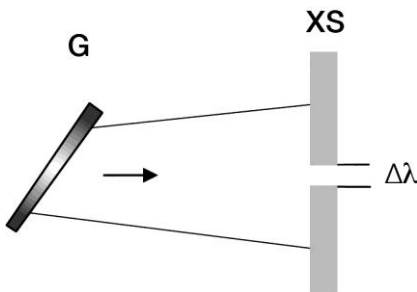


*Figure 13-10. Spectral resolution using a grating and a slit.* Polychromatic light incident on and diffracted by the grating G is not spectrally resolved; the grating merely diffracts each wavelength in the incident beam in a different direction. A spectral narrow band  $\Delta\lambda$  is obtained by using exit slit XS to prevent all wavelengths outside this band from passing to the detector.

<sup>187</sup> J. U. White, "Gratings as broad band filters for the infra-red," *J. Opt. Soc. Am.* **37**, 713-717 (1947).

<sup>188</sup> K. Knop, "Diffraction gratings for color filtering in the zero diffraction order," *Appl. Opt.* **17**, 3598-3603 (1978).

### 13.5.2. Gratings as biosensors<sup>189</sup>

Using surface plasmon resonance, surface relief diffraction gratings may be employed as optical biosensors to detect organic and biological molecules.<sup>190</sup> These biosensors detect changes in surface plasma waves, also called surface plasmon polaritons, as molecules interact (adsorb or desorb) with the surface of a metal-coated grating, along which electrons may move freely.

A light wave incident on the grating surface may transfer some of its energy to a surface plasma wave; this transferred energy causes localized changes in the density of the free electrons. For certain wavelengths, resonant oscillations of the free electrons are observed. These oscillations are sensitive to changes in the refractive index of the medium above the metal, the basis for their use as sensors. Both the intensity<sup>191</sup> and the wavelength<sup>192</sup> of the resonance are sensitive to changes in the local refractive index at the surface of the metal; that is, the transfer of energy from the incident wave to the surface plasma wave results in a change in the grating's diffracted efficiency (see Figure 9-20).

A typical grating-based biosensor uses a grating with a gold or silver coating, on which certain antibodies have been applied that bind only to specific macromolecules. A fluid that may contain the specific macromolecule is applied to the metal grating surface; if the macromolecule is present, it will bind to the antibodies and change the refractive index of the region directly above the metal coating.

---

<sup>189</sup> J. R. Sambles *et al.*, "Optical excitation of surface plasmons: an Introduction," *Contemporary Physics* **32**, 173-183 (1991).

<sup>190</sup> Y. Y. Teng and E. A. Stern, "Plasma radiation from metal grating surfaces," *Phys. Rev. Lett.* **19**, 511-514 (1967); H. Raether, *Surface Plasmons on Smooth and Rough Surfaces and on Gratings*, Springer-Verlag (Berlin, Germany: 1988), chapter 6; B. Liedberg *et al.*, "Surface plasmon resonance for gas detection and biosensing," *Lab. Sensors Actuat.* **4**, 299-304 (1983); J. Homola *et al.*, "Surface Plasmon Resonance Biosensors," in F. Ligler and C. R. Taitt, *Optical Biosensors: Present & Future*, 1<sup>st</sup> ed., Elsevier Science (Amsterdam, Netherlands: 2002), chapter 4.

<sup>191</sup> D. C. Cullen *et al.*, "Detection of immune-complex formation via surface plasmon resonance on gold-coated diffraction gratings," *Biosensors* **3**, 211-225 (1987).

<sup>192</sup> P. S. Vukusic *et al.*, "Surface plasmon resonance on gratings as a novel means for gas sensing," *Sens. Actuators B* **8**, 155 (1992).

### 13.5.3. Gratings in fiber-optic telecommunications<sup>193</sup>

In the late 1990s, surface-relief diffraction gratings became widely used in two types of equipment for fiber-optic telecommunications networks operating in the 1.3–1.7  $\mu\text{m}$  wavelength range. While other wavelength selective technologies exist (*e.g.*, interference filters, fiber Bragg gratings and array waveguide gratings), the cost advantage of surface-relief gratings becomes significant as the channel count increases, since a system with  $N$  channels requires  $N-1$  filters but only a single grating – the filters must act in series (in a cascade arrangement) but the grating acts on all channels in parallel. Moreover, as  $N$  increases, the spectral bandpass of the filters must decrease, further increasing their cost.

*Multiplexers & Demultiplexers.*<sup>194</sup> A multiplexer (see Figure 13-11(a)) is a component in a fiber-optic network that combines many input channels into one output channel; as the input channels have different wavelengths, the multiplexer can be considered a spectrograph used in reverse. A demultiplexer (Figure 13-11(b)) separates many wavelengths in a single input channel so that each is transmitted into a unique output channel (this is functionally equivalent to a spectrograph). Multiplexers and demultiplexers may be employed together to produce add-drop routers.

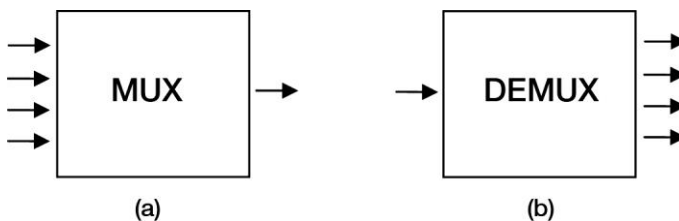


Figure 13-11. Fiber-optic network components. (a) Multiplexer: many input beams (each of a unique wavelength) are combined to propagate down the same output path. (b) Demultiplexer: the several signals in the (combined) input beam are separated by wavelength. For simplicity, only four wavelengths are shown.

---

<sup>193</sup> *E.g.*, see J.-P. Laude, *DWDM Fundamentals, Components, and Applications*, Artech House (Boston, Massachusetts: 2002).

<sup>194</sup> T. Kita and T. Harada, “Use of aberration-corrected concave gratings in optical demultiplexers,” *Appl. Opt.* **22**, 819–825 (1983).

*Optical Spectrum Analyzers.* In addition to serving in network components, gratings are used in optical spectrum analyzers which use a small fraction of the light in the network to monitor the intensity and stability of each channel. These systems are essentially spectrographs and may use plane or concave gratings.

### **13.5.4 Gratings as beam splitters**

Gratings can be used as beam splitters in conjunction with Moiré fringe applications or interferometers. Under normal illumination ( $\alpha = 0$ ), a grating with a symmetric groove profile will diffract both first-order beams with equal intensity. A diffraction grating used as a beam divider provides higher efficiencies when its groove profile is rectangular, whereas a grating used for spectroscopic purposes should have a sinusoidal or triangular groove profile.

Transmission gratings can be used as two-beam splitters (where the zero-order beam has negligible efficiency or is otherwise trapped), three-beam splitters (where the groove profile is chosen so that the zero-order beam has the same intensity as the two first-order beams), or for multiple beam sampling, depending on the choice of groove profile.<sup>195</sup>

### **13.5.5 Gratings as optical couplers**

Gratings can be used to couple light into and out of waveguide structures.<sup>196</sup> Generally the groove spacing  $d$  is specifically chosen to ensure that only one diffraction order (other than the zero order) propagates.

### **13.5.6 Gratings in metrological applications**

Diffraction gratings can be employed in a variety of metrological applications. The precise microscopic surface-relief pattern can be used

---

<sup>195</sup> E. G. Loewen, L. B. Mashev and E. K. Popov, "Transmission gratings as 3-way beam splitters," *Proc. SPIE* **815**, 66-72 (1987); E. K. Popov, E. G. Loewen and M. Nevière, "Transmission gratings for beam sampling and beam splitting," *Appl. Opt.* **35**, 3072-3075 (1996); E. G. Loewen and E. Popov, *Diffraction Gratings and Applications*, Marcel Dekker, Inc. (1997), ch. 5.

<sup>196</sup> T. Tamir and S. T. Peng, "Analysis and design of grating couplers," *Appl. Phys.* **14**, 235-254 (1977).

to calibrate atomic force microscopes (AFMs). Gratings can also be used in systems designed to measure displacement<sup>197</sup> and strain.<sup>198</sup>

---

<sup>197</sup> J.-A. Kim, K.-C. Kim, E. W. Bae, S. Kim and Y. K. Kwak, "Six-degree-of-freedom displacement measurement using a diffraction grating," *Rev. Sci. Instrum.* **71**, 3214-3219 (2000).

<sup>198</sup> B. Zhao and A. Asundi, "Strain microscope with grating diffraction method," *Opt. Eng.* **38**, 170-174 (1999).

# 14. ADVICE FOR USING GRATINGS

## 14.1. CHOOSING A SPECIFIC GRATING

If a diffraction grating is to be used only to disperse light by wavelength (rather than provide focusing as well), then choosing the proper grating is often a straightforward matter involving the specification of the blaze angle and groove spacing. In other instances, the problem is one of deciding on the spectrometric system itself. The main parameters that must be specified are

- Spectral region (wavelength range)
- Wavelength of peak efficiency
- Speed (focal ratio) or throughput
- Resolution or resolving power
- Dispersion
- Free spectral range
- Output optics
- Size limitations

The spectral region, spectral resolution and size requirements will usually lead to a choice of plane *vs.* concave design, as well as the coating (if the grating is reflecting). The size and weight of the system, the method of receiving output data, the intensity, polarization and spectral distribution of the energy available, *etc.*, must also be considered. The nature of the detection system, especially for array detectors, plays a major role in system design: its size, resolution, and image field flatness are critical issues in the specification of the optical system, and the sensitivity (*vs.* wavelength) of the detector will lead to a grating efficiency *vs.* wavelength specification.

Spectral resolution depends on many aspects of the optical system and the quality of its components. In some cases, the grating may be the limiting component (see Section 8.3). The decision here involves the size of the grating and the angle at which it is to be used, but not on the number of grooves on the grating or the groove spacing (see Chapter 2).

Speed (or throughput) determines the focal length as well as the sizes of the optical elements and of the system itself. Special coatings become

important in certain regions of the spectrum, especially the vacuum ultraviolet.

When thermal stability is important, gratings should be made on a low expansion material, such as Schott ZERODUR® or Corning ULE®.

Guidelines for specifying gratings are found in Chapter 16.

## **14.2. APPEARANCE**

In the early days of diffraction grating manufacture, R.W. Wood remarked that the best gratings were nearly always the worst ones in their cosmetic or visual appearance. While no one would go so far today, it is important to realize that a grating with certain types of blemishes may well perform better than one that appears perfect to the eye.

### **14.2.1. Ruled gratings**

Cosmetic defects on ruled gratings may be caused by small droplets of metal or oxide that have raised the ruling diamond, or streaks may be caused by temporary adhesion of aluminum to the sides of the diamond tool. On ruled concave gratings, one can usually detect by eye a series of concentric rings called a *target pattern*. It is caused by minor changes in tool shape as the diamond swings through the arc required to rule on a curved surface. Every effort is made to reduce the visibility of target patterns to negligible proportions.

Some ruled master gratings have visible surface defects. The most common sort of defect is a region of grooves that are burnished too lightly (in relation to the rest of the grating surface). While readily seen with the eye, such a region has little effect on spectroscopic performance.

### **14.2.2 Holographic gratings**

Holographic gratings are susceptible to a different set of cosmetic defects. *Comets* are caused by specks on the substrate; when the substrate is rotated as the photoresist is applied, these specks cause the photoresist to flow around them, leaving comet-like trails. Artifacts created during the recording process are also defects; these are holograms of the optical components used in the recording of the grating.

### **14.3. GRATING MOUNTING**

The basic rule of mounting a grating is that for any precise optical element: its shape should not be changed accidentally through excessive clamping pressure. This problem can be circumvented by kinematic (three-point) cementing, using a nonrigid cement, or by supporting the surface opposite the point where clamping pressure is applied.

If a grating is to be mounted from the rear, the relative orientations of the front and rear surfaces is more important than if the grating is to be mounted from the front. Front-mounting a plane grating, by contacting the mount to the front surface of the grating (near the edge of the grating and outside the free aperture), allows the cost of the substrate to be lower, since the relative parallelism of the front and back surfaces need not be so tightly controlled.

### **14.4. GRATING SIZE**

Grating size is usually dictated by the light throughput desired (and, in the case of concave gratings, imaging and instrument size limitations as well). Should none of the standard substrate sizes listed in the MKS *Diffraction Grating Catalog* be suitable to match an instrument design, these same gratings can be supplied on special size substrates. Special elongated substrate shapes are available for echelles and laser tuning gratings.

### **14.5. SUBSTRATE MATERIAL**

The standard material for small and medium-sized grating substrates is specially annealed borosilicate crown glass (BK-7). Low-expansion material (such as Schott ZERODUR®, Corning ULE®, Ohara CLEARCERAM®-Z or fused silica) can be supplied upon request. For large gratings (approximately 135 x 265 mm or larger), low-expansion material is standard; BK-7 can be requested as well. For certain applications, it is possible to furnish metal substrates (*e.g.*, copper or aluminum) that are good heat sinks.

### **14.6. GRATING COATINGS**

While evaporated aluminum is the standard coating for reflection gratings, fast-fired aluminum with overcoatings of magnesium fluoride ( $MgF_2$ ) can be used to enhance efficiency in the spectrum between 120

and 160 nm. For the extreme ultraviolet (below 50 nm), gold replica gratings are recommended. Gold replicas also have higher reflectivity in most regions of the infrared spectrum and are particularly useful for fiber-optic telecommunications applications in the S, C and L (infrared) transmission bands.\*

---

\* The transmission bands used in fiber-optic telecommunications are usually defined as follows: S (short) band: c. 1435 to 1535 nm, C (conventional) band: c. 1525 to 1565 nm, and L (long) band: c. 1565 to 1630 nm. These definitions are by no means universal, but between them they cover the near-IR amplification range of erbium-doped optical fibers.

# 15. HANDLING GRATINGS

A diffraction grating is a *first surface optic*, so its surface cannot be touched or otherwise come in contact with another object without damaging it and perhaps affecting its performance. Damage can take the form of contamination (as in the adherence of finger oils) or distortion of the microscopic groove profile in the region of contact. This chapter describes the reasons why a grating must be handled carefully and provides guidelines for doing so.

## 15.1. THE GRATING SURFACE

Commercially available diffraction gratings are replicated optics comprised of three layers: a substrate, a resin layer, and (usually) a reflective coating (see Chapter 5). Each layer serves a different purpose: (1) the metallic layer provides high reflectivity, (2) the resin layer holds the groove pattern and groove profile, and (3) the substrate (usually glass) keeps the optical surface rigid.

## 15.2. PROTECTIVE COATINGS

Since the groove profile is maintained by the resin (epoxy) layer, rather than the reflective (metallic) coating on top of it (see Figure 15-1), protective coatings such as those that meet the military specification MIL-M-13508 (regarding first-surface aluminum mirrors) do not serve their intended purpose. Even if the aluminum coating itself were to be well-protected against contact damage, it is too thin to protect the softer resin layer underneath it. Consequently, replicated gratings are not provided with contact- or abrasion-protecting coatings.

## 15.3. GRATING COSMETICS AND PERFORMANCE

Warnings against touching the grating surface notwithstanding, damage to the surface occasionally occurs. Contact from handling, mounting or packaging can leave permanent visible marks on the grating surface. Moreover, some gratings have cosmetic defects that do not adversely impair optical performance, or perhaps represent the best available quality for a grating with a particular set of specifications. For example, some gratings have 'worm tracks' due to mechanical ruling of the master grating from which the replicated grating was taken, others

have coating defects like spit or spatter, and others have 'pinholes' (tiny voids in the reflective coating), etc. The many possible classifications of surface defects and the many opportunities to render the surface permanently damaged conspire to make the surfaces of many gratings look less than cosmetically perfect.

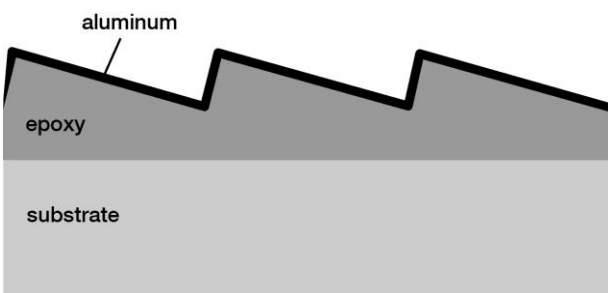


*Figure 15-1. Composition of a replica diffraction grating.* A section of a standard blazed grating with an aluminum coating is shown. Layer thicknesses are not shown to scale: generally, the aluminum film thickness is about 1  $\mu\text{m}$ , and the resin layer is between 10 and 50  $\mu\text{m}$ , depending on groove depth and grating size; the substrate thickness is usually between 3 and 100 mm.

While this damage may be apparent upon looking that the grating, it is not straightforward to determine the effect this damage has on the performance of the grating. Often the area affected by damage or contamination is a small fraction of the total area of the grating. Therefore, only a small portion of the total number of grooves under illumination may be damaged, displaced or contaminated. A damaged or contaminated region on the surface of a grating may have little, if any, noticeable effect on the performance of the optical system, because a diffraction grating is usually used as an integrating optic (meaning that all light of a given wavelength diffracted from the grating surface is brought to focus in the spectral order of interest). In contrast, a lens or mirror that does not focus (say, an eyeglass lens or a bathroom mirror) will show a distortion in its image corresponding to the damaged region of the optic. This familiar experience – the annoying effect of a chip on an eyeglass lens or a smudge on a bathroom mirror – has led many to assume that a similar defect on the surface of a grating will lead to a similar deficiency in performance. The most appropriate performance test of a grating with surface damage or cosmetic defects is not visual

inspection but instead to use the grating in its optical system and determine whether the entire system meets its specifications.

Damage to a region of grooves, or their displacement, will theoretically have some effect on the efficiency of the light diffracted from that region, as well as the total resolving power of the grating, but in practice such effects are generally not noticeable. Of more concern, since it may be measurable, is the effect surface damage may have on light scattered from the grating, which may decrease the signal-to-noise (SNR) of the optical system. Most forms of surface damage can be thought of as creating scattering centers where light that should be diffracted (according to the grating equation) is scattered into other directions instead.

#### **15.4. UNDOING DAMAGE TO THE GRATING SURFACE**

Damage to the microscopic groove profile is, unfortunately, irreversible; the resin layer will retain a permanent imprint. Contamination of the grating surface with finger oils, moisture, vacuum pump oil, etc. is also often permanent, particularly if the contaminated grating surface has been irradiated.

Sometimes surface contamination can be partially removed, and occasionally it can be removed completely, using a mild unscented dishwashing liquid. Care should be taken not to apply any pressure (even gentle scrubbing) to the grating surface. If contaminants remain, spectroscopic-grade solvents may be used; the purity of such solvents should be ascertained and only the purest form available used. The use of carbon dioxide ( $\text{CO}_2$ ) snow,<sup>199</sup> which sublimes after being applied to the grating surface, thereby carrying with it the contaminants, has also been used with some success. The key to cleaning a grating surface is to provide no friction (e.g., scrubbing) that might damage the delicate groove structure.

#### **15.5. GUIDELINES FOR HANDLING GRATINGS**

- *Never touch the grooved surface of a diffraction grating.* Handle a grating by holding it by its edges. If possible, use powder-free gloves while handling gratings.

---

<sup>199</sup> R. R. Zito, "Cleaning large optics with  $\text{CO}_2$  snow," *Proc. SPIE* **1236**, 952-972 (1990).

- *Never allow any mount or cover to come in contact with the grooved surface of a diffraction grating.* A grating that will be shipped should have its grooved surface protected with a specially-designed cover that does not touch the surface itself. Gratings that are not in use, either in the laboratory or on the manufacturing floor, should be kept in a closed box. Keep any oils that may be used to lubricate grating mount adjustments away from the front surface of the grating.
- *Do not talk or breathe over the grooved surface of a diffraction grating.* Wear a nose and face mask when it is required that you talk over the surface of a grating. Breath spray is particularly bad for reflection gratings, so one should not speak directly over the grating surface; instead, either turn away or cover the mouth (with the hand or a surgical mask).

## 16. GUIDELINES FOR SPECIFYING GRATINGS

Proper technical specifications are needed to ensure that the part supplied by the manufacturer meets the requirements of the customer. This is especially true for diffraction gratings, whose complete performance features may not be fully recognized. Documents that provide guidance in the specification of optical components, such as the ISO 10110 series ("Optics and optical instruments: Preparation of drawings for optical elements and systems"), do not clearly lend themselves to the specification of diffraction gratings. This chapter provides guidelines for generating clear and complete technical specifications for gratings.

Specifications should meet the following criteria.

- They should refer to *measurable* properties of the grating.
- They should be as *objective* as possible (avoiding judgment or interpretation).
- They should be *quantitative* where possible.
- They should employ common *units* where applicable (the SI system is preferred).
- They should contain *tolerances*.

A properly written engineering print for a diffraction grating will be clear and understandable to both the customer and the manufacturer.

### 16.1. REQUIRED SPECIFICATIONS

All grating prints should contain, at a minimum, the following specifications.

1. *Free Aperture.* The free aperture, also called the *clear aperture*, of a grating is the maximum area of the surface that will be illuminated. The free aperture is assumed to be centered within the *ruled area* (see below) unless otherwise indicated. For configurations in which the grating will rotate, such as in a monochromator, it is important to specify the free aperture as the maximum dimensions of the beam on the grating surface (*i.e.*, when the grating is rotated most obliquely to the incident beam). Also, it is important to ensure that the free aperture specifies an area that is completely circumscribed by the

ruled area, so that the illuminated area never includes part of the grating surface that does not have grooves. The free aperture of the grating is that portion of the grating surface for which the optical specifications apply (*e.g., Diffraction Efficiency, Wavefront Flatness or Curvature, Scattered Light* – see below).

2. *Ruled Area.* The ruled area of a grating is the maximum area of the surface that will be covered by the groove pattern. The ruled area is assumed to be centered on the substrate face unless otherwise indicated. By convention, the ruled area of a rectangular grating is specified as "groove length by ruled width" – that is, the grooves are parallel to the first dimension; for example, a ruled area of 30 mm x 50 mm indicates that the grooves are 30 mm long. Most rectangular gratings have their grooves parallel to the shorter substrate dimension. For gratings whose grooves are parallel to the longer dimension, it is helpful to specify "long lines" to ensure that the grooves are made parallel to the longer dimension.
3. *Substrate Dimensions.* The substrate dimensions (width, length, and thickness) should be called out, as should their tolerances. If the grating is designed to be front-mounted, the substrate specifications can be somewhat looser than if the grating surface will be positioned or oriented by the precise placement of the substrate. Front-mounting a grating generally reduces its cost and production time (see *Alignment* below). A grating substrate should have bevels on its active face, so that it is easier to produce and to reduce chipping the edges while in use. Bevel dimensions should be specified explicitly and should be considered in matching the *Ruled Area* (above) with the substrate dimensions.\* For custom (special-size) substrates, certain minimum bevel dimensions may be required to ensure that the grating is manufacturable – please contact us for advice.
4. *Substrate Material.* The particular substrate material should be specified. If the material choice is of little consequence, this can be left to the manufacturer, but especially for applications requiring substrates with low thermal expansion coefficients, or requiring gratings that can withstand high heat loads, the substrate material and its grade should be identified. For transmission gratings, the proper specification of the substrate material should include reference to the fact that the substrate will be used in transmission,

---

\* MKS standard bevels have a face width of 1.5 mm and are oriented at 45° to the two edges.

and may additionally refer to specifications for refractive index, inclusions, bubbles, striae, etc.

5. *Nominal Surface Figure*. Plane (flat) gratings should be specified as being planar; concave gratings should have a radius specified, and the tolerance in the radius should be indicated in either millimeters or fringes of red HeNe light ( $\lambda = 632.8$  nm) (a "wave" being a single wavelength, equaling 632.8 nm, and a "fringe" being a single half-wavelength, equaling 316.4 nm). Deviations from the nominal surface figure are specified separately as "wavefront flatness" or "wavefront curvature" (see below).
6. *Wavefront Flatness or Curvature*. This specification refers to the allowable deviation of the optical surface from its *Nominal Surface Figure* (see above). Plane gratings should ideally diffract plane wavefronts when illuminated by collimated incident light. Concave gratings should ideally diffract spherical wavefronts that converge toward wavelength-specific foci. In both cases, the ideal radius of the diffracted wavefront should be specified (it is infinite for a plane grating) and maximum deviations from the ideal radius should also be called out (e.g., the tolerance in the radius, higher-power irregularity in the wavefront). It is important to specify that grating wavefront testing be done in the diffraction order of use if possible, not in zero order, since the latter technique does not measure the effect of the groove pattern on the diffracted wavefronts. Deviations from a perfect wavefront are most often specified in terms of waves or fringes of red HeNe light. Generally, wavefront is specified as an allowable deviation from the nominal focus ("power") and allowable higher-order curvature ("irregularity").
7. *Groove Spacing or Frequency*. The number of grooves per millimeter, or the spacing between adjacent grooves, should be specified, but not both (unless one is subjugated to the other by labeling it as "reference"). For a grating whose groove spacing varies across the surface (e.g., an aberration-corrected concave holographic grating), the groove spacing (or frequency) is generally specified at the center of the grating surface.
8. *Groove Alignment*. Alignment refers to the angle between the groove direction and an edge of the grating substrate. Sometimes this angular tolerance is specified as a linear tolerance by stating the maximum displacement of one end of a groove (to an edge) relative to the other end of the groove. Generally, a tight alignment

specification increases manufacturing cost; it is often recommended that alignment be allowed to be somewhat loose and that the grating substrate dimensions not be considered for precise alignment but that the grating surface be oriented and positioned optically instead of mechanically (see comments in *Substrate Dimensions* above).

9. *Diffraction Efficiency.* Grating efficiency is usually specified as a maximum at a particular wavelength; often this is the *peak wavelength* (i.e., the wavelength of maximum efficiency). Occasionally efficiency specifications at more than one wavelength are specified. Either relative or absolute diffraction efficiency should be specified.
  - Relative efficiency is specified as the percentage of the power at a given wavelength that would be reflected by a mirror (of the same coating as the grating) that is diffracted into a particular order by the grating (that is, efficiency relative to a mirror).
  - Absolute efficiency is specified as the percentage of the power incident on the grating that is diffracted into a particular order by the grating.

In addition to the wavelength and the diffraction order, grating efficiency depends on the incidence and diffraction angles  $\alpha$  and  $\beta$ ; if these angles are not explicitly stated, the standard configuration (namely the Littrow configuration, in which the incident and diffracted beams are coincident) will generally be assumed. Unless otherwise noted on the curves themselves, all MKS efficiency curves are generated for the near-Littrow conditions of use with  $\alpha \approx \beta$ .

Generally, diffraction gratings are polarizing elements, so that the efficiency in both polarizations should be considered:

P-plane	TE	light polarized parallel to grooves
S-plane	TM	light polarized perpendicular to grooves

For each wavelength that has an efficiency specification, the following should be indicated: the wavelength, the efficiency (in percent), whether the efficiency specification is relative or absolute, the diffraction order, the polarization of the light, and the angles  $\alpha$  and  $\beta$ . In some cases, the bandwidth of the exit slit in the spectrometer used to measure the grating efficiency may need to be called out as well.

## **16.2. SUPPLEMENTAL SPECIFICATIONS**

Additional specifications are sometimes required based on the application in which the grating is to be used.

10. *Blaze Angle.* Although it is better to specify diffraction efficiency, which is a performance characteristic of the grating, sometimes the blaze angle is specified instead (or additionally). A blaze angle should be specified only if it is to be measured and verified (often done by measuring efficiency anyway), and a tolerance should be noted. In cases where both the diffraction efficiency and the blaze angle are specified, the efficiency specification should be controlling, and the blaze angle specification should be for reference only.
11. *Coating Material.* Generally, the *Diffraction Efficiency* specifications will dictate the coating material, but sometimes a choice exists and a particular coating should be specified. Additionally, dielectric coatings may be called out that are not implied by the efficiency specifications.
12. *Scattered Light.* Grating scattered light is usually specified by requiring that the fraction of monochromatic light power incident on the grating and measured a particular angle away from the diffracted order falls below a certain upper limit. The proper specification of scattered light would call out the test configuration, the polarization and wavelength of the incident light, the incidence angle, the solid angle subtended by the detector aperture, and the dimensions of the exit slit. Grating scatter is measured at MKS using red HeNe light.
13. *Cosmetics.* The cosmetic appearance of a diffraction grating does not correlate strongly with the performance of the grating, and for this reason specifications limiting the type, number and size of cosmetic defects are not recommended. Nevertheless, all MKS products undergo a rigorous cosmetic inspection before shipment.
14. *Imaging Characteristics.* Concave holographic gratings may be aberration-corrected, in which case they can provide focusing without the use of auxiliary optics. In these cases, imaging characteristics should be specified, generally by calling out the *full width at half maximum intensity* (FWHM) of the images.
15. *Damage Threshold.* In some instances, such as pulsed laser applications, diffracted gratings are subjected to beams of high power density that may cause damage to the delicate grating surface, in

which case the maximum power per unit area that the grating surface must withstand should be specified.

16. *Other specifications.* Other specifications that relate to the functional performance of the grating should be called out in the print. For example, if the grating must perform in extreme environments (e.g., a satellite or space-borne rocket, high heat and/or humidity environments), this should be noted in the specifications.

### **16.3. ADDITIONAL REQUIRED SPECIFICATIONS FOR CONCAVE ABERRATION-REDUCED GRATINGS**

Concave aberration-reduced gratings, often used in constant-deviation and flat-field spectrograph mounts (see Sections 7.5.3 and 7.5.5), have imaging properties that are tailored to the specific geometry of the spectrometer; that is, the grating recording coordinates  $\gamma$ ,  $r_c$ ,  $\delta$  and  $r_d$  depend on the use coordinates  $\alpha$ ,  $r$ ,  $\beta$  and  $r'$  (all of these quantities are defined in Chapter 7). Consequently, a concave aberration-reduced grating requires additional specifications to be fully described.

The cases for constant-deviation monochromators and flat-field spectrographs are given separately below. In all cases, a clear optical schematic showing the quantities defined is highly recommended, especially to ensure that the definition of angles is understood.

17. *Constant-deviation monochromator gratings.* Concave holographic gratings used in constant deviation monochromators should have the following three parameters specified (see Figure 16-1) to be defined uniquely:
  - the distance  $r$  from the entrance slit to the grating center (often called the *entrance arm* distance),
  - the distance  $r'$  from the exit slit to the grating center (the *exit arm* distance), and
  - the angle  $2K$  between these two arms (the *deviation angle*); alternatively, the *half-deviation angle*  $K$  may be specified provided it is clear which angle is called out.
18. *Flat-field spectrograph gratings.* Concave holographic gratings used in flat-field spectrographs require four parameters (see Figure 16-2):
  - the entrance arm distance  $r$ ,
  - the angle  $\alpha$  the entrance arm makes with the grating normal,

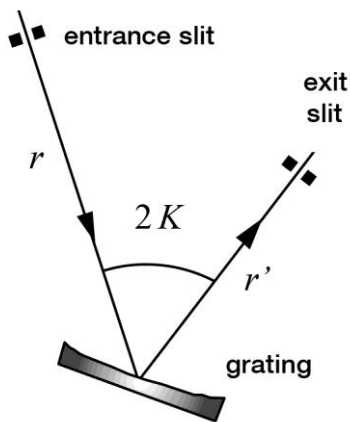


*Figure 16-1. Constant-deviation monochromator geometry.* The quantities that should be specified are the entrance arm distance  $r$ , the exit arm distance  $r'$ , and the angle  $2K$  between these arms.

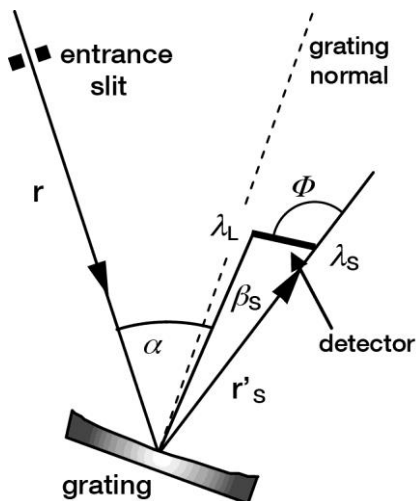


*Figure 16-2. Flat-field spectrograph geometry.* The quantities that should be specified are the incidence angle  $\alpha$ , the entrance arm distance  $r$ , the exit arm distance  $r's$  for the shortest wavelength in the spectrum to reach the detector, and the obliquity angle  $\phi$  of the detector. The detector is shown; the shortest and longest wavelengths  $\lambda_S$  and  $\lambda_L$  image at either end of the detector. [The distance  $r'_L$  from the grating center to the image of  $\lambda_L$  is not shown.]

- the distance  $r$ 's from the grating center to the image (on the detector) of the shortest wavelength  $\lambda_s$  in the spectrum, and
- the obliquity angle  $\phi$  of the detector (as described in 2.3.2).

An alternative set of parameters for defining a flat-field spectrograph is the set of quantities  $\alpha$ ,  $r$ ,  $l_H$  and  $\beta_H$ , where  $\alpha$  and  $r$  are as above and

- the distance  $l_H$  is measured from the grating center to the line defined by the detector, such that these two lines are perpendicular, and
- the angle  $\beta_H$  is the angle the line  $l_H$  makes with the grating normal (see Figure 16-3).

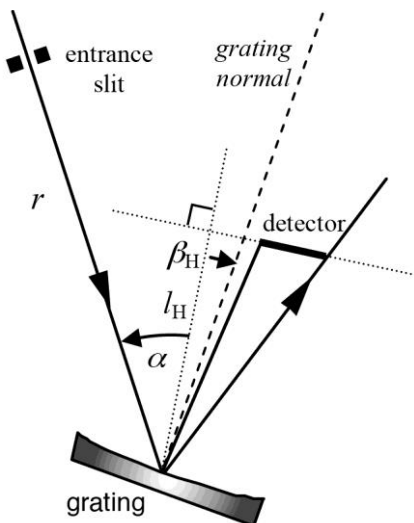


*Figure 16-3. Alternative flat-field spectrograph geometry.* A flat-field spectrograph can also be described uniquely by the following quantities: the incidence angle  $\alpha$ , the entrance arm distance  $r$ , the distance  $l_H$  (the line from the grating center to the line defined by the detector, such that these two lines are perpendicular), and the angle  $\beta_H$  that the line  $l_H$  makes with the grating normal.

Converting from the parameter set in Figure 16-3 to that in Figure 16-2 can be accomplished using the formulas

$$r' = l_H \sec(\beta_H - \beta_s), \quad r' L = l_H \sec(\beta_H - \beta_L). \quad (16-1)$$

# APPENDIX A. Sources of Error in Monochromator-Mode Efficiency Measurements of Plane Diffraction Gratings

Jeffrey L. Olson

While simple in principle, measuring the efficiency of diffraction gratings is a complex process requiring precise methods to achieve acceptable results. Every optical, mechanical, and electronic component comprising an efficiency measuring system is a potential source of error. Environmental factors may also contribute to the overall measurement uncertainty. Each source of error is identified and its effect on efficiency measurement is discussed in detail.

## A.O. INTRODUCTION

In his 1982 book *Diffraction Gratings*, M.C. Hutley makes the following statement regarding the measurement of diffraction grating efficiency:

“One seldom requires a very high degree of photometric accuracy in these measurements as one is usually content to know that a grating is 60% efficient rather than 50% and the distinction between, say, 61% and 60% is of little practical significance.”<sup>200</sup>

While this statement may have been true at the time it was written, it is no longer the case today. Certain industries, such as laser tuning and telecommunications, demand gratings with efficiencies approaching theoretical limits. The efficiency specifications for these gratings are well defined, and measurement errors as small as one percent may mean the difference between the acceptance and rejection of a particular grating.

In principle, measuring the efficiency of diffraction gratings is simple. A ratiometric approach is used in which the energy of a diffracted beam is compared to the energy of the incident beam. The incident beam may be

---

<sup>200</sup> M. C. Hutley, *Diffraction Gratings*, Academic Press (1982), p.168.

either measured directly (absolute measurement) or indirectly (relative measurement, by reflection from a reference mirror). Conversion from relative to absolute efficiency can be made easily by multiplying the known reflectance of the reference mirror by the relative efficiency of the grating. (Exceptions to this rule have been noted, namely 1800 to 2400 g/mm gold or copper gratings measured at wavelengths below 600 nm).<sup>201</sup>

As mentioned in Section 11.2, a monochromator mode efficiency-measuring instrument, in essence, is a double grating monochromator, with the grating under test serving as the dispersing element in the second monochromator. The first monochromator scans through the spectral range while the test grating rotates in order to keep the diffracted beam incident upon a detector that remains in a fixed position throughout the measurement.

A typical efficiency measuring apparatus (see Figure A-1) consists of a monochromator, collimator, polarizer, grating rotation stage, grating mount,

detector positioning stage, detector and associated optics, amplifier, and signal processing hardware. Once the beam exits the monochromator it is collimated, polarized, and, if necessary, stopped-down to a diameter appropriate for the grating being tested. The beam is then directed toward the grating to be tested where it is diffracted toward the detector. The electronic signal generated by the detector is amplified, filtered, and presented to the user via any number of devices ranging from a simple analog meter to a computer. In any case, a comparison is made between a reference signal, obtained by direct or indirect measurement of the incident beam, and the signal from the grating being tested.

Efficiency measurement results are normally reported on a graph (see Figure A-2) with wavelength on the X-axis and percent efficiency (absolute or relative) on the Y-axis. It is very unusual to see a published efficiency curve with error bars or some other indication of the measurement uncertainty. It must be understood that these measurements are not exact and may be in error by several percent. A complete understanding of the measurement process as well as the sources of error and how to minimize them would be of great value to the technician or engineer making the measurements as well as those

---

<sup>201</sup> E. G. Loewen and E. Popov, *Diffraction Gratings and Applications*, Marcel Dekker, Inc. (1997), p. 415.

involved in making decisions to accept or reject gratings based on efficiency.

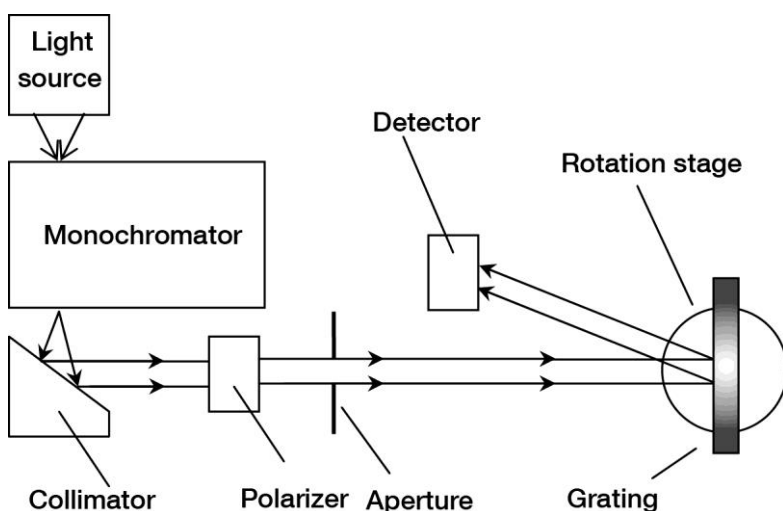


Figure A-1. Typical monochromator-mode efficiency measuring apparatus.

## A.1. OPTICAL SOURCES OF ERROR

### A.1.1. Wavelength error

Perhaps the most obvious error of an optical nature is an error in wavelength. If the monochromator does not accurately select the desired wavelength, efficiency peaks, anomalies, etc., will appear at the wrong spectral position on the efficiency curve. If the grating being measured is rotated to the appropriate incident angle for a given wavelength, the diffracted beam may partially or totally miss the detector if the wavelength is not correct. This is less of a problem in manually controlled instruments, since the operator can adjust the wavelength or grating rotation angle to obtain a maximum reading. On an automated instrument, however, a significant error may result unless the instrument has the ability to “hunt” for the efficiency peak.

Wavelength errors are usually caused by a failure of the monochromator indexing mechanism to move the grating to the correct rotation angle. Most computer-based monochromator systems employ

correction factors or calibration tables in firmware to correct systematic wavelength errors. Even so, many monochromators use open-loop stepper motor drives to position the grating. Since there is no explicit feedback from the rotation mechanism, the controller must assume that the grating is in the correct position. If the motor fails to move the proper number of steps due to binding in the mechanical system or for some other reason, the wavelength will be in error.

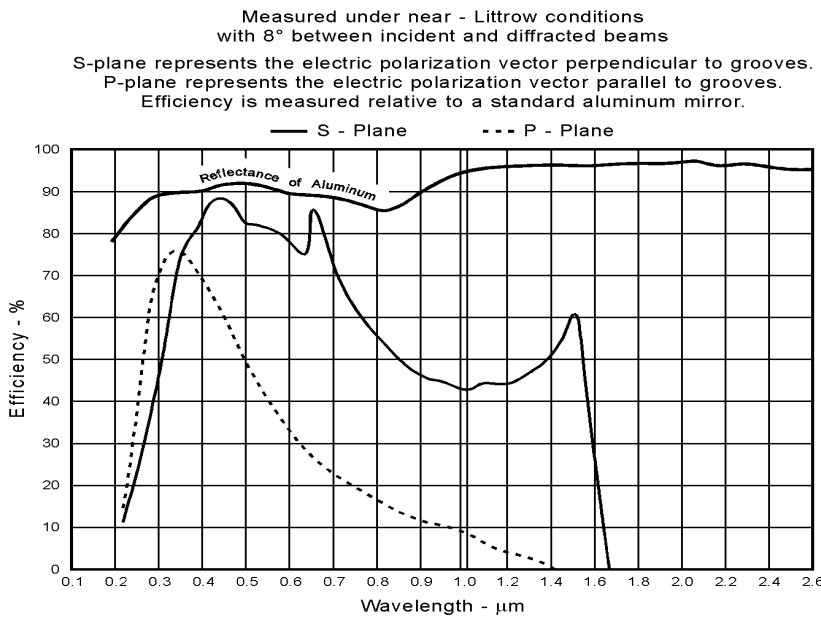


Figure A-2. Typical efficiency curve.

To ensure wavelength accuracy, periodic wavelength calibration should be done using a calibration lamp or other spectral line source. The author has used the Schumann-Runge O<sub>2</sub> absorption lines effectively for monochromator wavelength calibration in the far ultraviolet region near 193 nm. The well-defined Schumann-Runge transitions occurring at 192.6 nm are especially useful spectral features.<sup>202</sup>

<sup>202</sup> R. C. Sze and C. A. Smith, "High-temperature absorption studies of the Schumann-Runge band of oxygen at ArF laser wavelengths," *J. Opt. Soc. Am.* **B7**, 3, 462-475 (2000).

### A.1.2. Fluctuation of the light source intensity

One of the drawbacks of using a single detector system is that the light source intensity can change between the times the reference and sample measurements are made. With filament lamps, the intensity is proportional to the power dissipated in the filament. According to Ohm's law, power  $P$  is the product of current  $I$  and voltage  $E$ , and voltage is the product of current and resistance  $R$ , therefore:

$$P = IE = I(IR) = I^2R. \quad (A-1)$$

Typically, electrical power is applied to the lamp socket, rather than to the lamp directly. The contact resistance between the lamp and socket can be significant and is prone to change over time. If a constant voltage is applied to the socket and the contact resistance was to increase, the current, power, and lamp intensity will decrease as a result. If a constant current is applied instead, no change in power will occur as the result of a change in contact resistance (provided the filament resistance remains constant). For this reason, current-regulated, rather than voltage-regulated, power supplies are preferred whenever filament-type lamps are used. A photo-feedback system, in which a detector monitors and controls the lamp intensity, is also a good choice. Regardless of the type of light source used, it is always best that the sample and reference measurements be made in quick succession.

### A.1.3. Bandpass

As a rule, the bandpass of the light source should always be narrower than that of the grating under test. The bandpass  $B$  of the grating under test is estimated by the angular dispersion  $D$  of the grating, the distance  $r$  from the grating to the detector aperture, and the width  $w'$  of the exit aperture according to the equation:

$$B \approx \frac{w'}{rD}. \quad (A-2)$$

[Eq. (A-2) assumed the case where the aberrated image of the entrance slit is not wider than the exit aperture; see Section 8.3.]

Whenever a grating is measured using a source with a bandpass that is too broad, some of the outlying wavelengths will be diffracted away from the detector. In contrast, when the reference measurement is made using a mirror or by direct measurement of the incident beam, no dispersion occurs. Consequently, the detector captures all wavelengths

contained within the incident beam during the reference measurement, but not during the grating measurement (resulting in an artificial decrease in grating efficiency). Another consequence of measuring gratings using a light source with a broad bandpass is that sharp efficiency peaks will appear flattened and broadened, and may be several percent lower than if measured using a spectrally-narrow light source. Efficiency curves should, but often do not, state the bandpass of the source used to make the measurement. When using a monochromator, it is generally best to adjust the slits to obtain the narrowest bandpass that will provide an acceptable signal-to-noise ratio (SNR). Alternatively, a narrow band spectral source, such as a laser or calibration lamp, may be used in conjunction with a monochromator or interference filter to eliminate unwanted wavelengths.

#### A.1.4. Superposition of diffracted orders

According to the grating equation (see Eq. (2-1)), the first order at wavelength  $\lambda$  and the second order at wavelength  $\lambda/2$  will diffract at the same angle (see Section 2.2.2). Therefore, the light emerging from a monochromator exit slit will contain wavelengths other than those desired. The unwanted orders must be removed to accurately determine the efficiency at the desired wavelength. “Order-sorting” filters are most commonly used for this purpose. These are essentially high-pass optical filters that transmit longer wavelengths while blocking the shorter wavelengths.

Another problematic situation arises when the adjacent diffracted orders are very closely spaced. In this case, adjacent orders must be prevented from overlapping at the detector aperture, which would result in a significant error. This situation can be avoided by ensuring that the bandpass of the source is less than the free spectral range of the grating being tested. As shown in Section 2.7, the free spectral range  $F_\lambda$  is defined as the range of wavelengths  $\Delta\lambda$  in a given spectral order  $m$  that are not overlapped by an adjacent order, expressed by Eq. (2-29):

$$F_\lambda = \Delta\lambda = \frac{\lambda}{m}. \quad (2-29)$$

For an echelle being measured in the  $m = 100^{\text{th}}$  order at  $\lambda = 250$  nm, the free spectral range is 2.5 nm. The detector aperture must also be sufficiently narrow to prevent adjacent orders from being detected, but

not so narrow as to violate the “rule” regarding the bandpass of the light source and grating under test.

#### A.1.5. Degradation of the reference mirror

When a mirror is used to determine the incident light energy, its reflectance as a function of wavelength needs to be well characterized. Mirrors tend to degrade over time due to atmospheric exposure, and if not re-characterized periodically, optimistic measurements of grating efficiency will result. At the National Physical Laboratory (NPL) in England, an aluminum-coated silica flat was used as a reference mirror. This is nothing new, but in this case the “buried” surface of the mirror was used as the mirror surface instead of the metal surface itself. Since the aluminum is never exposed to the atmosphere, its reflectance is stable, and since the mirror was characterized through the silica substrate, its influence is automatically taken into account.<sup>203</sup> The restriction in using the buried surface method is that the incident beam must be normal to the mirror surface to avoid beam separation caused by multiple reflections from the front and buried surfaces. When an unprotected mirror surface is used as a reference, absolute measurements of its reflectance should be made on a regular basis.

#### A.1.6. Collimation

If the incident beam is not reasonably well collimated, the rays will fall upon the grating at a variety of angles and will be diffracted at different angles. In the case of a diverging diffracted beam, the beam will spread, possibly overfilling the detector. Since the reference beam does not encounter a dispersing element in its path (but the sample beam does), it is possible that all the energy will be collected during the reference measurement but not during the sample measurement, causing the measured efficiency to be low.

Whenever a monochromator-based light source is used it is difficult, if not impossible, to perfectly collimate the beam emerging from the exit slit in both planes. It is important to collimate the beam in the direction perpendicular to the grooves, but it is not as critical for the beam to be well collimated in the direction parallel to the grooves, since no diffraction occurs in that direction. A limiting aperture may be used to restrict the beam size and prevent overfilling the grating under test.

---

<sup>203</sup> M. C. Hutley, *Diffraction Gratings*, Academic Press (1982), p.169.

It should be emphasized that beam collimation is not nearly as important in an efficiency measuring system as it is in an imaging system, such as a spectrograph. It is only necessary to ensure that the detector collects all the diffracted light. The degree of collimation required largely depends on the dispersion of the grating under test, but in most cases a beam collimated to within  $0.1^\circ$  is adequate. For example, an angular spread of  $0.1^\circ$  in a beam incident upon a 1200 g/mm grating measured in the 1<sup>st</sup> order at 632.8 nm (Littrow configuration) will produce a corresponding spread in the diffracted beam of less than 1 mm over a distance of 500 mm.

#### A.1.7. Stray light or “optical noise”

The influence of stray radiation must always be taken into consideration when making efficiency measurements. If the level of background radiation is very high, the detector may be biased enough to result in a significant error. This is especially true when simple DC detection methods are used. Any bias introduced by background radiation must be subtracted from both the reference and sample measurements before the ratio is computed. For example, if the background radiation equals 2% of the reference beam, and the grating being tested measures 50% relative efficiency, the actual efficiency is 48/98 or 49%. This represents an error of 1% of the full-scale measured efficiency. In many cases simply operating the instrument in a dark lab or enclosure is sufficient to reduce background light to insignificant levels. Averaging is often used to “smooth out” noisy signals, but unlike other more random noise sources that tend to be bipolar, stray light-induced noise is always positive. Averaging several measurements containing a significant level of optical noise may bias the final measurement. In most cases, it is best to use phase-sensitive detection to remove the effects of unwanted radiation.

#### A.1.8. Polarization

Most efficiency curves display the S and P as well as the 45-degree polarization efficiency *vs.* wavelength. When making polarized efficiency measurements using an unpolarized source, it is necessary to use some form of optical element to separate the two polarization vectors. It is critical that the polarizer be aligned as closely as possible to be parallel (P plane) or perpendicular (S plane) to the grooves or a polarization mixing error will result. To determine the 45-degree polarization efficiency of a

grating, it seems easy enough to set the polarizer to 45 degrees and make the measurement, but unless the output from the light source is exactly balanced in both S and P planes, an error will result.

Figure A-3 shows the effect of source polarization on the measured efficiency of a hypothetical grating having efficiencies of 90% in the P plane and 50% in the S plane at some arbitrary wavelength. In one case the light source contains equal S and P intensities while the other has a 70:30 S-to-P ratio. In the case of the balanced light source, as the polarizer is rotated to 45°, the efficiency is 70%, exactly the average of the S and P measurements. On the other hand, the unbalanced source results in a measured efficiency of 60%. This represents an error of 10% of the full-scale measured value. For that reason, it is always recommended to make separate S and P measurements and then average them to determine the grating's 45-degree polarization efficiency.

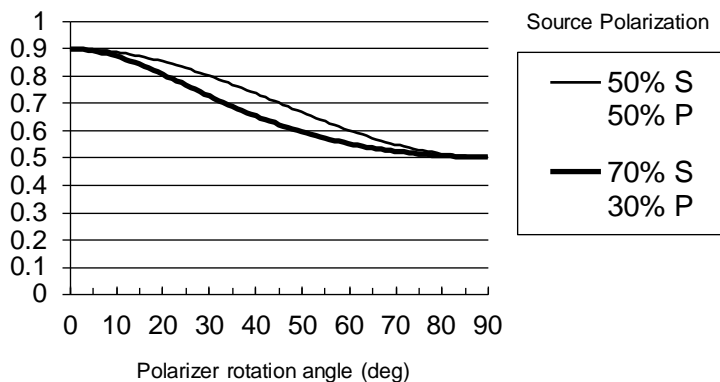


Figure A-3. Efficiency comparison with balanced and unbalanced source polarization ( $0^\circ = P$ ,  $90^\circ = S$ ).

#### A.1.9. Unequal path length

An error can result in a single detector system purely as the result of the optical path being different between the reference and sample measurements. This is especially true at UV wavelengths where the atmospheric absorption is significant. Different optical path lengths are

not as much of a problem in dual detector systems since the relative calibration of the two detectors can compensate for atmospheric effects.

## **A.2. MECHANICAL SOURCES OF ERROR**

### **A.2.1. Alignment of incident beam to grating rotation axis**

It is critical to align the incident beam to the rotation axis of the grating stage and mount. If not, the beam will “walk” across the grating surface at relatively low incident angles, and partially miss the grating surface at very high incident angles. Since the incident and diffracted beams are displaced from their correct location, it is entirely possible that all or part of the diffracted beam will miss the detector aperture.

### **A.2.2. Alignment of grating surface to grating rotation axis**

The effect of not having the grating surface located exactly over the rotation axis will be similar to that of not having the beam aligned to the grating rotation axis. Optimally, a grating mount that references the grating’s front surface, rather than the sides or back of the grating substrate, may be used to ensure alignment. This is often not practical since the contact points on the mount may leave an impression on the grating surface. To avoid this problem, an inclined lip or rail is sometimes used that makes contact with the grating on the extreme outer edge only. On beveled grating substrates this can be a source of error since the dimensional variation of the bevels can be significant. If the grating mount does not reference the front surface, an adjustment must be provided in order to accommodate gratings of various thicknesses.

### **A.2.3. Orientation of the grating grooves (tilt adjustment)**

On grating mounts that use the substrate to locate the grating to be tested, the plane in which the diffracted orders lie will be tilted if the grooves are not properly aligned with the sides of the grating substrate. This may cause the diffracted beam to pass above or below the detector aperture. Most gratings do not have perfect alignment of the grooves to the substrate, so it is necessary to incorporate a method for rotating the grating a small amount in order to compensate for groove misalignment.

#### **A.2.4. Orientation of the grating surface (tip adjustment)**

Due to some wedge in the grating substrate, for example, the grating surface may not be parallel to the grating rotation axis. This will cause the diffracted beam to fall above or below the detector aperture. On most grating mounts an adjustment is provided to correct this situation. Ideally the grating tip, tilt, and rotation axes all intersect at a common point on the grating surface, but in fact it is extremely rare to find a grating mount in which the tip axis does so. In most cases the tip axis is located behind or below the grating substrate, so when adjusted, the grating surface will no longer lie on the rotation axis. The ideal situation is one in which the grating is front-surface referenced on the mount so that no adjustment is needed.

#### **A.2.5. Grating movement**

It is essential that the grating being tested be held securely in the mount during the testing process. Vibration from motors and stages as well as the inertia generated by the grating as it is rotated may cause it to slip. Any motion of the grating relative to the mount will result in alignment errors and invalidate any measurements taken after the movement occurred.

### **A.3. ELECTRICAL SOURCES OF ERROR**

#### **A.3.1. Detector linearity**

In principle, all that is required to make satisfactory ratiometric measurements is a linear response from the sensing element and associated electronics. Nearly all detectors have response curves that exhibit non-linearity near saturation and cut off. It is extremely important to ensure that the detector is biased such that it is operating within the linear region of its response curve. In addition, the detector preamplifier and signal processing electronics must also have a linear response, or at least have the non-linearity well characterized for a correction to be applied. Neutral density filters may be inserted into the optical path to verify or characterize the detection system linearity. The following set of five calibrated neutral density filters is sufficient, in most cases, for verifying the detector response to within  $\pm 1\%$ :

Detector non-linearity becomes a major source of error when the reference and grating signals differ significantly in intensity. Unless the

linearity of the detector and associated electronics has been well established, using a mirror with a reflectance of 90% or higher as a reference may introduce an error if the grating being measured has an efficiency of 20%. This is analogous to sighting in a rifle at 100 yards and using it to shoot at targets 25 yards away. In some situations, it is best to use a well-characterized grating as nearly identical to the grating to be tested as possible. This method is especially useful for making “go/no-go” efficiency measurements. If the reference grating is carefully chosen to be one that is marginally acceptable, then the efficiency measuring instrument will have its greatest accuracy at the most critical point. All gratings measuring greater than or equal to 100% relative to the reference grating are assumed to be good and those below 100% are rejected. Of course, this method requires periodic recharacterization of the reference grating to maintain measurement integrity.

<i>Optical Density</i>	<i>Transmission*</i>
0.1	79%
0.3	50%
0.6	25%
1.0	10%
2.0	1%

\* rounded to nearest whole percent.

### A.3.2. Changes in detector sensitivity

Some efficiency measuring instruments use separate detectors for making the reference and grating measurements (these are not to be confused with systems that use secondary detectors to monitor light source fluctuations). Most, however, use a single detector for both the reference and grating measurements instead. There are very good reasons for doing this. First, detectors and the associated electronics are expensive, so using a single detector is far more cost effective. Detector response characteristics change over time, so frequent calibration is necessary in a dual-detector system to ensure that the photometric accuracy of each detector has not changed relative to the other. By using the same detector for sample and reference measurements, photometric accuracy is not an issue, since an error in the reference measurement will also be present in the grating measurement and consequently nullified.

### **A.3.3. Sensitivity variation across detector surface**

A significant error can result if the reference or diffracted beam is focused down to form a spot that is much smaller than the detector's active area. Some detectors, especially photomultipliers, may exhibit a sensitivity variation amounting to several percent as the spot moves across the detector surface. It is often sufficient to place the detector aperture far enough away from the detector such that the spot is defocused and just under-fills the active area. Alternately a diffuser or integrating sphere is sometimes used to distribute the light more uniformly across the detector surface.

### **A.3.4. Electronic noise**

Any form of optical or electronic noise can influence efficiency measurements. It is desirable to maintain the highest signal-to-noise ratio (SNR) possible, but often a trade-off must be made between signal strength and spectral resolution. Decreasing the monochromator slit width in order to narrow the bandpass of the source results in a reduced detector output signal. Care must be taken not to limit the intensity to a point where electronic (and optical) noise becomes a significant factor. In most cases, an SNR value of 200:1 is adequate.

## **A.4. ENVIRONMENTAL FACTORS**

### **A.4.1. Temperature**

Normally it is not necessary to perform efficiency measurements in an extremely well-regulated environment, but there are a few cases in which temperature control is needed. Whenever very high spectral resolution measurements are made (*c.*  $\Delta\lambda \leq 1$  nm), temperature variation within the monochromator may cause a significant wavelength drift. Temperature fluctuations may cause optical mounts to expand or contract resulting in a displacement of the beam. It is always a good idea to keep heat sources well away from all optical and mechanical components that may affect the grating being tested or the beam. It is also wise to allow gratings that are to be tested to acclimate in the same environment as the test instrument.

### **A.4.2. Humidity**

Humidity is not usually a significant error source, but since it can affect the system optics and electronics, it merits mentioning. A high humidity level may influence measurements at wavelengths where atmospheric absorption varies with relative humidity. Low humidity promotes the generation of static electricity that may threaten sensitive electronic components. In general, the humidity level should be maintained in a range suitable for optical testing.

### **A.4.3. Vibration**

Vibration becomes an error source when its amplitude is sufficient to cause the grating under test or any of the optical components to become displaced. If the vibration is from a source other than the instrument itself, then mounting the instrument on a vibration isolated optical bench will solve the problem. If the instrument itself is the vibration source, then the problem becomes a little more difficult. Stepper-motors are most often used to rotate and translate the grating being tested, as well as tune the monochromator, select filters, *etc.* As the motors ramp up to predetermined velocity, a resonant frequency is often encountered that will set up an oscillation with one or more mechanical components in the system. While it is sometimes necessary to pass through these resonant frequencies, it is never advisable to operate continuously at those frequencies. Most motion controllers have provisions for tuning the motion profile to minimize resonance. Some motion controllers allow micro-stepped operation of the motors, producing a much smoother motion. Although they are generally more expensive, servo controllers, amplifiers, and motors provide exceptional accuracy and very smooth motion.

## **A.5. SUMMARY**

Many of the error sources identified can be eliminated entirely, but only at the expense of decreased functionality. Greater accuracy can be obtained using an instrument that operates at a fixed wavelength in a fixed geometry and is only used to test gratings that have identical physical properties. When a large variety of gratings are to be tested, each with a different size, shape, groove frequency, wavelength range, test geometry, *etc.*, it is not practical to construct a dedicated instrument for each. In this case, a more complex instrument is required. In specifying

such an instrument, each source of error should be identified, and if possible, quantified. An error budget can then be generated that will determine if the instrument is able to perform at the desired level. Most likely it will not, and then a decision needs to be made regarding which features can be compromised, eliminated, or implemented on another instrument.

Disagreements often arise between measurements made of the same grating on different efficiency measuring instruments. Slight differences in test geometry, bandpass, and beam size can have a surprisingly large effect on efficiency measurements. What is sometimes difficult to understand is that it is possible for two instruments to measure the same grating and get different results that are valid!

Grating efficiency is largely determined by the groove properties of the master from which the grating was replicated, and to some degree the coating. It is very rare for a master, regardless of the process used to create it, to have perfectly uniform efficiency at every spot along its surface. In some cases, the efficiency may vary by several percent. If a grating is measured using a small diameter beam, then these efficiency variations are very noticeable compared to measurements made using a larger beam. If two different instruments are used to measure the same grating, it is possible that the beams are not the same size or, in the case of a small beam diameter, are not sampling the same spot on the grating surface. Both instruments are correct in their measurements, but still do not agree. For this reason, whenever comparisons between instruments are made, the differences in their configuration must be taken into consideration.

The goal of efficiency measurement is to characterize the grating under test, not the apparatus making the measurements. For this reason, efficiency curves should report not only the relative or absolute efficiency *vs.* wavelength, but the properties of the instrument making the measurement as well. Only then is it possible to reproduce the results obtained with any degree of accuracy.



## APPENDIX B. Lie aberration theory for grating systems

Besides the wavefront aberration theory described in Chapter 7, geometrical optics can be formulated in a manner in direct analogy with the Hamiltonian theory of classical dynamics.<sup>204</sup> The basis for this analogy is the recognition that Fermat's principle, which requires that a physical light path be an extremum, is equivalent to the requirement that this physical light path follow a trajectory governed by a Hamiltonian. The coordinates and momenta of a particle in classical mechanics therefore correspond to the coordinates and direction cosines of a light ray in optics, and the tools of classical mechanics can be applied directly to geometrical optics.

The characterization of optical systems using Lie transformations, hitherto applied to dynamical systems, was first developed by Dragt, who considered axially symmetric systems.<sup>205</sup> Later this formulation was extended by Goto and Kurosaki to optical systems without axial symmetry (but with a plane of symmetry).<sup>206</sup>

Dragt considered the coordinates  $x$  and  $y$  of a point in the object plane, as well as their direction cosines  $p$  and  $q$ , as the object *phase space variables* and primed quantities ( $x'$ ,  $y'$ ,  $p'$  and  $q'$ ) as their corresponding image phase space variables (see Figure B-1), and expressed the transformation of the ray in object space to the ray in image space (due to the optical system) as

$$W' = \mathbf{M}w \quad (B-1)$$

where  $\mathbf{M}$  is a *mapping* (or simply *map*), an operator that transforms coordinates in *object space* to corresponding coordinates in *image space*.

A transformation that maps coordinates in object space into coordinates in image space according to Fermat's principle is called *symplectic*. Dragt and Finn showed in 1976 that a symplectic map can be

---

<sup>204</sup> A. J. Dragt, E. Forest and K. B. Wolf, "Foundations of a Lie algebraic theory of geometrical optics," in *Lie Methods in Optics*, J. J. Sanchez-Mondragon and K. B. Wolf, eds. (Springer-Verlag, Berlin, 1984), ch. 4.

<sup>205</sup> A. J. Dragt, "Lie algebraic theory of geometric optics and optical aberrations," *J. Opt. Soc. Am.* **72**, 372-379 (1982).

<sup>206</sup> K. Goto and T. Kurosaki, "Canonical formulation for the geometrical optics of concave gratings," *J. Opt. Soc. Am.* **A10**, 452-465 (1993).

expressed in terms of Lie transformations.<sup>207</sup> More specifically, this map can be expressed as the product of Lie transformations, each of which is homogeneous in the object space coordinates (that is, all terms in each Lie transformation are of the same power in the independent variables). Furthermore, truncating the product at any power leaves a symplectic transformation, so lower-order imaging properties can be examined without considering the higher-order Lie transformations in the map. Goto and Kurosaki used Dragt's formalism to derive, using Lie algebraic theory rather than wavefront aberration theory, equations that are formally identical to the aberration coefficients  $F_{20}$ ,  $F_{02}$ ,  $F_{30}$ , etc. seen in Chapter 7.

---

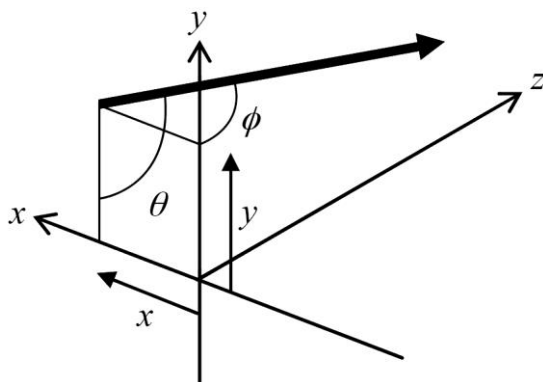


*Figure B-1. Definition of the object space variables.* The optical ray in object space has coordinate  $(x, y)$  in the object plane and direction defined by angles  $\theta$  and  $\phi$  (shown), whose direction cosines are  $p$  and  $q$ .

---

The transformation from object phase space to image phase space may be represented as a sequence of operations; for example, for diffraction by a grating, these operations are (in sequence)

1. transit from the object plane to the grating, through the distance  $r$ ,
2. rotation, through the angle  $\alpha$ , to a coordinate frame centered at the grating center and oriented with an axis along the grating normal,

---

<sup>207</sup> A. J. Dragt and J. M. Finn, "Lie series and invariant functions for analytical symplectic maps," *J. Math. Phys.* **17**, 2215-2227 (1976).

3. diffraction in this coordinate frame,
4. rotation through the angle  $\beta$ , and
5. transit from the grating to the image plane, through the distance  $r'$ .

An advantage of the Lie transformation approach over the wavefront aberration technique is that general points  $(x, y)$  in the object plane are naturally considered; which this is also true of wavefront aberration theory, the algebra is cumbersome and, as a result, most authors consider only a point source in the dispersion plane.

Another immediate advantage of the Lie transformation approach is that systems with more than one optical element can be addressed in a computationally straightforward manner, simply by appending transformations (in the sequence in which the optical ray encounters the optical elements).<sup>208</sup> Using wavefront aberration theory this is not straightforward, in large part because the grating surface coordinates appear explicitly in the optical path difference (see Eq. (7-5)). Many researchers overcame this complication by imposing intermediate foci between successive elements,<sup>209</sup> though Chrisp introduced the use of toroidal reference surfaces and provided an important advance in the development of wavefront aberration theory for multielement systems.<sup>210</sup>

As an example of the power of Lie algebraic techniques in the analysis of multielement optical system, below is the equation for defocus for a system of two aberration-reduced concave holographic gratings:<sup>211</sup>

<sup>208</sup> C. Palmer, W. R. McKinney and B. Wheeler, "Imaging equations for spectroscopic systems using Lie transformations. Part I - Theoretical foundations," *Proc. SPIE* **3450**, 55-66 (1998).

<sup>209</sup> T. Namioka, H. Noda, K. Goto and T. Katayama, "Design studies of mirror-grating systems for use with an electron storage ring source at the Photon Factory," *Nucl. Inst. Meth.* **208**, 215-222 (1983).

<sup>210</sup> M. Chrisp, "The theory of holographic toroidal grating systems," Ph. D. dissertation, U. London (1981); M. Chrisp, "Aberrations of holographic toroidal grating systems," *Appl. Opt.* **22**, 1508-1518 (1983).

<sup>211</sup> C. Palmer, B. Wheeler and W. R. McKinney, "Imaging equations for spectroscopic systems using Lie transformations. Part II - Multi-element systems," *Proc. SPIE* **3450**, 67-77 (1998).

$$\begin{aligned}
F_{20} = & \frac{\cos \beta_1 \cos \beta_2}{\cos \alpha_1 \cos \alpha_2} r_1 + \frac{\cos \alpha_1 \cos \alpha_2}{\cos \beta_1 \cos \beta_2} r'_2 + \frac{\cos \alpha_1 \cos \beta_2}{\cos \alpha_2 \cos \beta_1} D \\
& - \frac{2A_2^{[1]}r_1}{\cos \alpha_1 \cos \beta_1} \left[ \frac{\cos \beta_2}{\cos \alpha_2} D + \frac{\cos \alpha_2}{\cos \beta_2} r'_2 \right] \\
& - \frac{2A_2^{[2]}r'_2}{\cos \alpha_2 \cos \beta_2} \left[ \frac{\cos \alpha_1}{\cos \beta_1} D + \frac{\cos \beta_1}{\cos \alpha_1} r_1 \right] \\
& + \frac{4A_2^{[1]}A_2^{[2]}r_1r'_2D}{\cos \alpha_1 \cos \alpha_2 \cos \beta_1 \cos \beta_2}.
\end{aligned} \tag{B-2}$$

Here the subscripts on the angles and distances refer to each grating, and we have defined

$$D = r'_1 + r_2 \tag{B-3}$$

as the distance between the two gratings. The quantity  $A_2^{[i]}$  depends on the substrate curvature and groove pattern for the  $i^{\text{th}}$  grating.

## FURTHER READING

ASTM standard E131-02, Standard Terminology Relating to Molecular Spectroscopy, ASTM International (2003).

Ball, D. W., 2001. *The Basics of Spectroscopy*, SPIE Press (Bellingham, Washington).

Born, M., and E. Wolf, 1999. *Principles of Optics*, seventh expanded edition, Cambridge University Press (Cambridge, England).

Clark, B. J., T. Frost and M. A. Russell, 1993. *UV Spectroscopy: Techniques, instrumentation, data handling*, Chapman and Hall (London, England).

Davis, S. P., 1970. *Diffraction Grating Spectrographs*, Holt, Rinehart and Winston (New York, New York).

Ederer, D. L., ed., 1998. Selected Papers on VUV Synchrotron Radiation Instrumentation – Beam Line and Instrument Development, SPIE Milestone Series vol. **MS 152**, SPIE (Bellingham, Washington).

Harris, D. A. and C. L. Bashford, eds., 1987. *Spectrophotometry and Spectrofluorimetry*, IRL Press (Oxford, England).

Harrison, G. R., 1973. "The diffraction grating – an opinionated appraisal," *Appl. Opt.* **12**, 2039-2049.

Harvey, J. E. and R. N. Pfisterer, 2019. "Understanding diffraction grating behavior: including conical diffraction and Rayleigh anomalies from transmission gratings," *Opt. Eng.* **58**(8), 087105.

Hunter, W. R., 1985. "Diffraction Gratings and Mountings for the Vacuum Ultraviolet Spectral Region," *Spectrometric Techniques*, vol. IV., 63-180 (1985). This article provides a very thorough and detailed review of the use and manufacture of diffraction gratings.

Hutley, M. C., 1976. "Interference (holographic) diffraction gratings," *J. Phys.* **E9**, 513-520 (1976). This article offers more detail on holographic gratings and compares them with ruled gratings.

Hutley, M. C., 1982. *Diffraction Gratings*, Academic Press (New York, New York). This book provides a complete and thorough description of diffraction gratings, their manufacture and their application.

James, R. F. and R. S. Sternberg, 1969. *The Design of Optical Spectrometers*, Chapman and Hall (London, England).

J.-P. Laude, 2002. *DWDM Fundamentals, Components, and Applications*, Artech House (Boston, Massachusetts).

- Loewen. E. G., 1970. "Diffraction Gratings for Spectroscopy," *J. Physics E* **3**, 953-961.
- Loewen. E. G., M. Nevière and D. Maystre, 1977. "Grating Efficiency Theory as it Applies to Blazed and Holographic Gratings," *Appl. Optics* **16**, 2711-2721 (1977).
- Loewen, E. G., 1983. "Diffraction Gratings, Ruled and Holographic," in *Applied Optics and Optical Engineering*, vol. IX (chapter 2), R. Shannon, ed., Academic Press (New York, New York). This chapter describes developments in grating efficiency theory as well as those in concave grating aberration reduction.
- Loewen, E. G. and E. Popov, 1997. *Diffraction Gratings and Applications*, Marcel Dekker (New York, New York).
- Lyman, T, 1928. *The Spectroscopy of the Extreme Ultraviolet*, 2<sup>nd</sup> edition, Longman, Greens & Co. (London, England).
- Maystre, D., ed., 1993. *Selected Papers on Diffraction Gratings*, SPIE Milestone Series vol. **MS 83**, SPIE (Bellingham, Washington).
- McKinney, W.R., 1984. *Diffraction Gratings: Manufacture, Specification, and Application – Tutorial 25*, SPIE (Bellingham, Washington).
- Meltzer, R. J., 1969. "Spectrographs and Monochromators," in *Applied Optics and Optical Engineering*, vol. V (chapter 3), R. Shannon, ed., Academic Press (New York, New York).
- Peatman, W.B., 1997. Gratings, Mirrors and Slits: Beamline Design for Soft X-Ray Synchrotron Radiation Sources, Taylor & Francis (London, England).
- Perkampus, H.-H., 1992. *UV-VIS Spectroscopy and Its Applications*, Springer-Verlag (Berlin, Germany).
- Petit, R., ed., 1980. *Electromagnetic Theory of Gratings*, Springer-Verlag (New York, New York); volume 22 in "Topics in Current Physics" series.
- Richardson, D., 1969. "Diffraction Gratings", in *Applied Optics and Optical Engineering*, vol. V (chapter 2), R. Kingslake, ed., Academic Press (New York, New York).
- Samson, J. A. R., and D. L. Ederer, 2000. *Vacuum Ultraviolet Spectroscopy*, Academic Press (San Diego, California).
- Schroeder, D. J., 2000. *Astronomical Optics*, 2<sup>nd</sup> ed., Academic Press (San Diego, California). Chapters 12 through 15 serve as an excellent introduction to gratings and their instruments, with application toward stellar spectrometry. Chapters 2 through 5 form a clear and quite complete introduction to the ideas of geometrical optics used to design lens, mirror, and grating systems.

- Skoog, D. A., F. J. Holler and T. A. Nieman, 1998. *Principles of Instrumental Analysis*, fifth edition, Brooks/Cole. The sections on atomic and molecular spectroscopy serve as excellent introductions to the subject.
- Stover, J. C., 1990. *Optical Scattering*, McGraw-Hill, Inc. (New York, New York).
- Stroke, G. W. 1967. "Diffraction Gratings," in *Handbook of Physics* **29**, S. Flugge, ed. (Springer, Berlin).
- Strong, J., 1960. "The Johns Hopkins University and diffraction gratings," *J. Opt. Soc. Am.* **50**, 1148-1152.
- Werner, W., 1970. *Imaging Properties of Diffraction Gratings*, Uitgeverij Waltman (Delft, Netherlands).
- Williard, H. H., et al., 1988. *Instrumental Methods of Analysis*, seventh edition, Wadsworth (Belmont, California). The chapters on absorption and emission spectroscopy, and ultraviolet and visible spectroscopic instrumentation, are of particular interest.
- Wolfe, W. 1997. *Introduction to Grating Spectrometers*, SPIE Press (Bellingham, Washington).



# Grating Publications by MKS Personnel

Below is a partial list of publications by MKS scientists and engineers pertaining to diffraction gratings and their uses.

## Reference Books

E. G. Loewen and E. Popov, *Diffraction Gratings and Applications*, 1997 Marcel Dekker, Inc. (ISBN 0-8247-9923-2).

## Gratings in General

D. Richardson, "Diffraction Gratings," chapter 2, volume II of *Applied Optics and Optical Engineering*, R. Kingslake, ed. (Academic Press, New York: 1969)

E. G. Loewen, "Diffraction Gratings for Spectroscopy," *J. Physics E* **3**, 953-961 (1970).

E. G. Loewen, *Diffraction Grating Handbook*, first edition, Bausch & Lomb (1970).

G. R. Harrison and E. G. Loewen, "Ruled gratings and wavelength tables," *Appl. Opt.* **15**, 1744-1747 (1976).

E. G. Loewen, M. Nevière and D. Maystre, "Optimal design for beam sampling mirror gratings," *Appl. Opt.* **15**, 2937-2939 (1976).

E. G. Loewen, "Diffraction Gratings, Ruled and Holographic," chapter 2, volume IX of *Applied Optics and Optical Engineering*, R. Shannon, ed. (Academic Press, New York: 1983), pp. 33-71.

W. R. McKinney, Diffraction gratings: manufacture, specification and application, SPIE Tutorial T25 (1984).

E. G. Loewen, "What's new in gratings?" in *Instrumentation for Ground-Based Optical Astronomy, Present and Future*, L. B. Robinson, ed. (Springer-Verlag, 1987), pp. 118-123.

E. G. Loewen, "The Ruling and Replication of Diffraction Gratings," *Optics and Photonics News*, May 1991.

C. Palmer, *Diffraction Grating Handbook*, eighth edition, MKS Instruments, Inc. (2020). [E. G. Loewen wrote the first edition, originally published in 1970.]

C. Palmer, "Diffraction Gratings: The Crucial Dispersive Component," *Spectroscopy* **10**, 14-15 (1995).

## Grating Efficiency

- E. G. Loewen, D. Maystre, R. C. McPhedran and I. Wilson, "Correlation between efficiency of diffraction gratings and theoretical calculations over a wide spectral range," *Japanese J. Appl. Phys.* **14**, suppl. 1, 143-152 (1975).
- E. G. Loewen, M. Nevière and D. Maystre, "Grating efficiency theory as it applies to blazed and holographic gratings," *Appl. Opt.* **16**, 2711-2721 (1977).
- E. G. Loewen and M. Nevière, "Dielectric coated gratings: a curious property," *Appl. Opt.* **16**, 3009-3011 (1977).
- E. G. Loewen, M. Nevière and D. Maystre, "On an asymptotic theory of diffraction gratings used in the scalar domain," *J. Opt. Soc. Am.* **68**, 496-502 (1978).
- E. G. Loewen and M. Nevière, "Simple selection rules for VUV and XUV diffraction gratings," *Appl. Opt.* **17**, 1087-1092 (1978).
- I. Wilson, B. Brown and E. G. Loewen, "Grazing incidence grating efficiencies," *Appl. Opt.* **18**, 426-427 (1979).
- E. G. Loewen, M. Nevière and D. Maystre, "Efficiency optimization of rectangular groove gratings for use in the visible and IR regions," *Appl. Opt.* **18**, 2262-2266 (1979).
- E. G. Loewen, W. R. McKinney and R. McPhedran, "Experimental Investigation of Surface Plasmon Scatter from Diffraction Gratings," *Proc. SPIE* **503**, 187-197 (1984).
- L. B. Mashev, E. K. Popov and E. G. Loewen, "Asymmetrical trapezoidal grating efficiency," *Appl. Opt.* **26**, 2864-2866 (1987).
- L. B. Mashev, E. K. Popov and E. G. Loewen, "Optimization of grating efficiency in grazing incidence," *Appl. Opt.* **26**, 4738-4741 (1987).
- L. Mashev, E. Popov and E. G. Loewen, "Total absorption of light by a sinusoidal grating near grazing incidence," *Appl. Opt.* **27**, 152-154 (1988).
- E. Popov, L. Mashev and E. G. Loewen, "Total absorption of light by gratings in grazing incidence: a connection in the complex plane with other types of anomaly," *Appl. Opt.* **28**, 970-975 (1989).
- L. Mashev, E. Popov and E. G. Loewen, "Brewster effect for deep metallic gratings," *Appl. Opt.* **28**, 2538-2541 (1989).
- E. Popov, L. Tsonev, E. Loewen and E. Alipieva, "Spectral behavior of anomalies in deep metallic grooves," *J. Opt. Soc. Am.* **A7**, 1730-1735 (1990).
- E. G. Loewen, E. K. Popov, L. V. Tsonev and J. Hoose, "Experimental study of local and integral efficiency behavior of a concave holographic diffraction grating," *J. Opt. Soc. Am.* **A7**, 1764-1769 (1990).
- E. K. Popov, L. V. Tsonev and E. G. Loewen, "Scalar theory of transmission relief gratings," *Opt. Commun.* **80**, 307-311 (1991).

V. S. Valdes, W. R. McKinney and C. Palmer, "The differential method for grating efficiencies implemented in Mathematica," *Nucl. Inst. Meth.* **A347**, 216-219 (1994).

C. Palmer, J. Olson and M. M. Dunn, "Blazed diffraction gratings obtained by ion-milling sinusoidal photoresist gratings," *Proc. SPIE* **2622**, 112-121 (1995).

## Grating Imaging

W. R. McKinney and C. Palmer, "Numerical design method for aberration-reduced concave grating spectrometers," *Appl. Opt.* **26**, 3108-3118 (1987).

C. Palmer and W. R. McKinney, "Optimizing Angular Deviation for Fixed-Deviation Monochromators Modified by Use of Aberration-Reduced Holographic Gratings," *Proc. SPIE* **815**, 57-65 (1987).

C. Palmer, "Limitations of aberration correction in spectrometer imaging," *Proc. SPIE* **1055**, 359-369 (1989).

C. Palmer, "Theory of second generation holographic gratings," *J. Opt. Soc. Am.* **A6**, 1175-1188 (1989).

C. Palmer, "Absolute astigmatism correction for flat-field spectrographs," *Appl. Opt.* **28**, 1605-1607 (1989).

W. R. McKinney and C. Palmer, "Design of Grazing Incidence Monochromators Involving Unconventional Gratings," *Proc. SPIE* **1055**, 332-335 (1989).

C. Palmer and W.R. McKinney, "Equivalence of focusing conditions for holographic and varied line-space gratings," *Appl. Opt.* **29**, 47-51 (1990).

C. Palmer, "Second-order imaging properties of circular-field spectrographs," *Appl. Opt.* **29**, 1451-1454 (1990); erratum, *Appl. Opt.* **29**, 3990 (1990).

C. Palmer, "Deviation of second-order focal curves in common spectrometer mounts," *J. Opt. Soc. Am.* **A7**, 1770-1778 (1990).

C. Palmer and W. R. McKinney, "Imaging Theory of Plane-symmetric Varied Line-space Grating Systems," *Opt. Eng.* **33**, 820-829 (1994).

W. R. McKinney and C. Palmer, "Derivation of aberration coefficients for single-element plane-symmetric reflecting systems using Mathematica," *Proc. SPIE* **3150**, 97-104 (1997).

C. Palmer, W. R. McKinney and B. Wheeler, "Imaging equations for spectroscopic systems using Lie transformations. Part I - Theoretical foundations," *Proc. SPIE* **3450**, 55-66 (1998).

C. Palmer, B. Wheeler and W. R. McKinney, "Imaging equations for spectroscopic systems using Lie transformations. Part II - Multi-element systems," *Proc. SPIE* **3450**, 67-77 (1998).

C. Palmer and W. R. McKinney, "Imaging properties of varied line-space (VLS) gratings with adjustable curvature," *Proc. SPIE* **3450**, 87-102 (1998).

## Echelle Gratings

- G. R. Harrison, E. G. Loewen and R. S. Wiley, "Echelle gratings: their testing and improvement," *Appl. Opt.* **15**, 971-976 (1976).
- E. G. Loewen, D. Maystre, E. Popov and L. Tsonev, "Echelles: scalar, electromagnetic and real-groove properties," *Appl. Opt.* **34**, 1707-1727 (1995).
- J. Hoose *et al.*, "Grand Gratings: Bigger is Better, Thanks to Mosaic Technology," *Photonics Spectra* (December 1995).
- E. G. Loewen *et al.*, "Diffraction efficiency of echelles working in extremely high orders," *Appl. Opt.* **35**, 1700-1704 (1996).
- E. Popov *et al.*, "Integral method for echelles covered with lossless or absorbing thin dielectric layers," *Appl. Opt.* **38**, 47-55 (1999).

## Transmission Gratings

- E. G. Loewen, L. B. Mashev and E. K. Popov, "Transmission gratings as three-way beamsplitters," *Proc. SPIE* **815**, 66-72 (1981).
- E. K. Popov, L. V. Tsonev and E. G. Loewen, "Scalar theory of transmission relief gratings," *Opt. Commun.* **80**, 307-311 (1991).
- E. K. Popov, E. G. Loewen and M. Nevière, "Transmission gratings for beam sampling and beam splitting," *Appl. Opt.* **35**, 3072-3075 (1996).

## Mosaic Gratings

- J. Hoose *et al.*, "Grand Gratings: Bigger is Better, Thanks to Mosaic Technology," *Photonics Spectra* **29**, 118-120 (December 1995).
- T. Blasiak and S. Zheleznyak, "History and construction of large mosaic diffraction gratings," *Proc. SPIE* **4485**, 370-377 (2002).

## Grating Replication

- W. R. McKinney and L. Bartle, "Development in replicated nickel gratings," *Proc. SPIE* **315**, 170-172 (1981).
- E. G. Loewen, Replication of mirrors and diffraction gratings, SPIE Tutorial **T10** (1983).

## Master Grating – Holographic

- L. Mashev and S. Tonchev, "Formation of holographic diffraction gratings in photoresist", *Applied Physics A* **26**, 143-149 (1981).
- L. Mashev and S. Tonchev, "Formation of blazed holographic gratings", *Applied Physics B* **28**, 349-353 (1982).

L. Mashev and S. Tonchev, "Producing and measurement of holographic diffraction gratings", *Proc. Symp. "Physics and Electronics"* **I**, 233-236 (1982).

L. Mashev and S. Tonchev, "Diffraction efficiency of blazed holographic gratings", *Opt. Comm.* **47**, 5-7 (1983).

F. Canova, O. Uteza, J.-P. Chambaret, M. Flury, S. Tonchev, R. Fechner and O. Parriaux, "High-efficiency, broad band, high-damage threshold high-index gratings for femtosecond pulse compression", *Opt. Express* **15**, 15324-15334 (2007).

S. Tonchev, "Double-sided exposure for large blaze-angle saw-tooth grating manufacturing", *Proc. 2<sup>nd</sup> EOS Conference on Manufacturing of Optical Components (EOSMOC 2011)*, paper 4386 (2011).

### Master Grating - Ruling

R. S. Wiley, "Diamond's role in ruling diffraction gratings," *Proc. Int. Diamond Conf.*, 249-256 (1967).

E. G. Loewen, R. H. Burns and K. H. Kreckel, "Numerically controlled ruling engine with 1/10 fringe interferometric feedback for grids 600 mm square and scales 760 mm long," *J. Opt. Soc. Am.* **60**, 726A (1970).

E. G. Loewen, R. S. Wiley and G. Portas, "Large diffraction gratings ruling engine with nanometer digital control system," *Proc. SPIE* **815**, 88-95 (1987).

### Grating Testing

W. Anderson, G. Griffin, C. F. Mooney and R. Wiley, "Electron microscope method for measuring diffraction grating groove geometry," *Appl. Opt.* **4**, 999-1003 (1965).

G. R. Harrison, E. G. Loewen and R. S. Wiley, "Echelle gratings: their testing and improvement," *Appl. Opt.* **15**, 971-976 (1976).



# INDEX

- aberration, 84  
aberration coefficient, 84  
aberration reduction, 90  
aberration-reduced concave grating, 79  
Abney mount, 94  
absolute efficiency, 113  
add-drop routers, 200  
anamorphic magnification, 34  
angular deviation, 22, 98  
angular dispersion, 26  
anomalies, 115, 136  
astigmatism, 85  
astronomy, 192  
atomic spectroscopy, 185  
'B' engine, 40  
bandpass, 31  
beam splitters, 201  
blaze angle, 36  
blaze condition, 36  
blaze wavelength, 114  
blazing, 113  
'C' engine, 41  
camera, 70  
Carpenter prism. See grism  
classical diffraction, 22  
classical grating, 80  
collimator, 70  
colorimetry, 187  
coma, 88  
concave grating, 80  
conical diffraction, 22  
conservation of energy, 134  
constructive interference, 21  
cut-off filters, 168  
damage threshold, 66  
defocus, 85  
demultiplexer, 200  
deviation angle, 22, 98  
differential methods, 139  
diffraction, 19  
diffraction grating, 14  
diffraction limit, 102  
diffraction order, 21, 24  
diffuse scattered light, 142  
dispersion plane, 82  
dual-blaze grating, 67  
Eagle mount, 94  
echelles, 179  
efficiency, 35, 113  
efficiency curve, 114  
emission spectrum, 187  
energy density, 64  
energy distribution, 35  
esonant oscillations, 199  
excitation spectrum, 187  
*f*/number, 32  
Fermat's principle, 82  
fiber-optic telecommunications, 200  
finite conductivity, 126  
first generation holographic grating, 49, 80  
first surface optic, 207  
first-order Littrow blaze wavelength, 37  
flat-field spectrograph, 55, 96  
fluorescence spectroscopy, 187  
focal length, 32  
focal ratio, 32  
Foucault knife-edge test, 161  
free spectral range, 35  
full width at half maximum intensity, 30  
general ray, 82  
grating cosmetics, 207  
grating efficiency, 35  
grating equation, 21  
grating normal, 81  
grating prism. See grism  
grating scatter, 37, 141  
grating specifications, 211  
grating tangent plane, 82  
gratings as filters, 197

- grazing incidence, 179  
grism, 177  
groove density, 22  
groove frequency, 22  
groove pattern, 55, 79  
groove spacing, 19  
grooves per millimeter, 22  
half deviation angle, 23  
handling gratings, 209  
high vacuum, 64  
holographic grating, 45  
hyperspectral systems, 188  
imaging spectrographs, 98  
immersed grating, 183  
in-plane diffraction, 22  
in-plane scatter, 142  
instrumental analysis, 185  
instrumental bandpass, 111  
instrumental stray light, 141  
integral methods, 139  
interference grating. See  
    holographic grating  
interorder scatter, 144, 166  
ion etching, 131  
IR spectroscopy, 185  
laser tuning, 189  
Lie transformations, 235  
limit of resolution, 28  
line curvature, 85  
linear dispersion, 27  
linespread function, 103  
Littrow blaze condition, 37  
Littrow configuration, 22  
Littrow monochromator, 73  
Lyman ghosts, 143, 158  
magnification, 34, 103  
Mann engine, 40  
master grating, 14  
merit function, 92  
metrological applications, 201  
Michelson engine, 39  
molecular spectroscopy, 185  
monochromator, 69  
mosaic grating, 193  
multiplexer, 200  
obliquity factor, 28  
optical couplers, 201  
optical spectrum analyzers, 201  
order sorting, 25  
overfilling, 146  
overlapping spectra, 25  
Paschen-Runge mount, 94  
peak wavelength, 114  
perfect grating, 145  
pitch, 19  
plane grating, 69  
plate factor. See reciprocal linear  
    dispersion  
polarization, 115  
polarization conversion, 138  
pole ray, 82  
polychromator, 69  
principal plane, 82  
pulse stretching and compression,  
    191  
R number, 182  
Raman spectroscopy, 188  
Rayleigh anomalies, 136  
Rayleigh criterion, 29  
reciprocal linear dispersion, 27  
reciprocity theorem, 134  
reflection grating, 14, 19  
relative efficiency, 113  
relative humidity, 63  
replica grating, 14, 57  
replication tree, 59  
resolving power, 28  
resolving power vs. resolution, 31  
resonance anomalies, 136  
Rowland ghosts, 143, 155  
ruled gratings, 39  
ruling engine, 39  
ruling process, 42  
S plane, 115  
sagittal curvature, 81  
sagittal focal distance, 86  
sagittal magnification, 103  
sagittal plane, 82  
sagittal radius, 81  
satellites, 159

- scalar efficiency theories, 139  
scattered light, 37, 141  
second generation holographic grating, 50, 80  
Seya-Namioka monochromator, 98  
Sheridan grating, 48  
signal-to-noise ratio, 38, 170  
slit function, 170  
SNR. See signal-to-noise ratio  
spectral bandpass, 31  
spectral order, 21  
spectral resolution, 31  
spectrograph, 69  
spectrometer, 69  
spectroscopy, 13  
specular reflection, 22  
spot diagram, 101  
stigmatic image, 84  
stray light, 37, 141  
stray radiant energy, 141  
submaster, 57  
substrate curvature, 79  
substrate figure, 79  
subtractive dispersion, 74  
surface plasma wave, 137, 199  
surface plasmon polariton, 199  
synchrotron radiation, 197  
tangential curvature, 81  
tangential focal distance, 86  
tangential magnification, 103  
tangential plane, 82  
target pattern, 204  
temperature, 63  
threshold anomalies, 136  
TM plane, 115  
transfer coating, 58  
transmission grating, 19, 174  
triple monochromator, 75  
tunable filter, 198  
UV spectroscopy, 185  
varied line-space grating, 44, 80  
vector efficiency theories, 139  
visible spectroscopy, 185  
VLS grating. See varied line-space grating  
Wadsworth mount, 87, 96  
wavefront testing, 161  
wavenumbers, 181  
zero order, 22, 24